STUDY THE POTENTIAL OF INDIGENOUS MOSS AS A HEAVY METAL POLLUTION BIOMONITORING TOOL FOR THE KUMAON REGION (PITHORAGARH AND CHAMPAWAT DISTRICT) OF UTTARAKHAND (INDIA)

Thesis Submitted for the award of the Degree of

DOCTOR OF PHILOSOPHY

in

Botany

By

Dheeraj Gahtori

(41800636)

Supervised By

Dr. Ashish Vyas (12386)

Department of Microbiology & Biochemistry

(Professor)

Lovely Professional University

Co-Supervised by

Dr. Joginder Singh

Department of Botany (Professor)

Nagaland University, Lumami

LOVELY PROFESSIONAL UNIVERSITY, PUNJAB

2024

DECLARATION

I, hereby declare that the presented work in the thesis entitled "Study the potential of indigenous moss as a heavy metal pollution biomonitoring tool for the Kumaon region (Pithoragarh and Champawat district) of Uttarakhand (India)" in fulfillment of the degree of **Doctor of Philosophy (Ph. D.)** is outcome of research work carried out by me under the supervision of Dr. Ashish Vyas, working as Professor, in the Department of Microbiology, School of Bioengineering and Biosciences of Lovely Professional University, Punjab, India. In keeping with the general practice of reporting scientific observations, due acknowledgments have been made whenever the work described here has been based on the findings of another investigator. This work has not been submitted in part or full to any other University or Institute for the award of any degree.

(Signature of Scholar)

Name of the scholar: Dheeraj Gahtori

Registration No.: 41800636

Department/School: Department of Botany, School of Bioengineering & Biosciences

Lovely Professional University,

Punjab, India

CERTIFICATE

This is to certify that the work reported in the Ph. D. thesis entitled "Study the potential of indigenous moss as a heavy metal pollution biomonitoring tool for the Kumaon region (Pithoragarh and Champawat district) of Uttarakhand (India)" submitted in fulfillment of the requirement for the award of the degree of **Doctor of Philosophy (Ph.D.)** in the Department of Microbiology, School of Bioengineering and Biosciences, is a research work carried out by Dheeraj Gahtori, 41800636, is a bonafide record of his/her original work carried out under my supervision and that no part of the thesis has been submitted for any other degree, diploma or equivalent course.

(Signature of Supervisor)
Dr. Ashish Vyas
Professor
Department of Microbiology,
School of Bioengineering and Biosciences
Lovely Professional University,
Phagwara, Punjab 144 411
INDIA

(Signature of Co-Supervisor)
Dr. Joginder Singh
Professor
Professor
Department of Botany
Nagaland University, Lumami,
Zunheboto, Nagaland 798 627,
INDIA

ABSTRACT

Heavy metal pollution is a significant environmental problem that arises when heavy metal ions are discharged into the natural environment. Understanding the extent of metal pollution and locating its causes locally are the first steps in mitigating it. India, a developing country with an enormous population, experiences poor air quality due to industrial activities, heavy traffic density, and rural biomass burning. A significant part of India's economy depends on agriculture, which also contributes to air pollution through chemical fertilizers, pesticides, and crop residue burning.

The study was conducted in the Pithoragarh and Champawat districts of the Kumaon region of Uttarakhand. The area has a rich floral and faunal diversity. The economy depends upon local agricultural practices and small industrial activities. The region is also well known for its importance as a yatra route for the *Adikailash Yatra* and the famous *Mansoravar Yatra,* which is why it has a high tourism activity.

Before introducing the moss species for the biomonitoring study, the study area was surveyed thoroughly. Based on the availability of moss throughout the year and different ecological aspects, including sampling, four different moss species, *Thuidium cyambifolium, Rhynchostegiella divericatifolia, Fissidens anomalous,* and *Isopterygium elegance*, were selected for their physiological tolerance for chlorophyll, nitrate reductase and peroxidase activity against the heavy metals (Zinc, Lead, Copper and Cadmium).

The Phytotoxicity of the different metals on the chlorophyll content of the studied moss after 7 days and prolonged exposure of 15 days showed that among the tested moss, *T. cyambifolium* was the most tolerant for heavy metals as it exhibited a minimal decrease in chlorophyll content (chlorophyll a, b, and total chlorophyll) compared to other studied mosses against Zn, Pb, Cu, and Cd. As observed in the work, the loss in photosynthetic activity of moss at the high concentration was evident by decreased hill activity and oxygen evolution capacity of mosses. The nitrate reductase activity was in the order of *T. cyambifolium* > *R. divericatifolia*> *F. anomalus* > *I. elegens*. Compared to *T. cyambifolium,* the other three mosses showed a significant decrease in nitrate reductase activity when exposed to heavy metal treatments.

During this study, it was noted that Cd, Zn, Cu, and Pb treatments generally suppress peroxidase activity in moss plants, with the effect becoming more pronounced over time,

except for the unique response seen in *Thuidium cyambifolium*. It was found to be decreased consistently as observations were taken on the third, sixth, and fifteenth days. Initially, the value was found to be increased, and after that, it was reported to have decreased. This increase in enzyme activity could represent an appropriate protection against the overproduction of peroxide radicals under low concentrations of heavy metals. The peroxidase activity of the examined mosses against the Zn, Cu, Pb, and Cd was in order of *T. cyambifolium* > *R. divericatifolia* > *F. anomalus* > *I. elegens*.

Finally, based on the availability, ecological parameters, and physiological tolerance of mosses against different heavy metals, *Thuidium cymbifolium* was selected for the present biomonitoring study. The moss *T. cymbifolium* was collected at different seasonal intervals, i.e., winter, summer, and rainy seasons, for three consecutive years during the study. The present investigation comprised the study of the accumulation of Zinc, Copper, Lead, and Cadmium in eight different study sites located in the Champawat and Pithoragarh districts. Using moss bag transplants, these sites were divided into five zones based on their direction.

Moss bags containing *T. cymbifolium* were transplanted at approximately uniform elevations across diverse locations, differing in orientation and seasonal positioning, to examine the heavy metal accumulation in the moss. After the end of the season, the transplanted bags were collected and subjected to acid digestion to extract the metals using the atomic absorption spectrophotometer (AAS).

Through the investigation, the results from various sampling stations in Champawat and Pithoragarh district were correlated to the baseline levels of Zn, Cu, Pb, and Cd in different seasons. It was found that the highest accumulation of these heavy metals occurred during the summer season, followed by the winter season. The lowest accumulation was observed during the rainy season across all study sites. Among the five directions, the highest metal pollution was detected in the eastern, southern, and northern sampling sites, followed by the western sampling sites of districts Champawat and Pithoragarh.

The concentrations of these heavy metals exhibited considerable variation and outliers in decreasing order across the three seasons: summer, winter, and rain. Compared with the other two seasons, summer presented the highest accumulation of Zinc (1.972 mg/g) from the east direction of Pithorgarh and the south direction of Khetikhan (1.854 mg/g). At the same time, winter and rainy seasons showed the lowest accumulation of Zn (0.400 mg/g and 0.555

mg/g) from the city center of Thal and Champawat. Pb pollution in Champawat and Pithoragarh districts was recorded as 1.767 mg/g and 1.728 mg/g from the east direction of Thal and the north direction of Lohaghat during the summer, rainy, and winter seasons. Copper metal accumulation was minimal during the rainy season from the east direction of Ghat (0.463 mg/g) and from the west direction of Khetikhan (0.380 mg/g). Cadmium showed remarkable differences in accumulation compared to the other three studied metals in the summer, winter, and rainy seasons. Maximum accumulation from the north direction from the Thal and minimum accumulation from the north direction from the Ghat of district Pithoragarh were reported.

The primary sources of emissions responsible for the significant burden of metal deposition may be attributed to various environmental factors correlated with the distribution of emission sources. Moreover, variables such as traffic density, closeness to adjacent roads, precipitation, meteorological conditions, seasonal variations, sampling time, and dominant wind direction may also influence the occurrence of the phenomenon. Compared to other locations, the areas to the east and north of Pithoragarh and the south direction of Khetikhan and Barakote experienced high annual accumulations of zinc (Zn) and copper (Cu). The city center of Ghat, the northern direction of Pithoragarh from district Pithoragarh and west of Khetikhan, and the north direction of Lohaghat from Champawat district exhibited significant levels of lead (Pb) and cadmium (Cd) contamination. The high pollution load is due to the presence of a large number of vehicles and high levels of pollution in these popular tourist spots. Automobiles, specifically buses, cars, and other motor vehicles, are the sole means of transportation linking the foothills to these regions.

Variation of metal accumulation level and degree of contamination in different study sites of district Champawat and Pithoragarh in relation to contamination factor was also studied during the study. During three consecutive years, For Zinc, the city center of Munsiyari and the city center of Thal were reported under the C1 category with CF > 1, showing that these sites were recorded as unpolluted during the course of the study. The areas north of Lohaghat and Pithoragarh, south of Khetikhan and Ghat, and east of Barakote and Thal, along with the east and west directions of Barakote, fall under the C3 category. These regions' contamination factor (CF) ranges from 2 to 3.5, indicating slight pollution.

The city center of Lohaghat is classified as C1, indicating that the area is free from Pb pollution. The areas to the north, direction of Lohaghat, Pithoragarh, Ghat, and Munsiyari,

south of Lohaghat, Ghat, and Munsiyari, and in the east direction of Lohaghat, Barakote, Pithoragarh, and Thal, as well as the areas in the west direction of Barakote and Thal, were classified as C3 category showing that these sites had slight Pb pollution.

About Cu, the CF (contamination factor) in the range of 2-3.5 is observed in the city center of Pithoragarh and Ghat, Khetikhan, Barakote, and Thal from the north, east, and west directions. As a result, these sites were classified under the C3 category, indicating a slight pollution level. The city centres of Thal and Munsiyari fall under the C1 category and show that these sites were unpolluted with copper.

Regarding Cadmium (Cd), the contamination factor values for most sites in each direction ranged from 1 to 2. Consequently, these sites can be classified within the C2 category, indicating a slight pollution level. The contamination factor (CF) ranging from 2 to 3.5 is observed in the city center of Ghat and in the areas of Pithoragarh, Ghat, Thal, and Munsiyari, which were located in the east direction. Consequently, these sites are categorized as C3, denoting a minor degree of pollution, which shows that the area is unpolluted. The eastern and western directions of Khetikhan and Thal and the north direction of Thal have CFs in the range of 2 to 3.5. This indicates that these locations fall into the C3 category with a slight level of pollution.

ACKNOWLEDGMENT

First and foremost, I would like to express my deepest gratitude to God for granting me the strength, perseverance, and wisdom to undertake and complete this PhD journey. His guidance and blessings have been my foundation throughout this process.

I want to express my gratitude to my supervisor, Dr. Ashish Vyas, Professor, Department of Microbiology at the School of Bioengineering and Biosciences, for his scientific approach, scholarly supervision, creative ideas, constructive criticism, affectionate help, and encouragement to improve the quality of my research. Without his direction and support, this endeavor would not have been possible.

I am highly indebted to my co-supervisor, Dr. Joginder Singh, Professor, Department of Botany, Nagaland University, who helped and guided me to the best of his abilities. His constant supervision, scholarly guidance, and inspirational advice always kept me alive in my research.

I express my profound gratitude to Prof. Dinesh Kumar Saxena, Emeritus Professor, Department of Botany, Bareilly College, Bareilly, for his meticulous guidance, insightful critique, extensive expertise, scientific recommendations, and unwavering support, which were invaluable in conducting the research.

I am incredibly grateful to Dr. Manish Belwal, a senior colleague and Assistant Professor at HNB GPGC, Khatima, for his invaluable guidance and unwavering support in conducting the current project. I am also thankful to my senior, Dr. Chandra Mohan Mehta, Professor and Associate Dean, and my friend, Dr. Bhupendra Mathpal, Associate Professor, School of Agriculture LPU, for their help and support.

I want to convey my gratitude to my Parents, brother, and sister for their unwavering affection, selflessness, and faith in me. Your prayers, support, and encouragement have been the primary source of my strength.

I express profound gratitude towards my daughter, Aadrika, and my wife, Priyanka. The constant affection, endurance, and kindness that you have shown me have been the primary catalysts for my strength and motivation. Your unwavering support and encouragement have been crucial in helping me navigate through this challenging journey, and I am immensely grateful for your role as my anchor.

Finally, I thank the Department of Forest, Government of Uttarakhand and Department of Higher Education, Uttarakhand, and the worthy Principal, HNB GPGC Khatima, for permitting

me to pursue PhD and providing me with all the requisite infrastructure for carrying out research work.

This PhD journey has been challenging yet rewarding, and I am grateful to everyone who has contributed to it.

Dheeraj Gahtori
16-12-2024

TABLE OF CONTENTS

LIST OF TABLES

LIST OF FIGURE

LIST OF APPENDICES

Chapter 1: INTRODUCTION

Metals are considered an essential part of the Earth's geochemical systems; thus, nature is a primary source of metals in the atmosphere (Garrett, 2010). Metals are widespread, with varying concentrations in parent rock, soil, water, air, and all biological matter. These are persistent and hazardous, accumulating in the environment for years (Mitra et al., 2022). Heavy metals, such as arsenic, cadmium, mercury, and lead, seriously threaten the ecosystem with increased industrial and urban growth.

Metal pollutants originate from various human-generated sources, including industrial discharges, vehicle emissions, waste burning, agricultural methods, and natural occurrences such as forest fires and volcanic eruptions. They are discharged into the atmosphere as either particulate matter or gases, which can be carried over long distances through air currents. Following their release into the atmosphere, metal pollutants undergo a series of processes that involve deposition, dispersion, and transformation (Briffa et al., 2020).

In the deposition process, metal particles from the air settle onto soil, water bodies, and vegetation surfaces and enter the food chain. Dispersion of metal pollutants involves movement through the air, enabling their transport to distant locations from the source of emission (He et al., 2023). In the atmosphere, metal pollutants undergo a chemical and physical transformation, including oxidation, reduction, and complexation, which impact the behavior and toxicity of metal pollutants.

In India, most of the studies on pollution are based on the analysis of the atmospheric aerosols collected using particulate matter filters (Basha et al., 2010; Krishna, 2012; Agarwal et al., 2020; Yadav et al., 2022). Although it is a fast and active analysis method, it requires sophisticated and expensive technical apparatus (Clements et al., 2017). Few cost-effective techniques with desirable sensitivity to simultaneously measure multiple air pollutants are available (Puckett, 1988; Giordano et al., 2021). Using air samplers in remote regions of India is challenging due to the poor electrical infrastructure (Saxena et al., 2014; Singh et al., 2017). Monitoring using chemicals is considered potentially harmful to the environment (Kjellstrom et al., 2006; Pandey et al., 2014). Therefore, biomonitoring using biological organisms to collect data in specific aspects of the biosphere is now emerging as the sole solution.

In biomonitoring, the information is derived from analyzing specific substances within cells or observing alterations in the behaviour of the monitored organisms (Wolterbeek, 2002; Markert & Wunschmann, 2010; Zaghloul et al., 2020). Using bioindicators to monitor air pollution is an efficient

and cost-effective alternative to measure ambient air quality directly. This approach is particularly relevant when monitoring is to be done in extensive geographical areas (Ruhling & Tyler, 1968; Chakrabortty & Paratkar, 2006; Zaghloul et al., 2020) and allows an assessment of the total exposure over a specific time frame (Chakrabortty et al., 2006; Stefanuț et al., 2021).

Biomonitoring has significant advantages: it requires no costly sampling apparatus, and organisms are often used as biological monitors (Saxena et al., 2006). The concentrations in the monitored organisms are higher than in the system to be monitored, improving measurement accuracy. Many organisms reflect average external conditions over a specific period, which becomes a significant factor when monitoring levels exhibit rapid changes over time.

Ruhling and Tyler (1968) developed the idea of using moss as a biomonitor in the late 1960s. The simple idea behind this concept was that mosses, especially carpet-forming moss, take their nutrition from the ambient environment and atmospheric deposition. Mosses are non-vascular cryptophytes from the bryophyte group found in moist, damp, and shady places.

Mosses are considered an excellent biomonitor due to their ability to naturally acquire metals from both dry and wet depositions (Wilkie & La Farge, 2011; Ares et al., 2012; Cowden & Aherne, 2019; Swislowski et al., 2022). To monitor time-integrated bulk deposition of metals, particularly ectohydric mosses, have frequently been employed because they depend entirely on air for nutrient supply and take tiny amounts of water and minerals from the soil (Coskun et al., 2005; Boev et al., 2022).

Due to a weak cuticle and lack of a proper root system, moss works as a hyperaccumulator of metals and metal complexes within the plant system (Stankovic et al., 2018; Bargagli, 2016; Sabreena et al., 2022). Additionally, the presence of high levels of polyuronic acid in moss increases its high cation exchange capacity (Liu et al., 2022; Varela et al., 2023), and negligible translocation makes mosses able to absorb ions from a dilute solution (Kosior et al., 2020; Vergel et al., 2022). These properties make mosses efficient and sensitive integrators of atmospheric input. Mosses are also helpful for assessing pollution due to their capacity to absorb potentially hazardous substances. When airborne deposition takes place, initially, much of the accumulated metal is trapped in the form of particulate matter (Jiang et al., 2018; Swisłowski et al., 2022).

Since mosses primarily absorb nutrients from the surroundings, a correlation between the environment and the concentration of the element in moss samples has been discovered (Bettineli, 2002; Decker & Reski, 2020; Salemaa et al., 2020). Therefore, metal concentration in mosses is a valuable means of mapping metal deposition and finding airborne metal pollution.

Due to the ease of sampling and the lack of need for expensive technical equipment, mosses are a good biomonitor of atmospheric pollution (Saxena et al., 2006). Collecting moss from pollution-free background areas to highly polluted regions is easy and cost-effective. Collecting mosses in different weather, i.e., summer, winter, and rainy seasons, makes it possible to know the specific trace element pollution area. Obtaining a comprehensive understanding of temporal and spatial variations at a reasonable cost is highly challenging through alternative methods. Moss transplants, for instance, can effectively achieve this objective (Giordano, et al., 2005).

Chapter 2: REVIEW OF LITERATURE

In recent decades, pollution has become an increasingly evident problem, with its escalation primarily attributed to the developments and advancements of modern society. Consequently, the quality of the air has progressively deteriorated over time. The rising concentration of pollutants in the atmosphere can be attributed to several critical factors, including population growth, urban expansion, industrial activities, and vehicular emissions (Ghorani-Azam et al., 2016; Manisalidis et al., 2020; Gurjar, 2021).

Thermal power plants, steel manufacturing, cement production, petrochemical facilities, refineries, and mining operations are a few examples of industries that might be responsible for releasing significant amounts of pollutants into the atmosphere (Al-Mutairi et al., 2017; Kuttippurath et al., 2022).

Air pollution resulting from dust storms in desert regions and the emissions of smoke from forest and grass fires are beyond human control. This underscores air quality, which can be affected by various human activities and natural events. Pollution can originate in one country, while its repercussions may extend to other regions (Perera, 2018; Rissmann et al., 2020).

Air pollution may be stationary (manufacturing and chemical industries), mobile (transportation), agricultural sources (fertilizers and pesticides), and natural sources (volcanic eruption, forest and prairie fires, and dust storms) (Goyal, 2003; Perera, 2018; El Morabet, 2019). The transport sector alone consumes a quarter of all energy used in India, 98% of which is oil. Air pollution from this industry accounts for over half the total in many cities and may even go up to 80% under certain conditions (Guttikunda & Mohan, 2014).

In recent years, human intervention with the environment has risen in Uttarakhand due to rapid growth in tourism, construction projects, and other activities such as automobile emissions, fertilizer usage, garbage burning, and agricultural and sewage sludge dumping. These factors have significantly led to a rise in the concentration of environmental pollutants (Yarragunta et al., 2020; Gautam et al., 2021; Kumar et al., 2023). An increase in urbanization and agricultural activities negatively impacted the forest cover and the overall environment. Consequently, the forest area is reduced, which finally causes the degradation of the natural environment (Sawant et al., 2021; Joshi, 2021).

Previous studies have shown that roads have a range of negative impacts on their surrounding environments. These studies emphasize the need for extensive studies, particularly on heavy metals such as copper, iron, zinc, etc. (Lepneva et al., 1987; Pagotto et al., 2001; Adnan et al., 2022). Metal pollution adversely affects the ecosystem of flora, fauna, and other non-living components, resulting

in undesirable alterations and metabolic disruptions. These consequences often pose significant risks to human health and the environment (Hermann, 1990). Therefore, there is a critical need to establish widespread and robust monitoring networks for pollutant metals, enabling the development of strategies to address and mitigate these issues effectively (Hodson, 2004).

2.1 BIOMONITORING OF HEAVY METALS

Biological monitoring, or biomonitoring, can be broadly described as utilizing biological organisms and materials to acquire quantitative data about specific qualities of the biosphere (Wolterbeek, 2002; Cuny, 2012; Badamasi, 2017). A biomonitor should retain contaminants for an extended period in their tissues. Several workers previously considered various factors such as occurrence, specificity, species richness, accumulation ratio, and biodiversity when choosing biomonitoring species (Wolterbeek & Bode, 1995; Wolterbeek, 2002; Stefanuţ et al., 2018).

In biomonitoring, living organisms at various environmental or ecosystem levels have been evaluated, including ecological communities, populations, individuals, tissues, and cells (Markert, 1993; Cuny, 2012; Tiwari & Agarwal, 2022). This comprehensive approach allowed a direct primary assessment of the health of the ecosystem by providing information on the bioavailability of the contaminant. This method simplified chemical analysis by eliminating the problem of assessing traces of contaminants and eliminating the risk of misinterpretation caused by sudden changes in environmental parameters during sampling (Grodzinska et al., 1999; Reimann et al., 2001; Conti, 2008).

2.2 TYPES OF BIOMONITORING

Biomonitoring offers valuable insights that can complement the monitoring and modelling of air pollution near the emission source. Developing assessment criteria for biomonitoring data through objectively evaluating existing information is essential to establish a foundation for these programs. Additionally, the presentation scheme should be both suggestive and readily comprehensible, even for individuals without specialized knowledge (Sloof, 1993). Assessment scales are formulated for plant biomonitoring based on the comprehensive assessment of various monitoring programs. These scales also lay the groundwork for the spatial representation of monitoring (Kosta-Rick et al., 2001; Steinnes et al., 2003). Biomonitoring is of two types: passive and active monitoring.

2.2.1 PASSIVE BIOMONITORING

This method allows for the comprehensive analysis of the chemical properties of research sites, entire regions, and indigenous mosses to provide dependable insights into regional variations in airborne metal contamination (Kauss & Hamdy, 1985; Chaphekar, 1991). Numerous studies have

primarily used the passive or native method to assess the effectiveness of metal absorption from precipitation by moss (Ruhling et al., 1987, 1992; Ruhling, 1994; Słonina et al., 2021; Chaudhuri & Roy, 2024). Numerous extensive surveys have been employed to convert the concentrations obtained from biomonitors into absolute deposition values to gain a deeper understanding of metal deposition.

2.2.2 ACTIVE BIOMONITORING

Active monitoring involves using native moss to investigate a more extensive area by relocating it from other sites. Chaudhary and Roy (2024) state that active biomonitoring is employed for studies encompassing extensive regions (national or regional) as well as smaller areas (industrial or urban areas). This technique, known as the "Moss bag," was initially introduced by Goodman and Roberts (1972) and subsequently adapted by Little and Martin (1974).

According to Haseloff (1982), active biomonitoring techniques can be categorized into three types: (i) transplantation (plants are moved to a new location), (ii) test plant (involves using specific plant species to monitor pollution), and (iii) test chamber (where plants are exposed to controlled environments). In transplantation, appropriate organisms, primarily moss or lichen, are relocated from unpolluted to polluted areas (Tyler, 1990; Falla et al., 2000).

2.3 MOSS AS BIOMONITOR

Mosses are classified under the division Bryophyta in the plant kingdom. Among cryptogams, these have shown significant success in their potential application as monitors for heavy metal air quality (Saxena et al., 2014; Mahapatra et al., 2019; Gahtori et al., 2024). Through their capacity to intercept, retain, and accumulate contaminants, Ruhling and Tyler (1971) and Goodman and Roberts (1971) used mosses for the first time to monitor heavy metals in the atmosphere. Later on, these were used worldwide for ecological monitoring.

When aerial deposition occurs, a significant portion is initially trapped as particulate matter (Fernandez & Carballeira, 2002). Mosses take up nutrients mainly through their surface from their surroundings (Decker & Reski, 2020); thus, a correlation can be established between element level and environment (Adamo, 2003). Therefore, the metal concentration in mosses can identify airborne metal pollution (Fernandez et al., 2004).

2.3.1 MECHANISM OF METAL ACCUMULATION AND FACTORS AFFECTING BIOMONITORING PROCESS

Atmospheric metal particles can be absorbed by the moss as liquid solutes, mixed with gas, or

adhered to particles. After depositing the atmospheric particles on the moss surface, the absorption occurs through entrapment on the cell surface and attachment to the outermost cell wall through an ion exchange mechanism via diffusion and transport channels or proteins to intercellular spaces (Brown and Bates, 1990). The ion exchange mechanism is defined by the number of protons that can be exchanged with metal ions binding to the tissue (Soudzilovskaia et al., 2010). The absorption of metal, based upon the nature of the metal as well as the cations present at exchange sites that can either interfere with or catalyse the metal uptake (Rühling and Taylor, 1970). Mosses also possess polygalacturonic acid, functional groups like amine, phosphodiester, etc, and negatively charged groups like carboxyl and phosphoryl in their cell wall, which catalyse cation ion exchange (Wiersma et al., 1990; Popper et al., 2003). Metallic ions attach to these functional groups through chelation. The high counter-gradient of mosses smoothly facilitates the entry of ions into their system (Shakya et al., 2008). Literature suggests that even though mosses accumulate through both wet and dry deposition, accumulation through wet deposition is much higher compared to dry deposition. Wet deposition of metals into moss is influenced by the amount of precipitation and duration of precipitation (Berg et al., 1995).

Table 2.1: Some commonly used mosses for biomonitoring programs

S. No.	Moss	Heavy Metal(s)	References
1.	*Haplocladium angustifolium., H. microphyllum, Hypnum cupressiforme, Pleurozium schreberi, and Pseudocleropodium purum*	Zn, Pb, Cr, Cu, Cd, Ag, Co, As, Mn, Mo, Ni, and V	Jiang et al., 2018, 2020
2.	*Pleurosium shreberi*	Zn, Fe, Ni, Cu, Cr, Pb, Hg, and Cd	Yushin et al., 2020; Swislowski et al. 2021
3.	*Barbula constricta*	Zn, Pb, and Cu	Srivastava et al. 2014
4.	*Rhodobryum giganteum*	Zn, Pb, Cd, and Cu	Singh et al., 2017
5.	*Barbulalam barenensis, Hyophilainvoluta, Thuidiumgratum, Octoblepharum albidium* and *Calympere safzelii*	Pb, Cu, Zn, Fe, Cd, and Cr	Ojo et al., 2012

6.	*Hypnum cupressiforme*	As, Cd, Co, Cr, Cu, Fe, Hg, Ni, Pb, and Zn	Lazo et al. 2022
7.	*Rhacocarpus purpurascens*, *Sphagnum* sp. and *Thuidium delicatulum*	Al, Fe, Mn, Pb and Zn	Benitez et al. 2021
8.	*Racomitrium lanuginosum*, *Hylocomium splendens*, *Pseudocalliergon Brevifolium*	As, Cd, Cr, Cu, Ni, Zn, and Pb	Wilkie and Farge, 2018
9.	*Hypnum cupressiforme*	Al, As, V, Ni, Fe, Cr, Zn	Betsou et al., 2019
10.	*Grimmia pulvinata*	Cd	Vieille et al., 2021
11.	*Sphagnum girgensohnii*	Na, Mg, Al, Cl, K, Ca, Sc, V, Cr, Mn, Fe, Co, Ni, Zn, Se, As, Br, Rb, Mo, Sr, Sb, Ba, Cs, La, Sm, Tb, Ce, Hf, Ta, W, Th, and U	Shvetsova et al., 2019
12.	*Hypnum cupressiforme*	Zn, Cd, Pb, and Cu	Saxena et al. 2008
13.	*Racomitrium crispulum*	Zn, Cd , Pb, and Cu	Saxena and Afreen, 2009

2.4 ADVANTAGE OF MOSS AS A GOOD BIOMONITOR

Moss-based monitoring is a cost-effective method that utilizes both passive and active receptors. This approach integrates temporal and spatial effects and bioavailability, comprehensively assessing contamination from both pathways. The significant advantages of using moss as a biomonitor are as follows:

- Moss lacks cuticles, protective waxy surfaces, and water-conducting systems (Ruhling & Tyler, 1973; Budke & Goffinet, 2016).
- Roots are absent, and rhizoids do not perform absorption functions. Therefore, bryophytes draw minerals from atmospheric precipitations (Tyler, 1990; Nordstrom, 2019).
- Mosses are perennial and evergreen plants; researchers can study them all year round, which facilitates tracking the temporal variations in metal profiles (Dołęgowska & Migaszewski,

2014).

- Mosses contain phenolic compounds, which help in the preservation or slow degeneration of tissues (Bansal et al., 2024).
- Mosses are good bio-accumulators of metals even when pollutants are present at low levels (Steinnes, 1995).
- Mosses respond quickly to environmental changes (Wolterbeek & Bode, 1995).
- Biomonitoring with mosses is an easy and cheap method to detect the possible sources of heavy metals (Onianwa, 2001; Ding et al., 2024).
- They are excellent tools used for pollution biomonitoring (Zechmeister et al., 2003).
- They have a rapid absorption rate due to their high cation exchange capacity (Rippy et al., 2005).
- They have insecticidal and antimicrobial properties, which protect them from insects and microorganisms. Insects cannot chew mosses and remain intact (Subramoniam & Subhisha, 2005).

2.5 SELECTION OF SPECIES

The selection of moss species in biomonitoring studies is an essential step. While selecting the species, the primary factors taken into consideration are widespread geographical distribution, survival in extreme weather and highly polluted regions, growing habits throughout the year, sampling ease, accumulation factors, and background values of nearly the same age (Sloof et al., 1991; Markert, 1993). Another vital criterion is availability in the area of interest, uptake of atmospheric nutrients only, uptake of elements unaffected by local conditions, known mechanisms of elemental uptake, and low background concentrations (Chakrabortty & Paratkar, 2006).

2.6 NATIONAL AND MULTINATIONAL SURVEYS BY MOSSES

2.6.1 INTERNATIONAL

For the investigation of metal concentrations across a wide range of geographical areas, mosses have already been used (Rhuling et al., 1984; Markert & Weckert, 1989; Ross, 1990; Steinnes, 1993; Herpin et al., 1996; Markert et al., 2003). At the beginning of the 70s (Ruhling, 1994), mosses were used in many European countries for the atmospheric monitoring program to monitor local (Giordano et al., 2005) and regional (Fernandez & Carballeira, 2002) sites.

During the 1980s–1990s, several workers also conducted national surveys to assess atmospheric fallout (Faus-Kessler et al., 1999; Grodsinzska & Szarek-Lukaszewska, 2001). Otvos et al. (2003) initiated the first nationwide study on atmospheric metal deposition in Hungary by analysing moss. In Galicia (NW Spain), Fernandez et al. (2005) surveyed five mosses by sampling.

Temporal and spatial comparisons based on global surveys revealed the efficiency of moss as a valuable biological tool for long-term and large-scale monitoring. In Europe, the use of native moss populations for detection and tracking geographical patterns in atmospheric heavy metal pollution is well-established. Rasmussen et al. (1988) used moss analysis in a joint Nordic project in many European countries.

Since 1990, The International Cooperative Programme (ICP) on the effects of air pollution on Europe routinely evaluated atmospheric moss deposition after an interval of every five years. In April 2020, the latest report on ICP Vegetation was published for a study done during 2015-16 at 5100 sites across 28 countries across Europe and beyond (Frontasyeva et al., 2020).

TABLE 2.2: A HISTORICAL OVERVIEW OF EUROPEAN MOSS BIOMONITORING SURVEYS

Year	Surveys	Coordinator
1968	The Moss technique was initially introduced.	Ruhling and Tyler
1975	An initial comprehensive survey conducted across Sweden	Ruhling
1977	An initial comprehensive survey conducted across Norway	Steinnes
1985	Initial collaborative Nordic Survey conducted in Denmark, Finland, Norway, and Sweden	Rühling (supported by the Nordic Council of Ministers)
1990	The initial European survey, known as the Joint Nordic/Baltic survey	Rühling (Lund University, Sweden)
1995	A survey conducted in 28 European countries	Rühling and Steinnes
2000	The third survey (28 countries)	Buse A. (ICP Vegetation, UK)
2005	The fourth survey (28 countries)	Harmens, H. (ICPVegetation, UK)
2010	The fifth survey (27 countries)	Harmens H.
2015	Sixth European survey (36 countries)	Harmens, H. and Frontasyeva M., (JINR, Russian Federation)

(Source: *Frontasyeva* et al., 2020)

2.6.2 NATIONAL

At Shillong, India, Gupta (1995) initiated moss biomonitoring by examining the accumulation of Cd, Cu, Mg, Pb, and Zn in the moss species *Bryum argenteum*, *Plagiothecium denticulatum*, and *Sphagnum* sp. Saxena et al. (2000) transplanted and analyzed metal deposition near a petrol pump using the moss *Sphagnum cuspidatum.* Using the moss bags technique, Saxena et al. (2007) used *Rhodobryum roseum* and *Barbula vinealis* to monitor metal precipitation at Nainital during 2004-2005. Saxena et al. (2008) did a retrospective study of the environmental metal data of the past 100 years by examining herbarium voucher specimens of *Barbula* sp. Vats et al. (2010) analyzed eight different metals with the help of atomic absorption spectroscopy using moss species, *Barbula constricta* and *Physcomitrium cyathicarpum*. Srivastava et al. (2014) applied the moss *Barbula constricted* J. Linn. in Mussoorie City, Uttarakhand, India, to quantify the metal deposition of lead, copper, zinc, and cadmium in the atmosphere. Using mosses, Singh et al. (2017) employed a passive biomonitoring technique to examine the seasonal/annual trend in the Kumaon and Garhwal regions of Uttarakhand, India. On recent changes in air quality, Joshi & Afroz (2023) used a passive biomonitoring technique with moss *Sphagnum* sp. in Nainital, Bhimtal, and Mangoli region of Uttarakhand, India.

2.7 IMPACT OF SEASONAL VARIATION AND DISTANCE ON METAL POLLUTION

Moss displays distinct variations in metal data, reflecting seasonal fluctuations. Significant fluctuations in the concentration of heavy metals throughout the year using mosses have been documented by Markert and Weckert (1989). Based on empirical evidence, variations in metal concentrations have been documented in mosses during different seasons, and prominent researchers in this field have also elucidated the contributing factors (Gerdolet al., 2002; Pavlikova et al., 2021). Across Europe, a biomonitoring study was conducted by Fernandez and Carballeira (2002) and Rajfur et al. (2024) during all seasons and found that metal concentration fluctuations within moss samples throughout the year.

Several researchers have reported a rapid decrease in concentrations of elements emitted from localized sources as the distance increases from the source. These findings have been established by examining the correlation between proximity to the emitting source and metal bioaccumulation (Genoni et al., 2000; Gao et al., 2022).

Complex atmospheric process and their interactions with weather factors have been mainly attributed to the variations in measured concentrations over time. Daily, short-term fluctuations in pollutant levels are led by the daily shifts in routes of atmospheric transport combined with changing

dispersion. While these fluctuations can be quite wide-ranging, consistent seasonal patterns recur throughout the year.

2.8 SENSITIVITY OF MOSSES

Numerous research studies have evaluated mosses to compare with other pollution indicators, including lichens, grass, vascular plants, topsoil, and plant litter, to assess their capability to mirror pollution gradients and their respective capacities for accumulating pollutants in various regions. Many of these studies revealed that mosses exhibit greater sensitivity than lichens and others (Roos et al., 1994; Jafarova et al., 2023).

Some researchers observed that mosses could accumulate more metals on average than topsoil (Ojo et al., 2012). Similarly, mosses have been compared with parts of vascular plants and found to be more efficient accumulators (Ruhling & Tyler, 1968; Sienkiewicz & Czarnowska, 1994; Turkan et al., 1995; Onianwa, 2001).

2.9 TAXONOMY OF MOSS

Mosses are essential to any forest ecosystem (Turetsky et al., 2010; Eldridge et al., 2023). A rich diversity and abundance of mosses are found in the northern Himalayan region of India (Pande, 1958; Gangulee, 1969). Genus *Thuidium* belongs to the division Bryophyta, representing the class Bryopsida and order Hypnales of the Family Thuidiaceae. By far, most of these mosses are earth forms, although a few occupy rocks (Gangulee, 1969; Chopra, 1975). Usually, they grow on rocks, logs, forest soil, and stream banks (Tan et al., 2006).

2.10 IMPACT OF ENVIRONMENTAL STRESSES ON MOSS PHYSIOLOGY

The stress of air pollution is responsible for a change in the moss physiology and decreases pigment concentration (Sujetoviene & Galinyte, 2016; Uka et al., 2021). A study conducted by Hajek et al. (2014) and Meng et al. (2021) revealed that mosses exposed to pollution exhibited a notable reduction in several physiological parameters and depleted levels of crucial elements, including nitrogen, phosphorus, and potassium. Mandal and Mukherjee (2000) investigated the impact of prolonged exposure to automobile exhaust on photosynthetic CO_2 absorption, chlorophyll content, and starch and sugar levels in five plants cultivated along the highway edge.

The study conducted by Saxena and Arfeen (2006) revealed a notable decrease in chlorophyll content, carbohydrate, protein, nitrogen, and other metabolic activities in moss treated with heavy metals. Saxena & Saxena (2002) showed that due to exceptionally high metal detoxification

capability, *Spagnum* moss could tolerate elevated levels of metal precipitation. Variations in chlorophyll content and changes in pigment ratios served as significant indicators of environmental stress. Prior research has shown that these parameters offer valuable information on the tolerance levels of the species (Tuba, 1987; Tuba, et al., 1996). In the tolerant mosses, the overall chlorophyll content is minimally affected by the short exposure.

2.11 IMPACT OF ENVIRONMENTAL STRESSES ON THE ANTIOXIDANT DEFENSE SYSTEM OF PLANTS

Copper (Cu), zinc (Zn), cadmium (Cd), and lead (Pb) are heavy metals that suppress plant growth by inhibiting the function of nitrate reductase, an essential enzyme for nitrogen absorption (Singh et al., 2016). Under stress conditions, the plant generates reactive oxygen species (ROS). ROS-induced damage to plant cells. Plants possess antioxidant enzymes such as superoxide dismutase (SOD) and peroxidase (POD) which neutralize reactive oxygen species (ROS) and protect against damages caused by pollutants (Hasanuzzaman et al., 2020).

Metals such as Pb, Zn, Cd, and Cu are naturally present in higher environmental concentrations and can be phytotoxic when they reach excessive levels (L'Huiller et al., 1996). Enzyme nitrate reductase helps in primary metabolism and, for its catalytic activity, exhibits a complex regulation mechanism (Viegas & Silveira, 2002). Mosses exploit a highly efficient counter-gradient mechanism, accumulating substantial amounts of metals in their tissues (Cardinale et al., 2004).

Chapter 3: HYPOTHESIS

Conventional monitoring requires equipment, continuous manpower, and uninterrupted power supply, which is generally associated with high costs (Biomonitoring using Indigenous mosses is a cost-effective, self-sustainable, and nil or low maintenance tool for measuring atmospheric elemental precipitation)

Regular monitoring of atmospheric precipitation is chosen to provide information on the absolute magnitude of atmospheric deposition at selected sites.

Monitoring with plants is readily applicable throughout the year and everywhere without much preliminary preparation and involvement of instruments. One may be passive, which occurs naturally in the study areas, and another is an active biomonitor, in which the organisms are brought into the study areas for specific periods to know the trend and intensity.

It continuously gives a comprehensive overview of air pollution levels and can be utilized to assess and regulate the effectiveness of environmental policies.

Chapter 4: OBJECTIVE

1. Seasonal field survey of Kumaon for measuring bryocover, metadata and screening the tolerance bryophyte species.
2. Selection of tolerant moss after screening their physiological and other parameter.
3. Biomapping of metal precipitations on seasonal and annual bases by native and transplant bryophytes on different sites of Kumaon hills.
4. To study the seasonal variation of metal concentration levels and their precipitation.

Chapter 5: METHODOLOGY

5.1 STUDY AREA

Uttarakhand is geographically divided into two principal divisions, namely Kumaon and Garhwal. The Kumaon division is adjacent to Tibet and Nepal in the foothills of the Himalayas. Six districts comprise the Kumaon division: Almora, Bageshwar, Nainital, Champawat, Pithoragarh, and Udham Singh Nagar. Based on the 2011 census, the population of Kumaon is approximately 2.9 million, with a population density of 170 individuals per square kilometre. The area features elevated Himalayan foothills laden with pine forests. Indeed, urban areas make up 75% of the population of Kumaon (Negi & Bisht, 2018). During summer, the average temperature reaches 40°C, while in winter it drops much below freezing conditions to -2.9°C. The recorded mean precipitation is 1644 millimetres (Figure 5.1a).

Figure 5.1a. Map of Uttarakhand

A total of eight study sites, viz. Champawat, Lohaghat, Khetikhan, and Barakote from district Champawat and Pithoragarh, Ghat, Thal, and Munsiyari from district Pithoragarh, were selected for the proposed study. These sites are popular tourist destinations as well as hub for local economic activities.

5.1.1 DISTRICT CHAMPAWAT

Champawat (29.2783°N, 80.0535°E) is the eastern district of Uttarakhand. Its northern boundary is demarcated by Pithoragarh district, its eastern boundary by Nepal, its southern boundary by Udham Singh Nagar, its western boundary by Nainital, and its northwest boundary by Almora district. The district covers a total area of 1766 km^2. According to the census, the district's population in 2011 was 2,59,648. The annual mean temperature in Champawat is 24.6-35°C. The warmest month is June, with an average temperature of 32.1-45°C. January is the coldest month, with an average temperature of 8-20°C (Figure 5.1b).

The Champawat district is defined by its diverse geography, featuring expansive valleys, mountain ranges, cliffs, and numerous rivers and streams. Approximately 65% of the district is covered with dense forests, while the remaining 35% is used for grazing, agriculture, and other non-agricultural purposes. The plains host exotic and native vegetation, including *Madar*, *Babool*, *Teak*, *Eucalyptus*, *Jamun*, and others.

Champawat district in Uttarakhand is primarily an agricultural area with a significant portion of the workforce engaged in cultivation and agriculture-related activities. While the industrial sector is present, it's not as dominant as agriculture. The district has a few key industrial sectors.

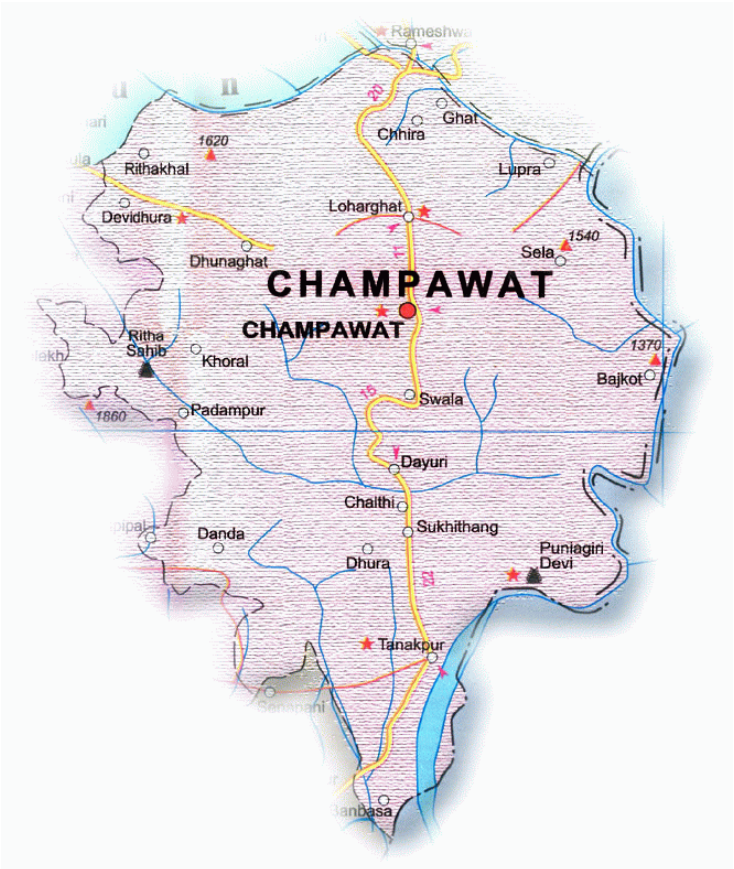

Figure 5.1b: Map of District Champawat.

5.1.1.1 CHAMPAWAT

Located at 1670 meters above sea level, Champawat is one of the easternmost towns in Uttarakhand. The region is famous for its picturesque natural beauty, variety of flora and fauna, and beautifully carved and constructed ancient temples. Large valleys, landscapes, mountain ranges, cliffs, and important rivers and rivulets form the geography of Champawat.

Altitude	:	1670 m. asl
Temperature	:	4°C – 35°C
Best Season	:	Round the year.

5.1.1.2 LOHAGHAT

Lohaghat is the town, and *Nagar Palika* is in the Champawat district. The place is well-known for its numerous cultural celebrations, such as *Devidhar Mela* and *Holi Rang Mahotsav*, is Lohaghat. The *Ramleela* of Lohaghat, one of the oldest in the Kumaon division, is the most unique feature of the area.

Altitude	:	1706 m. asl
Temperature	:	1.6°C – 36°C
Best Season	:	Round the year.

5.1.1.3 KHETIKHAN

The Khetikhan village is fortunate to have a beautiful view of the enormous pine forests and the snow-covered Himalayas. Raising cattle and farming are major sources of income for the economy. Since most men have moved to the cities for employment, the women of Khetikhan are responsible for agriculture, cattle rearing, and household chores.

Altitude	:	1815 m. asl
Temperature	:	-2°C – 29°C
Best Season	:	Round the year.

5.1.1.4 BARAKOTE

Barakote is a mid-size village in the Champawat district. It is 14 km from the sub-district headquarters in Lohaghat (the tehsildar office). According to the 2011 census, the population of Barakot is 1,122. The village's economy is based on cattle farming and agriculture.

Altitude	:	1600 m. asl
Temperature	:	2°C – 31°C
Best Season	:	Round the year.

5.1.2 DISTRICT PITHORAGARH

The district of Pithoragarh (30°00′N 80°20′E) is located in the easternmost region of Uttarakhand. It comprises approximately 13.29% of the state's territory and is home to 4.80% of its population. It ranks as the eighth most densely populated district in the state. The entire district is characterized by extensive mountainous terrain and experiences various climatic conditions, ranging from moderately warm during the summer to highly frigid winters. The higher areas of the district adjacent to Tibet/China experience year-round snow cover, while the meadows sustain snow for six months annually. Most of the district experiences winter snowfall and monsoon rainfall. Pithoragarh district has a rich ecological landscape with diverse flora and fauna. The district's vegetation includes various Bryophytes, Pteridophytes, Gymnosperms, Angiosperms, and rare orchid species at higher altitudes. Sal forests dominate the river valleys, and as the elevation increases, these are gradually replaced by pine forests. (Figure 5.1c).

Pithoragarh's industry is primarily driven by agriculture and tourism, with a focus on local produce and handicrafts. The district also has a growing tourism sector, particularly related to trekking, wildlife viewing, and cultural attractions.

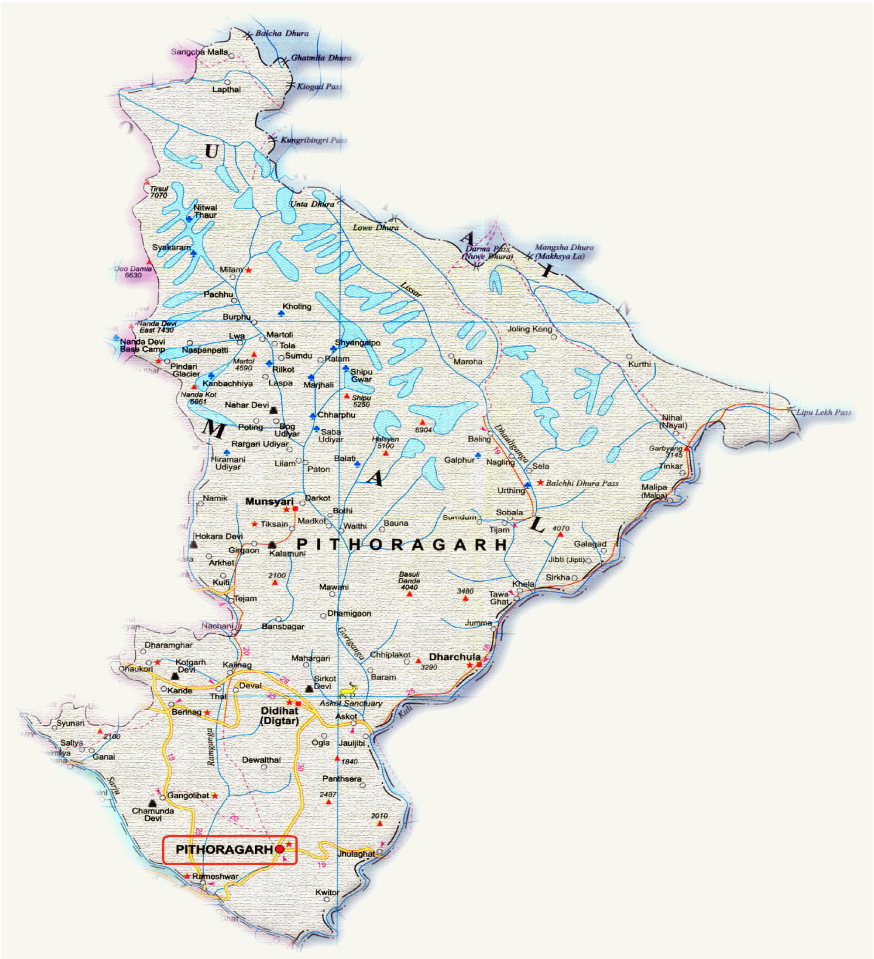

Figure 5.1c: Map of District Pithoragarh

5.1.2.1 PITHORAGARH

Pithoragarh, a renowned hill station in Uttarakhand, is currently the subject of significant tourist interest. The state provides opportunities for tourists to appreciate natural landscapes and engage in a range of adventurous activities, including white river rafting, hang-gliding, and skiing.

Altitude	:	1851 m. asl
Temperature	:	4°C – 31°C
Best Season	:	Round the year.

5.1.2.2 GHAT

Ghat is the junction of three districts: Pithoragarh, Champawat, and Almora. Topographically, it is a deep valley situated next to the *Saryu* River. The village's economy is based on cattle farming, agriculture, and local shops.

Altitude	:	633 m. asl
Temperature	:	8°C – 40°C
Best Season	:	Round the year.

5.1.2.3 THAL

Thal is a small town in the district of Pithoragarh, located on the banks of the Ramganga River. Thal town serves as a hub for regional trade with neighboring communities. Before traveling back to Tibet, *Bhotiya* traders traditionally frequented the Thal market to sell wool and utensils. The market also saw the exchange of garments from major cities and oil and chili products from *Sira* and *Sor.* A market was established in Thal under the *Mandi Parishad* scheme to support local farmers producing fruits, vegetables, and grains from nearby villages.

Altitude	:	800 m. asl
Temperature	:	9°C – 35°C
Best Season	:	Round the year.

5.1.2.4 MUNSIYARI

Munsiyari is an exquisite village in the Pithoragarh district, surrounded by the snow-capped peaks of the Himalayas. It offers stunning vistas of the natural landscape. The economy predominantly relies on tourism, subsistence agriculture, livestock farming, and associated industries. Numerous families depend on forests and other natural resources for their sustenance.

Altitude	:	2298 m. asl
Temperature	:	4°C – 31°C

Best Season : Round the year.

5.2 FIELD SAMPLING

5.2.1 SAMPLE COLLECTION

The three-month periodic survey, which represented one season, was done in sites located near the urban, suburban, and rural areas of the districts of Champawat and Pithoragarh. During sample collection, plastic gloves or a plastic bag over the hand were used. Adhering foreign materials, including the bark of the trees, lichen, dust and debris, were extensively eliminated from the samples in dry conditions. Only greenish and brown green parts of the moss were used.

5.2.2 CLEANING AND DRYING OF MOSS SAMPLES

After collecting the moss, any unnecessary parts were thoroughly eliminated to ensure it was contamination-free (Saxena & Saxena, 2000). The moss was then thoroughly rinsed with water to eliminate undesirable substances, followed by the final washing with distilled water. Finally, the moss was dried to a consistent mass at a temperature range of 30−35°C, which served as a reference for the calculations.

5.2.3 MAINTENANCE OF MOSS

Moss samples were maintained in the B.O.D. incubator. The chamber was well maintained with temperature, light, humidity, and moisture control devices to provide bryophytes a natural habitat and growth environment.

5.3 THE CONTROL SITE

The control moss was obtained from the forest core, which is considered the least impacted by human activity and, hence, not as affected by contamination. A collection of moss was obtained from the forests of Kranteshwar (29°18'22 N, 80°07'50 E) and Mayawati (29°22'18 N, 80°03'48 E) in the Champawat district, as well as from Chandak (29°36'44 N, 80°11'54 E) and Thalkedar (29°31'52 N, 80°14'20 E) in the Pithoragarh district.

5.4 MOSS SAMPLING

5.4.1 QUADRATE SAMPLING

Counting individual plants within a given population is extremely laborious and time-consuming. To study such a population, the area was divided into distinct, non-overlapping sampling

units (Temple, *et al.,* 1981). Five macro plots of 10 × 10 m were randomly selected from the central part of each control site of the forest. Five 40 cm × 40 cm quadrats were placed in different habitats within these macroplots. The quantitative data is presented as percentage cover. The dominance of bryophyte species was measured from the control site by calculating the importance value. The frequency, relative frequency, relative cover, and importance values were also calculated as follows (Jiang et al., 2011):

$$\text{Frequency (F) \%} = \frac{\text{Number of quadrats in which the species is present}}{\text{Total number of quadrats surveyed}} X\ 100$$

$$\text{Relative Frequency (Fr) \%} = \frac{\text{Frequency of a specific species}}{\text{Total frequency of all species}} X\ 100$$

$$\text{Relative Cover (Cr) \%} = \frac{\text{Average cover of a specific species}}{\text{Sum of average cover of all Species}} X\ 100$$

Importance Value (IV)%= Relative Frequency+Relative Density+Relative Abundance

$$\text{Relative Frequency (Fr) \%} = \frac{\text{Frequency of certain Species}}{\text{Sum of frequencies of allSpecies}} X\ 100$$

Frequency classes were categorized based on Raunkiaer's law as follows: Class A (0–20%), Class B (21–40%), Class C (41–60%), Class D (61–80%), and Class E (81–100%). Alpha diversity refers to the variety of species present within a specific site. The Shannon-Wiener index was employed to quantitatively assess and describe the diversity of moss species in the area (Magurran, 2003).

$$H' = -\sum pi\ ln\ pi$$

Here,

H' = Shannon-Weiner

pi = Proportional abundance of i^{th} species= (ni/N)

5.4.2 METEOROLOGICAL DATA OF STUDY SITES

Light parameters were taken with a light meter (Gossen, Germany, model no. SLM-110) and an infrared thermometer (Testo, 830 T2). Moisture was measured by a moisture meter (Korean-made), and air current was measured with an anemometer (F. W. Dwyer manufacturing company, Michigan City, U.S.A., model no. DEMPLO—01). Meteorological data were also collected from the satellite weather stations of ICAR-VPKAS, Almora, and G.B. Pant Horticulture Research Center.

5.5 PHYSIOLOGICAL TOLERANCE

SAMPLE PREPARATION

An initial field survey led to the selection of mosses for the tolerance study. Samples were obtained from the control location. To prevent dehydration-induced ultrastructural changes in cells, the collected moss samples were transported to the laboratory in polyethene bags and meticulously cleaned by removing small stones, soil, and dead remains (Ascaso & Galvan, 1976). Regular spraying with tap water at room temperature (about 25±2°C) was used to maintain the cultures in moist conditions. Before initiating heavy metal treatments, the samples were placed onto sterile Petri dishes filled with 10 mL of distilled water at room temperature. They were then allowed to acclimate under a 12:12-hour light-dark photoperiod for 3 to 5 days (Shakya et al., 2008).

SAMPLE TREATMENT

Fresh moss samples, approximately 5 g each, were treated by immersing them for 15 minutes in 500 ml solution of $CuCl_2$, $ZnCl_2$, $Pb(NO_3)_2$, and $CdCl_2$ at varying concentrations. For the control group, 5 g of each moss sample was immersed in double-deionized water for the same duration. Data collection occurred at 7-day and 15-day intervals. Each experimental treatment was conducted in triplicate. After treatment, the moss samples were rinsed three times with double-deionized water to remove any residual solution. The samples were then air-dried at room temperature until they reached a constant weight, ensuring consistency in measurement.

5.5.1 ESTIMATION OF CHLOROPHYLL AND TOTAL CHLOROPHYLL

Chlorophyll and total chlorophyll content were calculated using the method of Well & Allen, (1994) and Arnon, (1949). Pigments were extracted using 80% acetone under cold conditions. Fresh samples (0.5 g) were ground in a mortar with a known volume of acetone. The mixture was then filtered and centrifuged at 5000 rpm for 10 minutes. The absorbance of the resulting supernatant was measured at 663 nm and 645 nm, using acetone as a blank. The following formula estimated the amount of chlorophyll:

$$Chl - a = \left[(12.7\ X\ OD_{663} - 2.69\ X\ OD_{645})X\ \frac{V}{1000\ X\ w}\right] X\ 2$$

$$Chl - b = \left[(22.9\ X\ OD_{645} - 4.68\ X\ OD_{663})\ X\ \frac{V}{1000\ X\ w}\right]\ X\ 2$$

$$Total\quad Chlorophyll\ (mg/gmFW) = \left[\left(\frac{OD_{652}x1000}{34.5}\right)x\ \frac{V}{1000xw}\right]x2$$

where,

Chlorophyll content = mg/g fresh weight

V = acetone volume (ml)

W= weight of sample (gm)

5.5.2 NITRATE REDUCTASE ENZYME ACTIVITY

The analysis of nitrate reductase enzyme activity in plants followed the methodology outlined by Srivastava (1975) and Shankar et al. (2000). A fresh 0.5 g sample was placed in 20 ml black vials containing 8 ml of 0.1 M sodium phosphate buffer (pH 7.4), 1 ml of 0.2 M KNO_3, and 1 ml of 25% propanol. The vials were sealed and incubated in the dark for 30 minutes at 30°C. The enzyme activity was calculated by measuring the nitrite released in the mixture, which was assessed through a colorimetric reaction. After the assay, 1 ml of the incubation mixture was added to a test tube with 1 ml of 1N HCl and 1 ml of 0.2% N-(1-naphthyl) ethylenediamine dihydrochloride (NED). After a 20-minute reaction period, absorbance was assessed at 540 nm using a spectrophotometer. The nitrate content was expressed as millimole NO_2^- hr^{-1} gm^{-1} of fresh weight (FW).

5.5.3 PEROXIDASE ENZYME ACTIVITY

Peroxidase enzyme activity in moss was assessed following the methodology of Putter (1974) and Van Assche and Clijsters (1990). Enzyme extraction was done in a cold environment using 0.1 M sodium phosphate buffer (pH 7.4). The extract was centrifuged at 5000 rpm for 10 minutes, and the supernatant was collected as the enzyme source. The assay mixture included 1 ml of 0.1 M sodium phosphate buffer (pH 7.4), 1 ml of guaiacol, 2 ml of distilled water, and 1 ml of enzyme extract. The reaction was initiated by adding a drop of 3% hydrogen peroxide (H_2O_2), and absorbance was measured at 470 nm using a spectrophotometer at 15-second intervals until an increase in absorbance was observed. Enzyme activity was expressed as the change in optical density (ΔOD) $min^{-1}gm^{-1}$ of fresh weight (FW), calculated by noting the difference in absorbance over a 1-minute interval.

5.6 MOSS BAG PREPARATION AND TRANSPLANT

To prepare moss bags, 100 g of moss was thoroughly cleaned and placed into nylon bags with mesh dimensions of 16 × 16 cm and 2 mm (Ares et al., 2012). These bags were then deployed at various locations within the study area for active biomonitoring. For the deployment, moss bags were positioned at least 6 feet above the ground and were distributed in all four directions from the city center. Care was taken to ensure the bags were not placed under tree canopies (Saxena & Saxena, 2000). Each site was monitored for meteorological data, and the moss bags were retrieved during the

first week of March (for winter data, representing November to February), the first week of July (for summer data, representing March to June), and in November (for monsoon data, representing July to October). The collected bags were then transported to the laboratory for further analysis.

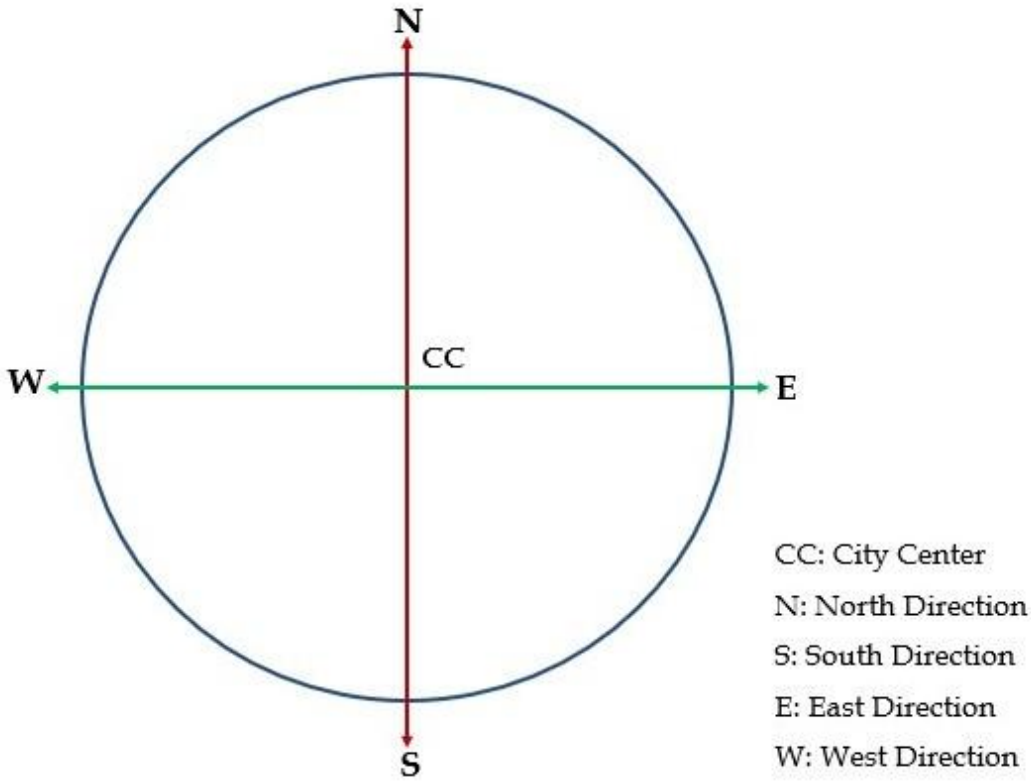

Figure 5.1d: General Scheme Plan for Monitoring.

5.7 ESTIMATION OF METALS

5.7.1 PLANT METAL ANALYSIS

Before analysis, the moss samples were cleaned to eliminate soil particles, dust, and other plant debris without washing the transplants (Barman, 1980) and dried at 70°C. 1 g of the dried material was digested using 5 ml of concentrated nitric acid (HNO_3) and 2 ml of perchloric acid ($HClO_4$). After digestion, the samples were filtered using Whatman No. 42 filter paper, and the filtrate was diluted to 50 ml using bi-distilled water. The resulting solution was analyzed using an atomic absorption spectrophotometer with hollow cathode lamps (ECIL AAS4139) (Kolthoff et al., 1971). Appropriate blanks were included to detect any potential contamination during the extraction process.

5.8 CONTAMINATION FACTOR (CF)

The contamination factor (CF) evaluates the degree of contamination caused by heavy metals in elemental concentration studies (Cesa et al., 2013; Monaci et al., 2021). It is determined using the formula provided by Fernandez and Carbelleria (2002).

$$\text{Contamination Factor(CF)} = \left[\frac{\text{Ci}}{\text{Cref}}\right]$$

Where:

- C_i is the concentration of elements in the moss samples after exposure at different monitoring sites.
- C_{ref} is the reference background concentration, determined as the average concentration of the three lowest levels of heavy metals among the sampling sites.

5.9 ANALYSIS OF DATA

STATISTICAL ANALYSIS

Data was collected in triplicate for analysing statistically. Results were expressed as mean ± standard error (Snedecor & Cochran, 1967). Analysis of variance (ANOVA) was employed to identify significant disparities in metal concentrations across varying distances and seasons, with significance thresholds established at $p < 0.05$. The Tukey Honestly Significant Difference (HSD) test was used for post-hoc comparisons to ascertain specific group differences.

Chapter 6: RESULT AND DISCUSSION

6.1 SAMPLING OF MOSS DIVERSITY

A total of 45 moss genera from 18 families were collected across various sites in Chandak and Thalkedar in the Pithoragarh district and Mayawati and Kranteshwar in the Champawat district (Table 6.1a and Figure 6.1a), illustrating the diversity and distribution patterns of the mosses. Thalkedar had the highest number of moss species reported, with 36 species, followed by Kranteshwar with 32, Chandak with 29, and Mayawati with 27. Notable findings included *Entodon luteonitens* (Entodontaceae), *Fissidens anomalus* (Fissidentaceae), and *Barbula funalis* (Pottiaceae), which were recorded at Chandak, and *Plagiochila* sp. (Plagiochilaceae), found exclusively at Mayawati. Most moss species were common across all sites. Four moss species, *Thuidium cyambifolium*, *Rhynchostegiella divericatifolia*, *Fissidens anomalus*, and *Isopterygium elegens* were the most frequently observed across all four control sites.

Table 6.1a: Distribution of different mosses reported from different collection sites

S. No.	Family	Moss	Chandak	Thalkedar	Mayawati	Kranteshwar
1	*Bartramiaceae*	*Bartramia pomiformis*	-	+	+	+
2		*B. subulata*	-	+	+	+
3		*Philonotis falcata*	+	+	+	+
4	*Brachytheciaceae*	*Rhynchostegiella divericatifolia*	+	+	+	+
5		*Brachythecium campestre*	+	-	-	+
6	*Bryaceae*	*Rhodobryum roseum*	+	+	+	+
7		*R. gigentium*	+	+	+	+
8		*Bryum cellulare*	+	+	+	+
9		*B. argentium*	-	+	+	-
10		*B. alpinum*	-	+	+	-
11		*Pohlia flexuosa*	-	+	+	+
12	Dicanaceae	*Campylopus gracilis*	+	-	+	-
13		*Dicranum scoparium*	-	+	-	+
14		*D. undulatum*	+	+	+	-
15	Encalyptaceae	*Encalypta vulgaris*	-	+	-	+
16	Entodontaceae	*Entodon subplicatus*	+	+	-	+

17		*E. luteonitens*	+	-	-	-
18	Fissidentaceae	*Fissidens anomalus*	+	+	+	+
19		*F. taxifolius*	-	+	-	+
20	Funariaceae	*Funaria hygrometrica*	+	+	-	+
21		*Physcomitrium cyathicarpum*	+	+	-	+
22	Grimmiaceae	*Racomitrium crispulum*	+	+	-	+
23		*Grimmia ovalis*	-	+	-	+
24	Hypnaceae	*Hylocomium splendens*	+	+	+	+
25		*Hypnum cupressiforme*	+	+	+	+
26	Meteoriaceae	*Aerobryopsis*	+	-	+	+
27	Mniaceae	*Mnium rostratum*	-	+	-	+
28		*Plagiomnium*	-	+	-	+
29	Plagiochilaceae	*Plagiochila*	-	-	+	-
30	Plagiotheciaceae	*Isopterigum elegans*	+	+	+	+
31	Polytricaceae	*Atricum undulatum*	+	+	+	+
32		*Polytricum juniperium*	+	+	-	-
33		*P. aloides*	+	-	-	+
34		*Pogonatum sp.*	-	+	+	-
35	Pottiaceae	*Barbula vinelis*	+	+	+	+
36		*B. constricta*	+	+	-	-
37		*B. funalis*	+	-	-	-
38		*B. obscura*	-	+	+	-
39		*Anoectangium clarum*	+	-	+	-
40		*A. thomsonii*	+	+	+	+
41		*Hyophila rosea*	-	+	-	+
42	Sphagnaceae	*Sphagnum squarrosum*	-	+	-	+
43	Thuidiaceae	*Thuidium tamariscellum*	+	+	+	+
44		*T. cyambifolium*	+	+	+	+
45		*T. delicatum*	+	-	+	-
TOTAL			29	36	27	32

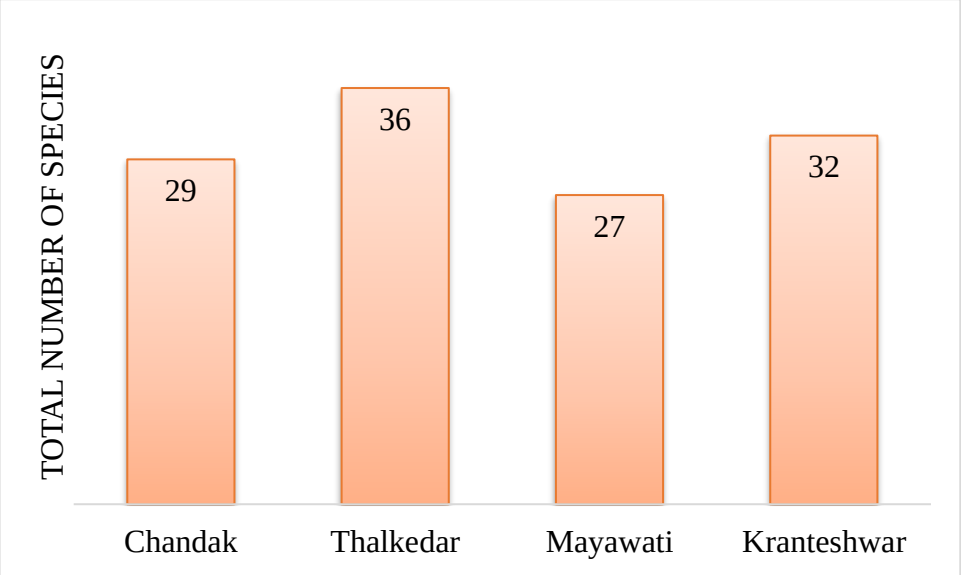

Figure 6.1a: Bar Diagram showing the distribution of moss species in different sites

Some mosses were most frequent in different investigation sites, namely Kranteshwar (Table 6.1 b), Mayawati (Table 6.1 c) of Champawat district and Chandak Forest (Table 6.1 d), and Thalkedar forest of district Pithoragarh (Table 6.1 e). The dominant moss family was Pottiacaceae, with seven species, followed by Bryaceae, with six species. Sahu and Asthana (2015) also concluded in their study that the Pithoragarh and Champawat regions had a rich biodiversity of mosses.

Table 6.1b: Analysis of different parameters of sampling for moss collected from Kranteshwar

S.No.	Moss	Frequency %	Relative Freq (Fr) %	Relative Density	Relative Abundance	Importance Value
1	*Bartramia pomiformis*	40	2.91	4.57	4.06	11.53
2	*Bartramia subulata*	32	2.33	1.73	1.92	5.98
3	*Philonotis falcata*	20	1.45	2.88	5.12	9.45
4	*Rhynchostegiella divericatifolia*	44	3.20	1.73	1.40	6.33
5	*Brachythecium campestre*	48	3.49	3.73	2.76	9.97
6	*Rhodobryum gigentium*	44	3.20	2.84	2.29	8.32
7	*R. roseum*	32	2.33	3.33	3.69	9.35
8	*Bryum cellulare*	16	1.16	1.69	3.74	6.59
9	*Pohlia flexuosa*	32	2.33	2.58	2.86	7.76
10	*Dicranum scoparium*	32	2.33	2.06	2.29	6.68
11	*Dicranum undulatum*	60	4.36	5.95	3.52	13.84
12	*Encalypta vulgaris*	48	3.49	2.34	1.73	7.57
13	*Entodon subplicatus*	12	0.87	3.54	10.47	14.88

14	*Fissidens anomalus*	60	4.23	2.04	1.26	7.53
15	*Fissidens taxifolius*	76	5.52	3.66	1.71	10.89
16	*Funaria hygrometrica*	60	4.36	2.11	1.25	7.72
17	*Physcomitrium cyathicarpum*	48	3.49	3.54	2.62	9.64
18	*Racomitrium crispulum*	56	4.07	2.37	1.50	7.94
19	*Grimmia ovalis*	28	2.03	4.78	6.06	12.88
20	*Hylocomium splendens*	60	4.36	3.26	1.93	9.55
21	*Hypnum cupressiforme*	72	5.23	2.13	1.05	8.42
22	*Aerobryopsis*	20	1.45	1.41	2.50	5.36
23	*Mnium rostratum*	60	4.36	1.29	0.76	6.41
24	*Plagiomnium*	24	1.74	8.74	12.93	23.42
25	*Isopterigum elegans*	76	5.52	1.76	0.82	8.10
26	*Atricum undulatum*	28	2.03	3.49	4.43	9.95
27	*Polytricum aloides*	28	2.03	3.66	4.64	10.33
28	*Barbula vinelis*	64	4.65	3.12	1.73	9.50
29	*Hyophila rosea*	40	2.91	2.16	1.91	6.98
30	*Sphagnum squarrosum*	32	2.33	2.09	2.31	6.73
31	*Thuidium tamariscellum*	64	4.65	8.20	4.55	17.40
32	*T. cyambifolium*	80	5.81	3.28	1.46	10.55

Table 6.1c: Analysis of different parameters of sampling for moss collected from Mayawati

S. No.	Moss	Frequency %	Relative Freq (Fr) %	Relative Density	Relative Abundance	Importance Value
1	*Bartramia pomiformis*	32	2.25	2.52	2.92	7.70
2	*Bartramia subulata*	48	3.38	3.37	2.60	9.35
3	*Philonotis falcata*	28	1.97	3.31	4.37	9.64
4	*Rhynchostegiella divericatifolia*	60	4.23	4.04	2.49	10.76
5	*Rhodobryum gigentium*	56	3.94	2.36	1.56	7.87
6	*R. roseum*	60	4.23	2.75	1.70	8.68
7	*Bryum cellulare*	20	1.41	3.26	6.03	10.70
8	*B. argentium*	8	0.56	2.80	12.95	16.31
9	*B. alpinum*	36	2.54	3.14	3.23	8.91

10	*Pohlia flexuosa*	44	3.10	3.92	3.30	10.32
11	*Campylopus gracilis*	60	4.23	4.04	2.49	10.76
12	*Dicranum undulatum*	72	5.07	2.48	1.27	8.82
13	*Fissidens anomalus*	60	4.23	2.04	1.26	7.53
14	*Hylocomium splendens*	56	3.94	3.44	2.27	9.66
15	*Hypnum cupressiforme*	40	2.82	2.04	1.89	6.75
16	*Aerobryopsis*	60	4.23	3.72	2.29	10.24
17	*Plagiochila*	72	5.07	2.39	1.23	8.68
18	*Isopterigum elegans*	68	4.79	3.24	1.76	9.79
19	*Atricum undulatum*	40	2.82	3.03	2.80	8.65
20	*Pogonatum*	24	1.69	4.02	6.19	11.90
21	*Barbula vinelis*	48	3.38	3.60	2.78	9.76
22	*B. obscura*	28	1.97	3.40	4.49	9.86
23	*Anoectangium thomsonii*	48	3.38	3.42	2.64	9.44
24	*A. clarum*	40	2.82	2.91	2.70	8.43
25	*Thuidium tamariscellum*	32	2.25	4.09	4.72	11.06
26	*T. cyambifolium*	80	5.63	5.74	2.65	14.03
27	*T. delicatum*	64	4.51	3.40	1.96	9.87

Table 6.1d: Analysis of different parameters of sampling for moss collected from Chandak

S. No.	Moss	Frequency %	Relative Freq (Fr) %	Relative Density	Relative Abundance	Importance Value
1	*Philonotis falcata*	28	2.08	5.16	7.80	15.04
2	*Rhynchostegiella divericatifolia*	48	3.57	1.81	1.59	6.97
9	*Brachythecium campestre*	48	3.57	2.33	2.06	7.96
4	*Rhodobryum gigentium*	44	3.27	2.77	2.67	8.72
5	*R. roseum*	56	4.17	4.89	3.70	12.76
6	*Bryum cellulare*	32	2.38	4.48	5.92	12.78
7	*Campylopus gracilis*	28	2.08	5.02	7.60	14.71
8	*Dicranum undulatum*	44	3.27	4.06	3.90	11.24
9	*Entodon subplicatus*	36	2.68	1.49	1.76	5.93
10	*E. luteonitens*	40	2.98	1.54	1.64	6.16

11	*Fissidens anomalus*	44	3.27	4.14	3.98	11.39
12	*Funaria hygrometrica*	20	1.49	5.16	10.92	17.56
13	*Physcomitrium cyathicarpum*	48	3.57	4.58	4.04	12.19
14	*Racomitrium crispulum*	44	3.27	3.59	3.45	10.31
15	*Hylocomium splendens*	60	4.46	2.54	1.79	8.79
16	*Hypunum cupressifore*	32	2.25	3.88	4.48	10.62
17	*Aerobryopsis*	56	4.17	4.55	3.44	12.16
18	*Isopterigum elegans*	76	5.65	1.91	1.06	8.63
19	*Atricum undulatum*	48	3.57	4.66	4.11	12.34
20	*Polytricum juniperium*	44	3.27	2.41	2.32	8.00
21	*Polytricum aloides*	40	2.98	2.17	2.30	7.45
22	*Barbula vinelis*	72	5.36	4.74	2.79	12.88
23	*B. constricta*	52	3.87	3.77	3.07	10.71
24	*B. funalis*	44	3.27	5.00	4.81	13.08
25	*Anoectangium thomsonii*	68	5.06	3.27	2.04	10.37
26	*A. clarum*	44	3.27	3.87	3.73	10.88
27	*Thuidium tamariscellum*	60	4.46	3.27	2.31	10.05
28	*T. cyambifolium*	76	5.65	3.40	1.90	10.95
29	*T. delicatum*	44	3.27	3.43	3.30	10.00

Table 6.1e: Analysis of different parameters of sampling for moss collected from Thalkedar

S.No.	Moss	Frequency %	Relative Freq (Fr) %	Relative Density	Relative Abundance	Importance Value
1	*Bartramia pomiformis*	44	2.76	3.57	3.41	9.75
2	*B. subulata*	48	3.02	3.89	3.41	10.32
3	*Philonotis falcata*	56	3.52	1.77	1.33	6.62
4	*Rhynchostegiella divericatifolia*	28	1.97	3.79	5.00	10.76
5	*Rhodobryum gigentium*	64	4.02	5.37	3.53	12.92
6	*R. roseum*	48	3.02	3.95	3.46	10.42
7	*Bryum cellulare*	64	4.02	2.55	1.68	8.25
8	*B. argentium*	44	2.76	1.48	1.41	5.65
9	*B. alpinum*	36	2.26	2.95	3.45	8.66

10	*Pohlia flexuosa*	64	4.02	2.47	1.62	8.11
11	*Dicranum scoparium*	76	4.77	2.79	1.54	9.11
12	*D. undulatum*	48	3.02	5.18	4.54	12.74
13	*Encalypta vulgaris*	56	3.52	4.05	3.04	10.62
14	*Entodon subplicatus*	12	0.75	5.29	18.53	24.57
15	*Fissidens anomalus*	48	3.38	2.07	1.59	7.04
16	*Fissidens taxifolius*	60	3.77	1.42	1.00	6.19
17	*Funaria hygrometrica*	36	2.26	2.60	3.04	7.91
18	*Physcomitrium cyathicarpum*	32	2.01	4.14	5.43	11.58
19	*Racomitrium crispulum*	60	3.77	2.66	1.86	8.29
20	*Grimmia ovalis*	48	3.02	4.51	3.95	11.48
21	*Hylocomium splendens*	56	3.52	4.40	3.31	11.23
22	*Hypnum cupressiforme*	52	3.27	3.38	2.73	9.38
23	*Mnium rostratum*	56	3.52	1.34	1.01	5.87
24	*Plagiomnium*	64	4.02	2.87	1.89	8.78
25	*Isopterigum elegans*	44	2.76	2.90	2.77	8.43
26	*Atricum undulatum*	56	3.52	3.52	2.64	9.68
27	*Polytricum juniperium*	44	2.76	2.18	2.08	7.02
28	*Pogonatum*	52	3.27	2.87	2.32	8.46
29	*Barbula vinelis*	48	3.02	4.46	3.90	11.38
30	*B. constricta*	36	2.26	5.26	6.14	13.67
31	*B. obscura*	28	1.76	2.60	3.91	8.27
32	*Anoectangium thomsonii*	52	3.27	1.45	1.17	5.89
33	*Hyophila rosea*	56	3.52	3.30	2.48	9.30
34	*Sphagnum squarrosum*	52	3.27	3.68	2.97	9.92
35	*Thuidium tamariscellum*	64	4.02	2.74	1.80	8.56
36	*T. cyambifolium*	84	5.28	1.61	0.81	7.69

The Shannon–Weiner index, an index for α diversity, showed more richness and evenness, with a value ranging between 3 and 3.31. It indicates that the area has a rich diversity of mosses (Fig. 6.1b). Bryophytes, generally mosses, are low-light-loving plants, and the core of the forest generally has low light due to higher plants. This condition favors the high diversity of mosses (Sheue et al., 2007).

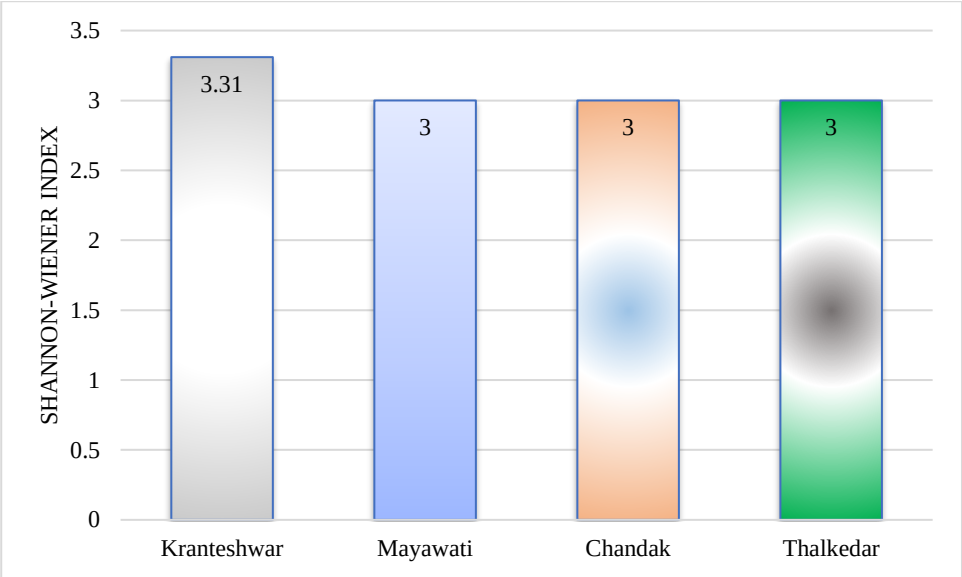

Fig 6.1b: Shannon-Wiener Diversity Index (H') of Alpha Diversity of moss in different sites

According to Raunkier's law, species were placed in their respective classes. The study depicts the maximum number of species in class C (56 taxa), followed by classes B (35 taxa), class D (21 taxa), class A (6 taxa), and class E (1 taxa) (Figure 6.1c). The only moss, *Thuidium cyambifolium*, falls under class E, which indicates that moss is most frequent in the study area. The importance value index (IVI) data indicates species diversity in a particular area. The dominant species in the study areas were *Thuidium cyambifolium, Fissidens taxifolium, Isopterigium elegens, Hypnum cupressiforme,* and *Rhynchostegiella divericatifolia*.

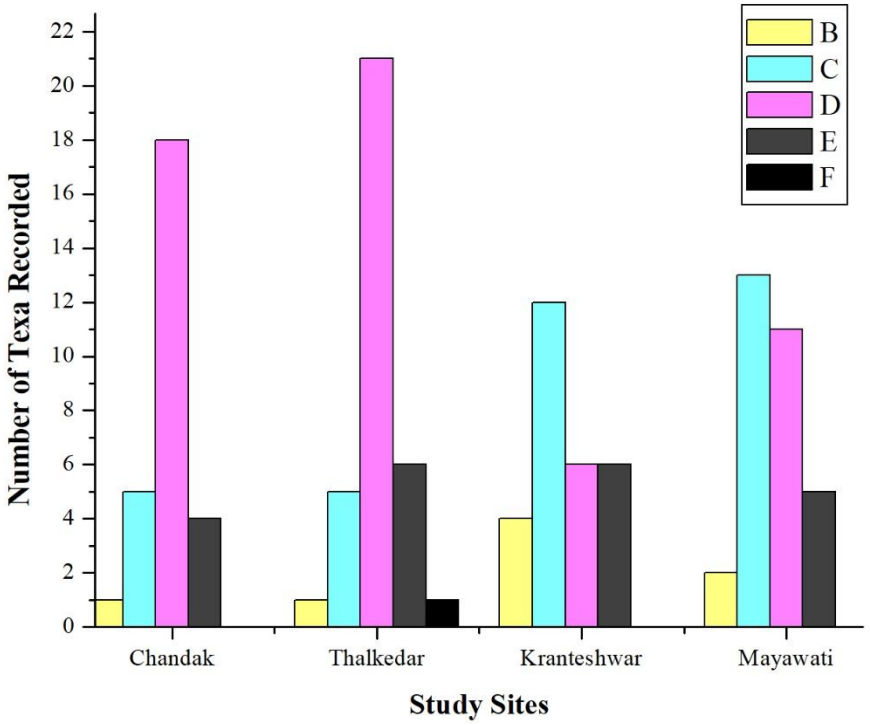

Fig. 6.1c: Frequency class distribution as per Raunkier's Class

The plants and the environment are interdependent. Mosses are a good biomonitor and bioindicator, so the richness of the mosses also reflects the environmental condition (Sinha et al., 2021; Barukial & Hazarika, 2023). Based on this preliminary survey for dominant moss, *Thuidium cyambifolium*, *Fissidens anomalus*, *Isopterigium elegens*, and *Rhynchostegiella divericatifolia* might be used to select a potential biomonitor by analyzing their tolerance against the zinc, lead, copper and cadmium.

6.2 METEOROLOGICAL STUDIES

The climate of the study area is influenced by its altitude and proximity to the Himalayan ranges, resulting in significant variability. Summers are relatively hot, while winters are cold, often dropping below 0°C. In Champawat district, temperatures range from a recorded low of 2.0°C to a high of 38.0°C. Rainfall in the state varies greatly, from 0 cm to 805.2 cm, with distribution influenced by geographical features such as slope and aspect. Approximately ¾ of the annual rainfall occurs during the monsoon season, typically from late June to September, while the remaining quarter falls in other seasons. Relative humidity ranges between 27% and 92% throughout the study period. The weather was generally cool from the month of April to October, featuring monsoon precipitation from the month of June to August and more temperate conditions from the month of September to November. Snowfall is infrequent, with occasional occurrences in January. The highest rainfall is recorded from July to October, totalling 805.2 mm Tables 6.2 a – 6.2 b.

Table 6.2a: Meteorological conditions at district Champawat during the period September 2019 to October 2022.

S. No.	YEAR	MONTH	TEMPERATURE (°C)			RAINFALL (mm)	WIND SPEED (Kmph)			RELATIVE HUMIDITY (%)
			MAX	AVG	MIN		MAX	AVG GUST	AVG	
1	2019	SEPTEMBER	29	24	15	402.1	5.6	5.4	3.2	86
2		OCTOBER	27	20	11	67.9	5.3	5.2	3.3	87
3		NOVEMBER	26	19	8	4.1	5.8	5.7	3.6	80
4		DECEMBER	20	13	3	124.8	5.6	5.4	3.5	63
5	2020	JANUARY	15	10	2	257.8	7.2	6.2	4.1	75
6		FEBRUARY	21	14	5	50.2	7.2	7	4.2	66
7		MARCH	23	18	8	126.7	8.8	8.7	5.4	63
8		APRIL	30	25	14	56.1	10.9	9.9	6.4	43
9		MAY	33	30	18	80.2	11.3	9.7	6.6	43
10		JUNE	32	29	19	292.5	8.1	6.9	4.5	63
11		JULY	30	28	19	805.2	6.4	6.3	3.6	82
12		AUGUST	29	26	18	531.4	6.7	6.3	3.9	88
13		SEPTEMBER	29	25	16	217.7	5.6	5	3	84
14		OCTOBER	29	23	13	4.4	5.8	5.8	3.7	63
15		NOVEMBER	25	18	7	5.5	6.2	5.6	3.6	52
16		DECEMBER	23	15	5	4.8	6.3	5.9	3.7	45
17	2021	JANUARY	22	15	4	20	7.1	6.7	4	50
18		FEBRUARY	25	18	7	11.8	10.3	8.3	5.2	43

19		MARCH	30	23	12	7.8	12.2	9.8	6.2	27
20		APRIL	32	27	14	28.1	14.7	11.8	7.7	26
21		MAY	31	27	16	257.6	10.2	9.3	6	57
22		JUNE	31	29	19	483.9	7.2	6.8	4.3	66
23		JULY	29	27	19	543.8	6.9	6.6	4.1	83
24		AUGUST	27	25	17	42.9	6.3	5.9	3.7	89
25		SEPTEMBER	27	23	15	108.8	5.9	5.9	3.6	89
26		OCTOBER	28	22	11	43.9	6	5.7	3.5	76
27		NOVEMBER	24	17	6	0	5.3	4.9	3.2	68
28		DECEMBER	19	12	2	13	5.8	5.2	3.4	60
29	2022	JANUARY	17	10	2	20.5	6.8	6.4	3.9	73
30		FEBRUARY	19	12	2	19	8.2	7.9	4.7	68
31		MARCH	32	23	10	0	11.4	8.2	5.1	29
32		APRIL	38	30	14	0.1	16.9	11.1	7.2	18
33		MAY	37	30	15	14.4	14.9	10.6	7	41
34		JUNE	37	31	19	37.4	14.4	10.5	7	42
35		JULY	29	25	17	223.9	6.8	6.5	3.9	85
36		AUGUST	28	24	16	177.1	6.6	6.6	4	88
37		SEPTEMBER	29	24	14	89.6	6.7	5.9	3.6	83
38		OCTOBER	26	20	9	47.1	6.1	5.8	3.7	77

Table 6.2b: Meteorological conditions at district Pithoragarh during the period September 2019 to October 2022.

S. No.	YEAR	MONTH	TEMPERATURE (°C)			RAINFALL (mm)	WIND SPEED (Kmph)			RELATIVE HUMIDITY (%)
			MAX	AVG	MIN		MAX	AVG GUST	AVG	
1	2019	SEPTEMBER	28	24	17	397.2	6.9	6.8	4.1	85
2		OCTOBER	26	21	13	59.9	7.5	7.1	4.6	76
3		NOVEMBER	24	19	11	7.2	8.4	6.9	5	61
4		DECEMBER	19	14	6	132.7	8.2	6.6	4.9	56
5	2020	JANUARY	15	10	4	217.1	8.7	7.1	5.2	71
6		FEBRUARY	19	14	6	51.6	9.2	8.2	5.7	64
7		MARCH	22	17	8	123.9	10.1	8.8	6.2	59
8		APRIL	27	23	13	81.6	11.6	10.1	7.1	42
9		MAY	30	26	16	135.6	11.8	10.6	7.1	47
10		JUNE	28	26	18	364.5	8.8	8.2	5.3	68
11		JULY	27	25	19	77.3	8	7.4	4.5	85
12		AUGUST	26	24	19	481.2	7.2	6.7	4.2	89
13		SEPTEMBER	27	24	17	223.3	7.1	6.8	4.3	86
14		OCTOBER	27	22	14	7.1	8.5	7.1	5.1	64
15		NOVEMBER	22	17	9	6	8.6	7.1	5.1	57
16		DECEMBER	20	14	6	0	9.1	7.1	5.4	46
17	2021	JANUARY	20	14	6	9.9	9.4	8.1	5.7	48
18		FEBRUARY	22	17	7	28.4	9.9	9.8	6.3	44

19		MARCH	27	23	11	8.2	11.6	10.7	7.3	28
20		APRIL	30	25	13	22.7	13.6	12.6	8.6	25
21		MAY	27	23	15	257.9	11.5	10.1	7	60
22		JUNE	27	25	18	528.7	9	8.3	5.4	69
23		JULY	26	23	19	381.8	7.2	7	4.4	86
24		AUGUST	24	22	18	450.9	6.8	6.4	4	91
25		SEPTEMBER	24	21	17	89.8	7.1	6.8	4.3	89
26		OCTOBER	24	20	13	165.8	8.4	7.4	5	77
27		NOVEMBER	21	16	7	0.5	8.6	7.3	5	69
28		DECEMBER	17	12	4	13.6	9.1	7.2	5.2	58
29	2022	JANUARY	15	11	4	14.1	8.8	8.1	5.2	69
30		FEBRUARY	17	12	3	26	10	9.2	5.9	68
31		MARCH	30	24	12	0.3	11.4	11.2	6.7	32
32		APRIL	35	28	15	0.8	13.5	13.1	8.1	22
33		MAY	34	27	16	24.4	12	11.6	7.4	46
34		JUNE	34	29	19	45.3	11.5	10.7	6.8	46
35		JULY	26	23	18	183.4	7.3	7.2	4.3	87
36		AUGUST	25	23	18	148.7	7.2	7	4.4	89
37		SEPTEMBER	25	22	16	108.2	7.5	7.7	4.7	86
38		OCTOBER	23	19	11	72.5	9	7.9	5.3	78

6.3 METALS PHYTOTOXICITY ON PHYSIOLOGICAL RESPONSE OF MOSS

6.3.1. EFFECT OF METAL TREATMENT ON MOSS CHLOROPHYLL

The phytotoxic effect of different heavy metals lead (Pb), cadmium (Cd), copper (Cu), and zinc (Zn)) on mosses *Thuidium cyambifolium, Rhynchostegiella divericatifolia, Fissidens anomalus,* and *Isopterygium elegens* were analyzed after 7 and 15 days of treatment. Two lower (5 mM, 10 mM) and two high (50 mM, 100 mM) applications were used to check the tolerance of mosses. Results are depicted in Table 6.3.1 a-d and Figures 6.3.1a to 6.3.1l.

6.3.1.1 EFFECT OF ZINC ON PHOTOSYNTHESIS PIGMENTS

The chlorophyll contents of four mosses, *Thuidium cyambifolium, R. divericatifolia, F. anomalous, and I. elegance*, were assessed for their tolerance to zinc at various concentrations over periods of 7 and 15 days, as shown in the accompanying table 6.3.1a and figure 6.3.1a-c.

***Chlorophyll-a*:**

After 7 days of zinc treatment at 5 mM concentration, the chlorophyll-a content was found to be highest with moss *Thuidium cyambifolium* (1.83 mg/g), followed by *F. anomalous* (1.72 mg/g), I. elegance (1.52 mg/g), and *R. divericatifolia* (1.36 mg/g). Here, it was observed that the zinc concentration in the studied moss species during the study significantly decreased the chlorophyll-a content in all four mosses after 7 and 15 days of treatment. A comparable trend was observed across various zinc concentrations (10, 50, and 100 mM) throughout the study.

***Chlorophyll-b*:**

After 7 days of zinc treatment at 5 mM concentration, the chlorophyll-b content was recorded as the highest in moss *Thuidium cyambifolium* (2.33 mg/g). Whereas, after 15 days of zinc treatment, the chlorophyll-b content was highest with the same moss, i.e., *Thuidium cyambifolium* (2.58 mg/g) at the same concentration. The findings also showed that, after 7 and 15 days of treatment, the content of chlorophyll-b in all four mosses significantly decreased as the zinc concentrations were raised to 10, 50, and 100 mM.

***Total Chlorophyll*:**

After 7 and 15 days of zinc treatment, the total chlorophyll content was highest in moss *Thuidium cyambifolium* at 5 mM concentration (4.18 and 4.57 mg/g, respectively). Based on data analysis (Figure 6.3.1 a-c), it was interesting to note that the moss *T. cyambifolium* was found to be the most tolerant among the other test mosses because the levels of chlorophyll (chlorophyll a, b, and total chlorophyll) showed the least amount of decline.

Table 6.3.1a Impact of Zinc toxicity on Chlorophyll a, b, and total Chlorophyll (mg/g FW) in various moss species at different concentrations following 7 and 15 days of treatment

	T. cyambifolium		***R. divericatifolia***		***F. anomalus***		***I. elegens***	
Chlorophyll a (mg/g FW)								
	7 Day	**15 Day**	**7 Day**	**15 Day**	**7 Day**	**15 Day**	**7 Day**	**15 Day**
Control	4.67±0.13a	4.45±0.13bc	2.57±0.17	1.56±0.17	2.43±0.16	1.54±0.11	2.36±0.17	2.06±0.13ab
5mM	3.83±0.09	3.38±0.08	1.36±0.08	0.66±0.06	1.72±0.09	1.74±0.12	1.52±0.13	1.48±0.05
10 mM	3.69±0.11	3.01±0.07	1.11±0.11	0.53±0.04	1.58±0.15	1.55±0.13	1.22±0.11	1.66±0.09
50 mM	2.53±0.13	2.36±0.12	0.83±0.09	0.43±0.04	1.29±0.11	1.29±0.13	1.06±0.13	1.38±0.13
100 mM	2.02±0.09	1.44±0.11	0.66±0.07	0.22±0.03	0.81±0.06	1.06±0.09	0.83±0.04ab	0.84±0.07
Chlorophyll b (mg/g FW)								
Control	5.62±0.15	5.21±0.11	3.61±0.18	3.01±0.14	3.41±0.16	2.54±0.11	3.31±0.14bc	1.98±0.13
5mM	4.33±0.12	3.58±0.14	2.01±0.11	2.01±0.11	2.21±0.11	2.33±0.08	2.36±0.11	1.91±0.06
10 mM	3.89±0.07	3.54±0.11	1.88±0.08	1.13±0.14	1.63±0.13ab	2.01±0.14ab	1.58±0.07	1.81±0.08
50 mM	3.36±0.09	3.39±0.08	1.59±0.11	1.09±0.12	1.39±0.12	1.58±0.12	1.36±0.12	1.62±0.07
100 mM	2.71±0.10	2.21±0.05ab	1.33±0.12	1.08±0.11	1.01±0.09abc	1.33±0.05	0.83±0.09	1.39±0.10
Total Chlorophyll (mg/g FW)								
Control	10.29±0.28	9.66±0.11	6.18±0.11	4.57±0.16	5.84±0.22	4.08±0.19	5.67±0.12ab	4.04±0.19ab
5mM	8.16±0.12	6.96±0.17	3.37±0.19	2.67±0.13	3.93±0.11	4.07±0.11	3.88±0.13	3.39±0.17
10 mM	7.58±0.10	6.55±0.12	2.99±0.11	1.66±0.14	3.21±.012	3.56±0.14abc	2.80±0.11	3.47±0.12
50 mM	5.89±0.13	5.75±0.09ab	2.42±0.13	1.52±0.13ab	2.68±0.12	2.87±0.13	2.45±0.12	2.74±0.11
100 mM	4.73±0.12	3.65±0.11	1.99±0.08	1.30±0.12	1.82±0.13ab	2.39±0.15ab	1.66±0.08	2.23±0.13

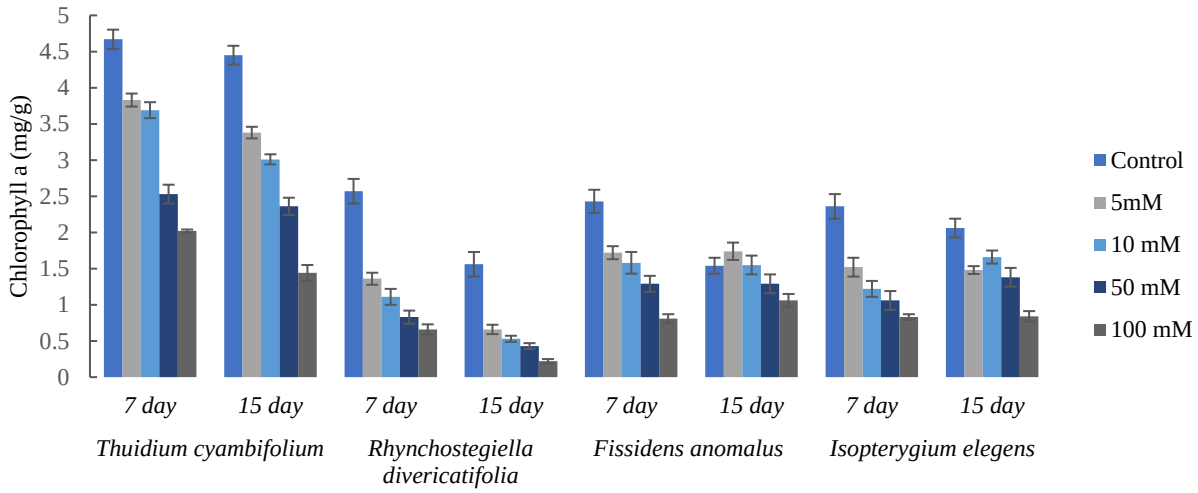

Figure 6.3.1a: Impact of various Zinc concentrations on chlorophyll 'a' after 7 and 15 days of exposure

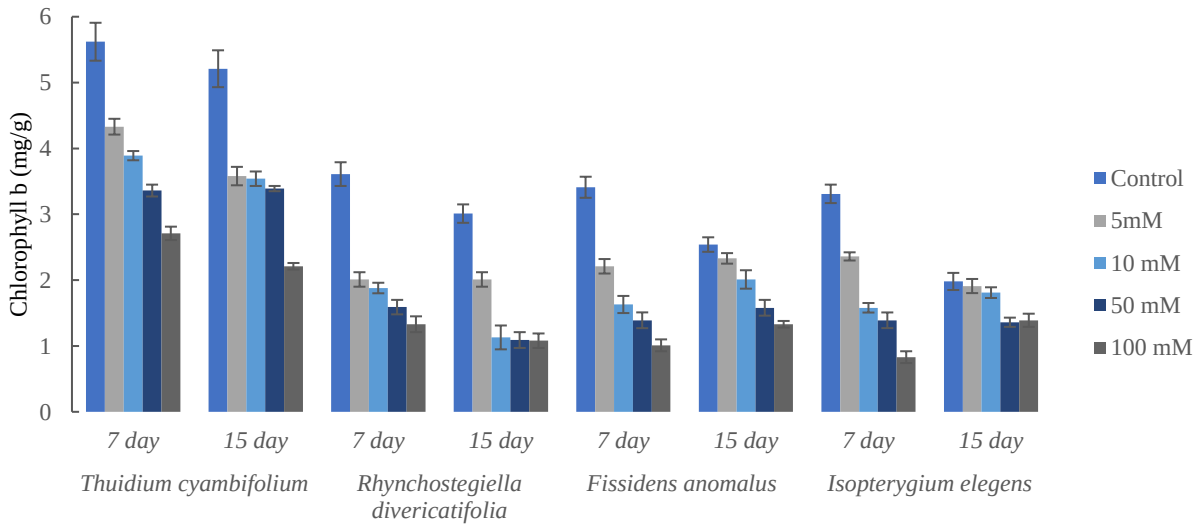

Figure 6.3.1b: Impact of various Zinc concentrations on chlorophyll 'b' after 7 and 15 days of exposure

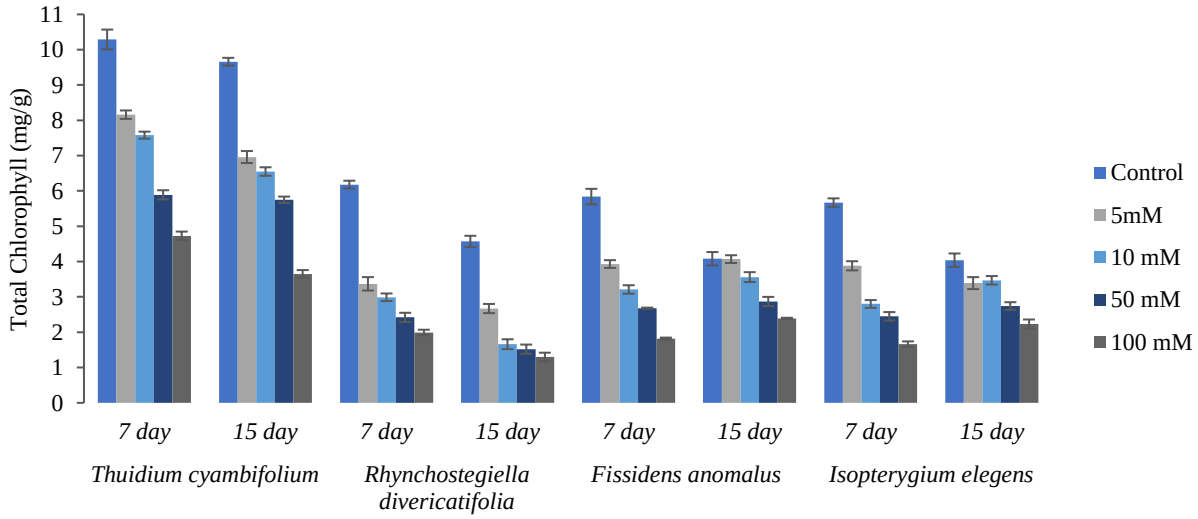

Figure6.3.1c: Impact of various Zinc concentrations on total chlorophyll after 7 and 15 days of exposure

6.3.1.2 EFFECT OF LEAD ON PHOTOSYNTHESIS PIGMENTS

The chlorophyll contents of four mosses, *Thuidium cyambifolium, R. divericatifolia, F. anomalous*, and *I. elegance* were assessed for their tolerance to lead at various concentrations over periods of 7 and 15 days, as shown in the accompanying table 6.3.1b and figure 6.3.1d-f.

***Chlorophyll-a*:**

By treating the lead to moss *Thuidium cyambifolium* at 5 mM concentration, after 7 days, the chlorophyll-a content was found to be highest, i.e., 3.01 mg/g, and least with moss *F. anomalous* (1.08 mg/g). Interestingly, after 15 days of treatment, the chlorophyll-a was also highest with moss *Thuidium cyambifolium* (2.79 mg/g) at 5 mM. As the lead concentration in the studied moss species increased during the study, the chlorophyll-a content significantly decreased in all four mosses after 7 and 15 days of treatment. A similar pattern was recorded in different concentrations of lead (10, 50 and 100 mM) during the study period.

***Chlorophyll-b*:**

After 7 days of lead treatment at 5 mM, the chlorophyll-b was highest in moss *T. cyambifolium* (3.72 mg/g). However, after 15 days of zinc treatment, the chlorophyll-b was highest again in *T. cyambifolium* (3.33 mg/g) at 5 mM concentration. The results showed that, after 7 and 15 days of treatment, the chlorophyll-b content in all four mosses significantly decreased as the lead concentrations increased from 10 mM to 100 mM.

***Total Chlorophyll*:**

After 7 days of lead treatment, the total chlorophyll content of moss *T. cyambifolium* at 5 mM concentration was highest (6.32 mg/g). After 15 days, *T. cyambifolium* again had a maximum chlorophyll content (5.84 mg/g) at 5 mM concentration. Based on the data analysis, it was interesting to note that the moss *T. cyambifolium* was most tolerant among other test mosses, as it has shown a minor decrease in chlorophyll content against the lead treatment.

Table 6.3.1b: Impact of Lead toxicity on Chlorophyll a, b, and total Chlorophyll (mg/g FW) in various moss species at different concentrations following 7 and 15 days of treatment

	T. cyambifolium		***R. divericatifolia***		***F. anomalus***		***I. elegens***	
Chlorophyll a (mg/g FW)								
	7 Day	**15 Day**	**7 Day**	**15 Day**	**7 Day**	**15 Day**	**7 Day**	**15 Day**
Control	4.67±0.13a	4.45±0.13a	2.57±0.17a	1.56±0.17a	2.43±0.16a	1.54±0.11a	2.36±0.17a	2.06±0.13a
5mM	3.01±0.16b	2.79±0.16b	2.45±0.07b	0.66±0.06	2.12±0.13b	0.91±0.10	2.11±0.14	1.79±0.19
10 mM	2.98±0.12bc	2.65±0.17c	1.08±0.12	0.53±0.06a	1.87±0.05	0.81±0.07	1.98±0.11bc	1.66±0.04
50 mM	2.74±0.13c	1.57±0.13	0.64±0.06	0.43±0.10a	1.62±0.08	0.51±0.06	1.81±0.16	1.51±0.12
100 mM	1.73±0.15	1.45±0.11	0.49±0.08	0.22±0.07	1.01±0.09	0.21±0.04ab	1.54±0.13ab	0.91±0.04
Chlorophyll b (mg/g FW)								
Control	5.62±0.15	5.21±0.11	3.61±0.18	3.01±0.14	3.41±0.16	2.54±0.11	3.31±0.14bc	1.98±0.13
5mM	4.72±0.10	4.33±0.11	3.58±0.16ab	1.96±0.15	2.91±0.39	1.95±0.20	3.29±0.15ab	1.84±0.11
10 mM	3.58±0.09	2.84±0.07	3.23±0.11	0.81±0.10	2.12±0.11	1.54±0.14	3.01±0.20	1.78±0.10
50 mM	3.05±0.13	2.54±0.15	3.03±0.12	0.72±0.04	1.72±0.06	1.45±0.12ab	2.89±0.07	1.31±0.07
100 mM	2.14±0.09	1.62±0.08	1.87±0.10	0.67±0.11bc	1.18±0.17	1.33±0.06ab	1.29±0.09	1.29±0.08
Total Chlorophyll (mg/g FW)								
Control	10.29±0.28	9.66±0.11	6.18±0.11	4.57±0.16	5.84±0.22	4.08±0.19	5.67±0.12ab	4.04±0.19ab
5mM	7.73±0.22	7.12±0.17	6.03±0.19	2.62±0.15	5.03±0.14	2.86±0.06	5.40±0.12	3.63±0.14
10 mM	6.56±0.10	5.49±0.12	4.31±0.10	0.61±0.05	3.99±0.13	2.35±0.11ab	4.99±0.06	3.44±0.11abc
50 mM	5.79±0.21	4.11±0.11	3.67±0.06	1.15±0.09	3.34±0.16	1.96±0.13	4.70±0.13	2.82±0.11
100 mM	3.87±0.16	3.07±0.19	2.36±0.13	0.89±0.04	2.19±0.12	1.54±0.12	2.83±0.12	2.20±0.13abc

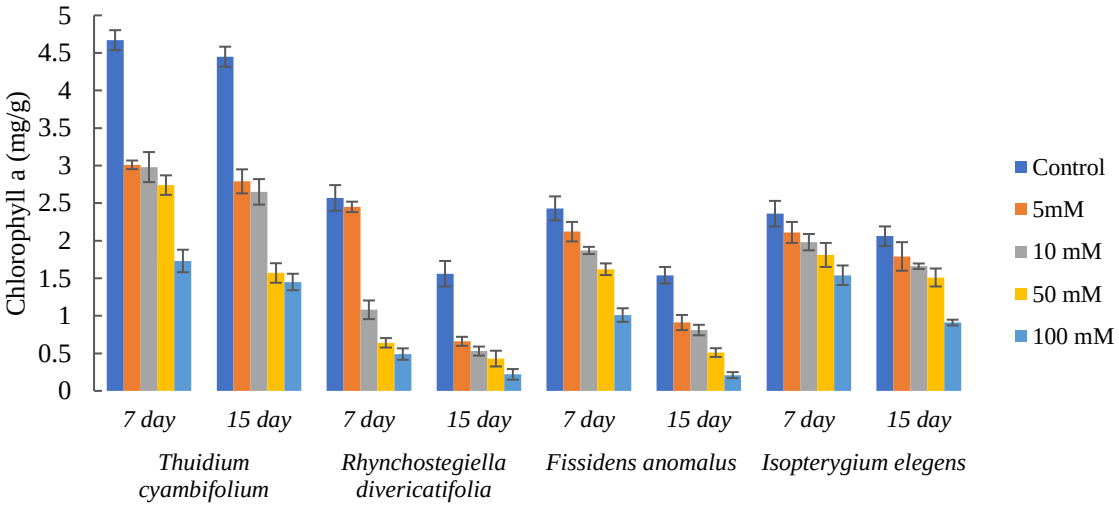

Figure 6.3.1d: Impact of various Lead concentrations on chlorophyll 'a' after 7 and 15 days of exposure

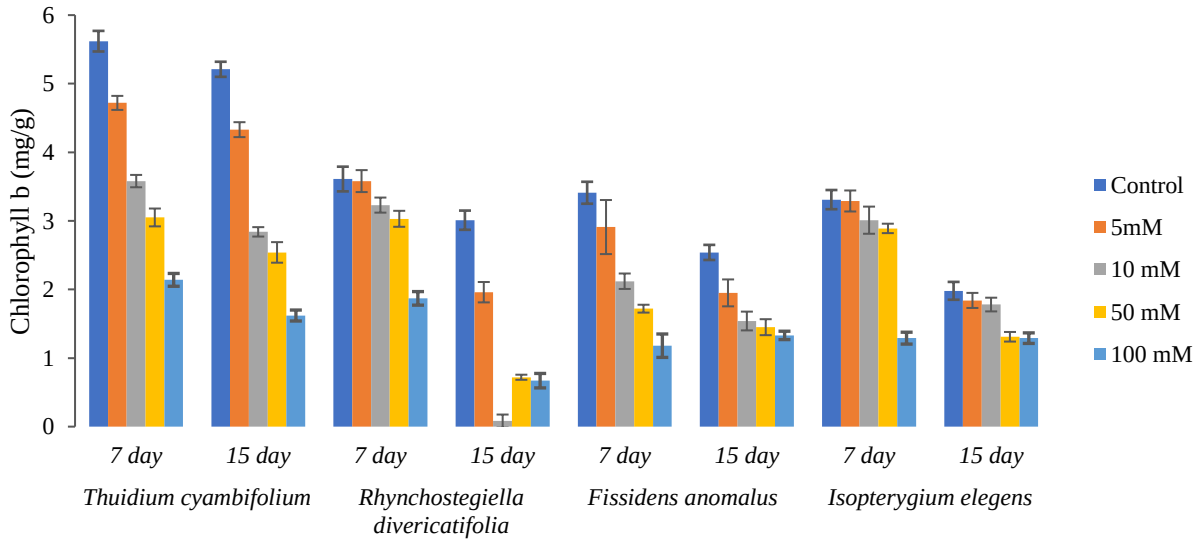

Figure 6.3.1e: Impact of various Lead concentrations on chlorophyll 'b' after 7 and 15 days of exposure

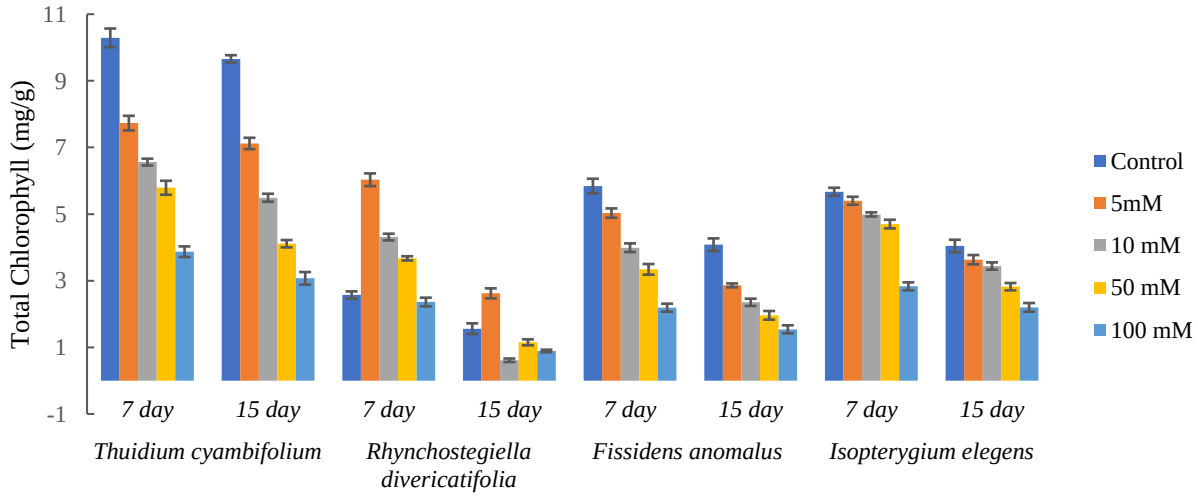

Figure 6.3.1f: Impact of various Lead concentrations on total chlorophyll after 7 and 15 days of exposure

6.3.1.3 EFFECT OF COPPER ON PHOTOSYNTHESIS PIGMENTS

The chlorophyll contents of four mosses, *T. cyambifolium, R.divericatifolia, F. anomalous*, and *I. elegance*, were screened against copper to study metal tolerance (Table 6.3.1c and Figure 6.3.1g-i.) at different concentrations after 7 and 15 days.

***Chlorophyll a*:**

The moss *T. cyambifolium* had the highest chlorophyll-a content (3.23 mg/g) after 7 days of treatment with copper at a 5 mM concentration. This was followed by *R. divericatifolia* (1.29 mg/g), *I. elegance* (1.22 mg/g), and *F. anomalous* (1.02 mg/g). After 7 and 15 days of treatment, there was a significant decrease in the amount of chlorophyll-a in all four mosses as the concentration of copper increased.

***Chlorophyll b*:**

After being exposed to a 5 mM concentration of copper for 7 and 15 days, the moss *T. cyambifolium* showed a high chlorophyll-b content of 4.01 mg/g. *R. divericatifolia* was identified as the second most copper-tolerant moss, with a chlorophyll-b content of 2.44 mg/g. The findings also demonstrated that, following 7 and 15 days of treatment, there was a significant drop in chlorophyll-b in all four mosses as the concentration of copper increased.

***Total Chlorophyll*:**

After 7 days and 15 days of a 5 mM concentration of copper treatment, the total chlorophyll content was highest in moss *T.cyambifolium.* Whereas *R. divericatifolia* with total chlorophyll content, i.e. (2.44 mg/g), was reported as the second highest tolerant moss against copper. Based on the data analysis here also, it was interesting to note that the moss *R. divericatifolia* was found to be the second highest tolerant among other test mosses, as it showed the least amount of decline in total chlorophyll content in response to the copper treatment.

able 6.3.1c: Impact of Copper toxicity on Chlorophyll a, b, and total Chlorophyll content (mg/g FW) in various moss species at different concentrations following 7 and 15 days of treatment

	T. cyambifolium		***R. divericatifolia***		***F. anomalus***		***I. elegens***	
Chlorophyll a (mg/g FW)								
	7 Day	**15 Day**	**7 Day**	**15 Day**	**7 Day**	**15 Day**	**7 Day**	**15 Day**
Control	4.67±0.13a	4.45±0.13bc	2.57±0.17	1.56±0.17	2.43±0.16	1.54±0.11	2.36±0.17	2.06±0.13ab
5mM	3.23±0.07	2.85±0.08	1.29±0.04	0.95±0.07	1.02±0.05	0.85±0.06	1.22±0.13	0.94±0.07
10 mM	2.07±0.05	1.74±0.07	0.95±0.05	0.71±0.03	0.83±0.05	0.59±0.06	1.01±0.07	0.77±0.09
50 mM	1.83±0.07bc	1.54±0.07	0.81±0.06	0.54±0.07	0.69±0.03	0.41±0.05	0.73±0.04	0.51±0.02
100 mM	1.64±0.04	1.33±0.06	0.77±0.07	0.44±0.06	0.44±0.05	0.32±0.03	0.51±0.05	0.33±0.03ab
Chlorophyll b (mg/g FW)								
Control	5.62±0.15	5.21±0.11	3.61±0.18	3.01±0.14	3.41±0.16	2.54±0.11	3.31±0.14bc	1.98±0.13
5mM	4.01±0.09	3.51±0.12	2.44±0.12	1.94±0.10	1.95±0.12	1.66±0.09	1.85±0.08	1.39±0.14
10 mM	3.55±0.08	2.79±0.09	2.29±0.17	1.74±0.08	1.69±0.14	1.32±0.08	1.66±0.07	1.14±0.09
50 mM	2.21±0.11	1.92±0.07	1.84±0.16	1.26±0.07	1.01±0.11	0.84±0.06	1.29±0.06	0.81±0.06ab
100 mM	1.73±0.08	1.44±0.05	1.68±0.11	0.95±0.09	0.74±0.09	0.55±0.05	0.84±0.09	0.66±0.03
Total Chlorophyll (mg/g FW)								
Control	10.29±0.28	9.66±0.11	6.18±0.11	4.57±0.16	5.84±0.22	4.08±0.19	5.67±0.12ab	4.04±0.19ab
5mM	7.24±0.09	6.36±0.11	3.73±0.16	2.89±0.07	2.97±0.13	2.51±0.14	3.07±0.14	2.33±0.11
10 mM	5.62±0.07	4.53±0.09	3.24±0.19	2.45±.07	2.52±0.11	1.91±0.13	2.67±0.11	1.91±0.14
50 mM	4.04±0.11	3.46±0.07	2.65±0.09	1.81±0.04	1.7±0.07	1.25±0.14	2.02±0.13	1.32±0.11
100 mM	3.37±0.08	2.77±0.05	2.45±0.07	1.39±0.11	1.18±0.07	0.87±0.08	1.35±0.12	0.99±0.09

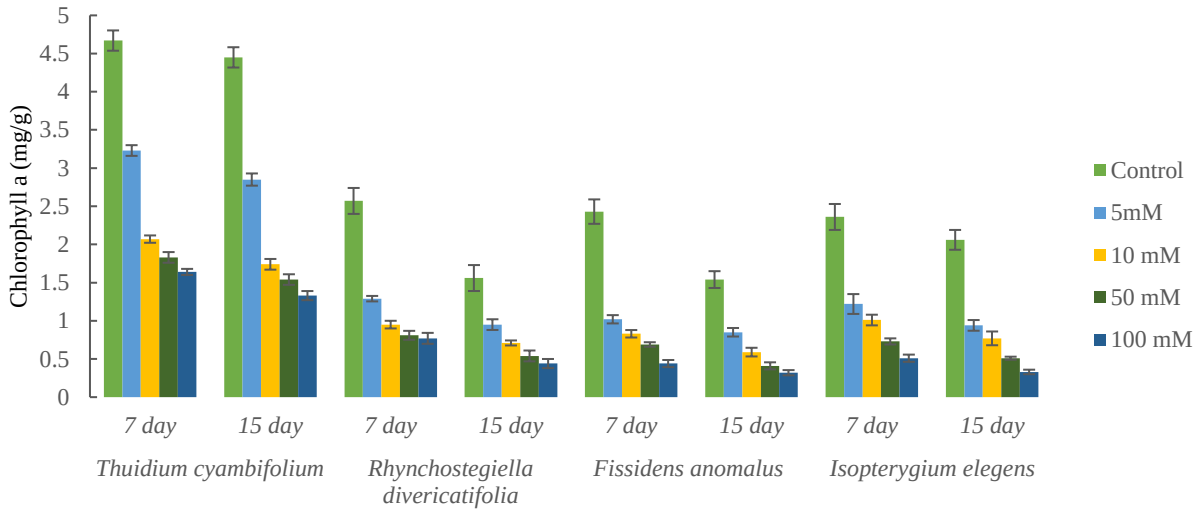

Figure 6.3.1g: Impact of various Copper concentrations on chlorophyll 'a' after 7 and 15 days of exposure

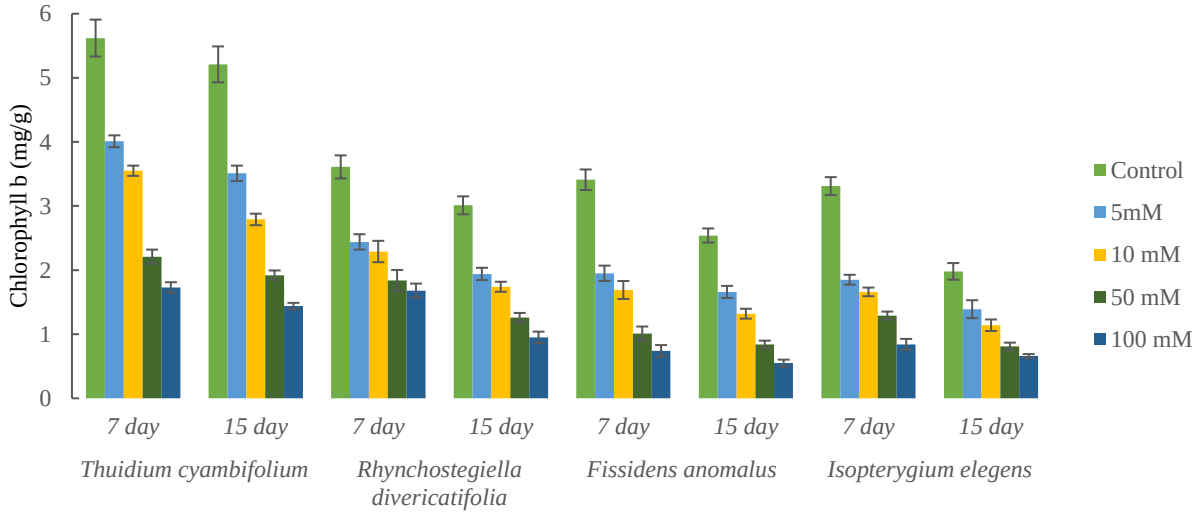

Figure 6.3.1h: Impact of various Copper concentrations on chlorophyll 'b' after 7 and 15 days of exposure

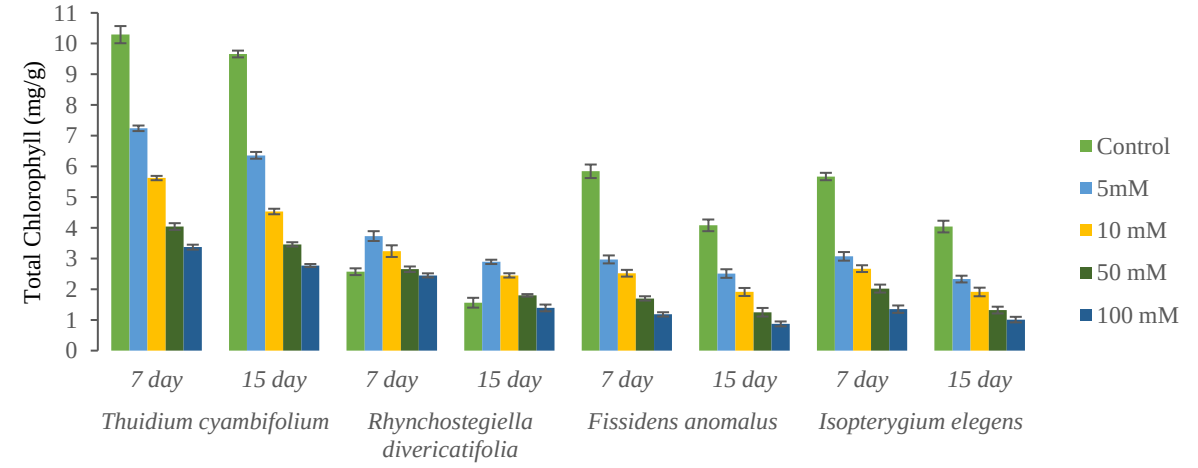

Figure 6.3.1i: Impact of various Copper concentrations on total chlorophyll after 7 and 15 days of exposure

6.3.1.4 EFFECT OF CADMIUM ON PHOTOSYNTHESIS PIGMENTS

The chlorophyll contents of four mosses, *T. cyambifolium, R. divericatifolia, F. anomalous,* and *I. elegance*, were screened for their metal tolerance at various concentrations of cadmium over periods of 7 and 15 days, as shown in Table 6.3.1d and figure 6.3.1j-l.

***Chlorophyll a*:**

After 7 days of treatment with 5 mM cadmium, the moss *T. cyambifolium* exhibited the highest chlorophyll-a content (1.99 mg/g). After 15 days of cadmium treatment at 5 mM concentration, the moss *T. cyambifolium* showed the maximum chlorophyll content (1.14 mg/g).

***Chlorophyll b*:**

After 7 days of cadmium treatment at the concentration of 5 mM, the highest content of chlorophyll-b was found with moss *T. cyambifolium* (3.65 mg/g). However, after 15 days of treatment, the same moss occurred with the highest chlorophyll content (2.31mg/g) at a lower concentration, i.e. 5 mM concentration of cadmium.

***Total Chlorophyll*:**

After 7 days of cadmium treatment, the total chlorophyll was found to be highest in moss *T. cyambifolium* at 5 mM concentration (4.71 mg/g) i.e. highest concentration of cadmium. After 15 days, the highest chlorophyll content, i.e. 3.68 mg/g, was recorded with *T. cyambifolium* at 5 mM concentration, i.e., the lowest concentration of cadmium. Based on data analysis (Figures 6.3.1 j-l) here, it was also interesting to note that the moss *T. cyambifolium* was found to be most tolerant among other studied mosses, as it showed the least decrease in chlorophyll content against the cadmium treatment.

Table 6.3.1d: Impact of Cadmium toxicity on Chlorophyll a, b, and total chlorophyll (mg/g FW) in various moss species at different concentrations following 7 and 15 days of treatment

	T. cyambifolium		***R. divericatifolia***		***F. anomalus***		***I. elegens***	
Chlorophyll a (mg/g FW)								
	7 Day	**15 Day**	**7 Day**	**15 Day**	**7 Day**	**15 Day**	**7 Day**	**15 Day**
Control	4.67±0.13a	4.45±0.13bc	2.57±0.17	1.56±0.17	2.43±0.16	1.54±0.11	2.36±0.17	2.06±0.13ab
5mM	3.49±0.04ab	3.08±0.06	1.14±0.07	1.13±0.13	1.01±0.11	0.84±0.05	1.01±0.03	0.81±0.7
10 mM	2.55±0.13	2.24±0.05	1.08±0.08	0.84±0.07	0.72±0.05ab	0.68±0.09	0.84±0.07	0.73±0.08
50 mM	1.85±0.04bc	1.55±0.09	0.91±0.03	0.65±0.11	0.66±0.03	0.47±0.07	0.73±0.08	0.66±0.07
100 mM	1.55±0.11	1.36±0.07bc	0.65±0.09	0.47±0.07ab	0.51±0.04	0.22±0.03	0.54±0.06	0.49±0.05
Chlorophyll b (mg/g FW)								
Control	5.62±0.15	5.21±0.11	3.61±0.18	3.01±0.14	3.41±0.16	2.54±0.11	3.31±0.14bc	1.98±0.13
5mM	3.65±0.17	3.31±0.19bc	1.58±0.05bc	1.17±0.13	1.91±0.13	1.74±.12	2.14±.08ab	1.73±0.07
10 mM	3.01±0.12	2.82±0.16	1.14±0.09	1.02±0.13	1.76±0.15	1.45±0.16	1.49±0.06	1.29±0.08
50 mM	2.47±0.16ab	2.07±0.05	1.08±0.04	0.92±0.06	0.95±.18	1.09±0.10	0.94±0.08	0.77±0.09
100 mM	2.01±0.15	1.55±0.07	0.91±0.10	0.71±0.07	0.77±0.08	0.54±0.04	0.73±0.04ab	0.54±0.11
Total Chlorophyll (mg/g FW)								
Control	10.29±0.28	9.66±0.11	6.18±0.11	4.57±0.16	5.84±0.22	4.08±0.19	5.67±0.12ab	4.04±0.19ab
5mM	7.14±0.14	6.39±0.12	2.72±0.17	2.30±0.12	2.92±0.14	2.58±0.11	3.15±0.13	2.54±0.07
10 mM	5.56±0.07	5.06±0.09	2.22±0.16	1.86±0.6	2.48±0.11	2.13±0.08	2.33±0.11	2.02±0.09ab
50 mM	4.32±0.10	3.6±0.10	1.99±0.18	1.57±0.06	1.61±0.07	1.56±0.07	1.67±0.07	1.43±0.05
100 mM	3.56±0.04	1.91±0.13	1.56±0.08	1.18±0.09	1.28±0.03	0.76±0.05	1.27±0.09	1.03±0.11

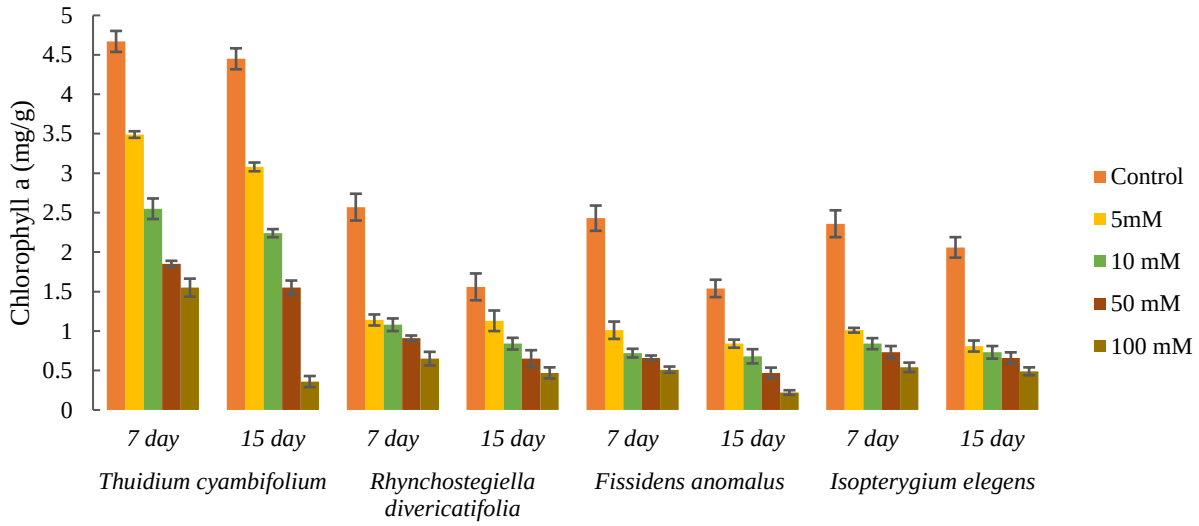

Figure 6.3.1j: Impact of various Cadmium concentrations on chlorophyll 'a' after 7 and 15 days of exposure

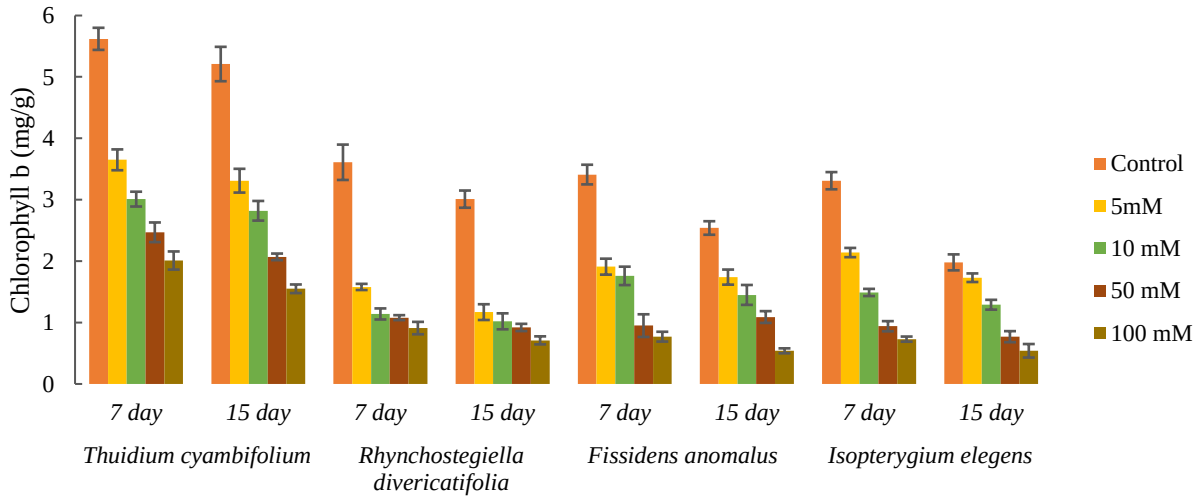

Figure 6.3.1k: Impact of various Cadmium concentrations on chlorophyll 'b' after 7 and 15 days of exposure

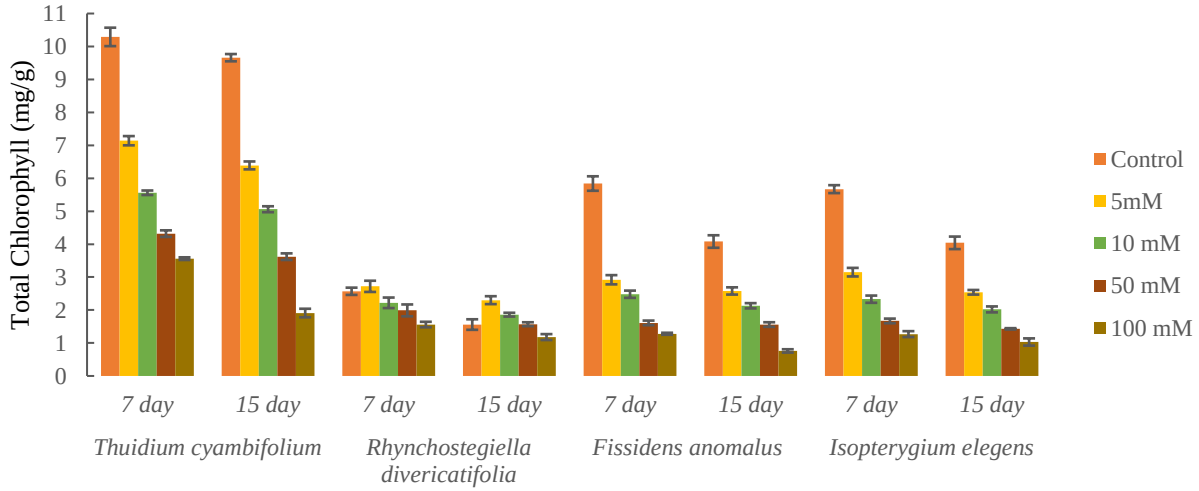

Figure 6.3.1l: Impact of various Cadmium concentrations on total chlorophyll after 7 and 15 days of exposure

The study aimed to observe the effects of four different metal treatments on the chlorophyll content of native moss plants from selected study sites of Champawat and Pithoragarh districts. For this purpose, Samples of mosses (*T. cyambifolium*, *R. divericatifolia*, *F. anomalous*, and *I. elegance*) were collected to monitor the effects and tolerance of these mosses against different heavy metals viz., Zinc, Lead, Cadmium and Copper. Four moss samples were brought to the laboratory and processed for removal of contaminations. Then, these moss samples were randomly sprayed with selected heavy metals of different concentrations, i.e. 5 mM, 10 mM, 50 mM and 100 mM of Zinc, lead, cadmium and copper, for 20 minutes and incubated for 7 and 15 days. Over the past two decades, several prominent bryologists have researched using bryophytes to assess ecosystem pollution, particularly heavy metals (Jozwiak & Jozwiak, 2009; Rajfur, 2013; Mahapatra et al., 2019). Significant focus has been placed on studying the accumulation of analytes by indicator species in field studies and laboratory settings (Agnan et al., 2017; Zinicovscaia et al., 2018).

It was found that these heavy metals caused some damage to their chloroplasts as the natural colour was changed in most of these treated moss samples. Based on this, it might be possible that these concentrations of the used heavy metals are phytotoxic. Numerous studies have demonstrated that mosses are an effective biomonitor for heavy metals across various habitats through various mechanisms (Backor et al., 2023). Previously, a study conducted by Shakya et al. (2008) examined the impact of copper (Cu), zinc (Zn), and lead (Pb) on the chlorophyll levels of two mosses and leafy liverwort and observed that the accumulation of copper had a substantial inhibitory effect on chlorophyll a, chlorophyll b, and total chlorophyll in both the mosses and the leafy liverwort. They also reported that the rise in Cu accumulation is associated with notable reductions in chlorophyll a, chlorophyll b, total chlorophyll, and the chlorophyll a to b ratio. This phenomenon indicates the inhibitory impact of Cu on pigment biosynthesis, potentially a metal specific to this metal (Chettri et al., 1998; Panda & Choudhury, 2005).

Based on the comprehensive screening and data analysis conducted in this investigation and by comparing the results with Chrysargyris et al. (2021) regarding the chlorophyll content of *T. cyambifolium*, it was found that *T. cyambifolium* demonstrated the highest tolerance among the tested moss species. This conclusion is supported by its minimal reduction in chlorophyll content in response to metal treatments, except for *R. divericatifolia*, which exhibited the second-highest tolerance to copper. Chlorophyll content degradation has been previously documented in moss treated with Cr, Cu, and Zn (Vajpayee et al., 2000; Panda et al., 2003). Relative moderate Copper (Cu) is highly poisonous to plants, even when exposed to micromolar levels (Carbal, 2003). However, it is also a crucial

micronutrient for stimulating plant growth. Copper inhibition of the photosynthetic electron transport chain and degradation of chlorophyll have been reported by Quartacci et al. (2001) and Patsikka et al. (2002). Nevertheless, it is essential to note that a significant amount of copper can harm lower and higher plants. However, there have been documented cases of copper tolerance in mosses (Venkataraman, et al., 1992). Mosses, being low molecular protein organisms, are less toxic than copper and can be very valuable for bio-mapping, especially in environments with high copper concentrations.

At lower concentrations, Pb has been reported to have a limited effect on the degradation of chlorophyll biosynthesis. However, the inhibitory effect might also extend to the photo activity side at higher concentrations and continuous exposure. Prior studies have documented a decline in chlorophyll levels when exposed to Cr, Cu, Pb, and Zn (Vajpayee et al., 2000; Panda et al., 2005). Mosses possess a robust counter gradient system that enables them to collect substantial amounts of metals in their tissues (Van Assche & Clijsters, 1990; Cardinale et al., 2004). Shakya et al. (2008) also revealed that Lead exhibited lower phytotoxicity than Copper and reduced the total chlorophyll content in test mosses. Similarly, reductions in total chlorophyll content have been observed in various plants exposed to heavy metal stress, including Cd, Cu, Pb, Mg, and Ni (Panda et al., 2003; Fatoba & Udoh, 2008; Chmielowska-Bąk & Deckert, 2021).

This study concludes that the accumulation of heavy metals like Cu, Zn, Pb, and Cd in mosses induces stress, leading to chlorophyll degradation. Heavy metal accumulation primarily impacts chloroplast ultrastructure, resulting in lipid peroxidation of photosynthetic membranes, degradation of pigments, inhibition of PSII activity and electron transport, reduced carboxylation efficiency of Rubisco, and a decline in the net photosynthetic rate (Zhou et al., 2017; Wang et al., 2022).

The chlorophyll pigments are essential for the effective absorption of solar energy. According to reports, the restriction of photosynthesis in plants by increased metal concentrations is not due to cellular acidification but rather to the chemical reactivity or the anions generated during its hydration. It has also been found that this inhibition is reversible (Vincent, 1980; Srivastava, 2004). Metals typically reduce the chlorophyll-a and chlorophyll-b levels in lower plants (bryophytes) and higher plants (Sheoran et al., 1990; Ouzounidou, 1993). The present study revealed that *T. cyambifolium* was the most tolerant to the accumulation of heavy metals.

6.3.2. IMPACT OF VARIOUS METALS TREATMENT ON NITRATE REDUCTASE ACTIVITY (NRA)

This study aimed to evaluate the impact of Copper, Lead, Zinc, and Cadmium on nitrate reductase activity in moss plants, namely *Thuidium cyambifolium, Rhynchostegiella divericatifolia, Fissidens anomalus* and *Isopterygium elegens*. During the present study, the NRA activity of selected mosses was measured for 3 days, 6 days, and 15 days for both controlled conditions with different concentrations of metals (5mM, 10mM, 50mM, and 100mM metals treatment).

6.3.2.1 EFFECT OF ZINC ON NITRATE REDUCTASE ACTIVITY

In *T. cyambifolium*, it was noted that NR activity decreased at the 5mM Zn treatment by approximately 3.023, 2.690, and 2.395 μmole $min^{-1}g^{-1}$ FW during 3, 6, and 15 days. In *R. divericatifolia*, during the 3rd, 6th, and 15th days after treatment, the values were 2.908 μmole $min^{-1}g^{-1}$ FW, 2.588 μmole $min^{-1}g^{-1}$ FW, 2.303 μmole $min^{-1}g^{-1}$ FW. In contrast, in *F. anomalous* 2.598 μmole $min^{-1}g^{-1}$ FW, 2.312 μmole min^{-1} g^{-1} FW, 2.308 μmole $min^{-1}g^{-1}$ FW in *I. elegens* when treated with different Zn concentrations, the NRA values were found to be decreased by 2.885 μmole $min^{-1}g^{-1}$ FW, 2.568 μmole $min^{-1}g^{-1}$ FW, 2.285 μmole $min^{-1}g^{-1}$ FW (Table 6.3.2a and figure 6.3.2.1a-c).

As the concentration of metal treatments increased to 100 mM, the NR activity for *T. cyambifolium* declined considerably to 0.958 μmole $min^{-1}g^{-1}$ FW on the 3rd day. Further, it decreased to 0.177 μmole $min^{-1}g^{-1}$ FW on the 15th day. In *R. divericatifolia,* the rate of nitrate reductase activity (NRA) showed a substantial decrease, reaching 0.894 μmole $min^{-1}g^{-1}$ FW on the 3rd day and further dropping to 0.165 μmole $min^{-1}g^{-1}$ FW on the 15th day. The *F. anomalous* NRA exhibited a considerable decline, reaching 0.689 μmole $min^{-1}g^{-1}$ FW on the 3rd day and 0.127 μmole $min^{-1}g^{-1}$ FW on the 15th day. The activity of *I. elegens* NRA was seen to reduce dramatically to 0.879 μmole $min^{-1}g^{-1}$ FW on the 3rd day and further decrease to 0.163 μmole $min^{-1}g^{-1}$ FW on the 15th day (Table 6.3.2a and figure 6.3.2.1a-c).

6.3.2.2 EFFECT OF LEAD ON NITRATE REDUCTASE ACTIVITY

In *T. cyambifolium*, it was noted that NR activity decreased at the 5mM Zn treatment by approximately 3.434, 2.696, and 2.116 μmole $min^{-1}g^{-1}$ FW during 3, 6, and 15 days. In *R. divericatifolia*, during 3, 6, and 15 days of treatment, the values were recorded as 3.215 μmole $min^{-1}g^{-1}$ FW, 2.524 μmole $min^{-1}g^{-1}$ FW, 1.555 μmole $min^{-1}g^{-1}$ FW. In contrast, in *F. anomalous* 3.015 μmole $min^{-1}g^{-1}$ FW, 2.367 μmole min^{-1} g^{-1} FW, 1.858 μmole $min^{-1}g^{-1}$ FW in *I. elegens* when treated with

different Zn concentrations, the NRA values were found to be decreased by 3.065 µmole $min^{-1}g^{-1}$ FW, 2.406 µmole $min^{-1}g^{-1}$ FW, 1.483 µmole $min^{-1}g^{-1}$ FW (Table 6.3.2 and figure 6.3.2.2a-c).

As the concentration of metal treatments increased to 100 mM, the NR activity for *T. cyambifolium* declined considerably to 1.101 µmole $min^{-1}g^{-1}$ FW on the 3rd day. Further, it decreased to 0.201 µmole $min^{-1}g^{-1}$ FW on the 15th day. In *R. divericatifolia,* the rate of nitrate reductase activity (NRA) showed a substantial decrease, reaching 0.0.845 µmole $min^{-1}g^{-1}$ FW on the 3rd day and further dropping to 0.066 µmole $min^{-1}g^{-1}$ FW on the 15th day. The *F. anomalous* NRA exhibited a considerable decline, reaching 0.654 µmole $min^{-1}g^{-1}$ FW on the 3rd day and 0.199 µmole $min^{-1}g^{-1}$ FW on the 15th day. The activity of *I. elegens* NRA was seen to reduce dramatically to 0.747 µmole $min^{-1}g^{-1}$ FW on the 3rd day and further decrease to 0.139 µmole $min^{-1}g^{-1}$ FW on the 15th day (Table 6.3.2b and figure 6.3.2.2a-c).

6.3.2.3 EFFECT OF COPPER ON NITRATE REDUCTASE ACTIVITY

In *T. cyambifolium,* it was noted that NR activity decreased at the 5mM Zn treatment by approximately 3.497, 2.832 and 2.294 µmole $min^{-1}g^{-1}$ FW during 3, 6, and 15 days. In *R. divericatifolia*, during 3, 6, and 15 days of treatment, the values were recorded as 3.324 µmole $min^{-1}g^{-1}$ FW, 2.692 µmole $min^{-1}g^{-1}$ FW, 1.767 µmole $min^{-1}g^{-1}$ FW. In contrast, in *F. anomalous* 3.156 µmole $min^{-1}g^{-1}$ FW, 2.556 µmole min^{-1} g^{-1} FW, 1.677 µmole $min^{-1}g^{-1}$ FW in *I. elegens* when treated with different Zn concentrations, the NRA values were found to be decreased by 3.192 µmole $min^{-1}g^{-1}$ FW, 2.586 µmole $min^{-1}g^{-1}$ FW, 2.094 µmole $min^{-1}g^{-1}$ FW (Table 6.3.2c and figure 6.3.2.3a-c).

As the concentration of metal treatments increased to 100 mM, the NR activity for *T. cyambifolium* declined considerably to 0.994 µmole $min^{-1}g^{-1}$ FW on the 3rd day. Further, it decreased to 0.529 µmole $min^{-1}g^{-1}$ FW on the 15th day. In *R. divericatifolia,* the rate of nitrate reductase activity (NRA) showed a substantial decrease, reaching 0.833 µmole $min^{-1}g^{-1}$ FW on the 3rd day and further dropping to 0.166 µmole $min^{-1}g^{-1}$ FW on the 15th day. The *F. anomalous* NRA exhibited a considerable decline, reaching 0.764 µmole $min^{-1}g^{-1}$ FW on the 3rd day and 0.061 µmole $min^{-1}g^{-1}$ FW on the 15th day. The activity of *I. elegens* NRA was seen to reduce dramatically to 0.647 µmole $min^{-1}g^{-1}$ FW on the 3rd day and further decrease to 0.120 µmole $min^{-1}g^{-1}$ FW on the 15th day (Table 6.3.2c and figure 6.3.2.3a-c).

6.3.2.4 EFFECT OF CADMIUM ON NITRATE REDUCTASE ACTIVITY

In *T. cyambifolium*, it was noted that NR activity decreased at the 5mM Zn treatment by approximately 2.613, 2.160, and 1.786 µmole $min^{-1}g^{-1}$ FW during 3, 6, and 15 days. In *R. divericatifolia*, during 3, 6, and 15 days of treatment, the values were recorded as 2.404 µmole $min^{-1}g^{-1}$ FW, 1.988 µmole $min^{-1}g^{-1}$ FW, 1.644 µmole $min^{-1}g^{-1}$ FW. In contrast, in *F. anomalous* 2.468 µmole $min^{-1}g^{-1}$ FW, 2.041 µmole min^{-1} g^{-1} FW, 1.688 µmole $min^{-1}g^{-1}$ FW in *I. elegens* when treated with different Zn concentrations, the NRA values were found to be decreased by 1.914 µmole $min^{-1}g^{-1}$ FW, 1.583 µmole $min^{-1}g^{-1}$ FW, 1.309 µmole $min^{-1}g^{-1}$ FW (Table 6.3.2d and Figure 6.3.2.4a-c).

As the concentration of metal treatments increased to 100 mM, the NR activity for *T. cyambifolium* declined considerably to 1.777 µmole $min^{-1}g^{-1}$ FW on the 3rd day. Further, it decreased to 0.373 µmole $min^{-1}g^{-1}$ FW on the 15th day. In *R. divericatifolia,* the rate of nitrate reductase activity (NRA) showed a substantial decrease, reaching 1.335 µmole $min^{-1}g^{-1}$ FW on the 3rd day and further dropping to 0.210 µmole $min^{-1}g^{-1}$ FW on the 15th day. The *F. anomalous* NRA exhibited a considerable decline, reaching 0.754 µmole $min^{-1}g^{-1}$ FW on the 3rd day and 0.119 µmole $min^{-1}g^{-1}$ FW on the 15th day. The activity of *I. elegens* NRA was seen to reduce dramatically to 0.587 µmole $min^{-1}g^{-1}$ FW on the 3^{rd} day and further decrease to 0.092 µmole $min^{-1}g^{-1}$ FW on the 15th day (Table 6.3.2d and Figure 6.3.2.4a-c).

Table 6.3.2a: Effect of Zinc on Nitrate Reductase Enzyme Activity (µmole $min^{-1}g^{-1}$ FW) in different moss at different concentrations for 3, 6, and 15 days of lab treatment

	Thuidium cyambifolium			*Rhynchostegiella divericatifolia*			*Fissidens anomalus*			*Isopterygium elegens*		
	3 days	**6 Days**	**15 days**	**3 days**	**6 Days**	**15 days**	**3 days**	**6 Days**	**15 days**	**3 days**	**6 Days**	**15 days**
Control	3.789±0.12	3.716±0.16	2.807±0.13	3.654±0.12	3.215±0.15	2.742±0.18	3.685±0.14	3.747±0.15	2.762±0.10	3.612±0.15	3.654±0.14	2.711±0.13
5mM	3.023±0.11	2.690±0.11	2.395±0.06	2.908±0.15	2.588±0.09	2.303±0.21	2.598±0.13	2.312±0.21	2.058±0.14	2.885±0.14	2.568±0.19	2.285±0.16
10mM	2.571±0.19	2.005±0.16	1.564±0.04	2.314±0.08	1.802±0.11	1.408±0.06	1.355±0.17	1.837±0.09	1.433±0.03	2.317±0.14	1.807±0.17	1.410±0.13
50mM	1.824±0.17	1.186±0.19	0.771±0.07	1.744±0.15	1.134±0.19	0.737±0.11	1.784±0.15	1.160±0.16	0.754±0.15	1.722±0.069	1.119±0.12	0.728±0.05
100mM	0.958±0.11	0.412±0.11	0.177±0.05	0.894±0.09	0.384±0.12	0.165±0.09	0.689±0.09	0.296±0.034	0.127±0.14	0.879±0.11	0.378±0.09	0.163±0.11

Table 6.3.2b: Effect of Lead on Nitrate Reductase Enzyme Activity (µmole $min^{-1}g^{-1}$ FW) in different moss at different concentrations for 3, 6, and 15 days of lab treatment

	Thuidium cyambifolium			*Rhynchostegiella divericatifolia*			*Fissidens anomalus*			*Isopterygium elegens*		
	3 days	**6 Days**	**15 days**	**3 days**	**6 Days**	**15 days**	**3 days**	**6 Days**	**15 days**	**3 days**	**6 Days**	**15 days**
Control	3.789±0.12	3.716±0.16	2.807±0.13	3.654±0.12	3.215±0.15	2.742±0.18	3.685±0.14	3.747±0.15	2.762±0.10	3.612±0.15	3.654±0.14	2.711±0.13
5mM	3.434±0.12	2.696±0.15	2.116±0.15	3.215±0.14	2.524±0.14	1.555±0.14	3.015±0.11	2.367±0.13	1.858±0.13	3.065±0.11	2.406±0.12	1.483±0.14
10mM	2.582±0.11	1.962±0.15	1.491±0.13	2.258±0.13	1.716±0.16	0.991±0.15	1.184±0.11	0.900±0.13	0.684±0.14	2.183±0.15	1.659±0.19	0.958±0.14
50mM	1.671±0.21	0.902±0.14	0.487±0.06	1.354±0.16	0.731±0.09	0.213±0.05	1.047±0.04	0.565±0.07	0.305±0.06	1.498±0.19	0.809±0.11	0.236±0.05
100mM	1.101±0.07	0.470±0.09	0.201±0.07	0.845±0.10	0.361±0.04	0.066±0.06	0.654±0.06	0.279±0.08	0.119±0.01	0.747±0.06	0.319±0.11	0.139±0.09

Table 6.3.2c: Effect of Copper on Nitrate Reductase Enzyme Activity (µmole $min^{-1}g^{-1}$ FW) in different moss at different concentrations for 3, 6, and 15 days of lab treatment

	Thuidium cyambifolium			*Rhynchostegiella divericatifolia*			*Fissidens anomalus*			*Isopterygium elegens*		
	3 days	**6 Days**	**15 days**	**3 days**	**6 Days**	**15 days**	**3 days**	**6 Days**	**15 days**	**3 days**	**6 Days**	**15 days**
Control	3.789±0.12	3.716±0.16	2.807±0.13	3.654±0.12	3.215±0.15	2.742±0.18	3.685±0.14	3.747±0.15	2.762±0.10	3.612±0.15	3.654±0.14	2.711±0.13
5mM	3.497±0.16	2.833±0.32	2.294±0.14	3.324±0.11	2.692±0.25	1.767±0.05	3.156±0.28	2.556±0.11	1.677±0.21	3.192±0.11	2.586±0.24	2.094±0.14
10mM	2.427±0.19	1.578±0.18	1.025±0.09	2.225±0.05	1.446±0.01	0.611±0.13	2.081±0.12	1.353±0.19	0.571±0.08	2.145±0.15	1.394±0.07	0.906±0.07
50mM	1.884±0.16	0.999±0.19	0.613±0.05	1.583±0.16	0.839±0.12	0.333±0.12	1.435±0.12	0.761±0.21	0.214±0.14	1.452±0.12	0.770±0.16	0.408±0.11
100mM	0.994±0.12	0.780±0.09	0.529±0.03	0.833±0.15	0.358±0.08	0.166±0.07	0.764±0.08	0.329±0.11	0.061±0.004	0.647±0.14	0.278±0.10	0.120±0.09

Table 6.3.2d: Effect of Cadmium on Nitrate Reductase Enzyme Activity (µmole $min^{-1}g^{-1}$ FW) in different moss at different concentrations for 3, 6, and 15 days of lab treatment

	Thuidium cyambifolium			*Rhynchostegiella divericatifolia*			*Fissidens anomalus*			*Isopterygium elegens*		
	3 days	**6 Days**	**15 days**	**3 days**	**6 Days**	**15 days**	**3 days**	**6 Days**	**15 days**	**3 days**	**6 Days**	**15 days**
Control	3.788±0.11	3.716±0.16	2.807±0.13	3.654±0.12	3.215±0.15	2.742±0.18	3.685±0.14	3.747±0.15	2.762±0.10	3.612±0.15	3.654±0.14	2.711±0.13
5mM	2.613±0.14	2.160±0.17	1.789±0.19	2.404±0.21	1.988±0.19	1.644±0.21	2.468±0.16	2.041±0.11	1.688±0.17	1.914±0.13	1.583±0.10	1.309±0.16
10mM	2.544±0.15	1.773±0.11	1.236±0.14	2.356±0.16	1.642±0.25	1.144±0.26	2.316±0.12	1.614±0.147	1.125±0.13	1.744±0.24	1.215±0.19	0.847±0.11
50mM	2.051±0.17	1.122±0.16	0.614±0.16	1.547±0.17	0.846±0.17	0.463±0.15	1.147±0.13	0.627±0.15	0.343±0.16	0.847±0.15	0.463±0.13	0.253±0.14
100mM	1.777±0.23	0.705±0.14	0.373±0.18	1.335±0.15	0.530±0.11	0.210±0.19	0.754±0.13	0.299±0.18	0.119±0.15	0.587±0.19	0.233±0.14	0.092±0.009

The study shows that higher concentrations of Zn led to a considerable decrease in NRA activity in mosses compared to the control. The most pronounced effects were detected at a 100mM concentration of Zn. High amounts of Zn have an adverse effect on the SH-group of the NR enzyme, leading to a decrease in its activity. The findings of this study corroborate the conclusions reached by previous researchers (Luna et al., 2000; Jayasri & Suthindhiran, 2017; Filova et al., 2021). In a previous study by Panda and Choudhury (2005), the impact of Zn on nitrate reductase activity was also highlighted, and their findings align with the results of the current study.

Lead has several harmful impacts on plant biosystems. In a previous study, Saxena et al. (2008) similarly investigated the impact of various lead concentrations on two mosses, i.e., *Rhodobryum roseum* and *Hypnum cupressforme.* They reported that a similar declining pattern was revealed at higher concentrations of Lead. Thus, the present results were also supported by his work. In *T. cyambifolium,* the NR activity decreased significantly with increasing metal concentration, with the highest decrease observed at 100 mM concentration of Pb. *R. divericatifolia* had a similar pattern of reduced activity, particularly when exposed to greater metal concentrations. This trend was also observed in *F. anomalus* and *I. elegens.*

The findings revealed the significant impact of Cu metal treatments on NRA activity, as depicted in Figure 6.3.2.3a-c. Saxena and Arfeen (2009) found similar results in their study on *Racomitrium crispulum*. Following a 15-day treatment with elevated copper (Cu) levels, a significant reduction in nitrate reductase activity (NRA) was noted. In the same way, Panda and Choudhury (2005) conducted a study to examine the impact of copper on the activity of nitrate reductase and the reactions to oxidative stress in the abundant moss *Polytrichum commune*. An interesting observation was that *Thuidium cyambifolium* exhibited a minor reduction in NR activity. The study shows that higher concentrations of Cu metal had a considerable negative impact on NRA activity in moss plants, with the most severe impacts reported at 100 mM Zn. The decrease in Nitrate reductase activity in moss treated with Cu at high concentrations (50 mM to 100 mM) can be related to either the suppression of enzyme synthesis or the decrease of enzyme activity. Therefore, the current findings align with the findings of renowned bryologists (Saxena & Arfeen, 2009; Harmens et al., 2013; Wang et al., 2024), who also verified that an increase in heavy metal content leads to a decrease in NR activity in mosses. In an earlier study, Munne-Bosch and Alegre (2002) examined how heavy metals impact the physiological responses of mosses. They found that environmental stress, including metal exposure, directly influences Nitrate Reductase (NR) activity.

Cadmium is a highly toxic heavy metal known for its harmful impacts on plant systems. Table 6.3.2d and Figure 6.3.2.4a-c show a significant declining trend of nitrate reductase activity in *T. cyambifolium* followed by *R. divericatifolia, F. anomalus,* and *I. elegens.* The nitrate reductase activity (NRA) of *T. cyambifolium* exhibited the slightest decrease after 15 days of cadmium (Cd) exposure, particularly at the highest concentration of 100 mM, compared to other mosses. Saxena and Arfeen (2009) reported similar findings in *Racomitrium crispulum*, where nitrate reductase activity (NRA) decreased after 15 days of treatment with higher doses of cadmium. A decrease in NRA after a prolonged period of metal treatments with various concentrations reported in the present study and similar declining patterns in NRA values were also confirmed by previous workers (Saxena & Arfeen, 2006b; Wahid et al., 2007; Lopez-Luna et al., 2012; Sainger et al., 2014).

The results indicate that NR activity in the studied mosses was reported in order to *T. cyambifolium* > *R. divericatifolia* > *F. anomalus* > *I. elegens.* The inhibition of nitrate reductase (NR) activity is thought to result from metal interactions at various sites, disrupting numerous enzymes containing functional sulfhydryl groups involved in NADH binding. This interference disrupts the protein synthesis pathway (Vyas & Puranik, 1995; Saxena & Arfeen, 2006b). Over prolonged incubation, NR activity declines even at lower metal concentrations, indicating that metal application inhibits nitrate reductase activity in plant tissues (Hu & Liang, 2015)

Earlier studies also revealed that environmental stress has an adverse effect on NRA (Gou et al., 2020; Isaza et al., 2020; Bian et al., 2020). Nitrate reductase is possibly the most responsive to water stress; as the water imbalance encouraged by metal treatment is responsible for decreased NR activity.

The findings demonstrate that the activity of NR in the examined mosses was observed in the following order: *T. cyambifolium* > *R. divericatifolia* > *F. anomalus* > *I. elegens*. Compared to *T. cyambifolium*, the other three mosses showed a significant decrease in NR activity when exposed to heavy metal treatments. Hence, the findings indicate that *T. cyambifolium* can be investigated as the predominant moss species in response to heavy metal treatments. The inhibition of NR activity is believed to be caused by the interaction of metals at various places, which inhibits a significant number of enzymes with a functional sulphydryl group involved in NADH binding. This interaction disrupts the protein synthesis pathway (Vyas & Puranik, 1995; Hussain et al., 2020; Rashid et al., 2021). During an extended incubation period, the activity of NR declines even at lower doses.

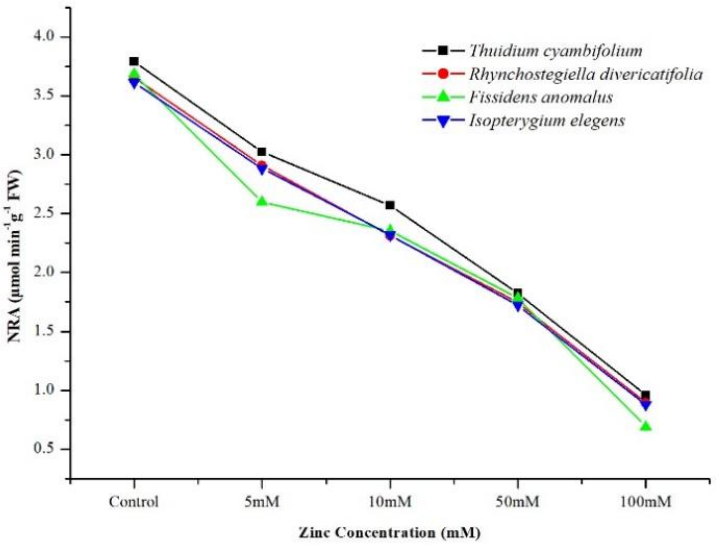

Figure 6.3.2.1a: Effect of Zinc (Zn) on NRA activity after 3 days of exposure

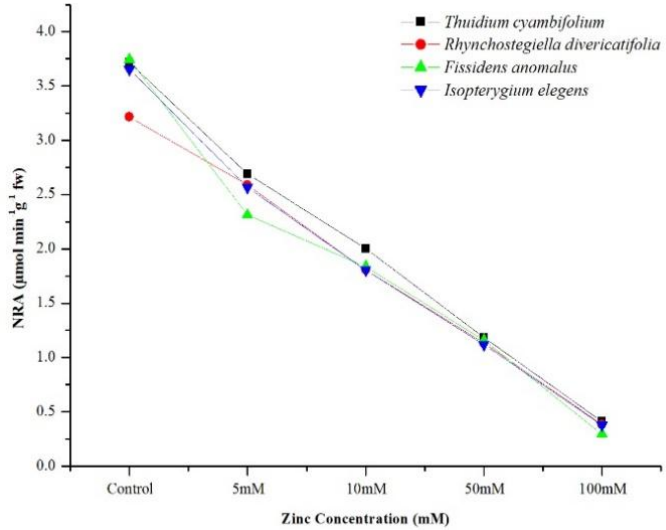

Figure 6.3.2.1b: Effect of Zinc (Zn) on NRA activity after 6 days of exposure

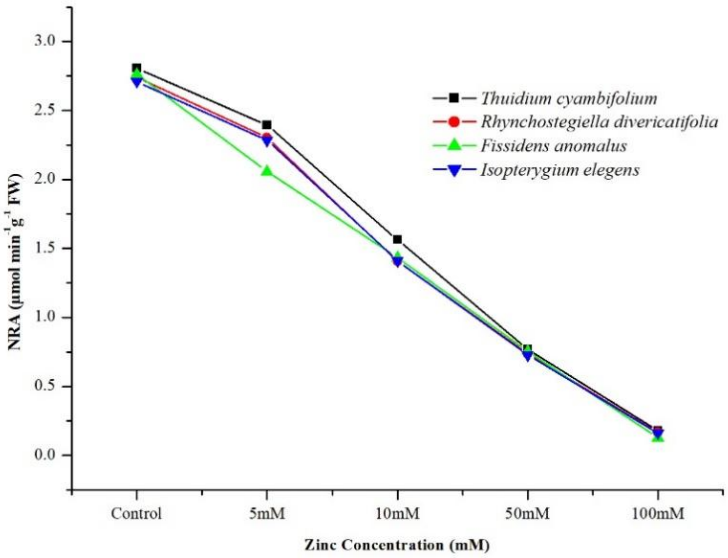

Figure 6.3.2.1c: Effect of Zinc (Zn) on NRA activity after 15 days of exposure

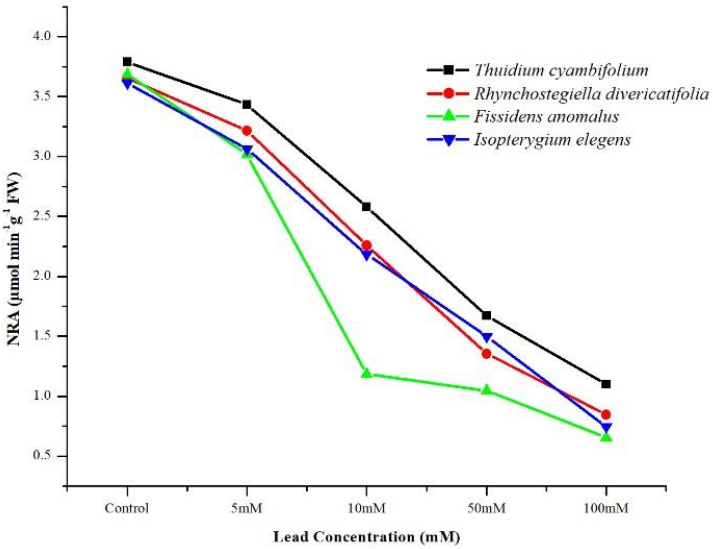

Figure 6.3.2.2a: Effect of Lead (Pb) on NRA activity after 3 days of exposure

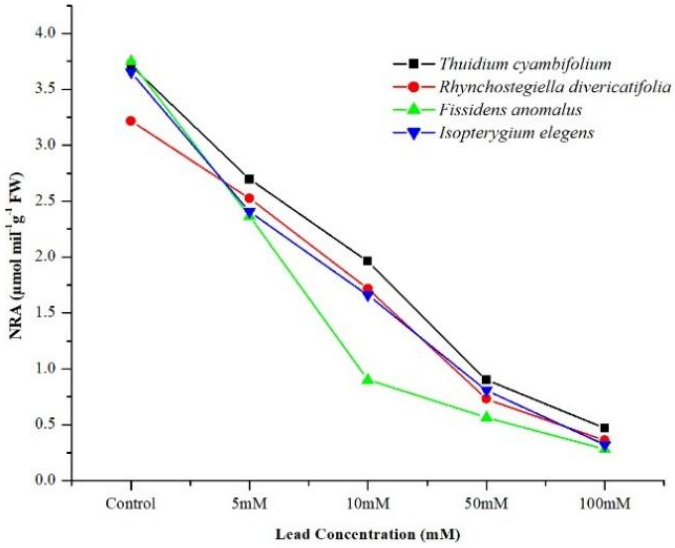

Figure 6.3.2.1b: Effect of Lead (Pb) on NRA activity after 6 days of exposure

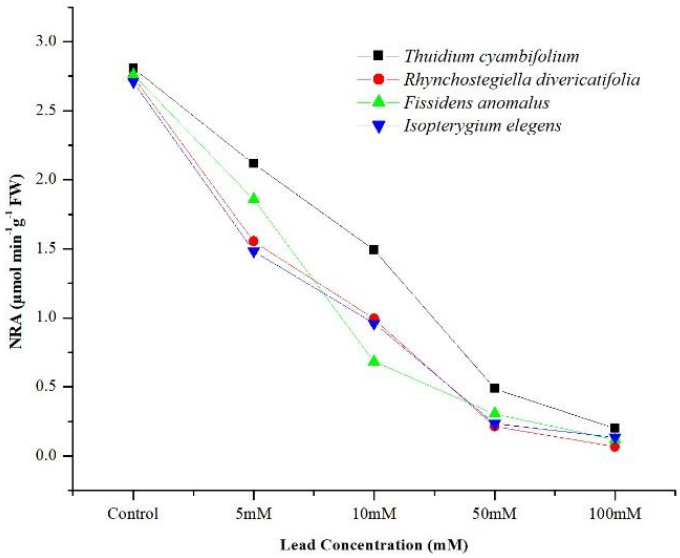

Figure 6.3.2.2c: Effect of Lead (Pb) on NRA activity after 15 days of exposure

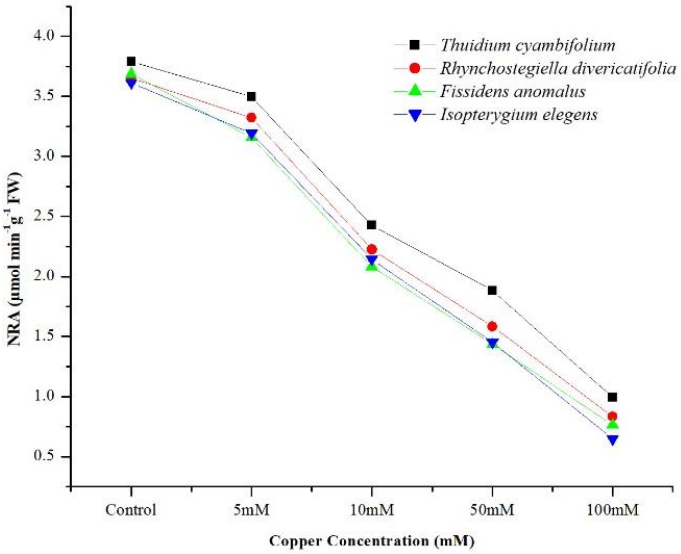

Figure 6.3.2.3a: Effect of Copper (Cu) on NRA activity after 3 days of exposure

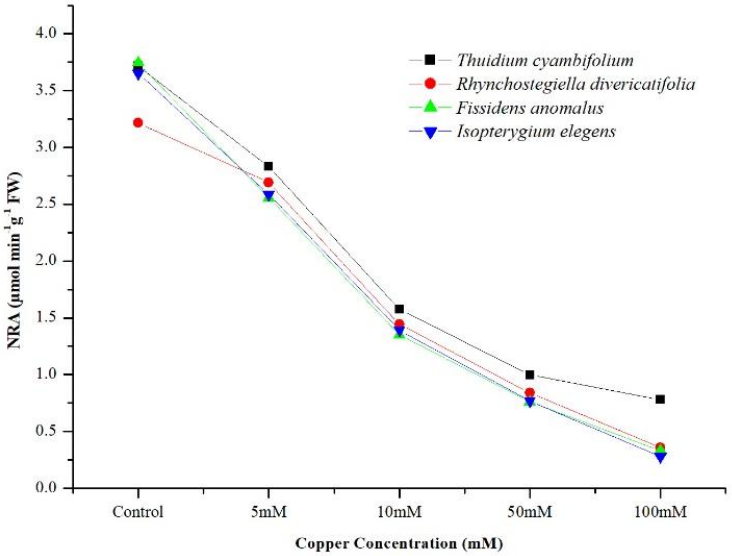

Figure 6.3.2.3b: Effect of Copper (Cu) on NRA activity after 6 days of exposure

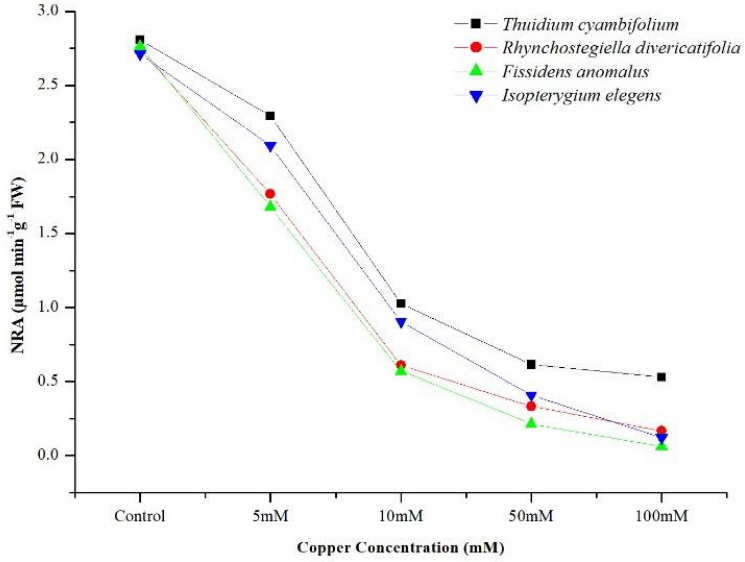

Figure 6.3.2.3c: Effect of Copper (Cu) on NRA activity after 15 days of exposure

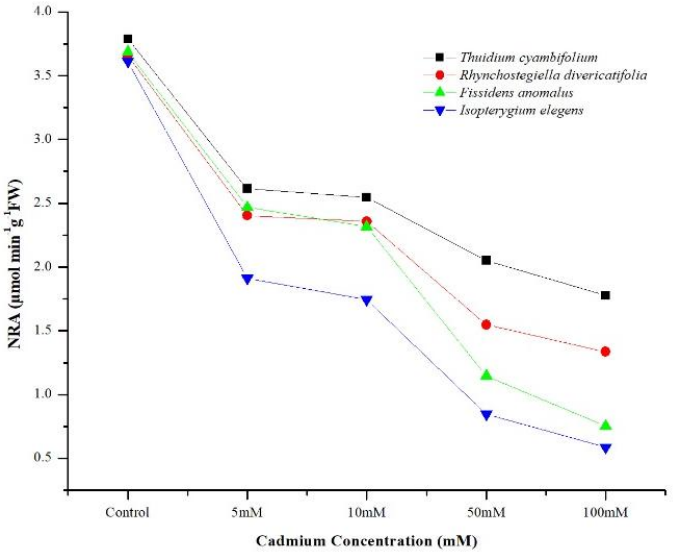

Figure 6.3.2.4a: Effect of Cadmium (Cd) on NRA activity after 3 days of exposure

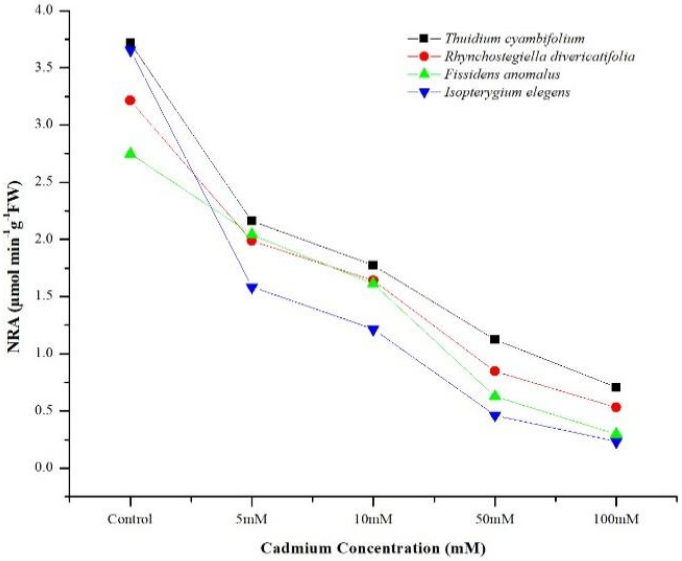

Figure 6.3.2.4b: Effect of Cadmium (Cd) on NRA activity after 6 days of exposure

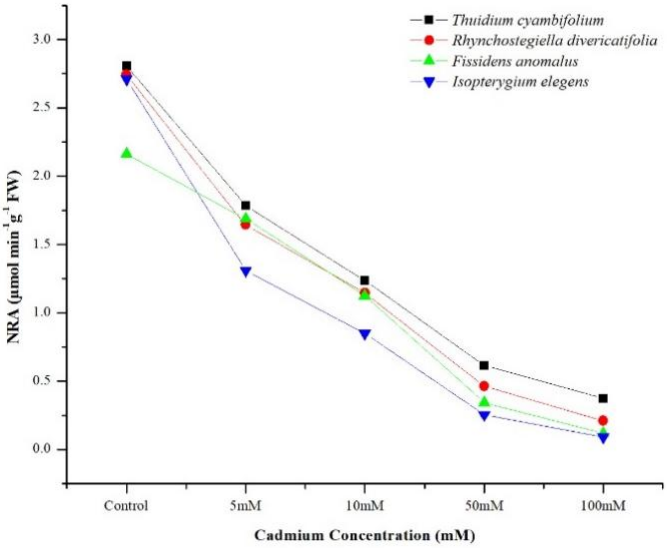

Figure 6.3.2.4c: Effect of Cadmium (Cd) on NRA activity after 15 days of exposure

6.3.3. EFFECT OF METALS ON PEROXIDASE ACTIVITY (POX) OF MOSSES

The effect of Copper, Lead, Zinc, and Cadmium studied on peroxidase activity (POX) in selected mosses, namely *Thuidium cyambifolium, Rhynchostegiella divericatifolia, Fissidens anomalous,* and *Isopterygium elegance*. During the present investigation, the POX activity was measured for 3 days, 6 days, and 15 days for both controlled conditions with different concentrations of metals (5mM, 10mM, 50mM, and 100mM metals treatment).

6.3.3.1 EFFECT OF ZINC ON PEROXIDASE ACTIVITY

In *Thuidium cyambifolium,* on the third day of Zn treatment, the peroxidase value increased at a 5mM Zn concentration (1.356 ΔOD min^{-1} gm^{-1} FW) compared to the control. This increase continued until a 10mM concentration (1.467 ΔOD min^{-1} gm^{-1} FW). The POX value decreased from 0.616 ΔOD min^{-1} gm^{-1} FW to 0.426 ΔOD min^{-1} gm^{-1} FW, with the concentration increased from 50mM to 100mM (Table 6.3.3.1 and Figure 6.3.3.1a). After the sixth day, the POX value was reported as 0.855 ΔOD min^{-1} gm^{-1} FW at a 5mM Zn concentration and found to be sharply decreased at 10 mM (0.565 ΔOD min^{-1} gm^{-1} FW), 50 mM (0.535 ΔOD min^{-1} gm^{-1} FW), and 100 mM (0.366 ΔOD min^{-1} gm^{-1} FW) (Figure 6.3.3.1b). After fifteen days of Zn treatment, the POX value was observed as 0.542 ΔOD min^{-1} gm^{-1} FW at 5 mM concentration and found to be sharply decreased at 10 mM (0.411 ΔOD min^{-1} gm^{-1} FW), 50 mM (0.333 ΔOD min^{-1} gm^{-1} FW), and 100 mM (0.178 ΔOD min^{-1} gm^{-1} FW) (Figure 6.3.3.1c).

In *Rhynchostegiella divericatifolia*, a declining trend was observed in peroxidase values for the different Zn concentrations. The peroxidase value was 1.233 ΔOD min^{-1} gm^{-1} FW on the third day at a 5 mM Zn concentration. It was decreased to 1.145 ΔOD min^{-1} gm^{-1} FW at 10 mM concentration. At 50 mM concentration, it was recorded as 0.574 ΔOD min^{-1} gm^{-1} FW, and at 100 mM, the POX value was reported as 0.486 ΔOD min^{-1} gm^{-1} FW (Table 6.3.3.1 and Figure 6.3.3.1a). After the sixth day, the POX value was reported as 0.825 ΔOD min^{-1} gm^{-1} FW at a 5mM Zn concentration and found to be sharply decreased at 10 mM (0.564 ΔOD min^{-1} gm^{-1} FW), 50 mM (0.402 ΔOD min^{-1} gm^{-1} FW), and 100 mM (0.379 ΔOD min^{-1} gm^{-1} FW) (Figure 6.3.3.1b). After fifteen days of Zn treatment, the POX value was observed as 0.523 ΔOD min^{-1} gm^{-1} FW at 5 mM concentration and found to be sharply decreased at 10 mM (0.345 ΔOD min^{-1} gm^{-1} FW), 50 mM (0.256 ΔOD min^{-1} gm^{-1} FW), and 100 mM (0.122 ΔOD min^{-1} gm^{-1} FW) (Figure 6.3.3.1c).

In *Fissidens anomalous,* on the third day of Zn treatment, the peroxidase value in comparison control increased to 1.123 ΔOD min^{-1} gm^{-1} FW at a 5mM Zn concentration. This increase continued

until a 10mM concentration (1.368 ΔOD min^{-1} gm^{-1} FW). The POX value declined from 0.684 ΔOD min^{-1} gm^{-1} FW to 0.537 ΔOD min^{-1} gm^{-1} FW when the concentration of Zn increased from 50mM to 100mM (Table 6.3.3.1 and Figure 6.3.3.1a). After the sixth day, the POX value was reported as 0.845 ΔOD min^{-1} gm^{-1} FW at a 5mM Zn concentration and found to be sharply decreased at 10 mM (0.574 ΔOD min^{-1} gm^{-1} FW), 50 mM (0.414 ΔOD min^{-1} gm^{-1} FW), and 100 mM (0.389 ΔOD min^{-1} gm^{-1} FW) (Figure 6.3.3.1b). After fifteen days of Zn treatment, the POX value was observed as 0.533 ΔOD min^{-1} gm^{-1} FW at 5 mM concentration and found to be sharply decreased at 10 mM (0.378 ΔOD min^{-1} gm^{-1} FW), 50 mM (0.268 ΔOD min^{-1} gm^{-1} FW), and 100 mM (0.113 ΔOD min^{-1} gm^{-1} FW) (Figure 6.3.3.1c).

In *Isopterygium elegens,* on the third day of Zn treatment, the peroxidase value increased at a 5mM Zn concentration (1.144 ΔOD min^{-1} gm^{-1} FW) compared to the control. This increase continued until a 10mM concentration (1.243 ΔOD min^{-1} gm^{-1} FW). The POX value decreased from 50mM to 100mM Zn concentration from 0.678 ΔOD min^{-1} gm^{-1} FW to 0.453 ΔOD min^{-1} gm^{-1} FW (Table 6.3.3.1 and Figure 6.3.3.1a). After the sixth day, the POX value was reported as 0.853 ΔOD min^{-1} gm^{-1} FW at a 5mM Zn concentration and found to be sharply decreased at 10 mM (0.512 ΔOD min^{-1} gm^{-1} FW), 50 mM (0.485 ΔOD min^{-1} gm^{-1} FW), and 100 mM (0.343 ΔOD min^{-1} gm^{-1} FW) (Figure 6.3.3.1b). After fifteen days of Zn treatment, the POX value was observed as 0.432 ΔOD min^{-1} gm^{-1} FW at 5 mM concentration and found to be sharply decreased at 10 mM (0.354 ΔOD min^{-1} gm^{-1} FW), 50 mM (0.203 ΔOD min^{-1} gm^{-1} FW), and 100 mM (0.132 ΔOD min^{-1} gm^{-1} FW) (Figure 6.3.3.1c).

6.3.3.2 EFFECT OF LEAD ON PEROXIDASE ACTIVITY

In *Thuidium cyambifolium,* on the third day of Pb treatment, the peroxidase value increased at a 5mM Pb concentration (1.293 ΔOD min^{-1} gm^{-1} FW) compared to the control. This increase continued until a 10mM concentration (1.417 ΔOD min^{-1} gm^{-1} FW). The POX value decreased from 0.713 ΔOD min^{-1} gm^{-1} FW to 0.572 ΔOD min^{-1} gm^{-1} FW with increased Pb concentration from 50mM to 100mM (Table 6.3.3.2 and Figure 6.3.3.2a). After the sixth day, the POX value was reported as 0.984 ΔOD min^{-1} gm^{-1} FW at a 5mM Pb concentration and found to be decreased at 10 mM (0.602 ΔOD min^{-1} gm^{-1} FW), 50 mM (0.582 ΔOD min^{-1} gm^{-1} FW), and 100 mM (0.366 ΔOD min^{-1} gm^{-1} FW) (Figure 6.3.3.2b). After fifteen days of Pb treatment, the POX value was observed as 0.653 ΔOD min^{-1} gm^{-1} FW at 5 mM concentration and found to be sharply decreased at 10 mM (0.361 ΔOD min^{-1} gm^{-1} FW), 50 mM (0.342 ΔOD min^{-1} gm^{-1} FW), and 100 mM (0.245 ΔOD min^{-1} gm^{-1} FW) (Figure 6.3.3.2c).

In *Rhynchostegiella divericatifolia*, on the third day of Pb treatment, the peroxidase value started to increase at a 5mM Pb concentration (1.241 ΔOD min^{-1} gm^{-1} FW) compared to the control. This increase continued until a 10mM concentration (1.386 ΔOD min^{-1} gm^{-1} FW). The POX value decreased from 0.688 ΔOD min^{-1} gm^{-1} FW to 0.542 ΔOD min^{-1} gm^{-1} FW with an increase in the concentration from 50 mM to 100 mM (Table 6.3.3.2 and Figure 6.3.3.2a). After the sixth day, the POX value was reported as 0.952 ΔOD min^{-1} gm^{-1} FW at a 5mM Pb concentration and found to be sharply decreased at 10 mM (0.598 ΔOD min^{-1} gm^{-1} FW), 50 mM (0.535 ΔOD min^{-1} gm^{-1} FW), and 100 mM (0.414 ΔOD min^{-1} gm^{-1} FW) (Figure 6.3.3.2b). After fifteen days of Pb treatment, the POX value was observed as 0.583 ΔOD min^{-1} gm^{-1} FW at 5 mM concentration and found to be sharply decreased at 10 mM (0.312 ΔOD min^{-1} gm^{-1} FW), 50 mM (0.299 ΔOD min^{-1} gm^{-1} FW), and 100 mM (0.201 ΔOD min^{-1} gm^{-1} FW) (Figure 6.3.3.2c).

In *Fissidens anomalus*, on the third day of Pb treatment, the peroxidase value started to increase at a 5mM Pb concentration (1.185 ΔOD min^{-1} gm^{-1} FW) compared to the control. This increase continued until a 10mM concentration (1.339 ΔOD min^{-1} gm^{-1} FW). The POX value decreased from 0.698 ΔOD min^{-1} gm^{-1} FW to 0.522 ΔOD min^{-1} gm^{-1} FW with the increase in the concentration of Pb from 50 to 100 mM (Table 6.3.3.2 and Figure 6.3.3.2a). After the sixth day, the POX value was reported as 0.928 ΔOD min^{-1} gm^{-1} FW at a 5mM Pb concentration and found to be sharply decreased at 10 mM (0.587 ΔOD min^{-1} gm^{-1} FW), 50 mM (0.527 ΔOD min^{-1} gm^{-1} FW), and 100 mM (0.385 ΔOD min^{-1} gm^{-1} FW) (Figure 6.3.3.2b). After fifteen days of Pb treatment, the POX value was observed as 0.635 ΔOD min^{-1} gm^{-1} FW at 5 mM concentration and found to be sharply decreased at 10 mM (0.341 ΔOD min^{-1} gm^{-1} FW), 50 mM (0.336 ΔOD min^{-1} gm^{-1} FW), and 100 mM (0.234 ΔOD min^{-1} gm^{-1} FW) (Figure 6.3.3.2c).

In *Isopterygium elegens*, on the third day of Pb treatment, the peroxidase value started to increase at a 5mM Pb concentration (1.020 ΔOD min^{-1} gm^{-1} FW) compared to the control. This increase continued until a 10mM concentration (1.245 ΔOD min^{-1} gm^{-1} FW). The POX value decreased from 0.578 ΔOD min^{-1} gm^{-1} FW to 0.514 ΔOD min^{-1} gm^{-1} FW with increased Pb concentration from 50 mM to 100 mM (Table 6.3.3.2 and Figure 6.3.3.2a). After the sixth day, the POX value was reported as 0.961 ΔOD min^{-1} gm^{-1} FW at a 5mM Pb concentration and found to be sharply decreased at 10 mM (0.548 ΔOD min^{-1} gm^{-1} FW), 50 mM (0.498 ΔOD min^{-1} gm^{-1} FW), and 100 mM (0.454 ΔOD min^{-1} gm^{-1} FW) (Figure 6.3.3.2b). After fifteen days of Pb treatment, the POX value was observed as 0.498 ΔOD min^{-1} gm^{-1} FW at 5 mM concentration and found to be sharply decreased at 10 mM (0.356 ΔOD min^{-1} gm^{-1} FW), 50 mM (0.312 ΔOD min^{-1} gm^{-1} FW), and 100 mM (0.256 ΔOD min^{-1} gm^{-1} FW) (Figure 6.3.3.2c).

6.3.3.3 EFFECT OF COPPER ON PEROXIDASE ACTIVITY

Compared to the control, the peroxidase value in *Thuidium cyambifolium* increased to 1.132 ΔOD min-1 gm-1 FW on the third day of Pb treatment with 5mM Cu concentration. The observed rise persisted until reaching a concentration of 10mM (1.321 ΔOD min-1 gm-1 FW). The POX value declined from 0.782 ΔOD min-1 gm-1 FW to 0.595 ΔOD min-1 gm-1 FW with increased Cu concentration from 50 mM to 100 mM (Table 6.3.3.3 and Figure 6.3.3.3a). On the sixth day, the peroxidase value rose at a 5mM Cu concentration (0.664 ΔOD min-1 gm-1 FW) compared to the control medium. This increase persisted until reaching a concentration of 10mM (0.878 ΔOD min-1 gm-1 FW). The POX value declined from 0.514 ΔOD min-1 gm-1 FW to 0.389 ΔOD min-1 gm-1 FW with increased Cu concentration from 50 mM to 100 mM (Figure 6.3.3.3b). Fifteen days later, the peroxidase value rose when exposed to a 5mM Cu concentration (0.425 ΔOD min-1 gm-1 FW) compared to the control. This increase persisted until reaching a concentration of 10mM (0.554 ΔOD min-1 gm-1 FW). The POX value declined from 0.246 ΔOD min-1 gm-1 FW to 0.234 ΔOD min-1 gm-1 FW with increased Cu concentration from 50 mM to 100 mM (Figure 6.3.3.3c).

In *Rhynchostegiella divericatifolia*, on the third day of Cu treatment, the peroxidase value increased at a 5mM Cu concentration (1.022 ΔOD min^{-1} gm^{-1} FW) compared to the control. This increase continued until a 10mM concentration (1.172 ΔOD min^{-1} gm^{-1} FW). The POX value decreased from 0.652 ΔOD min^{-1} gm^{-1} FW to 0.554 ΔOD min^{-1} gm^{-1} FW with the increase in the Cu concentration from 50 mM to 100 mM (Table 6.3.3.3 and Figure 6.3.3.3a). After the sixth day, the POX value was reported as 0.726 ΔOD min^{-1} gm^{-1} FW at a 5mM Cu concentration and found to be sharply decreased at 10 mM (0.511 ΔOD min^{-1} gm^{-1} FW), 50 mM (0.435 ΔOD min^{-1} gm^{-1} FW), and 100 mM (0.294 ΔOD min^{-1} gm^{-1} FW) (Figure 6.3.3.3b). After fifteen days of Cu treatment, the POX value was observed as 0.489 ΔOD min^{-1} gm^{-1} FW at 5 mM concentration and found to be sharply decreased at 10 mM (0.399 ΔOD min^{-1} gm^{-1} FW), 50 mM (0.203 ΔOD min^{-1} gm^{-1} FW), and 100 mM (0.199 ΔOD min^{-1} gm^{-1} FW) (Figure 6.3.3.3c).

In *Fissidens anomalus*, on the third day of Cu treatment, the POX value was reported as 1.009 ΔOD min^{-1} gm^{-1} FW at a 5mM Cu concentration and found to be sharply decreased at 10 mM (0.982 ΔOD min^{-1} gm^{-1} FW), 50 mM (0.552 ΔOD min^{-1} gm^{-1} FW), and 100 mM (0.483 ΔOD min^{-1} gm^{-1} FW) (Table 6.3.3.3 and Figure 6.3.3.3a). After the sixth day, the POX value was reported as 0.621 ΔOD min^{-1} gm^{-1} FW at a 5mM Cu concentration and found to be sharply decreased at 10 mM (0.534 ΔOD min^{-1} gm^{-1} FW), 50 mM (0.332 ΔOD min^{-1} gm^{-1} FW), and 100 mM (0.195 ΔOD min^{-1} gm^{-1} FW) (Figure 6.3.3.3b). After fifteen days of Cu treatment, the POX value was observed as 0.451 ΔOD min-

^{1} gm^{-1} FW at 5 mM concentration and found to be sharply decreased at 10 mM (0.358 ΔOD min^{-1} gm^{-1} FW), 50 mM (0.257 ΔOD min^{-1} gm^{-1} FW), and 100 mM (0.212 ΔOD min^{-1} gm^{-1} FW) (Figure 6.3.3.3c).

In *Isopterygium elegens,* on the third day of Cu treatment, the peroxidase value started to increase at a 5mM Cu concentration (1.032 ΔOD min^{-1} gm^{-1} FW) compared to the control. This increase continued until a 10mM concentration (1.297 ΔOD min^{-1} gm^{-1} FW). The POX value decreased from 0.689 ΔOD min^{-1} gm^{-1} FW to 0.489 ΔOD min^{-1} gm^{-1} FW with an increased concentration of Cu from 50 mM to 100 mM (Table 6.3.3.3 and Figure 6.3.3.3a). After the sixth day, the POX value was reported as 0.898 ΔOD min^{-1} gm^{-1} FW at a 5mM Cu concentration and found to be sharply decreased at 10 mM (0.545 ΔOD min^{-1} gm^{-1} FW), 50 mM (0.468 ΔOD min^{-1} gm^{-1} FW), and 100 mM (0.313 ΔOD min^{-1} gm^{-1} FW) (Figure 6.3.3.3b). After fifteen days of Cu treatment, the POX value was observed as 0.467 ΔOD min^{-1} gm^{-1} FW at 5 mM concentration and found to be sharply decreased at 10 mM (0.378 ΔOD min^{-1} gm^{-1} FW), 50 mM (0.235 ΔOD min^{-1} gm^{-1} FW), and 100 mM (0.233 ΔOD min^{-1} gm^{-1} FW) (Figure 6.3.3.3c).

6.3.3.4 EFFECT OF CADMIUM ON PEROXIDASE ACTIVITY

In *Thuidium cyambifolium,* on the third day of Cd treatment, the peroxidase value started to increase at a 5mM Cd concentration (0.967 ΔOD min^{-1} gm^{-1} FW) compared to the control. This increase continued until a 10mM concentration (1.025 ΔOD min^{-1} gm^{-1} FW). When the concentration of Cd rose from 50 mM to 100 mM, the POX value dropped from 0.777 ΔOD min^{-1} gm^{-1} FW to 0.674 ΔOD min^{-1} gm^{-1} FW (Table 6.3.3.4 and Figure 6.3.3.4a). After the sixth day, the POX value was reported as 0.992 ΔOD min^{-1} gm^{-1} FW at a 5mM Cd concentration and found to be sharply decreased at 10 mM (0.673 ΔOD min^{-1} gm^{-1} FW), 50 mM (0.589 ΔOD min^{-1} gm^{-1} FW), and 100 mM (0.498 ΔOD min^{-1} gm^{-1} FW) (Figure 6.3.3.4b). After fifteen days of Cd treatment, the POX value was observed as 0.651 ΔOD min^{-1} gm^{-1} FW at 5 mM concentration and found to be sharply decreased at 10 mM (0.586 ΔOD min^{-1} gm^{-1} FW), 50 mM (0.462 ΔOD min^{-1} gm^{-1} FW), and 100 mM (0.423 ΔOD min^{-1} gm^{-1} FW) (Figure 6.3.3.4c).

In *Rhynchostegiella divericatifolia*, a declining trend was observed in peroxidase values for the different Cd concentrations. The peroxidase value was 0.857 ΔOD min-1 gm-1 FW on the third day at a 5 mM Cd concentration. This increase continued until a 10mM concentration (0.897 ΔOD min^{-1} gm^{-1} FW). When the concentration of Cd rose from 50 mM to 100 mM, the POX value dropped from 0.698 ΔOD min^{-1} gm^{-1} FW to 0.568 ΔOD min^{-1} gm^{-1} FW (Table 6.3.3.4 and Figure 6.3.3.4a).

After the sixth day, the POX value was reported as 0.921 ΔOD min^{-1} gm^{-1} FW at a 5mM Cd concentration and found to be sharply decreased at 10 mM (0.598 ΔOD min^{-1} gm^{-1} FW), 50 mM (0.586 ΔOD min^{-1} gm^{-1} FW), and 100 mM (0.479 ΔOD min^{-1} gm^{-1} FW) (Figure 6.3.3.4b). After fifteen days of Cd treatment, the POX value was observed as 0.589 ΔOD min^{-1} gm^{-1} FW at 5 mM concentration and found to be sharply decreased at 10 mM (0.522 ΔOD min^{-1} gm^{-1} FW), 50 mM (0.367 ΔOD min^{-1} gm^{-1} FW), and 100 mM (0.356 ΔOD min^{-1} gm^{-1} FW) (Figure 6.3.3.4c).

In *Fissidens anomalus*, on the third day of Cd treatment, the peroxidase value started to increase at a 5mM Cd concentration (0.715 ΔOD min^{-1} gm^{-1} FW) and found to be sharply decreased at 10 mM (0.648 ΔOD min^{-1} gm^{-1} FW), 50 mM (0.589 ΔOD min^{-1} gm^{-1} FW), and 100 mM (0.345 ΔOD min^{-1} gm^{-1} FW) (Table 6.3.3.4 and Figure 6.3.3.4a). After the sixth day, the POX value was reported as 0.987 ΔOD min^{-1} gm^{-1} FW at a 5mM Cd concentration and found to be sharply decreased at 10 mM (0.588 ΔOD min^{-1} gm^{-1} FW), 50 mM (0.555 ΔOD min^{-1} gm^{-1} FW), and 100 mM (0.397 ΔOD min^{-1} gm^{-1} FW) (Figure 6.3.3.4b). After fifteen days of Cd treatment, the POX value was observed as 0.552 ΔOD min^{-1} gm^{-1} FW at 5 mM concentration and found to be sharply decreased at 10 mM (0.501 ΔOD min^{-1} gm^{-1} FW), 50 mM (0.402 ΔOD min^{-1} gm^{-1} FW), and 100 mM (0.322 ΔOD min^{-1} gm^{-1} FW) (Figure 6.3.3.4c).

In *Isopterygium elegens,* on the third day of Cd treatment, the peroxidase value started to increase at a 5mM Cd concentration (0.884 ΔOD min^{-1} gm^{-1} FW) compared to the control. This increase continued until a 10mM concentration (0.985 ΔOD min^{-1} gm^{-1} FW). This increase continued until a 10mM concentration (0.897 ΔOD min^{-1} gm^{-1} FW). When the concentration of Cd rose from 50 mM to 100 mM, the POX value dropped from 0.648 ΔOD min^{-1} gm^{-1} FW to 0.589 ΔOD min^{-1} gm^{-1} FW (Table 6.3.3.4 and Figure 6.3.3.4a). After the sixth day, the POX value was reported as 0.933 ΔOD min^{-1} gm^{-1} FW at a 5mM Cd concentration and found to be sharply decreased at 10 mM (0.568 ΔOD min^{-1} gm^{-1} FW), 50 mM (0.512 ΔOD min^{-1} gm^{-1} FW), and 100 mM (0.458 ΔOD min^{-1} gm^{-1} FW) (Figure 6.3.3.4b). After fifteen days of Cd treatment, the POX value was observed as 0.554 ΔOD min^{-1} gm^{-1} FW at 5 mM concentration and found to be sharply decreased at 10 mM (0.432 ΔOD min^{-1} gm^{-1} FW), 50 mM (0.389 ΔOD min^{-1} gm^{-1} FW), and 100 mM (0.367 ΔOD min^{-1} gm^{-1} FW) (Figure 6.3.3.4c).

Table 6.3.3.1: Effect of Zinc on Peroxidase Enzyme Activity (ΔOD $min^{-1}gm^{-1}FW$) at various concentrations after 3, 6, and 15 days of lab treatment

	Thuidium cyambifolium			***Rhynchostegiella divericatifolia***			***Fissidens anomalus***			***Isopterygium elegens***		
	3 day	**6 Day**	**15 day**	**3 day**	**6 Day**	**15 day**	**3 day**	**6 Day**	**15 day**	**3 day**	**6 Day**	**15 day**
Control	0.658	0.575	0.441	0.663	0.578	0.453	0.652	0.512	0.412	0.686	0.585	0.446
	±0.008	±0.005	±0.002	±0.008	±0.007	±0.006	±0.003	±0.006	±0.008	±0.004	±0.008	±0.007
5 mM	1.356	0.855	0.542	1.233	0.825	0.523	1.123	0.845	0.533	1.144	0.853	0.432
	±0.008	±0.004	±0.006	±0.007	±0.001	±0.005	±0.007	±0.008	±0.007	±0.004	±0.005	±0.009
10 mM	1.467	0.565	0.411	1.145	0.564	0.345	1.368	0.574	0.378	1.243	0.512	0.354
	±0.007	±0.006	±0.004	±0.007	±0.002	±0.003	±0.005	±0.003	±0.008	±0.006	±0.008	±0.008
50 mM	0.616	0.535	0.333	0.574	0.402	0.256	0.684	0.414	0.268	0.678	0.485	0.203
	±0.003	±0.007	±0.008	±0.005	±0.009	±0.007	±0.009	±0.006	±0.005	±0.008	±0.003	±0.007
100 mM	0.426	0.366	0.178	0.486	0.379	0.122	0.537	0.389	0.113	0.453	0.343	0.132
	±0.008	±0.009	±0.005	±0.005	±0.007	±0.005	±0.008	±0.005	±0.007	±0.008	±0.007	±0.008

Table 6.3.3.2: Effect of Lead on Peroxidase Enzyme Activity (ΔOD $min^{-1}gm^{-1}FW$) at various concentrations after 3, 6, and 15 days of lab treatment

	Thuidium cyambifolium			***Rhynchostegiella divericatifolia***			***Fissidens anomalus***			***Isopterygium elegens***		
	3 day	**6 Day**	**15 day**	**3 day**	**6 Day**	**15 day**	**3 day**	**6 Day**	**15 day**	**3 day**	**6 Day**	**15 day**
Control	0.658 ±0.008	0.575 ±0.005	0.441 ±0.002	0.663 ±0.008	0.578 ±0.007	0.453 ±0.006	0.652 ±0.003	0.512 ±0.006	0.412 ±0.008	0.686 ±0.004	0.585 ±0.008	0.446 ±0.007
5 mM	1.293 ±0.007	0.984 ±0.008	0.653 ±0.007	1.386 ±0.006	0.952 ±0.008	0.583 ±0.005	1.185 ±0.005	0.928 ±0.007	0.635 ±0.006	1.02 ±0.007	0.961 ±0.004	0.498 ±0.007
10 mM	1.417 ±0.009	0.602 ±0.008	0.361 ±0.006	1.241 ±0.008	0.598 ±0.004	0.312 ±0.006	1.339 ±0.004	0.587 ±0.009	0.341 ±0.005	1.245 ±0.005	0.548 ±0.008	0.356 ±0.009
50 mM	0.713 ±0.007	0.582 ±0.003	0.342 ±0.007	0.688 ±0.007	0.535 ±0.004	0.299 ±0.008	0.698 ±0.007	0.527 ±0.005	0.336 ±0.007	0.578 ±0.006	0.498 ±0.004	0.312 ±0.006
100 mM	0.572 ±0.008	0.484 ±0.007	0.243 ±0.008	0.542 ±0.008	0.414 ±0.008	0.201 ±0.002	0.522 ±0.007	0.385 ±0.009	0.234 ±0.002	0.514 ±0.007	0.454 ±0.007	0.256 ±0.005

Table 6.3.3.3: Effect of Copper on Peroxidase Enzyme Activity (ΔOD $min^{-1}gm^{-1}FW$) at various concentrations after 3, 6, and 15 days of lab treatment

	Thuidium cyambifolium			***Rhynchostegiella divericatifolia***			***Fissidens anomalus***			***Isopterygium elegens***		
	3 day	**6 Day**	**15 day**	**3 day**	**6 Day**	**15 day**	**3 day**	**6 Day**	**15 day**	**3 day**	**6 Day**	**15 day**
Control	0.658 ±0.008	0.575 ±0.005	0.441 ±0.002	0.663 ±0.008	0.578 ±0.007	0.453 ±0.006	0.652 ±0.003	0.512 ±0.006	0.412 ±0.008	0.686 ±0.004	0.585 ±0.008	0.446 ±0.007
5 mM	1.132 ±0.004	0.664 ±0.007	0.425 ±0.004	1.022 ±0.003	0.726 ±0.009	0.489 ±0.006	1.009 ±0.004	0.621 ±0.007	0.451 ±0.006	1.032 ±0.007	0.898 ±0.008	0.467 ±0.009
10 mM	1.321 ±0.006	0.878 ±0.007	0.554 ±0.004	1.172 ±0.005	0.511 ±0.007	0.399 ±0.005	0.982 ±0.009	0.534 ±0.003	0.358 ±0.004	1.297 ±0.009	0.545 ±0.008	0.378 ±0.006
50 mM	0.782 ±0.007	0.514 ±0.006	0.246 ±0.002	0.652 ±0.006	0.435 ±0.005	0.203 ±0.008	0.552 ±0.009	0.332 ±0.006	0.257 ±0.005	0.689 ±0.004	0.468 ±0.008	0.233 ±0.006
100 mM	0.595 ±0.002	0.389 ±0.006	0.234 ±0.007	0.454 ±0.008	0.294 ±0.002	0.199 ±0.006	0.483 ±0.005	0.195 ±0.008	0.212 ±0.003	0.489 ±0.009	0.313 ±0.005	0.235 ±0.007

Table 6.3.3.4 Effect of Cadmium on Peroxidase Enzyme Activity (ΔOD $min^{-1}gm^{-1}FW$) at various concentrations after 3, 6, and 15 days of lab treatment

	Thuidium cyambifolium			***Rhynchostegiella divericatifolia***			***Fissidens anomalus***			***Isopterygium elegens***		
	3 day	**6 Day**	**15 day**	**3 day**	**6 Day**	**15 day**	**3 day**	**6 Day**	**15 day**	**3 day**	**6 Day**	**15 day**
Control	0.658 ±0.008	0.575 ±0.005	0.441 ±0.002	0.663 ±0.008	0.578 ±0.007	0.453 ±0.006	0.652 ±0.003	0.512 ±0.006	0.412 ±0.008	0.686 ±0.004	0.585 ±0.008	0.446 ±0.007
5 mM	0.967 ±0.008	0.992 ±0.002	0.651 ±0.009	0.857 ±0.005	0.921 ±0.008	0.589 ±0.005	0.715 ±0.004	0.987 ±0.004	0.552 ±0.006	0.884 ±0.005	0.933 ±0.003	0.554 ±0.004
10 mM	1.025 ±0.003	0.673 ±0.003	0.586 ±0.002	0.897 ±0.005	0.598 ±0.007	0.522 ±0.004	0.648 ±0.002	0.588 ±0.004	0.501 ±0.003	0.895 ±0.002	0.568 ±0.007	0.432 ±0.002
50 mM	0.777 ±0.005	0.589 ±0.003	0.462 ±0.002	0.698 ±0.004	0.586 ±0.009	0.367 ±0.008	0.589 ±0.003	0.555 ±0.002	0.402 ±0.004	0.648 ±0.005	0.512 ±0.008	0.389 ±0.004
100 mM	0.674 ±0.003	0.498 ±0.003	0.423 ±0.002	0.568 ±0.003	0.479 ±0.005	0.356 ±0.006	0.345 ±0.001	0.397 ±0.003	0.322 ±0.004	0.589 ±0.009	0.458 ±0.006	0.367 ±0.006

The study shows that the peroxidase activity during 3, 6, and 15 days was significantly decreased in *Thuidium cyambifolium*. Interestingly, *Rhynchostegiella divericatifolia*, *Isopterygium elegance*, and *Fissidens anomalous* reported a similar decreasing pattern. These findings indicate that Zinc treatment generally suppresses peroxidase activity in moss plants, with the effect becoming more pronounced over time, except for the unique response seen in *Thuidium cyambifolium* (Table 6.3.3.1 and Figures 6.3.3.1 a-l). Previous studies have experimentally demonstrated that environmental stress, such as metal exposure, directly affects Peroxidase activity (POD) (Munné-Bosch & Alegre, 2002; Saxena & Arfeen, 2009; Onele et al., 2018). Its activity varies depending on the species and the metals applied, and an increase in POD activity is often considered a stress management enzyme (Reddy & Prasad, 1992; Shaw, 1995; Aydoğan et al., 2017). In previous studies, it has been confirmed that the high value of stress enzymes might be due to oxidative stress created during the time of equilibrium between the reactive oxygen species (ROS) and antioxidant becomes unbalanced due to abnormal intracellular behavior due to environmental events during season to season (Barenyi & Karause, 1985; Mittler & Zilinskas, 1994).

These findings indicate that Lead treatment generally suppresses POD activity in moss plants, with the effect becoming more pronounced over time, except for the unique response seen in *Thuidium cyambifolium***.** Previously, Saxena et al. (2008) have also reported a similar inclining and declining pattern in POD on two different mosses, i.e., *Rhodobryum roseum* and *Hypnum cupessiforme*, in their study. Some previous workers also explored the fact that the peroxidase enzyme plays an important role in plant growth. Pollution load increases the peroxidase activity, which can be inferred to be due to reactive oxygen generated under stress caused by air pollution (Rai & Panda, 2015; Bansal et al., 2016), and the scavenging properties of POD seem to be enhanced under pollution stress (Elstner & Osswald, 1994). The findings of the present work also follow Okamoto et al., 2001, and Saxena and Arfeen, 2009, who observed that high POX activity in plants might indicate oxidative stresses.

As some of the sampling sites of the present study were urban and agricultural areas, they might be responsible for the source of copper. Copper (Cu) is a crucial micronutrient for plant growth and development. However, excessive Cu can disrupt several physiological processes, including the synthesis of pigments, the photosynthetic process, the metabolism of nitrogen and protein, and the absorption of minerals (Demirevska Kepova et al., 2004; Kumar et al., 2021; Zeng et al., 2021).

Cadmium was found to have a less effective impact on peroxidase activity than other metal concentrations. A more robust Cd enrichment capacity exhibited a better tolerance to Cd stress due to its efficient antioxidant defence system (Hassan et al., 2020). As the metal concentrations were enhanced, the peroxidase values were reduced, indicating stress in physiological tolerance. Similar observations were also reported by Okamoto et al., 2001, and Saxena and Arfeen, 2009.

The results indicate that the peroxidase activity in the mosses studied was observed in the order *T. cyambifolium* > *R. divericatifolia* > *F. anomalous*> *I. elegance.* When compared to the four tested mosses, *T. cyambifolium* exhibited greater tolerance. Therefore, due to these findings, T. cyambifolium was selected for additional biomonitoring research.

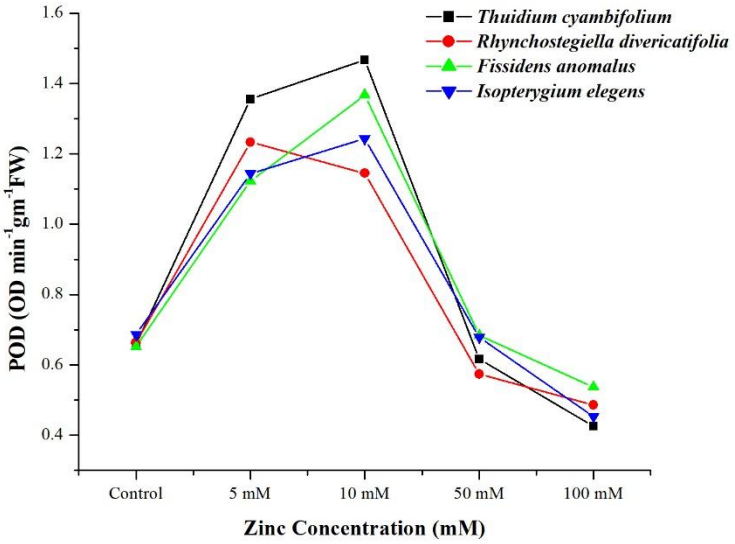

Figure 6.3.3.1a: Effect of Zinc (Zn) on Peroxidase Enzyme Activity after 3 days of exposure

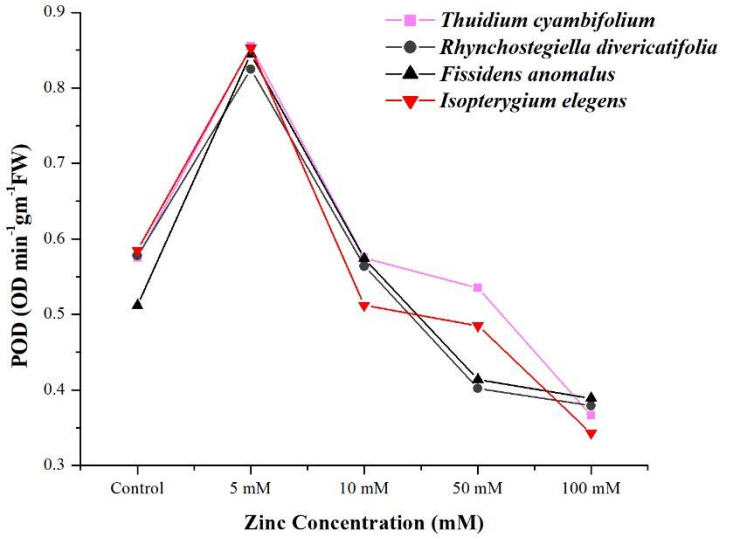

Figure 6.3.3.1b: Effect of Zinc (Zn) on Peroxidase Enzyme Activity after 6 days of exposure

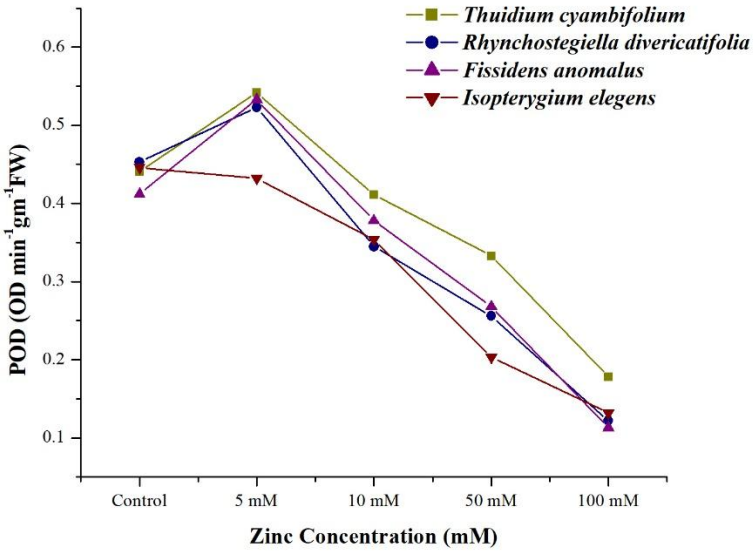

Figure 6.3.3.1c: Effect of Zinc (Zn) on Peroxidase Enzyme Activity after 15 days of exposure

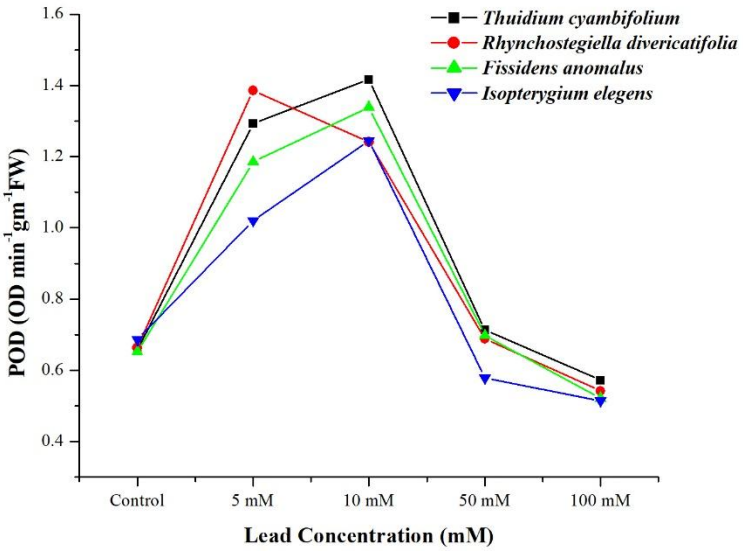

Figure 6.3.3.2a: Effect of Lead (Pb) on Peroxidase Enzyme Activity after 3 days of exposure

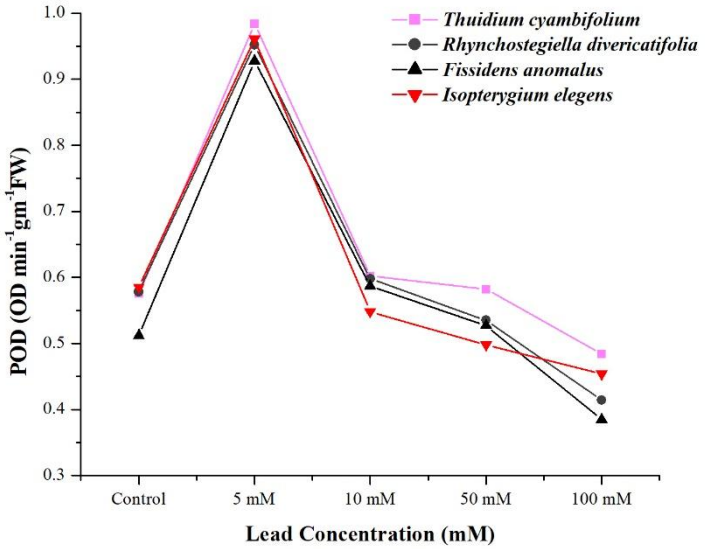

Figure 6.3.3.2b: Effect of Lead (Pb) on Peroxidase Enzyme Activity after 6 days of exposure

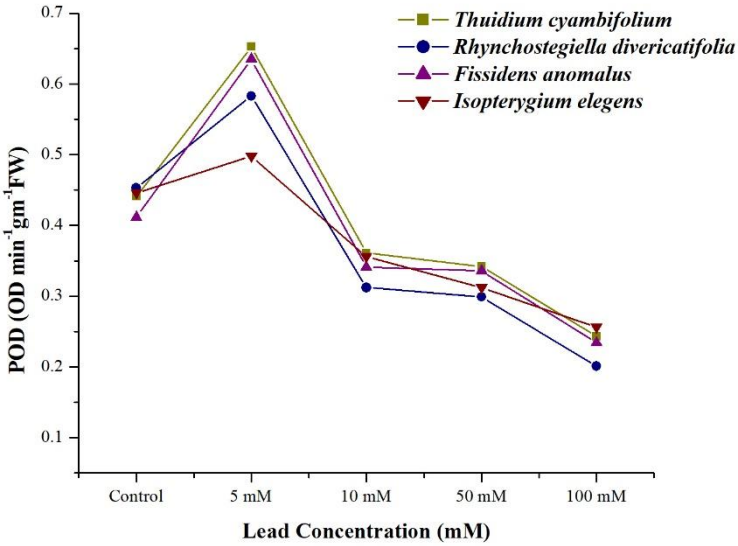

Figure 6.3.3.2c: Effect of Lead (Pb) on Peroxidase Enzyme Activity after 15 days of exposure

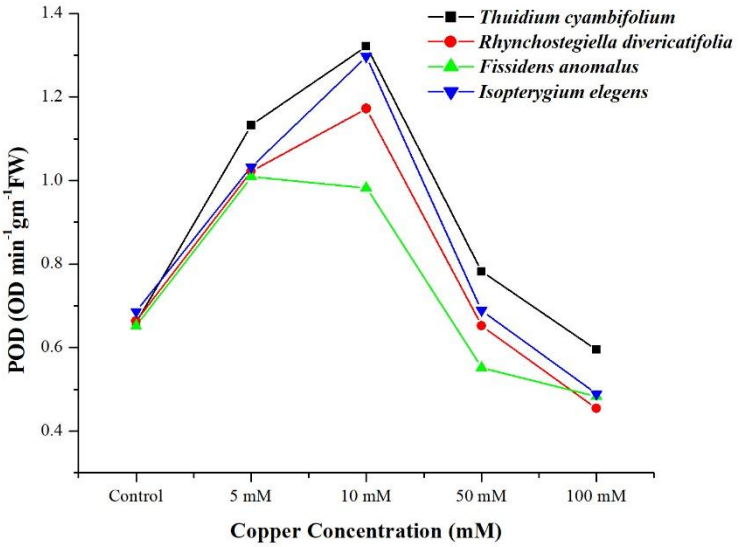

Figure 6.3.3.2a: Effect of Copper (Cu) on Peroxidase Enzyme Activity after 3 days of exposure

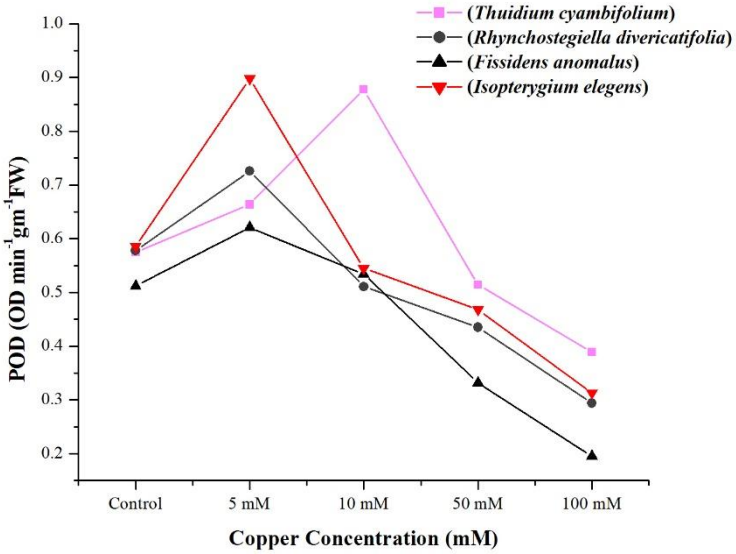

Figure 6.3.3.2b: Effect of Copper (Cu) on Peroxidase Enzyme Activity after 6 days of exposure

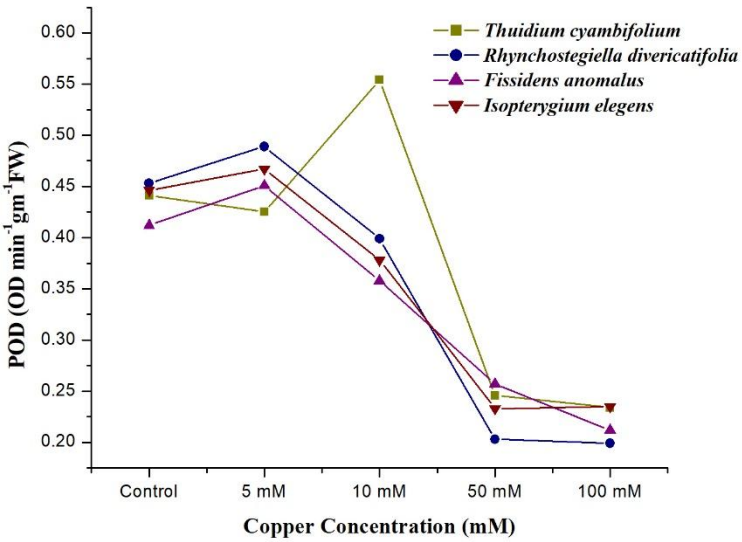

Figure 6.3.3.2c: Effect of Copper (Cu) on Peroxidase Enzyme Activity after 15 days of exposure

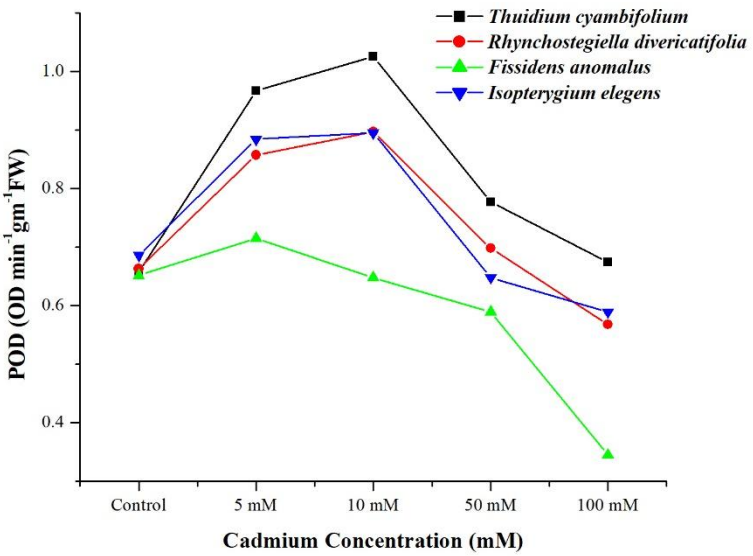

Figure 6.3.3.2a: Effect of Cadmium (Cd) on Peroxidase Enzyme Activity after 3 days of exposure

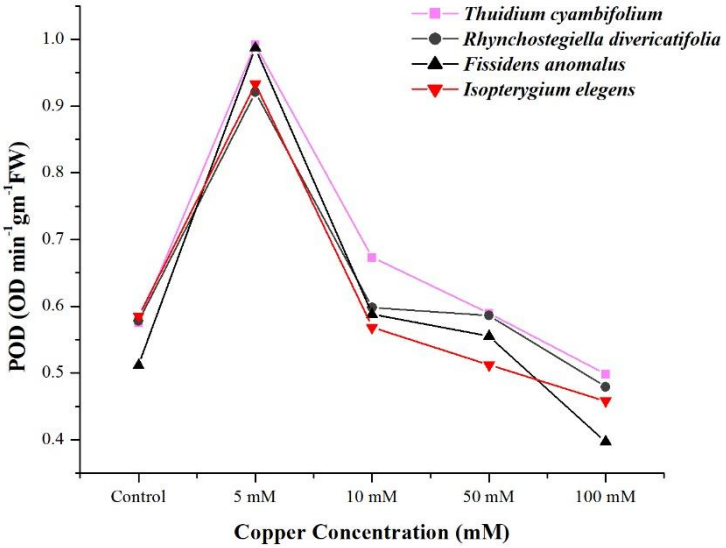

Figure 6.3.3.2b: Effect of Cadmium (Cd) on Peroxidase Enzyme Activity after 6 days of exposure

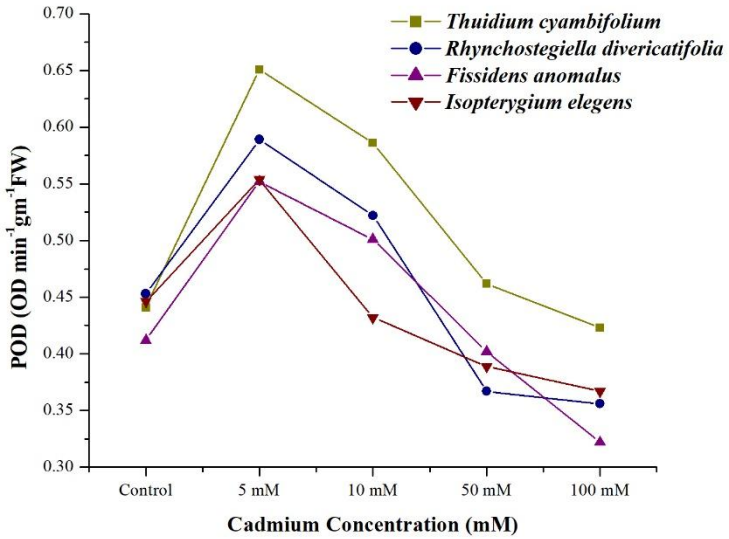

Figure 6.3.3.2c: Effect of Cadmium (Cd) on Peroxidase Enzyme Activity after 15 days of exposure

6.4. TAXONOMICAL STUDY:

The taxa *Thuidium cymbifolium* (Dozy & Molk) Dozy & Molk. was collected from the field and taxonomically explored in the lab under stereo binoculars with the support of different flora. A detailed line diagram of moss was prepared with the help of *Camera Lucida* and presented in plate 1. Furthermore, the Central National Herbarium, Botanical Survey of India (BSI) also verified the authenticity of the plant. Kolkata (Annexure 1).

Figure 6.4 : *Thuidium cymbifolium* (Dozy & Molk) Dozy & Molk. growing in a natural habitat.

The plants exhibit dioicous growth, measuring up to or exceeding 10 cm in length, and are characterized by their large yellow-green to deep green coloration (perhaps brownish in age), forming compact mats. The primary stem is crawling, often exhibiting regular bipinnate branching with distinct central strands. The paraphyllia is compact about the stems and has lanceolate to filiform shapes. Erectopatent, ovate-lanceolate triangular stem leaves terminate in a long arista created by the excurrent costa and plicate up to 3 mm in length. The branched leaves are erectopatent, concave ovate, lanceolate, and have an acute apex upon drying. The botanical capsule is cylindrical and possesses a double peristome.

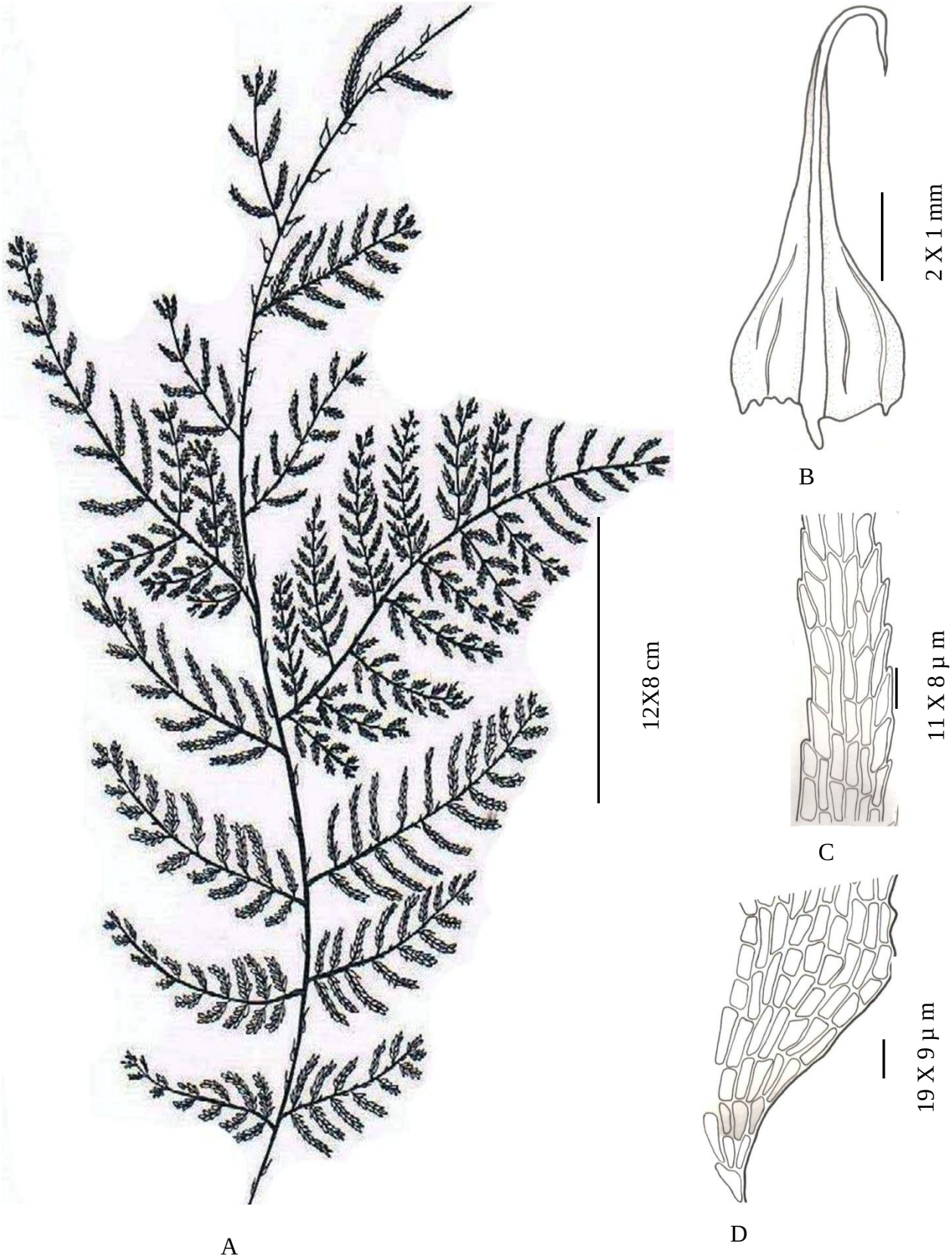

Plate 1: *Thuidium cymbifolium* (Dozy et Molk.) Dozy et Molk. (A) Complete plant, (B) a leaf, (C) mid-leaf cells, (D) Basal Cell

6.5. SEASONAL METAL ACCUMULATION AT DIFFERENT STUDY SITES FROM DIFFERENT DIRECTIONS IN CHAMPAWAT DISTRICT

6.5.1 Champawat

6.5.1a Zinc

The seasonal metal load of Zn in moss *Thuidium cymbifolium* (Dozy & Molk) Dozy & Molk. at different directions from Champawat during the study (from 2020 to 2022) is presented in Table (6.5.1a) and Figures (6.5.1a-c).

In the summer season, the maximum Zn accumulation was measured in the East direction from 2020 (1.365 mg/g DW) and 2022 (1.959 mg/g DW), and in 2021, the same was reported highest from the north direction (1.689 mg/g DW). The minimum deposition was recorded in the moss at the city center (0.852 mg/g DW, 0.927 mg/g DW, and 0.952 mg/g DW) throughout the study period.

During the rainy season, maximum zinc accumulation was reported from the east in 2020 (0.971 mg/g DW) and 2021 (1.114 mg/g DW), and it was reported maximum from the west direction (1.270 mg/g DW) in 2022. The rainy season had the minimum concentration in the city center in all three consecutive years of study (0.602 mg/g DW) in 2020, (0.562 mg/g DW) in 2021, and (0.655 mg/g DW) in 2022.

In winter, the highest metal load was measured at different sites in different years, i.e., towards the east during 2020 (1.180 mg/g DW) and in the west direction during 2021 (1.368 mg/g DW) and 2022 (1.580 mg/g DW). The minimum values were measured from the city center in all three years (0.525 mg/g DW, 0.682 mg/g DW, and 0.833 mg/g DW, respectively). All the study sites exhibited seasonal significant differences ($p \leq 0.05$) in Zn concentration compared to baseline concentration.

6.5.1b. Lead:

Seasonal accumulation of Pb in moss *T. cymbifolium* at different sampling sites of Champawat is shown in Table (6.5.1b) and Figures (6.5.1d-f). Results revealed seasonal non-significant different ($p \leq 0.05$) values at most sites during the study period.

The comparative study during the summer season of all three years shows a high value of Pb reported from the city center (0.976 mg/g DW) in 2020, from the north (1.274 mg/g DW) and south (1.565 mg/g DW) in 2021 and 2022, respectively. The lowest concentration was measured towards the west (0.656 mg/g DW, 0.948 mg/g DW, and 1.090 mg/g DW) in 2020, 2021, and 2022, respectively.

During the rainy season, the maximum deposition for Pb was reported from the south direction as 0.594 mg/g DW, 0.778 mg/g DW, and 0.976 mg/g DW, and the minimum as 0.484 mg/g DW, 0.533 mg/g DW, and 0.643 mg/g DW at the south direction during 2020, 2021, and 2022, respectively.

In winter, maximum mean Pb values were recorded at the city center (0.721 mg/g DW) in 2020 from the south direction (1.007 mg/g DW) in 2021 and the east (1.278 mg/g DW) in 2022. Its minimum value was reported in the north direction (0.556 mg/g DW and 0.652 mg/g DW) during 2020 and 2021, respectively, and in the west direction (0.816 mg/g DW) during 2022. The results showed significantly different values than baseline deposition across all sites over three consecutive years.

6.5.1c. Copper:

Table (6.5.1c) and Figures (6.5.1g-i) illustrate the seasonal Cu concentration accumulated in moss *T. cymbifolium* at different collection sites of Champawat in 2020, 2021, and 2022.

Results revealed that in summer, maximum Cu accumulation was recorded from the south direction in 2020 (0.785 mg/g DW) and 2022 (1.119 mg/g DW), respectively. Furthermore, minimum values were found from the west direction in 2020 (0.557 mg/g DW), 2021 (0.648 mg/g DW), and 2022 (0.740 mg/g DW).

In the rain, the city center had the highest lead concentration during 2020, 2021, and 2022 (0.538 mg/g DW, 0.670 mg/g DW, and 0.726 mg/g DW), respectively. However, the lowest values were measured at 0.347 mg/g DW, 0.372 mg/g DW, and 0.392 mg/g DW in 2020, 2021, and 2022 towards the west at 1 Km.

During the winter, the highest deposition was reported from the city center (0.641 mg/g DW and 0.751 mg/g DW) in 2020 and 2021, while in the east direction (0.833 mg/g DW) during 2022. Its lowest values were observed in the north direction (0.446 mg/g DW) during 2020 and from the west in 2021 and 2022 (0.550 mg/g DW and 0.613 mg/g DW), respectively. Over baseline deposition, all sites revealed significant differences ($p \leq 0.05$) results in all three studied years.

6.5.1d. Cadmium:

Observation of seasonal accumulations of Cd in moss *T. cymbifolium* at different collection sites of Champawat City during the years 2020, 2021, and 2022 are represented in Table (6.5.1d) and Figures (6.5.1j-l).

Results revealed that maximum Cd accumulation in the moss occurred during summer at different sites, whereas rains recorded minimum metal levels. In addition, the values of baseline concentration during rain were below the detection limit in 2020 and 2021. Seasonally non-significant ($p \leq 0.05$) values were found at almost all the study sites of Champawat.

In summer, the level of Cd was found to diversify and analyzed maximum in the north direction during 2020 (0.089 mg/g DW), in the west direction in 2021 (0.111 mg/g DW), and in the south in 2022 (0.133 mg/g DW). A decline in Cd values was observed in moss collected from the city center (0.021 mg/g DW) in 2020, (0.023 mg/g DW) in 2021, and (0.026 mg/g DW) in 2021 in the moss analyzed.

The levels of Cd pollution during the rainy season were measured in 2020 (0.090 mg/g DW), 2021 (0.105 mg/g DW), and 2022 (0.128 mg/g DW), with a high concentration toward the east. In all three years under study, the west direction had the lowest load (0.019 mg/g DW, 0.032 mg/g DW, and 0.045 mg/g DW).

During winter, the maximum concentration of Cd in 2020 was 0.039 mg/g DW in the west; in 2021, it was measured at 0.097 mg/g DW; in 2022, it was exhibited at 0.106 mg/g DW at the city center. At the same time, a decrease in Cd values was observed in the east direction in 2020, 2021, and 2022 as 0.019 mg/g DW, 0.040 mg/g DW, and 0.054 mg/g DW, respectively.

6.5.2. Lohaghat:

6.5.2a. Zinc:

The results of metal bio mapping of Zn through moss *T. cymbifolium* at different study sites of Lohaghat during the years 2020, 2021, and 2022 are presented in Table (6.5.2a) and Figures (6.5.2 a-c).

The metal deposition in the moss was highest in summer, followed by rain and winter. On the other hand, the seasonal non-significant difference ($p \leq 0.05$) was observed repeatedly at most of the locations over three consecutive years..

Metal accumulation in the moss was observed to occur in a sequence of summer> winter> rain. Yet, the seasonal difference was not statistically significant ($p \leq 0.05$) at nearly all the sites for three successive years.

Observations show that maximum zinc accumulation during summer was recorded in different

directions. North had accumulated 1.482 mg/g DW (2020), east showed 1.763 mg/g DW (2021), and west 1 Km depicted 2.051 mg/g DW of zinc in 2022. The minimum Zn level was found at the city center in all three consecutive years of study, i.e., 0.778 mg/g DW, 1.067 mg/g DW, and 1.241 mg/g DW, respectively.

In the rainy season, deposition was recorded up to 0.876 mg/g DW (2020), 1.058 mg/g DW (2021), and 1.354 mg/g DW (2022) in the north direction, while the minimum deposition was recorded in the years 2020 (0.536 mg/g DW),2021 (0.671 mg/g DW), and 2022 (0.869 mg/g DW) from the east direction.

In winter, the highest values evaluated in all three years of the study, i.e., 2020, 2021, and 2022, were 1.121 mg/g DW, 1.470 mg/g DW, and 1.640 mg/g DW towards the north direction, respectively. At the same time, the lowest concentration was recorded from the city center during 2020 (0.642 mg/g DW) and in the east direction during 2021 (0.853 mg/g DW) and 2022 (1.045 mg/g DW). All values were significantly different ($p \leq 0.05$) compared to baseline deposition.

6.5.2b. Lead:

Table (6.5.2b) and Figures (6.5.2d-f) depict the seasonal Pb concentration accumulated in moss *T. cymbifolium* at different collection sites of Lohaghat. Results revealed seasonally significant different ($p \leq 0.05$) values at some sites during 2020, 2021, and 2022.

In 2020 and 2021, Pb accumulation during the summers was highest in the north (1.547 mg/g DW and 1.853 mg/g DW), and in 2022, it was reported high from the city center (1.850 mg/g DW). Additionally, minimal values were recorded at the city center in 2020 (0.621 mg/g DW) and 2021 (1.253 mg/g DW). However, in 2022, the lowest deposition (1.308 mg/g DW) was reported from the west direction.

In the rainy season, the highest values were recorded in the south (1.226 mg/g DW) in 2020, in the north (1.491 mg/g DW) in 2021, and in the west (1.674 mg/g DW) in 2022. In contrast, the lowest values were observed from the city center in 2020 (0.277 mg/g DW), in 2021 (0.378 mg/g DW), and during 2022 (0.562 mg/g DW), respectively.

The winter season had the highest concentration in the north direction (1.323 mg/g DW) in 2020, (1.581 mg/g DW) in 2021, and (1.664 mg/g DW) in 2022. However, the lowest values were measured at the city center: 0.433 mg/g DW in 2020, 0.641 mg/g DW in 2021, and 0.753 mg/g DW

in 2022, respectively. Over baseline concentration, all sites revealed significant differences ($p \leq 0.05$) results in all three studied years.

6.5.2c. Copper:

Seasonal results of mapping of Cu through moss *T. cymbifolium* at the different directions of Lohaghat during various seasons of the years 2020, 2021, and 2022 are presented in Table (6.5.2c) and Figures (6.5.2g-i). Most sites exhibited seasonally non-significant differences ($p \leq 0.05$) results.

In the summer, the highest metal accumulation was measured in the north direction of the city during 2020 (0.979 mg/g DW), while from the city center, the same was reported highest during 2021 (1.164 mg/g DW) and 2022 (1.627 mg/g DW. The lowest values were found from the west direction (0.873 mg/g DW and 0.981 mg/g DW in 2020 and 2021, respectively, and during 2022 (1.157 mg/g DW) from the south direction.

During the rainy season, *T. cymbifolium* exhibited the maximum level of metal concentration in the south direction (0.748 mg/g DW) during 2020. The same was reported highest from the east direction (0.863 mg/g DW) in 2021 and the city center (1.023 mg/g DW) in 2022. At the same time, a consistent trend was observed for minimum values. The lowest metal concentration was found towards the city center (0.566 mg/g DW) in 2020, from the north direction (0.764 mg/g DW) in 2021 and the west direction (0.582 mg/g DW) in 2022.

Winter season revealed a consistent trend, with maximum Cu concentration in the west direction (0.864 mg/g DW) during 2020 and from the city center in 2021 and 2022 (0.987 mg/g DW and 1.334 mg/g DW), respectively. The lowest values were measured in the east direction during 2020 (0.740 mg/g DW), from the south direction (0.845 mg/g DW) in 2021, and during 2022, the same was reported lowest (1.026 mg/g DW) from the west direction. All the values in the three consecutive years of the study showed significantly different values ($p \leq 0.05$) compared to baseline concentration.

6.5.2d. Cadmium:

The amount of Cd accumulated in moss *T. cymbifolium* at different sampling stations of Lohaghat during various seasons of 2020, 2021, and 2022 are shown in Table (6.5.2d) and Figures (6.5.2j-l).

Results revealed that moss *T. cymbifolium* accumulated the lowest Cd in the rainy season and

the highest in summer. A seasonal non-significant variation ($p \leq 0.05$) was found in most sites. Furthermore, the baseline concentration values during rain were below the detection limit in 2020 and 2021.

In summer, the east direction showed the highest metal accumulation during 2020 (0.087 mg/g DW) and from the city center (0.109 mg/g DW and 0.128 mg/g DW) in 2021 and 2022, respectively. However, during 2020, the lowest values were reported from the north (0.052 mg/g DW), and in 2021 and 2022, the same was reported lowest from the east direction (0.067 mg/g DW and 0.089 mg/g DW).

During the rainy season, maximum Cd concentration was found in the north direction in 2020 (0.028 mg/g DW) and 2022 (0.065 mg/g DW), while during 2021, the same was reported high in the south direction (0.053 mg/g DW). Cadmium concentration declined to 0.022 mg/g DW and 0.037 mg/g DW during 2020 and 2021 in the city center and 0.051 mg/g DW towards east 2022, respectively.

The winter season exhibited a consistent pattern for the highest and lowest concentrations. The maximum concentration was found in the west direction in 2020 (0.055 mg/g DW) and from the city center in 2021 (0.075 mg/g DW) and 2022 (0.085 mg/g DW), respectively. The minimum values were recorded as 0.038 mg/g DW during 2020 in the south direction and from the east direction in 2021 (0.056 mg/g DW) and 2022 (0.064 mg g^{-1} DW).

6.5.3. Khetikhan:

6.5.3a. Zinc:

Results of seasonal accumulation of Zn in moss *T. cymbifolium* at different sampling sites of Khetikhan during the years 2020, 2021, and 2022 are presented in Table (6.5.3a) and Figures (6.5.3j-l).

Data revealed that *T. cymbifolium* accumulates Zn at the highest level in the summer, followed by winter and rainy seasons. However, almost all values were found seasonally non-significantly different ($p \leq 0.05$) at most sites during the three consecutive years of study.

Summer exhibited the maximum zinc accumulation from the south direction in 2020 (1.873 mg/g DW), followed by 2021(1.973 mg/g DW) and 2022 (2.347 mg/g DW). However, minimum accumulation was found in the west direction in 2020 (1.344 mg/g DW) and at the city center in 2021 (1.514 mg/g DW) and 2022 (1.654 mg/g DW).

In the rainy season, the highest and lowest Zn depositions were reported from the north direction during 2020 (1.243 mg/g DW) and 2021 (1.233 mg/g DW) and from the south direction in 2022 (1.372 mg/g DW). However, the lowest values were measured towards the city center (0.551 mg/g DW) in 2020, (0.634 mg/g DW) in 2021, and (0.724 mg/g DW) in 2022.

In the winter season, the highest value was recorded from the south direction in 2020 (1.530 mg/g DW). In 2021, it was reported high from the north direction (1.621 mg/g DW) and in 2022 from the south direction (1.842 mg/g DW), whereas the minimum concentration was observed at the city center during 2020 (0.686 mg/g DW), 2021 (0.745 mg/g DW) and 2022 (0.853 mg/g DW). Over baseline concentration, all sites revealed significantly different ($p \leq 0.05$) results in all three years.

6.5.3b. Lead:

The results of biomapping of lead through moss *T. cymbifolium* at different directions of Khetikhan during 2020, 2021, and 2022 are presented in Table (6.5.2 b) and Figures (6.5.3d-f). Seasonally non-significant difference ($p \leq 0.05$) was found at most sites in the three consecutive years. East direction recorded the maximum metal accumulation in the years 2020 (1.039 mg/g DW) and 2021 (1.563 mg/g DW), while towards the north, it was reported in 2022 (1.350 mg/g DW). The lowest Pb level was found at the city center in the three years, i.e., 0.765 mg/g DW (2020), 0.819 mg/g DW (2021), and 0.948 mg/g DW (2022).

During the rainy season, the value rose upto 0.553 mg/g DW (2020), 1.130 mg/g DW (2021), and from the south direction, 0.876 mg/g DW (2022). However, the lowest values were reported at the city center in the year 2020 (0.344 mg/g DW), 2021 (0.422 mg/g DW), and from the north direction (0.688 mg/g DW) during the year 2022.

In winter, the maximum concentration was reported in the west direction during 2020 (0.752 mg/g DW), from the east during 2021 (1.264 mg/g DW), and during 2021, reported 1.061 mg/g DW from the west direction. At the same time, the lowest concentration was reported at the city center during 2020 (0.408 mg/g DW), 2021 (0.525 mg/g DW), and 2022 (0.703 mg/g DW).

6.5.3c. Copper:

Seasonal accumulation of copper in moss *T. cymbifolium* at different sampling sites of Khetikhan during the years 2020, 2021, and 2022 are depicted in Table (6.5.3c) and Figures (6.5.3g-i). Results show that the maximum Cu accumulation in the moss occurred during summer at different sites,

whereas rain recorded minimum metal level in rain.

In summer, the peak concentration of Cu was reported from the north during 2020 (1.125 mg/g DW) and 2020 (1.568 mg/g DW), while in 2022, it was reported high from the city center (1.241 mg/g DW). The minimum deposition of Cu was measured from the transplants harvested from the west during 2020 (0.543 mg/g DW), from the city center during 2021 (0.934 mg/g DW), and again from the west during 2022 (0.954 mg/g DW).

Rain values for Cu were found to be maximum in the north in 2020 (0.627 mg/g DW), in the south direction in 2021 (1.229 mg/g DW), and in the north direction in 2022 (0.722 mg/g DW). The minimum deposition was recorded in the transplants harvested from the west direction in 2020 (0.226 mg/g DW), from the city center in 2021 (0.676 mg/g DW), and towards the west direction in 2022 (0.344 mg/g DW).

In the winter season, the maximum copper accumulation was reported from the north in 2020 (0.752 mg/g DW), 2021 (0.838 mg/g DW), and 2022 (0.958 mg/g DW). The values declined to 0.372 mg/g DW in 2020 in the west direction, 0.451 mg/g DW in 2021 from the city center, and 0.584 mg/g DW in 2022 in the east direction. Statistically significant differences in values over baseline concentration were observed at all sites throughout the three consecutive years.

6.5.3d. Cadmium:

Seasonal accumulation of cadmium in moss *T. cymbifolium* at different collection sites of Khetikhan during the years 2020, 2021 and 2022 are represented in table 6.5.3d and Figures (6.5.3j-l).

Results show that maximum Cd accumulation in the moss occurred during summer at different sites, whereas rains recorded minimum metal levels. In addition, the baseline concentration values during the rain season were below the detection limit in 2020 and 2021.

In summer, the level of Cd was analyzed at its maximum in the west direction during 2020 (0.115 mg/g DW), 2021 (0.129 mg/g DW), and 2022 (0.196 mg/g DW). Minimum Cd values were reported from the moss collected from the city centre in 2020 (0.062 mg/g DW), 2021 (0.070 mg/g DW), and 2022 (0.072 mg/g DW).

In rain, the Cd contamination level was reported to be maximum in the east direction (0.058

mg/g DW) in 2020, from the west (0.077 mg/g DW) in 2021, and in 2022 (0.116 mg/g DW). The minimum metal load was found high in the south direction during 2020 (0.033 mg/g DW), 2021 (0.040 mg/g DW), and at the city centre in 2022 (0.057 mg/g DW).

During winter, the maximum concentration of Cd was found in the west direction in 2020 (0.093 mg/g DW), 2021 (0.100 mg/g DW), and 2022 (0.144 mg/g DW). Conversely, decreases in Cd values were observed at the city center during 2020 (0.046 mg/g DW), 2021 (0.051 mg/g DW), and 2022 (0.046 mg/g DW).

6.5.4. Barakote:

6.5.4a. Zinc:

The results of biomapping of Zn through moss T. cymbifolium at different collection sites of Barakote during the years 2020, 2021, and 2022 are presented in Table (6.5.4a) and Figures (6.5.4 a-c).

The moss was observed to accumulate the metal in summer, followed by winter and rain. However, a significant seasonal difference ($p \leq 0.05$) was found at most of the sites in three consecutive years of investigations (2020, 2021, and 2022).

The maximum metal accumulation was recorded in the summer from the east direction in 2020 (1.360 mg/g DW), 2021 (1.563 mg/g DW), and 2022 (1.770 mg/g DW). The minimum Zn level was found at city center in 2020 (0.778 mg/g DW), in 2020 (0.818 mg/g DW) and 2021 (0.873 mg/g DW).

In the rainy season, the values rose consistently to a concentration of 1.066 mg/g DW in 2020, 1.130 mg/g DW in 2021 in the east direction, and 1.366 mg/g DW in 2022 in the west direction. However, the lowest values were found towards the city center in the years 2020 (0.404 mg/g DW), 2021 (0.429 mg/g DW), and 2022 (0.444 mg/g DW).

In winter, the highest accumulation of Zn was evaluated from the east direction in 2020 (1.146 mg/g DW), 2021 (1.264 mg/g DW), and 2021 (1.544 mg/g DW). At the same time, the lowest concentration was found in the city center during 2020 (0.483 mg/g DW), 2021 (0.532 mg/g DW), and 2022 (0.574 mg/g DW).

6.5.4b. Lead:

Table (6.5.4b) and Figures (6.5.4 d-f) depict observations of seasonal accumulation of Pb in moss T. cymbifolium at different sampling sites of Barakote during 2020, 2021, and 2022.

In the summer season, Pb values were found to be maximum in the east direction in 2020 (1.162 mg/g DW) and 2022 (1.843 mg/g DW), and 1.364 from the west direction in 2021. Minimum deposition was calculated in transplants harvested from the south (0.564 mg/g DW) in 2020 and 2021 (0.767 mg/g DW) in 2022 and in the north direction (1.061 mg/g DW).

During the rainy season, the maximum lead accumulation was reported in the west direction (0.462 mg/g DW) in 2020, in the east direction (0.557 mg/g DW) during 2021, and in the north direction (0.852 mg/g DW) in 2022. The minimum lead accumulation was reported from the south (0.258 mg/g DW) in 2020 and 2021 (0.370 mg/g DW), and in 2022, it was reported high from the north direction (0.546 mg/g DW).

In the winter season, the west direction was identified to accumulate a maximum level of lead in 2020 (0.671 mg/g DW), 2021 (0.966 mg/g DW), and in the east direction in 2022 (1.346 mg/g DW). The values declined to 0.429 mg/g DW in 2020 in the north direction, 0.631 mg/g DW in 2021, and 0.754 mg/g DW in 2022 in the south direction.

6.5.4c. Copper:

Seasonal accumulation of Cu in moss *T. cymbifolium* at different sampling sites of Barakote during 2020, 2021, and 2022 are illustrated in Table (6.5.4c) and Figures (6.5.4 g-i).

Seasonal and annual data revealed that T. cymbifolium accumulates copper in the order summer>winter>rain season. Almost all values were found seasonally significantly different ($p \leq 0.05$) at most of the sites during three consecutive years of study (2020, 2021, and 2022).

In the summer season, the maximum Cu accumulation was recorded in the north direction in 2020 (1.354 mg/g DW), in 2021 (1.561 mg/g DW), and in the south direction in 2022 (1.973 mg/g DW). Transplants collected from the west direction during 2020 (0.769 mg/g DW) and from the city center during 2021 (0.904 mg/g DW) and 2022 (0.945 mg/g DW) accumulated the minimum metal.

During the rainy season, the highest deposition was observed from the north in 2020 (0.772 mg/g DW) and 2021 (0.842 mg/g DW) and from the south in 2022 (1.255 mg/g DW). The lowest metal accumulation was reported from the east (0.361 mg/g DW) in 2020 (0.452 mg/g DW) in 2021, and from the city center in 2022.

Results depict that moss *T. cymbifolium* accumulated the maximum metal in the winter season in the north direction: 1.149 mg/g DW in 2020, 1.322 mg/g DW in 2021, and 1.650 mg/g DW from the south direction in 2022. The minimum values were recorded in the west direction in 2020 (0.653 mg/g DW) and from the city center in 2021 (0.692 mg/g DW) and 2022 (0.756 mg/g DW).

6.5.4d. Cadmium:

The amount of Cd accumulated in moss *T. cymbifolium* at different sampling stations of Barakote during different seasons of 2020, 2021, and 2022 are presented in Table (6.5.4d) and Figures (6.5.4 j-l).

Results revealed that moss *T. cymbifolium* accumulates the lowest Cd in the rainy season. A seasonal significant variation ($p \leq 0.05$) was found at most of the sites. The baseline concentration values during rain were non-detectable in 2020 and 2021.

In the summer, the north direction during 2020 (0.106 mg/g DW), 2021 (0.126 mg/g DW), and from the east direction during 2022 (0.154 mg/g DW) was identified to accumulate a maximum level of Cd. In addition, minimum values were recorded at the city center in 2020 (0.064 mg/g DW), 2021 (0.082 mg/g DW), and 2022 (0.088 mg/g DW).

During the rainy season, the maximum cadmium concentration was found at the city centre in 2020 (0.037 mg/g DW), 2021 (0.055 mg/g DW) from the west direction during 2022 (0.069 mg/g DW) in the three consecutive years of study. Cd concentration declined up to 0.023 mg/g DW (2020), 0.036 mg/g DW (2021) at south 3 Km, and 0.058 mg/g DW (2022) in the east direction.

Winter exhibited maximum concentration in the west direction (0.051 mg/g DW) in 2020 and (0.088 mg/g DW) in 2022, while at the north (0.070 mg/g DW) during 2021. Its minimum value was measured in the east direction during 2020 (0.039 mg/g DW), 2021 (0.054 mg/g) and 2022 (0.058 mg/g)

6.5.5. Pithoragarh:

6.5.5a. Zinc:

The results of biomapping of Zn through moss *T. cymbifolium* at different collection sites of Pithoragarh during the years 2020, 2021, and 2022 are presented in Table 6.5.5a and Figures (6.5.5 a-c). Results reveal seasonally non-significant differences ($p \leq 0.05$) values at different study sites.

Summer observations show a consistent trend for the maximum and minimum zinc accumulation. The highest concentration was recorded from the north direction in 2020 (1.862 mg/g DW), from the east direction in 2021 (1.929 mg/g DW), and from the south direction in 2022 (2.357 mg/g DW). Furthermore, minimum values were found at the city center during 2020 (0.858 mg/g DW), 2021 (1.030 mg/g DW), and 2022 (1.302 mg/g DW).

In the rainy season, the highest values recorded during 2020 were 0.639 mg/g DW, 2021 was 0.834 mg/g DW in the north direction, and 1.644 mg/g DW (2022) in the east direction. The lowest values were observed towards the east direction in 2020 (0.427 mg/g DW) from the west in 2021 (0.732 mg/g DW), and 0.968 mg/g DW from the city center in 2022.

In winter, the highest concentrations were observed from the north direction in 2020 (1.449 mg/g DW), 2021 (1.691 mg/g DW), and 2022 (2.307 mg/g DW). The lowest values were recorded at the city center in 2020 (0.846 mg/g DW), 2021 (0.944 mg/g DW), and 2022 (1.141 mg/g DW).

6.5.5b. Lead:

The results of biomapping of Pb through moss *T. cymbifolium* at different collection sites of Pithoragarh during the year 2020, 2021, and 2022 are presented in Table (6.5.5b) and Figures (6.5.5 d-f).

The moss was observed to accumulate the metal in the sequence summer> winter> rain. However, a seasonally non-significant difference ($p \leq 0.05$) was found at most sites in three consecutive years.

In the summer, the city center recorded maximum metal accumulation in 2020 (1.433 mg/g DW), 2021 (1.640 mg/g DW), and 2022 (2.192 mg/g DW). The minimum Pb level was found in the south direction in 2020 (0.742 mg/g DW) and 2021 (1.060 mg g^{-1}), while in 2022, the same was reported as minimal from the west direction (1.246 mg/g DW).

During rains, the values consistently trended to 0.748 mg/g DW in 2020, 1.036 mg/g DW in 2021, and 1.245 mg/g DW in 2022 at the city center. However, the lowest values were exhibited in the years 2020 (0.287 mg/g DW), 2021 (0.459 mg/g DW), and 2022 (0.629 mg/g DW) in the north direction.

In the winter season, the highest values evaluated were 0.956 mg/g DW in 2020 in the west direction, 1.246 mg/g DW in 2021 from the north, and 1.201 mg/g DW in 2022 at the city center. At the same time, the lowest concentration was found towards the south during 2020 (0.528 mg/g DW) and 2021 (0.726 mg/g DW) and in the east direction during 2022 (0.863 mg/g DW).

6.5.5c. Copper:

The results of biomapping of Cu through moss *T. cymbifolium* at different transplant sites

during the years 2020, 2021, and 2022 are presented in Table (6.5.5c) and Figures (6.5.5 g-i).

Results show that maximum Cu accumulation in the moss has occurred during summer at different sites, whereas, rain recorded minimum metal level. Results reveal seasonally non-significant differences ($p \leq 0.05$) values at different study sites (2020, 2021 and 2022).

The maximum deposition of Cu in summer was 1.695 mg/g DW (2020), 1.995 mg/g DW (2021), and 2.163 mg/g DW (2022) towards the north direction. Whereas it was measured minimum in the transplants harvested from the city center during 2020 (0.863 mg/g DW), 2021 (0.955 mg/g DW), and 2022 (1.013 mg/g DW).

In the rainy season, the values for Cu were found to be maximum in the north direction in 2020 (0.870 mg/g DW) in 2022 (1.534 mg/g DW) and from the east direction in 2021 (1.133 mg/g DW). Meanwhile, the minimum deposition was measured in moss harvested from the city center (0.348 mg/g DW) in 2020, (0.618 mg/g DW) in 2021, and (0.732 mg/g DW) in 2022.

In the winter season, the north direction was identified to accumulate a maximum level of copper in 2020 (1.239 mg/g DW), 2021 (1.661 mg/g DW), and 2022 (1.859 mg/g DW). The values declined to 0.554 mg/g DW in 2020, 0.668 mg/g DW in 2021, and 0.758 mg/g DW in 2022.

The highest annual average was measured at 0.870 mg/g DW (2020), 1.534 mg/g DW (2022) from the north direction and 1.133 mg/g DW (2021) in the east direction. Statistically significant differences in values over baseline concentration were observed at all sites throughout the three consecutive years.

6.5.5d. Cadmium:

Seasonal and annual accumulation of Cd in moss *T. cymbifolium* at different transplant sites during the years 2020, 2021, and 2022 are represented in Table (6.5.5d) and Figures (6.5.5 j-l).

Results show that maximum Cd accumulation in the moss has occurred during summer at different sites, whereas, rain recorded minimum metal level. In addition, the values of baseline concentration during rain were below the detection limit in the years 2020 and 2021. Seasonally non-significant ($p \leq 0.05$) values were found at almost all the study sites of Pithoragarh.

In summer, the level of Cd was analyzed at its maximum at the city center during 2020 (0.105

mg/g DW), 2021 (0.125 mg/g DW), and 2022 (0.146 mg/g DW). A decline in Cd value was found in moss collected from the north (0.069 mg/g DW) during 2020 and from the west in 2021 (0.066 mg/g DW) and 2022 (0.093 mg/g DW).

In the rainy season contamination level of Cd was found high in the east direction during 2020 (0.056 mg/g DW), in 2021 (0.071 mg/g DW), and in 2022 (0.083 mg/g DW). While the minimum load was found at the same sites during the different years, it was measured at 0.018 mg/g DW (2020), 0.035 mg/g DW (2021), and 0.047 mg/g DW (2022) in the west direction.

During winter, the highest accumulation of Cd in 2020 was found to be 0.086 mg/g DW in the east direction and from the south direction during 2021 (0.085 mg/g DW) and (0.107 mg/g DW) in 2022. A decrease in Cd value was observed at the city center in 2020 (0.054 mg/g DW) and in the south in 2021 (0.085 mg/g DW) and 2022 (0.107 mg/g DW).

6.5.6. Ghat:

6.5.6a. Zinc:

The results of biomapping of Zn through moss *T. cymbifolium* at different collection sites of Ghat during the years 2020, 2021, and 2022 are depicted in Table (6.5.6a) and Figures (6.5.6 a-c).

The moss was found to accumulate the metal in the sequence summer> winter> rain. However, the seasonally non-significant difference ($p \leq 0.05$) was found at almost all the sites in the three consecutive years.

The summer season recorded the maximum metal accumulation in 2020 (1.816 mg/g DW) in the south direction, in the west during 2021 (2.172 mg/g DW), and in the east during 2022 (2.352 mg/g DW). The minimum Zn level was found at city center (0.960 mg/g DW) in 2020 and (1.101 mg/g DW) in 2021 and (1.390 mg/g DW) during 2022.

In the rainy season, the values increased to 0.760 mg/g from the city center in 2020. In 2021 (0.968 mg/g DW) and 2022 (1.227 mg/g DW), the concentration was reported high from the south direction. However, the lowest values were measured from the east direction in the years 2020 (0.355 mg/g DW), 2021 (0.568 mg/g DW), and 2022 (0.649 mg/g DW).

In winter, the highest values were evaluated from the south in 2020 (1.359 mg/g DW), 2021 (1.568 mg/g DW), and 2022 (1.861 mg/g DW). At the same time, the lowest concentration was found in the

north during 2020 (0.845 mg/g DW) and in the city center during 2021 (1.035 mg/g DW) and 2022 (1.232 mg/g DW). Furthermore, all values were significantly different ($p \leq 0.01, 0.05$) compared to baseline concentration.

6.5.6b. Lead:

Table (6.5.6b) and Figures (6.5.6 d-f) depict the seasonal Pb concentration accumulated in moss *T. cymbifolium* at different collection sites of Ghat. Results reveal seasonally significant different ($p \leq 0.01, 0.05$) values at most sites during 2020, 2021 and 2022.

Results revealed that maximum lead (Pb) accumulation during summer was towards the city center in 2020 (1.543 mg/g DW), from the north in 2021 (2.058 mg/g DW) and 2022 (2.353 mg/g DW). Minimum values were found in the west in 2020 (1.074 mg/g DW) and from the east direction in 2021 (1.559 mg/g DW) and in 2022 (1.951 mg/g DW).

In rain, the highest concentration was observed towards the north (0.965 mg/g DW) in 2020 and from the city center in 2021(1.136 mg/g DW) and in 2022 (1.354 mg/g DW). However, the lowest values were measured at 0.554 mg/g DW in 2020 from the west, 0.659 mg/g DW in 2021, and 0.509 mg/g DW in 2022 towards the east.

In winter, the highest values were recorded from the city center in 2020 (1.080 mg/g DW), in 2021 (1.355 mg/g DW), and in 2022 (1.684 mg/g DW). The lowest deposition was reported in the east direction (0.675 mg/g DW) in 2020, 0.867 mg/g DW in 2021, and 0.964 mg/g DW in 2022. Over baseline concentration, all sites revealed significantly different ($p \leq 0.05$) results in all three studied years.

6.5.6c. Copper:

The results of biomapping of copper through moss *T. cymbifolium* at different sampling sites of Ghat during different seasons of 2020, 2021, and 2022 are presented in Table (6.5.6c) and Figures (6.5.6 g-i). Results revealed seasonally non-significant different ($p \leq 0.05$) values during 2020, 2021 and 2022.

Results revealed that maximum Cu accumulation during summer was towards the north during 2020 (1.113 mg/g DW), towards the south in 2021 (1.361 mg/g DW), and in the west direction in 2022 (1.171 mg/g DW). Minimum values were found at the east in 2020 (0.663 mg/g DW) and 2021 (0.842 mg/g DW) and from the city center in 2022 (1.143 mg/g DW).

The highest and lowest values show a consistent trend for metal in the rainy season. The maximum concentration was observed at the city center in 2020 (0.682 mg/g DW) and 2021 (0.744 mg/g DW), and in 2022, the same was reported high from the north direction (0.856 mg/g DW). The lowest values were measured at 0.250 mg/g DW, 0.468 mg/g DW, and 0.650 mg/g DW in the east direction during 2020, 2021, and 2022, respectively.

In the winter season, elevated metal load was found in the south direction (0.842 mg/g DW) in 2020 and the north (0.968 mg/g DW) and 1.358 mg/g DW in 2022. In contrast, the minimum deposition was observed in the east during 2020 (0.478 mg/g DW), whereas in the west in 2021 (0.742 mg/g DW) and from the city center in 2022 (0.877 mg/g DW). Over baseline concentration, all sites revealed significantly different ($p \leq 0.05$) results in all three studied years.

6.5.6d. Cadmium:

The results of the seasonal accumulation in moss *T. cymbifolium* at different sampling sites of Ghat during the years 2020, 2021, and 2022 are presented in Table (6.5.6d) and Figures (6.5.6 j-l). The results show that maximum Cd accumulation in the moss occurred during summer at different sites, whereas rain recorded a minimum metal level.

In summer, the level of Cd was analyzed maximum towards the city center during 2020 (0.123 mg/g DW), 2021 (0.137 mg/g DW), and at 3 Km of the south during 2022 (0.138 mg/g DW). There was a decrease in Cd values in transplants collected from the north direction (0.045 mg/g DW) in 2020, in the west direction in 2021 (0.062 mg/g DW), and 2022 (0.085 mg/g DW).

In rains, the Cd contamination level was high in the east direction during 2020, 2021, and 2022 (0.025 mg/g DW, 0.051 mg/g DW, and 0.084 mg/g DW), respectively. Its minimum load was found towards the north (0.015 mg/g DW and 0.023 mg/g DW) in 2020 and 2021 and towards the city center (0.054 mg/g DW) during 2022.

A maximum concentration of Cd during winter was reported from the east direction, 0.055 mg/g DW (2020), 0.076 mg/g (2021), and 0.112 mg/g (2022). In contrast, the same was measured minimum in the north direction during 2020 (0.027 mg/g DW) and 2021 (0.044 mg/g DW) and at the city center in 2022 (0.076 mg/g DW).

6.5.7. Thal:

6.5.7a. Zinc:

Table (6.5.7a) and Figures (6.5.7 a-c) depict the seasonal variations for Zn concentration in moss *T. cymbifolium* at different collection sites of Thal. Results revealed seasonally non-significant different ($p \leq 0.05$) values at some study sites during 2020, 2021, and 2022.

The moss was observed to have accumulated the metal in the summer> winter> rain sequence. However, a significant seasonal difference ($p \leq 0.05$) was found at most of the sites in the three consecutive years (2020, 2021, and 2022).

In summer, the highest values show diversified metal load in the east direction in 2020 (1.176 mg/g DW), in the west in 2021 (1.513 mg/g DW), and at 1.925 mg/g DW in 2022. The minimum Zn was found towards the city center in 2020 (0.678 mg/g DW), 2021 (0.734 mg/g DW), and 2022 (0.883 mg/g DW).

In the rainy season, the values rose consistently to the concentration of 0.488 mg/g DW in 2020 and 1.034 mg/g DW in 2022 from the west direction of 0.673 mg/g DW. However, the lowest values were found at the city center in 2020 (0.138 mg/g DW), 2021 (0.234 mg/g DW), and 2022 (0.344 mg/g DW).

In winter, the highest values were evaluated in the east direction in 2020 (0.836 mg/g DW), 2021 (1.137 mg/g DW), and in the west direction in 2022 (1.559 mg/g DW). At the same time, the lowest deposition was found at the city center in 2020 (0.383 mg/g DW) and 2021 (0.437 mg/g DW) and in 2021 (0.556 mg/g DW). Furthermore, all values were significantly different ($p \leq 0.05$) compared to the baseline concentration.

6.5.7b. Lead:

Seasonal and annual accumulation of Pb in moss *T. cymbifolium* at different sampling sites of Chamba during the years 2020, 2021, and 2022 are depicted in Table (6.5.7b) and Figures (6.5.7 d-f).

Results revealed that at different sites, there is maximum Pb in the moss during summer and minimum during rain. ANOVA revealed almost significant values in 2020, 2021, and 2022.

In the summer, the peak concentration of Pb was reported as 1.143 mg/g DW (2020) and 1.460 mg/g DW (2021) in the west, whereas the same was 1.814 mg/g DW (2022) in the south direction. However, the minimum deposition was reported in transplants harvested from the south direction in 2020

(0.553 mg/g DW) and from the city center in 2021 (0.708 mg/g DW) and 2022 (0.744 mg/g DW).

The rain value for Pb was found to be maximum in the west direction in 2020 (0.468 mg/g DW), 2021 (0.643 mg/g DW), and 2022 (0.983 mg/g DW). Its minimum concentration was measured in moss harvested in the south direction in 2020 (0.136 mg/g DW), in the west in 2021 (0.321 mg/g DW), and in the north direction in 2022 (0.342 mg/g DW).

In the winter season, the west direction was identified to accumulate a maximum level of lead in 2020 (0.884 mg/g DW), 2022 (1.472 mg/g DW), and the south side in 2021 (1.247 mg/g DW). The values declined up to 0.304 mg/g DW (2020) in the south, 0.367 mg/g DW (2021) at the city center, and 0.416 mg/g DW (2022) towards the east direction. Results show significantly different values over baseline concentration at all the sites in all three consecutive years.

6.5.7c. Copper:

Seasonal and annual accumulation of Cu in moss *T. cymbifolium* at different sampling sites of Chamba during the years 2020, 2021, and 2022 are depicted in Table (6.5.7c) and Figures (6.5.7 g-i). Results revealed seasonally significant different ($p \leq 0.05$) values at almost all the sites.

Observations revealed that maximum Cu accumulation during summer was in the north direction, measuring 1.258 mg/g DW (2020), and from the west direction in 2021 (1.541 mg/g DW), while 1.880 mg/g DW (2022) was in the south. Its minimum values were found towards the city center in 2020 (0.732 mg/g DW), in 2021 (0.811 mg/g DW), and from the north in 2021 (0.813 mg/g DW).

During the rain, the highest concentration was observed at the city center in 2020 (0.535 mg/g DW) and 0.586 mg/g DW in 2021. In 2022, the highest value was reported from the west direction (0.955 mg/g DW). However, the lowest values were measured in the south direction in 2020 (0.258 mg/g DW, and in 2021 (0.347 mg/g DW), while in 2022, the same was reported minimum from the north direction (0.528 mg/g DW).

The winter season showed the maximum Cu accumulation in the east direction (0.950 mg/g DW) in 2020, from the west direction (1.233 mg/g DW) in 2021, and in 2022 (1.406 mg/g DW) in 2022. This declined to 0.544 mg/g DW in 2020 from the city center, in 2021 (0.647 mg/g DW) in the north direction, and 0.658 mg/g DW in 2022 at the city center. Over baseline concentration, all sites revealed significant differences ($p \leq 0.05$) results in all three studied years.

6.5.7d. Cadmium:

The amount of Cd accumulated in moss *T. cymbifolium* at different sampling stations of Thal during various seasons of 2020, 2021, and 2022 are shown in Table (6.5.7d) and Figures (6.5.7 j-l). Results revealed that moss *T. cymbifolium* accumulates the lowest Cd in the rain season. A seasonal non-significant variation ($p \leq 0.05$) was found at most of the sites.

The minimum cadmium level was found at different sites in all three years: towards the west in 2020 (0.179 mg/g DW), from the north direction in 2021 (0.198 mg/g DW), and from the east direction in 2022 (0.225 mg/g DW). In addition, minimum values were recorded as 0.099 mg/g DW (2020) in the south direction, 0.071 mg/g DW (2021), and 0.077 mg/g DW (2022) in the city center.

Rain season shows the maximum Cd concentration in the north direction in 2020 (0.063 mg/g DW) and 2021 (0.083 mg/g DW), while in the east direction (0.139 mg/g DW) in 2021. Concentration declined up to 0.025 mg/g DW from the west direction in 2020, while at 0.047 mg/g DW (2021) and 0.044 mg/g DW (2022) at the city center.

The winter season had a maximum concentration in the north direction in 2020 (0.098 mg/g DW), 2021 (0.115 mg/g DW), and 2022 (0.185 mg/g DW). The minimum values were recorded at the city center during 2020 (0.045 mg/g DW), 2021(0.052 mg/g DW), and 2022 (0.062 mg g^{-1}).

6.5.8. Munsiyari:

6.5.8a. Zinc:

The results of biomapping of zinc through moss *T. cymbifolium* at different collection sites of Munsiyari during 2020, 2021, and 2022 are presented in Table (6.5.8a) and Figures (6.5.8 a-c). It was observed in the analysis that the moss accumulated the metal in the sequence of summer> winter> rain. Seasonally non-significant difference ($p \leq 0.05$) was found at most sites in the three consecutive years.

In summer, the south direction recorded the maximum metal accumulation in 2020 (1.471 mg/g DW), 2021 (2.091 mg/g DW), and 2022 (2.314 mg/g DW). However, the lowest values were observed at the city center in 2020 (0.707 mg/g DW) and 2021 (0.856 mg/g DW) and at the north 5 km in 2022 (0.916 mg/g DW).

In rain, zinc values rose to 0.381 mg/g DW in 2020 in the east direction, 0.581 mg/g DW in

2021 from the west direction, and 0.957 mg/g DW in 2022 in the west direction. The minimum zinc accumulation was reported towards the north (0.255 mg/g DW) and from the city center in 2020 (0.338 mg/g DW) and in 2022 (0.390 mg/g DW).

The highest values were evaluated in winter towards the south direction in 2020 (1.249 mg/g DW), 2021 (1.563 mg/g DW), and 2022 (1.861 mg/g DW). At the same time, the lowest concentration was found towards the city center in 2020 (0.383 mg/g DW), 2021 (0.561 mg/g DW), and 2022 (0.640 mg/g DW).

6.5.8b. Lead:

The Pb values at different sampling sites of Munsiyari during the seasons 2020, 2021, and 2022 were presented in a table (6.5.8b) and Figures (6.5.8 d-f). Results revealed that moss accumulated the lowest Pb in rain and the highest in summer. A seasonally significant variation was detected ($p \leq 0.05$) at almost all the sites of Munsiyari.

In the summer season, the west direction was identified to accumulate a maximum level of Pb during 2020 (0.965 mg/g DW) and 2022 (1.638 mg/g DW), while in 2021 (1.084 mg/g DW), it was the highest from the south direction. The values declined to 0.658 mg/g DW in 2020, 0.758 mg/g DW in 2021, and 0.913 mg/g DW in 2022 towards the city center.

In the rain, the consistent peak concentration of Pb was 0.381 mg/g DW (2020) from the east direction, 0.581 mg/g DW (2021), and 0.957 mg/g DW (2022) in the west direction. In contrast, the concentration was measured at the minimum in moss samples harvested from the north direction during 2020 (0.150 mg/g DW) and from the city center in 2021 (0.317 mg/g DW) and 2022 (0.337 mg/g DW).

In winter, values of Pb were found maximum in the south direction (0.563 mg/g DW) in 2020, (0.861 mg/g DW) in 2021, and from the west direction during 2022 (1.248 mg/g DW). Whereas minimum deposition was measured in moss harvested from the city center in 2020 (0.322 mg/g DW), 2021 (0.374 mg/g DW), and 2022 (0.383 mg/g DW). Statistically significant differences in values were observed at all sites over the baseline concentration throughout all three consecutive years..

6.5.8c. Copper:

Seasonal and annual accumulation of Cu in moss *T. cymbifolium* at different sampling sites of Pithoragarh during the years 2020, 2021, and 2022 are presented in Table (6.5.8c) and Figures (6.5.8

g-i).

Data revealed that *T. cymbifolium* accumulates Cu in summer> winter> rain season. However, almost all values were found to be seasonally significantly different ($p \leq 0.05$) at most of the sites during three consecutive years of study (2020, 2021, and 2022).

In summer, the maximum Cu accumulation was recorded in the south direction during the years 2020 (1.263 mg/g DW), 2021 (1.562 mg/g DW), and from the north direction in 2022 (1.878 mg/g DW). Moss samples harvested from the city center accumulated the minimum metal in all three consecutive years (0.745 mg/g DW, 0.817 mg/g DW, and 0.837 mg/g DW).

In rain, the highest concentration was observed at different sites in different years, i.e., at the city center in 2020 (0.513 mg/g DW), in the north direction in 2021 (0.678 mg/g DW), and in 2022 (0.965 mg/g DW). The same diversified trend was observed for the minimum concentration towards the east direction in 2020 (0.155 mg/g DW) (2020) and in 2021 (0.361 mg/g DW), while at the city center, it was 0.545 mg/g DW in 2022.

The maximum metal load in the winter season was found in the south direction as 1.036 mg/g DW in 2020, 1.355 mg/g DW in 2021, and 1.579 mg/g DW in 2022. The minimum values were recorded in the east direction in 2020 (0.468 mg/g DW), 2021 (0.556 mg/g DW), and 2022 (0.621 mg/g DW) from the city center. All the study sites exhibited significant differences ($p \leq 0.05$) in Cu compared to baseline concentration.

6.5.8d. Cadmium:

Results of cadmium load in moss *T. cymbifolium* at different sampling stations of Munsiyari during various seasons of 2020, 2021, and 2022 are shown in Table (6.5.8d) and Figures (6.5.8 j-l).

Observation exhibited that moss *T. cymbifolium* accumulates the lowest Cd in the rain season. A seasonally non-significant variation ($p \leq 0.05$) was found at most of the sites.

In summer, the maximum level of Cd was accumulated towards the east direction during 2020 (0.135 mg/g DW), 2021 (0.159 mg/g DW), and 2022 (0.186 mg/g DW). Its minimum values were measured at 0.052 mg/g DW, 0.072 mg/g DW, and 0.079 mg/g DW at the city center during 2020, 2021, and 2022, respectively.

During the rains, the maximum Cd concentration was found towards the city center (0.035

mg/g DW) in 2020, in the east direction (0.049 mg/g DW) in 2021, and (0.064 mg/g DW) in 2022. The concentration declined to 0.016 mg/g DW (2020) and 0.030 mg/g DW (2022) in the west direction, while it was 0.053 mg/g DW (2021) in the city center.

Winter had a maximum concentration in the east direction (0.065 mg/g DW, 0.084 mg/g DW, and 0.114 mg/g DW) and a minimum in the west direction (0.039 mg/g DW and 0.045 mg/g DW) in 2020 and 2021, whereas it was reported 0.062 mg/g DW at city center during 2022.

Table 6.5.1a: Seasonal variation in Zinc (mg/g DW) in *Thuidium cyambifolium* at different directions in Champawat during the years 2020, 2021, and 2022

Directions	Summer			Rain			Winter		
	2020	2021	2022	2020	2021	2022	2020	2021	2022
Baseline	0.234±0.018	0.326±0.013	0.387±0.010	0.094±0.007	0.135±0.025	0.147±0.013	0.132±0.008	0.165±0.025	0.265±0.011
City Center	0.852^{bc}± 0.043	0.927^{cd} ± 0.030	0.952^{d} ± 0.032	0.525^{c} ± 0.060	0.562^{c} ± 0.010	0.655^{c} ± 0.011	0.602^{b} ± 0.021	0.682^{d} ± 0.014	0.833^{c} ± 0.015
East	1.365^{b} ± 0.069	1.537^{cd} ± 0.076	1.959^{b} ± 0.040	0.971^{b} ± 0.019	1.114^{a} ± 0.010	1.046^{d} ± 0.011	1.180^{a} ± 0.032	1.287^{b} ± 0.012	1.366^{d} ± 0.031
North	1.286^{c} ± 0.059	1.689^{c} ± 0.049	1.923^{d} ± 0.055	0.840^{b} ± 0.019	0.981^{b} ± 0.014	0.852^{c} ± 0.013	0.944^{c} ± 0.022	1.136^{c} ± 0.020	1.433^{d} ± 0.025
South	1.227^{c} ± 0.053	1.511^{d} ± 0.059	1.745^{b} ± 0.066	0.853^{b} ± 0.018	1.002^{b} ± 0.016	0.960^{d} ± 0.011	0.853^{d} ± 0.037	1.117^{c} ± 0.013	1.283^{cd} ± 0.021
West	1.172^{cd} ± 0.050	1.344^{e} ± 0.063	1.365^{e} ± 0.042	0.906^{a} ± 0.019	1.047^{a} ± 0.013	1.270^{ab} ± 0.020	1.143^{ab} ± 0.011	1.368^{a} ± 0.023	1.580^{b} ± 0.014

Table 6.5.1b: Seasonal variation in Lead (mg/g DW) in *Thuidium cyambifolium* at different directions in Champawat during the years 2020, 2021, and 2022

Directions	Summer			Rain			Winter		
	2020	2021	2022	2020	2021	2022	2020	2021	2022
Baseline	0.163±0.019	0.236±0.016	0.264±0.011	0.032±0.007	0.044±0.011	0.057±0.009	0.052±0.008	0.059±0.009	0.088±0.009
City Center	0.976^{b} ± 0.016	1.143^{b} ± 0.022	1.240^{c} ± 0.027	0.539^{c} ± 0.040	0.678^{b} ± 0.018	0.755^{b}± 0.023	0.721^{c} ± 0.009	0.742^{b} ± 0.042	0.832^{b} ± 0.012
East	0.761^{d} ± 0.018	1.049^{c} ± 0.023	1.183^{d} ± 0.032	0.556^{b} ± 0.015	0.756^{b} ± 0.013	0.865^{bc} ± 0.021	0.682^{bc} ± 0.009	0.993^{c} ± 0.028	1.278^{b} ± 0.022
North	0.766^{de} ± 0.018	1.274^{c} ± 0.019	1.431^{de} ± 0.030	0.508^{c} ± 0.011	0.614^{d} ± 0.013	0.686^{cd} ± 0.010	0.556^{e} ± 0.011	0.652^{d} ± 0.012	0.835^{d} ± 0.017
South	0.856^{b} ± 0.011	1.238^{c} ± 0.022	1.565^{b} ± 0.021	0.594^{c} ± 0.022	0.778^{b} ± 0.025	0.976^{b} ± 0.015	0.781^{b} ± 0.030	1.007^{b} ± 0.027	1.165^{bc} ± 0.010
West	0.656^{e} ± 0.026	0.948^{e} ± 0.021	1.090^{e} ± 0.009	0.484^{b} ± 0.025	0.533^{c} ± 0.020	0.643^{e} ± 0.019	0.603^{ef} ± 0.007	0.765^{d} ± 0.017	0.816^{d} ± 0.029

.

- Values are represented as mean ± SE
- Means with the same letter are not significantly different.
- Tukeys's Honest Significant Difference (HSD) Test was performed at α=0.05 and Cv=4.289

Table 6.5.1c: Seasonal variation in Copper (mg/g DW) in *Thuidium cyambifolium* at different directions in Champawat during the years 2020, 2021, and 2022

Directions	Summer			Rain			Winter		
	2020	2021	2022	2020	2021	2022	2020	2021	2022
Baseline	0.135±0.017	0.158±0.011	0.165±0.018	0.035±0.008	0.037±0.007	0.046±0.005	0.056±0.008	0.062±0.006	0.076±0.009
City Center	0.775^{bc} ± 0.015	0.976^{bc} ± 0.018	0.957^{c} ± 0.024	0.538^{bc} ± 0.021	0.670^{ab} ± 0.031	0.726^{c} ± 0.034	0.641^{bc} ± 0.033	0.751^{b} ± 0.017	0.774^{bc} ± 0.010
East	0.629^{d} ± 0.019	0.746^{e} ± 0.011	0.966^{f} ± 0.025	0.368^{c} ± 0.055	0.466^{d} ± 0.014	0.664^{cd} ± 0.019	0.549^{de} ± 0.031	0.667^{e} ± 0.004	0.833^{e} ± 0.013
North	0.739^{f} ± .015	0.766^{f} ± 0.020	0.879^{f} ± 0.015	0.347^{d} ± 0.013	0.372^{e} ± 0.023	0.392^{f} ± 0.014	0.446^{e} ± 0.019	0.561^{e} ± 0.020	0.778^{f} ± 0.018
South	0.785^{de} ± 0.022	0.797^{e} ± 0.011	1.119^{e} ± 0.012	0.456^{c} ± 0.026	0.530^{d} ± 0.026	0.665^{de} ± 0.023	0.533^{d} ± 0.028	0.638^{f} ± 0.018	0.771^{d} ± 0.019
West	0.557^{e} ± 0.011	0.648^{e} ± 0.011	0.740^{f} ± 0.011	0.377^{cd} ± 0.017	0.461^{d} ± 0.016	0.471^{e} ± 0.023	0.519^{d} ± 0.015	0.550^{d} ± 0.019	0.613^{d} ± 0.019

Table 6.5.1d: Seasonal variation in Cadmium (mg/g DW) in *Thuidium cyambifolium* at different directions in Champawat during the years 2020, 2021, and 2022

Directions	Summer			Rain			Winter		
	2020	2021	2022	2020	2021	2022	2020	2021	2022
Baseline	0.010 ± 0.001	0.022 ± 0.006	0.041 ± 0.007	ND	ND	0.006 ± 0.001[a]	0.008 ± 0.001	0.011 ± 0.004	0.017 ± 0.009
City Center	0.067^{a} ± 0.004	0.097^{a} ± 0.004	0.106^{a} ± 0.012	0.021^{a} ± 0.006	0.023^{b} ± 0.001	0.026^{b} ± 0.011	0.034^{a} ± 0.0007	0.070^{a} ± 0.005	0.076^{a} ± 0.006
East	0.090^{a}± 0.006	0.105^{a} ± 0.014	0.128^{a} ± 0.015	0.019^{a} ± 0.006	0.040^{a} ± 0.009	0.054^{a} ± 0.011	0.041^{a} ± 0.003	0.047^{b} ± 0.003	0.062^{c} ± 0.004
North	0.089^{a} ± 0.009	0.108^{ab} ± 0.004	0.117^{a} ± 0.012	0.029^{a} ± 0.007	0.032^{a} ± 0.007	0.048^{a} ± 0.008	0.031^{a} ± 0.007	0.048^{a} ± 0.009	0.057^{a} ± 0.010
South	0.086^{a} ± 0.010	0.089^{a} ± 0.004	0.133^{a} ± 0.005	0.028^{a} ± 0.002	0.037^{a} ± 0.005	0.045^{a} ± 0.002	0.033^{a} ± 0.010	0.059^{a} ± 0.002	0.061^{a} ± 0.012
West	0.088^{a} ± 0.010	0.111^{a} ± 0.007	0.113^{a} ± 0.003	0.026^{a} ± 0.004	0.041^{a} ± 0.002	0.055^{a} ± 0.013	0.039^{b} ± 0.003	0.056^{b} ± 0.004	0.068^{c} ± 0.011

- Values are represented as mean ± SE
- Means with the same letter are not significantly different.
- Tukeys's Honest Significant Difference (HSD) Test was performed at α=0.05 and Cv=4.289

Table 6.5.2 a: Seasonal variation in Zinc (mg/g DW) in *Thuidium cyambifolium* at different directions in Lohaghat during the years 2020, 2021, and 2022

Directions	Summer			Rain			Winter		
	2020	2021	2022	2020	2021	2022	2020	2021	2022
Baseline	0.234±0.018	0.326±0.013	0.387±0.010	0.094±0.007	0.135±0.025	0.147±0.013	0.132±0.008	0.165±0.025	0.265±0.011
City Center	0.778 ^{cd} ± 0.010	1.067 ^{b} ± 0.020	1.241 ^{c} ± 0.0222	0.730^{c} ± 0.021	0.806 ^{b} ± 0.029	1.072 ^{d} ± 0.011	0.642^{b} ± 0.018	1.157 ^{cd} ± 0.024	1.460 ^{cd} ± 0.014
East	1.245 ^{c}± 0.026	1.763 ^{bc} ± 0.026	1.769 ^{c} ± 0.019	0.536 ^{bc} ± 0.029	0.671 ^{bc} ± 0.019	0.869 ^{b} ± 0.019	0.855 ^{b} ± 0.025	0.853 ^{bc} ± 0.024	1.045 ^{b} ± 0.012
North	1.482 ^{b}± 0.029	1.429 ^{d}± 0.026	1.555 ^{c}± 0.027	0.876^{b}± 0.012	1.058 ^{b}± 0.012	1.354 ^{a}± 0.015	1.121 ^{b}± 0.018	1.470 ^{b}± 0.017	1.64 ^{bc}± 0.025
South	1.186 ^{c} ± 0.037	1.429 ^{de} ± 0.033	1.623 ^{cd} ± 0.021	0.732^{c} ± 0.014	0.864 ^{cd} ± 0.011	1.078 ^{c} ± 0.023	0.892 ^{d}± 0.020	1.062 ^{c}± 0.015	1.365 ^{bc}± 0.019
West	1.168 ^{cd} ± 0.023	1.547 ^{bc} ± 0.012	2.051 ^{c} ± 0.010	0.654^{b} ± 0.017	0.811 ^{b} ± 0.022	1.069 ^{d} ± 0.017	0.762 ^{d} ± 0.017	1.149 ^{b} ± 0.014	1.371 ^{cd} ± 0.027

Table 6.5.2b: Seasonal variation in Lead (mg/g DW) in *Thuidium cyambifolium* at different directions in Lohaghat during the years 2020, 2021, and 2022

Directions	Summer			Rain			Winter		
	2020	2021	2022	2020	2021	2022	2020	2021	2022
Baseline	0.163±0.019	0.236±0.016	0.264±0.011	0.032±0.007	0.044±0.011	0.057±0.009	0.052±0.008	0.059±0.009	0.088±0.009
City Center	0.621 ^{e} ± 0.020	1.253 ^{b} ± 0.012	1.850 ^{b}± 0.026	0.277 ^{d} ± 0.008	0.378 ^{cd} ± 0.015	0.562 ^{c} ± 0.016	0.433 ^{d} ± 0.023	0.641 ^{b} ± 0.022	0.753 ^{bc} ± 0.016
East	1.377 ^{a} ± 0.019	1.452 ^{ab} ± 0.013	1.633 ^{b} ± 0.020	1.077 ^{a} ± 0.009	1.189 ^{a} ± 0.009	1.277 ^{a} ± 0.022	1.199 ^{a} ± 0.019	1.377 ^{a} ± 0.013	1.477 ^{a} ± 0.012
North	1.547 ^{b} ± 0.015	1.853 ^{b} ± 0.025	1.847 ^{b} ± 0.018	0.974 ^{a} ± 0.018	1.491 ^{a} ± 0.013	1.166 ^{a} ± 0.017	1.323 ^{a} ± 0.022	1.581 ^{a} ± 0.006	1.664 ^{a} ± 0.018
South	1.375 ^{a} ± 0.014	1.517 ^{b} ± 0.020	1.625 ^{b} ± 0.015	1.226 ^{a} ± 0.020	1.084 ^{a} ± 0.015	1.194 ^{a} ± 0.019	1.176 ^{a} ± 0.014	1.271 ^{a} ± 0.011	1.284 ^{a} ± 0.023
West	1.135 ^{a} ± 0.028	1.268 ^{cd} ± 0.013	1.308 ^{d} ± 0.016	0.887 ^{a} ± 0.019	0.903 ^{a} ± 0.022	1.674 ^{a} ± 0.021	0.844 ^{ab} ± 0.018	1.092 ^{b} ± 0.007	1.281 ^{b} ± 0.027

- Values are represented as mean ± SE
- Means with the same letter are not significantly different.
- Tukeys's Honest Significant Difference (HSD) Test was performed at α=0.05 and Cv=4.289

Table 6.5.2c: Seasonal variation in Copper (mg/g DW) in *Thuidium cyambifolium* at different directions in Lohaghat during the years 2020, 2021, and 2022

Directions	Summer			Rain			Winter		
	2020	2021	2022	2020	2021	2022	2020	2021	2022
Baseline	0.135±0.017	0.158±0.011	0.165±0.008	0.035±0.008	0.037±0.007	0.046±0.005	0.056±0.008	0.062±0.006	0.076±0.004
City Center	0.944 ^{a} ± 0.018	1.164 ^{a} ± 0.019	1.627 ^{a} ± 0.022	0.566 ^{b} ± 0.011	0.777 ^{a} ± 0.019	1.023 ^{a} ± 0.011	0.774 ^{a} ± 0.016	0.987 ^{a} ± 0.013	1.334 ^{a} ± 0.020
East	0.899 ^{c} ± 0.032	1.138 ^{d} ± 0.018	1.166 ^{de} ± 0.020	0.733 ^{b} ± 0.013	0.863 ^{b} ± 0.017	0.947 ^{b} ± 0.011	0.740 ^{c} ± 0.017	0.880 ^{c} ± 0.012	1.175 ^{bc} ± 0.017
North	0.979 ^{d} ± 0.014	1.075 ^{d} ± 0.018	1.382 ^{d} ± 0.020	0.626 ^{b} ± 0.018	0.764 ^{bc} ± 0.018	0.885 ^{c} ± 0.018	0.846 ^{c} ± 0.020	0.970 ^{c} ± 0.021	1.253 ^{c} ± 0.017
South	0.877 ^{cd} ± 0.016	1.069 ^{d} ± 0.020	1.157 ^{e} ± 0.026	0.748 ^{ab} ± 0.021	0.856 ^{d} ± 0.010	0.871 ^{b} ± 0.017	0.755 ^{c} ± 0.015	0.845 ^{e} ± 0.018	1.018 ^{c} ± 0.027
West	0.873 ^{cd} ± 0.019	0.981 ^{c} ± 0.013	1.173 ^{d} ± 0.026	0.643 ^{a} ± 0.018	0.765 ^{ab} ± 0.0149	0.849 ^{c} ± 0.015	0.864 ^{b} ± 0.015	0.877 ^{b} ± 0.017	1.026 ^{c} ± 0.026

Table 6.5.2d: Seasonal variation in Cadmium (mg/g DW) in *Thuidium cyambifolium* at different directions in Lohaghat during the years 2020, 2021, and 2022

Directions	Summer			Rain			Winter		
	2020	2021	2022	2020	2021	2022	2020	2021	2022
Baseline	0.010±0.001	0.022±0.006	0.041±0.007	ND	ND	0.006 ± 0.001	0.006±0.001	0.011±0.004	0.017±0.009
City Center	0.072 ^{a} ± 0.003	0.109 ^{ab} ± 0.006	0.128 ^{ab} ± 0.007	0.022 ^{a} ± 0.005	0.037 ^{a} ± 0.005	0.055 ^{a} ± 0.004	0.045 ^{a} ± 0.004	0.075 ^{a} ± 0.004	0.085 ^{a} ± 0.005
East	0.087 ^{a} ± 0.004	0.067 ^{ab} ± 0.007	0.089 ^{bc} ± 0.006	0.026 ^{a} ± 0.004	0.047 ^{a} ± 0.004	0.051 ^{a} ± 0.003	0.043 ^{a} ± 0.002	0.056 ^{a} ± 0.003	0.064 ^{a} ± 0.004
North	0.052 ^{a} ± 0.004	0.087 ^{ab} ± 0.004	0.120 ^{a} ± 0.007	0.028 ^{a} ± 0.001	0.050 ^{a} ± 0.003	0.065 ^{a} ± 0.006	0.040 ^{a} ± 0.005	0.061 ^{a} ± 0.002	0.094 ^{ab} ± 0.003
South	0.053 ^{a} ± 0.005	0.087 ^{a} ± 0.005	0.093 ^{a} ± 0.005	0.027 ^{a} ± 0.002	0.053 ^{a} ± 0.003	0.056 ^{a} ± 0.003	0.038 ^{a} ± 0.009	0.059 ^{a} ± 0.003	0.069 ^{a} ± 0.002
West	0.073 ^{ab} ± 0.006	0.085 ^{ab} ± 0.008	0.094 ^{bc} ± 0.004	0.037 ^{a} ± 0.002	0.046 ^{a} ± 0.003	0.055 ^{a} ± 0.002	0.055 ^{a} ± 0.003	0.064 ^{a} ± 0.004	0.081 ^{a} ± 0.005

- Values are represented as mean ± SE
- Means with the same letter are not significantly different.
- Tukeys's Honest Significant Difference (HSD) Test was performed at α=0.05 and Cv=4.289

Table 6.5.3a: Seasonal variation in Zinc (mg/g DW) in *Thuidium cyambifolium* at different directions in Khetikhan during the years 2020, 2021, and 2022

Directions	Summer			Rain			Winter		
	2020	2021	2022	2020	2021	2022	2020	2021	2022
Baseline	0.234±0.018	0.326±0.013	0.387±0.010	0.094±0.007	0.135±0.025	0.147±0.013	0.132±0.008	0.165±0.025	0.265±0.011
City Center	1.368 ^{a} ± 0.010	1.514 ^{b} ± 0.013	1.654 ^{a} ± 0.017	0.551 ^{bc} ± 0.015	0.634 ^{bc} ± 0.024	0.724 ^{c} ± 0.015	0.686 ^{b} ± 0.012	0.745 ^{cd} ± 0.027	0.853 ^{c} ± 0.022
East	1.371 ^{b} ± 0.011	1.670 ^{d} ± 0.020	1.840 ^{c} ± 0.020	1.134 ^{a} ± 0.015	1.092 ^{a} ± 0.060	1.242 ^{c} ± 0.014	1.186 ^{a} ± 0.011	1.231 ^{bcd} ± 0.017	1.657 ^{b} ± 0.015
North	1.552 ^{b} ± 0.017	1.876 ^{bc} ± 0.014	2.328 ^{a} ± 0.018	1.243 ^{a} ± 0.032	1.233 ^{a} ± 0.009	1.356 ^{a} ± 0.022	1.437 ^{a} ± 0.025	1.621 ^{a} ± 0.013	1.747 ^{b} ± 0.026
South	1.873 ^{a} ± 0.026	1.973 ^{de} ± 0.009	2.347 ^{a} ± 0.025	1.224 ^{a} ± 0.012	1.141 ^{a} ± 0.008	1.372 ^{a} ± 0.019	1.530 ^{a} ± 0.025	1.145 ^{b} ± 0.019	1.842 ^{a} ± 0.019
West	1.344 ^{b} ± 0.020	1.639 ^{bc} ± 0.034	1.867 ^{b} ± 0.024	0.951 ^{a} ± 0.023	0.839 ^{b} ± 0.017	1.232 ^{bc} ± 0.014	1.169 ^{a} ± 0.022	1.431 ^{a} ± 0.022	1.565 ^{b} ± 0.026

Table 6.5.3b: Seasonal variation in Lead (mg/g DW) in *Thuidium cyambifolium* at different directions in Khetikhan during the years 2020, 2021, and 2022

Directions	Summer			Rain			Winter		
	2020	2021	2022	2020	2021	2022	2020	2021	2022
Baseline	0.163±0.019	0.236±0.016	0.264±0.011	0.032±0.007	0.044±0.011	0.057±0.009	0.052±0.008	0.059±0.009	0.088±0.009
City Center	0.765 ^{c} ± 0.017	0.819 ^{d} ± 0.016	0.948 ^{d} ± 0.015	0.344 ^{d} ± 0.010	0.422 ^{cd} ± 0.013	0.747 ^{b} ± 0.021	0.408 ^{def} ± 0.014	0.525 ^{c} ± 0.018	0.703 ^{c} ± 0.016
East	1.039 ^{c} ± 0.018	1.563 ^{a} ± 0.021	1.275 ^{d} ± 0.013	0.553 ^{b} ± 0.011	1.130 ^{a} ± 0.013	0.834 ^{bcde} ± 0.024	0.751 ^{b} ± 0.018	1.264 ^{b} ± 0.010	1.022 ^{cd} ± 0.013
North	0.869 ^{cd} ± 0.016	1.131 ^{d} ± 0.012	1.350 ^{d} ± 0.014	0.527 ^{c} ± 0.016	0.766 ^{c} ± 0.017	0.668 ^{cde} ± 0.019	0.728 ^{cd} ± 0.012	0.841 ^{ce} ± 0.013	0.976 ^{c} ± 0.028
South	0.848 ^{bc} ± 0.020	0.970 ^{c} ± 0.019	1.254 ^{d} ± 0.012	0.451 ^{d} ± 0.017	0.761 ^{b} ± 0.018	0.876 ^{bc} ± 0.018	0.566 ^{c} ± 0.021	0.828 ^{cde} ± 0.012	1.054 ^{cd} ± 0.020
West	0.948 ^{c} ± 0.021	1.375 ^{bc} ± 0.011	1.226 ^{d} ± 0.017	0.551 ^{b} ± 0.016	0.955 ^{a} ± 0.019	0.794 ^{d} ± 0.013	0.752 ^{bc} ± 0.012	1.134 ^{b} ± 0.016	1.061 ^{c} ± 0.016

- Values are represented as mean ± SE
- Means with the same letter are not significantly different.
- Tukeys's Honest Significant Difference (HSD) Test was performed at α=0.05 and Cv=4.289

Table 6.5.3c: Seasonal variation in Copper (mg/g DW) in *Thuidium cyambifolium* at different directions in Khetikhan during the years 2020, 2021, and 2022

Directions	Summer			Rain			Winter		
	2020	2021	2022	2020	2021	2022	2020	2021	2022
Baseline	0.135±0.017	0.158±0.011	0.165±0.008	0.035±0.008	0.037±0.007	0.046±0.005	0.056±0.008	0.062±0.006	0.076±0.004
City Center	$0.901^{a} \pm 0.013$	$0.934^{c} \pm 0.016$	$1.241^{be} \pm 0.015$	$0.347^{d} \pm 0.022$	$0.676^{ab} \pm 0.015$	$0.636^{cd} \pm 0.013$	$0.583^{bc} \pm 0.012$	$0.451^{c} \pm 0.014$	$0.757^{cd} \pm 0.016$
East	$0.643^{d} \pm 0.019$	$1.174^{cd} \pm 0.029$	$1.074^{ef} \pm 0.018$	$0.445^{c} \pm 0.019$	$0.744^{c} \pm 0.008$	$0.443^{e} \pm 0.017$	$0.445^{e} \pm 0.015$	$0.452^{f} \pm 0.014$	$0.584^{f} \pm 0.008$
North	$1.125^{c} \pm 0.022$	$1.568^{b} \pm 0.016$	$0.157^{c} \pm 0.023$	$0.627^{b} \pm 0.010$	$1.132^{a} \pm 0.018$	$0.722^{d} \pm 0.020$	$0.752^{c} \pm 0.014$	$0.838^{d} \pm 0.015$	$0.958^{e} \pm 0.013$
South	$0.746^{e} \pm 0.013$	$1.458^{ab} \pm 0.012$	$1.183^{e} \pm 0.013$	$0.535^{c} \pm 0.023$	$1.229^{a} \pm 0.012$	$0.667^{de} \pm 0.022$	$0.640^{d} \pm 0.023$	$0.654^{f} \pm 0.023$	$0.822^{d} \pm 0.018$
West	$0.543^{e} \pm 0.017$	$1.031^{c} \pm 0.013$	$0.954^{e} \pm 0.014$	$0.226^{e} \pm 0.015$	$0.746^{b} \pm 0.013$	$0.344^{f} \pm 0.013$	$0.372^{e} \pm 0.020$	$0.555^{d} \pm 0.011$	$0.670^{d} \pm 0.017$

Table 6.5.3d: Seasonal variation in Cadmium (mg/g DW) in *Thuidium cyambifolium* at different directions in Khetikhan during the years 2020, 2021, and 2022

Directions	Summer			Rain			Winter		
	2020	2021	2022	2020	2021	2022	2020	2021	2022
Baseline	0.010±0.001	0.022±0.006	0.041±0.007	ND	ND	0.006 ± 0.001^{a}	0.006±0.001	0.011±0.004	0.017±0.009
City Center	$0.062^{a} \pm 0.003$	$0.070^{ab} \pm 0.005$	$0.072^{ab} \pm 0.005$	$0.041^{a} \pm 0.004$	$0.047^{a} \pm 0.002$	$0.057^{a} \pm 0.003$	$0.046^{a} \pm 0.003$	$0.051^{a} \pm 0.003$	$0.058^{a} \pm 0.006$
East	$0.091^{a} \pm 0.006$	$0.117^{ab} \pm 0.010$	$0.141^{a} \pm 0.016$	$0.058^{a} \pm 0.010$	$0.075^{a} \pm 0.004$	$0.113^{a} \pm 0.005$	$0.064^{a} \pm 0.003$	$0.090^{a} \pm 0.004$	$0.120^{a} \pm 0.010$
North	$0.074^{a} \pm 0.007$	$0.085^{ab} \pm 0.004$	$0.113^{a} \pm 0.010$	$0.036^{a} \pm 0.012$	$0.049^{a} \pm 0.006$	$0.061^{a} \pm 0.012$	$0.048^{a} \pm 0.012$	$0.059^{a} \pm 0.009$	$0.085^{ab} \pm 0.007$
South	$0.098^{a} \pm 0.009$	$0.127^{a} \pm 0.008$	$0.135^{a} \pm 0.004$	$0.033^{a} \pm 0.006$	$0.040^{a} \pm 0.006$	$0.069^{a} \pm 0.010$	$0.063^{a} \pm 0.007$	$0.081^{a} \pm 0.010$	$0.099^{a} \pm 0.003$
West	$0.115^{ab} \pm 0.003$	$0.104^{ab} \pm 0.007$	$0.196^{a} \pm 0.009$	$0.053^{a} \pm 0.011$	$0.077^{a} \pm 0.004$	$0.116^{a} \pm 0.006$	$0.093^{a} \pm 0.008$	$0.100^{a} \pm 0.005$	$0.144^{a} \pm 0.005$

- Values are represented as mean ± SE
- Means with the same letter are not significantly different.
- Tukeys's Honest Significant Difference (HSD) Test was performed at α=0.05 and Cv=4.289

Table 6.5.4a: Seasonal variation in Zinc (mg/g DW) in *Thuidium cyambifolium* at different directions in Barakote during the years 2020, 2021, and 2022

Directions	Summer			Rain			Winter		
	2020	2021	2022	2020	2021	2022	2020	2021	2022
Baseline	0.234±0.018	0.326±0.013	0.387±0.010	0.094±0.007	0.135±0.025	0.147±0.013	0.132±0.008	0.165±0.025	0.265±0.011
City Center	$0.778^{cd} \pm 0.007$	$0.818^{de} \pm 0.021$	$0.873^{d} \pm 0.019$	$0.404^{de} \pm 0.020$	$0.429^{d} \pm 0.009$	$0.444^{a} \pm 0.015$	$0.483^{cd} \pm 0.014$	$0.532^{ef} \pm 0.014$	$0.574^{d} \pm 0.017$
East	$1.360^{b} \pm 0.024$	$1.563^{bc} \pm 0.019$	$1.770^{c} \pm 0.017$	$1.066^{ab} \pm 0.016$	$1.130^{a} \pm 0.020$	$1.362^{b} \pm 0.021$	$1.146^{a} \pm 0.023$	$1.264^{bc} \pm 0.021$	$1.544^{c} \pm 0.015$
North	$0.945^{d} \pm 0.028$	$1.125^{e} \pm 0.020$	$1.364^{f} \pm 0.019$	$0.549^{c} \pm 0.012$	$0.766^{c} \pm 0.021$	$0.867^{c} \pm 0.018$	$0.665^{d} \pm 0.011$	$0.841^{d} \pm 0.019$	$1.118^{e} \pm 0.020$
South	$0.794^{d} \pm 0.010$	$0.970^{f} \pm 0.022$	$1.536^{d} \pm 0.023$	$0.471^{ef} \pm 0.021$	$0.777^{d} \pm 0.017$	$0.957^{d} \pm 0.017$	$0.547^{e} \pm 0.020$	$0.828^{d} \pm 0.014$	$1.188^{d} \pm 0.017$
West	$1.163^{cd} \pm 0.012$	$1.375^{de} \pm 0.024$	$1.737^{c} \pm 0.021$	$0.879^{a} \pm 0.013$	$0.955^{a} \pm 0.023$	$1.366^{a} \pm 0.019$	$0.948^{c} \pm 0.015$	$1.134^{b} \pm 0.014$	$1.484^{b} \pm 0.029$

Table 6.5.4b: Seasonal variation in Lead (mg/g DW) in *Thuidium cyambifolium* at different directions in Barakote during the years 2020, 2021, and 2022

Directions	Summer			Rain			Winter		
	2020	2021	2022	2020	2021	2022	2020	2021	2022
Baseline	0.163±0.019	0.236±0.016	0.264±0.011	0.032±0.007	0.044±0.011	0.057±0.009	0.052±0.008	0.059±0.009	0.088±0.009
City Center	$0.752^{cd} \pm 0.009$	$0.931^{c} \pm 0.015$	$1.171^{c} \pm 0.028$	$0.331^{d} \pm 0.013$	$0.433^{c} \pm 0.006$	$0.569^{c} \pm 0.017$	$0.429^{de} \pm 0.015$	$0.659^{b} \pm 0.022$	$0.839^{b} \pm 0.028$
East	$1.162^{b} \pm 0.014$	$1.352^{b} \pm 0.027$	$1.843^{a} \pm 0.015$	$0.344^{c} \pm 0.018$	$0.557^{cd} \pm 0.018$	$0.852^{bcd} \pm 0.019$	$0.634^{c} \pm 0.015$	$0.844^{de} \pm 0.014$	$1.346^{b} \pm 0.018$
North	$0.654^{f} \pm 0.010$	$0.834^{e} \pm 0.024$	$1.061^{af} \pm 0.024$	$0.271^{d} \pm 0.017$	$0.449^{ef} \pm 0.016$	$0.546^{f} \pm 0.012$	$0.429^{f} \pm 0.019$	$0.631^{d} \pm 0.016$	$0.758^{d} \pm 0.024$
South	$0.564^{d} \pm 0.019$	$0.767^{f} \pm 0.019$	$1.075^{e} \pm 0.026$	$0.258^{e} \pm 0.021$	$0.370^{d} \pm 0.016$	$0.559^{d} \pm 0.020$	$0.451^{de} \pm 0.022$	$0.563^{e} \pm 0.019$	$0.754^{f} \pm 0.020$
West	$1.117^{a} \pm 0.019$	$1.364^{bc} \pm 0.017$	$1.818^{b} \pm 0.022$	$0.462^{b} \pm 0.016$	$0.553^{c} \pm 0.026$	$0.849^{cd} \pm 0.018$	$0.671^{cde} \pm 0.020$	$0.966^{c} \pm 0.019$	$1.246^{b} \pm 0.021$

- Values are represented as mean ± SE
- Means with the same letter are not significantly different.
- Tukeys's Honest Significant Difference (HSD) Test was performed at α=0.05 and Cv=4.289

Table 6.5.4c: Seasonal variation in Copper (mg/g DW) in *Thuidium cyambifolium* at different directions in Barakote during the years 2020, 2021, and 2022

Directions	Summer			Rain			Winter		
	2020	2021	2022	2020	2021	2022	2020	2021	2022
Baseline	0.135±0.017	0.158±0.011	0.165±0.008	0.035±0.008	0.037±0.007	0.046±0.005	0.056±0.008	0.062±0.006	0.076±0.004
City Center	0.864 ^{ab} ± 0.024	0.904 ^{cd} ± 0.007	0.945 ^{cd} ± 0.026	0.449 ^{cd} ± 0.015	0.475 ^{d} ± 0.009	0.518 ^{e} ± 0.022	0.661 ^{b} ± 0.020	0.692 ^{b} ± 0.011	0.756 ^{cd} ± 0.019
East	0.953 ^{c} ± 0.024	1.174 ^{c} ± 0.019	1.246 ^{d} ± 0.025	0.361 ^{cd} ± 0.013	0.452 ^{d} ± 0.014	0.567 ^{d} ± 0.022	0.644 ^{cd} ± 0.029	0.747 ^{de} ± 0.023	0.963 ^{d} ± 0.014
North	1.354 ^{b} ± 0.020	1.561 ^{b} ± 0.024	1.854 ^{b} ± 0.024	0.772 ^{a} ± 0.018	0.842 ^{b} ± 0.016	1.144 ^{b} ± 0.013	1.149 ^{a} ± 0.009	1.322 ^{b} ± 0.009	1.568 ^{b} ± 0.021
South	0.970 ^{bc} ± 0.016	1.455 ^{ab} ± 0.025	1.973 ^{a} ± 0.015	0.655 ^{b} ± 0.024	0.769 ^{b} ± 0.022	1.255 ^{a} ± 0.019	0.863 ^{c} ± 0.021	1.229 ^{c} ± 0.017	1.650 ^{a} ± 0.024
West	0.769 ^{d} ± 0.013	1.031 ^{c} ± 0.022	1.261 ^{d} ± 0.016	0.447 ^{bc} ± 0.014	0.555 ^{cd} ± 0.026	0.720 ^{d} ± 0.019	0.653 ^{c} ± 0.016	0.746 ^{c} ± 0.018	0.948 ^{c} ± 0.020

Table 6.5.4d: Seasonal variation in Cadmium (mg/g DW) in *Thuidium cyambifolium* at different directions in Barakote during the years 2020, 2021, and 2022

Directions	Summer			Rain			Winter		
	2020	2021	2022	2020	2021	2022	2020	2021	2022
Baseline	0.010±0.001	0.022±0.006	0.041±0.007	ND	ND	0.006 ± 0.001 ^{a}	0.006±0.001	0.011±0.004	0.017±0.009
City Center	0.064 ^{a} ± 0.003	0.082 ^{ab} ± 0.005	0.088 ^{ab} ± 0.005	0.037 ^{a} ± 0.004	0.055 ^{a} ± 0.002	0.066 ^{a} ± 0.003	0.046 ^{a} ± 0.004	0.064 ^{a} ± 0.003	0.079 ^{a} ± 0.004
East	0.082 ^{a} ± 0.005	0.117 ^{ab} ± 0.005	0.154 ^{abc} ± 0.003	0.023 ^{a} ± 0.003	0.036 ^{a} ± 0.003	0.058 ^{a} ± 0.004	0.039 ^{a} ± 0.007	0.054 ^{a} ± 0.003	0.058 ^{a} ± 0.004
North	0.106 ^{a} ± 0.006	0.126 ^{ab} ± 0.007	0.145 ^{a} ± 0.010	0.032 ^{a} ± 0.007	0.046 ^{a} ± 0.006	0.063 ^{a} ± 0.004	0.049 ^{a} ± 0.009	0.070 ^{a} ± 0.005	0.087 ^{a} ± 0.005
South	0.068 ^{a} ± 0.009	0.091 ^{a} ± 0.006	0.126 ^{a} ± 0.005	0.034 ^{a} ± 0.005	0.045 ^{a} ± 0.004	0.067 ^{a} ± 0.004	0.048 ^{a} ± 0.015	0.065 ^{a} ± 0.005	0.078 ^{a} ± 0.006
West	0.090 ^{ab} ± 0.007	0.104 ^{ab} ± 0.005	0.126 ^{abc} ± 0.005	0.033 ^{a} ± 0.004	0.044 ^{a} ± 0.004	0.069 ^{a} ± 0.004	0.051 ^{a} ± 0.004	0.063 ^{a} ± 0.007	0.088 ^{a} ± 0.002

- Values are represented as mean ± SE
- Means with the same letter are not significantly different.
- Tukeys's Honest Significant Difference (HSD) Test was performed at α=0.05 and Cv=4.289

Table 6.5.5a: Seasonal variation in Zinc (mg/g DW) in *Thuidium cyambifolium* at different directions in Pithoragarh during the years 2020, 2021, and 2022

Directions	Summer			Rain			Winter		
	2020	2021	2022	2020	2021	2022	2020	2021	2022
Baseline	0.234±0.018	0.326±0.013	0.387±0.010	0.094±0.007	0.135±0.025	0.147±0.013	0.132±0.008	0.165±0.025	0.265±0.011
City Center	0.858 ^{bc} ± 0.015	1.030 ^{bc} ± 0.028	1.302 ^{bc} ± 0.036	0.443 ^{cd} ± 0.010	0.736 ^{b} ± 0.015	0.968 ^{b} ± 0.016	0.846 ^{a} ± 0.008	0.944 ^{ab} ± 0.016	1.141 ^{ab} ± 0.018
East	1.779 ^{a} ± 0.016	1.929 ^{a} ± 0.016	2.315 ^{a} ± 0.022	0.427 ^{d} ± 0.016	0.760 ^{bc} ± 0.020	1.644 ^{a} ± 0.015	1.254 ^{a} ± 0.014	1.654 ^{a} ± 0.024	1.958 ^{a} ± 0.020
North	1.862 ^{a} ± 0.013	1.926 ^{a} ± 0.022	2.351 ^{a} ± 0.033	0.639 ^{c} ± 0.018	0.834 ^{c} ± 0.020	1.145 ^{b} ± 0.022	1.449 ^{a} ± 0.025	1.691 ^{a} ± 0.029	2.037 ^{a} ± 0.024
South	1.565 ^{b} ± 0.021	1.832 ^{c} ± 0.015	2.357 ^{a} ± 0.021	0.568 ^{de} ± 0.011	0.820 ^{d} ± 0.020	1.316 ^{ab} ± 0.017	1.020 ^{c} ± 0.019	1.570 ^{a} ± 0.023	1.770 ^{a} ± 0.020
West	1.264 ^{bc} ± 0.015	1.469 ^{cd} ± 0.011	1.839 ^{bc} ± 0.017	0.555 ^{b} ± 0.019	0.732 ^{bc} ± 0.013	1.150 ^{cd} ± 0.023	1.053 ^{bc} ± 0.018	1.155 ^{b} ± 0.021	1.471 ^{bc} ± 0.021

Table 6.5.5b: Seasonal variation in Lead (mg/g DW) in *Thuidium cyambifolium* at different directions in Pithoragarh during the years 2020, 2021, and 2022

Directions	Summer			Rain			Winter		
	2020	2021	2022	2020	2021	2022	2020	2021	2022
Baseline	0.163±0.019	0.236±0.016	0.264±0.011	0.032±0.007	0.044±0.011	0.057±0.009	0.052±0.008	0.059±0.009	0.088±0.009
City Center	1.433 ^{a} ± 0.016	1.640 ^{a} ± 0.013	2.192 ^{a} ± 0.012	0.748 ^{b} ± 0.012	1.036 ^{a} ± 0.025	1.245 ^{a} ± 0.013	0.638 ^{def} ± 0.023	0.863 ^{c} ± 0.014	1.592 ^{a} ± 0.012
East	0.843 ^{d} ± 0.021	1.160 ^{c} ± 0.021	1.438 ^{c} ± 0.016	0.440 ^{c} ± 0.027	0.561 ^{cd} ± 0.019	0.752 ^{de} ± 0.011	0.661 ^{bc} ± 0.015	0.762 ^{de} ± 0.029	0.863 ^{e} ± 0.010
North	0.948 ^{c} ± 0.011	1.161 ^{d} ± 0.024	1.541 ^{cd} ± 0.020	0.287 ^{d} ± 0.020	0.459 ^{ef} ± 0.013	0.629 ^{def} ± 0.020	0.775 ^{c} ± 0.023	1.246 ^{a} ± 0.014	1.045 ^{c} ± 0.025
South	0.742 ^{c} ± 0.031	1.060 ^{de} ± 0.013	1.370 ^{c} ± 0.020	0.344 ^{de} ± 0.018	0.554 ^{c} ± 0.018	0.767 ^{c} ± 0.024	0.528 ^{cd} ± 0.016	0.726 ^{d} ± 0.013	0.957 ^{de} ± 0.026
West	0.829 ^{d} ± 0.018	1.175 ^{d} ± 0.012	1.246 ^{d} ± 0.019	0.457 ^{b} ± 0.019	0.584 ^{c} ± 0.025	0.847 ^{cd} ± 0.014	0.956 ^{b} ± 0.013	0.848 ^{d} ± 0.013	1.131 ^{c} ± 0.033

- Values are represented as mean ± SE
- Means with the same letter are not significantly different.
- Tukeys's Honest Significant Difference (HSD) Test was performed at α=0.05 and Cv=4.289

Table 6.5.5c: Seasonal variation in Copper (mg/g DW) in *Thuidium cyambifolium* at different directions in Pithoragarh during the years 2020, 2021, and 2022

Directions	Summer			Rain			Winter		
	2020	2021	2022	2020	2021	2022	2020	2021	2022
Baseline	0.135±0.017	0.158±0.011	0.165±0.008	0.035±0.008	0.037±0.007	0.046±0.005	0.056±0.008	0.062±0.006	0.076±0.004
City Center	0.863 ^{ab} ± 0.016	0.955 ^{c} ± 0.009	1.013 ^{c} ± 0.018	0.348 ^{d} ± 0.020	0.618 ^{bc} ± 0.012	0.732 ^{bc} ± 0.039	0.554 ^{bc} ± 0.016	0.668 ^{d} ± 0.020	0.758 ^{d} ± 0.011
East	1.579 ^{a} ± 0.011	1.757 ^{a} ± 0.021	2.051 ^{a} ± 0.018	0.854 ^{a} ± 0.014	1.133 ^{a} ± 0.017	1.468 ^{a} ± 0.019	1.147 ^{a} ± 0.022	1.574 ^{a} ± 0.009	1.753 ^{a} ± 0.011
North	1.695 ^{a} ± 0.013	1.995 ^{a} ± 0.012	2.163 ^{a} ± 0.027	0.870 ^{a} ± 0.012	1.036 ^{a} ± 0.013	1.534 ^{a} ± 0.018	1.239 ^{a} ± 0.015	1.661 ^{a} ± 0.018	1.859 ^{a} ± 0.014
South	1.364 ^{a} ± 0.024	1.565 ^{a} ± 0.017	1.814 ^{b} ± 0.021	0.767 ^{a} ± 0.015	0.837 ^{a} ± 0.015	1.171 ^{a} ± 0.025	1.159 ^{a} ± 0.012	1.523 ^{a} ± 0.023	1.562 ^{a} ± 0.025
West	1.386 ^{a} ± 0.020	1.571 ^{a} ± 0.021	1.759 ^{b} ± 0.026	0.543 ^{ab} ± 0.019	0.864 ^{a} ± 0.018	1.165 ^{a} ± 0.022	1.079 ^{a} ± 0.021	1.183 ^{a} ± 0.019	1.474 ^{a} ± 0.021

Table 6.5.5d: Seasonal variation in Cadmium (mg/g DW) in *Thuidium cyambifolium* at different directions in Pithoragarh during the years 2020, 2021, and 2022

Directions	Summer			Rain			Winter		
	2020	2021	2022	2020	2021	2022	2020	2021	2022
Baseline	0.010±0.001	0.022±0.006	0.041±0.007	ND	ND	0.006 ± 0.001	0.006±0.001	0.011±0.004	0.017±0.009
City Center	0.105 ^{a} ± 0.009	0.125 ^{ab} ± 0.006	0.146 ^{a} ± 0.009	0.044 ^{a} ± 0.004	0.048 ^{a} ± 0.005	0.056 ^{a} ± 0.003	0.054 ^{a} ± 0.004	0.074 ^{a} ± 0.004	0.067 ^{a} ± 0.005
East	0.096 ^{a} ± 0.004	0.108 ^{ab} ± 0.012	0.115 ^{abc} ± 0.008	0.056 ^{a} ± 0.004	0.071 ^{a} ± 0.002	0.083 ^{a} ± 0.003	0.086 ^{a} ± 0.004	0.095 ^{a} ± 0.004	0.094 ^{a} ± 0.003
North	0.069 ^{a} ± 0.008	0.089 ^{ab} ± 0.002	0.111 ^{a} ± 0.007	0.029 ^{a} ± 0.004	0.048 ^{a} ± 0.007	0.066 ^{a} ± 0.004	0.056 ^{a} ± 0.004	0.077 ^{a} ± 0.002	0.093 ^{ab} ± 0.003
South	0.079 ^{a} ± 0.006	0.098 ^{a} ± 0.007	0.129 ^{a} ± 0.011	0.044 ^{a} ± 0.003	0.055 ^{a} ± 0.004	0.075 ^{a} ± 0.004	0.065 ^{a} ± 0.005	0.085 ^{a} ± 0.004	0.107 ^{a} ± 0.005
West	0.078 ^{ab} ± 0.008	0.066 ^{b} ± 0.047	0.093 ^{bc} ± 0.014	0.018 ^{a} ± 0.004	0.035 ^{a} ± 0.004	0.047 ^{a} ± 0.006	0.065 ^{a} ± 0.014	0.043 ^{a} ± 0.005	0.074 ^{a} ± 0.003

- Values are represented as mean ± SE
- Means with the same letter are not significantly different.
- Tukeys's Honest Significant Difference (HSD) Test was performed at α=0.05 and Cv=4.289

Table 6.5.6a: Seasonal variation in Zinc (mg/g DW) in *Thuidium cyambifolium* at different directions in Ghat during the years 2020, 2021, and 2022

Directions	Summer			Rain			Winter		
	2020	2021	2022	2020	2021	2022	2020	2021	2022
Baseline	0.234±0.018	0.326±0.013	0.387±0.010	0.094±0.007	0.135±0.025	0.147±0.013	0.132±0.008	0.165±0.025	0.265±0.011
City Center	0.960 ^{b} ± 0.015	1.101 ^{b} ± 0.035	1.390 ^{b} ± 0.016	0.760 ^{a} ± 0.010	0.921 ^{a} ± 0.010	1.088 ^{a} ± 0.018	0.937 ^{a} ± 0.025	1.035 ^{a} ± 0.033	1.232 ^{a} ± 0.016
East	1.183 ^{c} ± 0.013	1.433 ^{d} ± 0.014	2.352 ^{a} ± 0.021	0.355 ^{d} ± 0.034	0.568 ^{d} ± 0.021	0.649 ^{f} ± 0.017	0.857 ^{b} ± 0.026	1.163 ^{cd} ± 0.013	1.372 ^{d} ± 0.012
North	1.546 ^{b} ± 0.029	1.847 ^{ab} ± 0.021	2.170 ^{b} ± 0.016	0.429 ^{d} ± 0.025	0.648 ^{d} ± 0.013	0.792 ^{cd} ± 0.027	0.845 ^{c} ± 0.025	1.123 ^{c} ± 0.012	1.548 ^{c} ± 0.028
South	1.816 ^{a} ± 0.020	1.932 ^{a} ± 0.017	1.653 ^{d} ± 0.0290	0.639 ^{cd} ± 0.021	0.968 ^{bc} ± 0.016	1.227 ^{b} ± 0.023	1.359 ^{b} ± 0.019	1.568 ^{a} ± 0.019	1.861 ^{a} ± 0.016
West	1.740 ^{a} ± 0.024	2.172 ^{a} ± 0.023	2.253 ^{a} ± 0.026	0.429 ^{c} ± 0.012	0.674 ^{cd} ± 0.023	0.756 ^{f} ± 0.020	1.249 ^{a} ± 0.020	1.439 ^{a} ± 0.017	1.839 ^{a} ± 0.024

Table 6.5.6b: Seasonal variation in Lead (mg/g DW) in *Thuidium cyambifolium* at different directions in Ghat during the years 2020, 2021, and 2022

Directions	Summer			Rain			Winter		
	2020	2021	2022	2020	2021	2022	2020	2021	2022
Baseline	0.163±0.019	0.236±0.016	0.264±0.011	0.032±0.007	0.044±0.011	0.057±0.009	0.052±0.008	0.059±0.009	0.088±0.009
City Center	1.543 ^{a} ± 0.021	1.744 ^{a} ± 0.013	2.263 ^{a} ± 0.023	0.909 ^{a} ± 0.012	1.136 ^{a} ± 0.029	1.354 ^{a} ± 0.019	1.080 ^{a} ± 0.013	1.355 ^{a} ± 0.014	1.684 ^{a} ± 0.012
East	1.078 ^{bc} ± 0.021	1.559 ^{a} ± 0.032	1.951 ^{a} ± 0.016	0.556 ^{b} ± 0.025	0.659 ^{bc} ± 0.016	0.771 ^{cde} ± 0.031	0.675 ^{bc} ± 0.014	0.867 ^{d} ± 0.012	0.964 ^{de} ± 0.024
North	1.661 ^{a} ± 0.016	2.058 ^{a} ± 0.027	2.259 ^{a} ± 0.030	0.965 ^{b} ± 0.026	1.018 ^{b} ± 0.012	1.137 ^{b} ± 0.023	0.992 ^{b} ± 0.019	1.217 ^{b} ± 0.016	1.346 ^{b} ± 0.031
South	1.372 ^{a} ± 0.019	1.862 ^{a} ± 0.034	2.353 ^{a} ± 0.027	0.747 ^{b} ± 0.024	0.991 ^{a} ± 0.021	0.948 ^{b} ± 0.013	0.864 ^{b} ± 0.020	1.042 ^{b} ± 0.031	1.230 ^{ab} ± 0.033
West	1.074 ^{ab} ± 0.018	1.648 ^{a} ± 0.034	1.959 ^{a} ± 0.029	0.554 ^{b} ± 0.029	0.726 ^{b} ± 0.026	0.833 ^{d} ± 0.019	0.743 ^{bcd} ± 0.025	0.874 ^{cd} ± 0.026	1.060 ^{c} ± 0.016

- Values are represented as mean ± SE
- Means with the same letter are not significantly different.
- Tukeys's Honest Significant Difference (HSD) Test was performed at α=0.05 and Cv=4.289

Table 6.5.6c: Seasonal variation in Copper (mg/g DW) in *Thuidium cyambifolium* at different directions in Ghat during the years 2020, 2021, and 2022

Directions	Summer			Rain			Winter		
	2020	2021	2022	2020	2021	2022	2020	2021	2022
Baseline	0.135±0.017	0.158±0.011	0.165±0.008	0.035±0.008	0.037±0.007	0.046±0.005	0.056±0.008	0.062±0.006	0.076±0.004
City Center	$0.955^{a} \pm 0.016$	$1.070^{ab} \pm 0.016$	$1.143^{b} \pm 0.018$	$0.582^{a} \pm 0.017$	$0.744^{a} \pm 0.020$	$0.842^{b} \pm 0.019$	$0.663^{ab} \pm 0.006$	$0.761^{b} \pm 0.012$	$0.877^{b} \pm 0.011$
East	$0.663^{d} \pm 0.016$	$0.842^{e} \pm 0.022$	$1.160^{de} \pm 0.028$	$0.250^{de} \pm 0.024$	$0.468^{d} \pm 0.025$	$0.650^{cd} \pm 0.016$	$0.478^{e} \pm 0.022$	$0.850^{cd} \pm 0.025$	$1.078^{c} \pm 0.021$
North	$1.113^{c} \pm 0.026$	$1.351^{c} \pm 0.019$	$1.664^{c} \pm 0.023$	$0.552^{bc} \pm 0.023$	$0.645^{d} \pm 0.012$	$0.856^{c} \pm 0.017$	$0.777^{c} \pm 0.015$	$0.968^{c} \pm 0.029$	$1.112^{d} \pm 0.027$
South	$1.041^{b} \pm 0.018$	$1.361^{b} \pm 0.020$	$1.638^{c} \pm 0.012$	$0.462^{c} \pm 0.013$	$0.657^{c} \pm 0.032$	$0.755^{cd} \pm 0.022$	$0.842^{c} \pm 0.019$	$0.967^{d} \pm 0.034$	$1.358^{b} \pm 0.025$
West	$0.859^{cd} \pm 0.026$	$0.858^{d} \pm 0.031$	$1.171^{d} \pm 0.015$	$0.324^{de} \pm 0.027$	$0.548^{cd} \pm 0.023$	$0.695^{d} \pm 0.016$	$0.645^{c} \pm 0.024$	$0.742^{c} \pm 0.014$	$0.978^{c} \pm 0.020$

Table 6.5.6d: Seasonal variation in Cadmium (mg/g DW) in *Thuidium cyambifolium* at different directions in Ghat during the years 2020, 2021, and 2022

Directions	Summer			Rain			Winter		
	2020	2021	2022	2020	2021	2022	2020	2021	2022
Baseline	0.010±0.001	0.022±0.006	0.041±0.007	ND	ND	0.006 ± 0.001^{a}	0.006±0.001	0.011±0.004	0.017±0.009
City Center	$0.123^{a} \pm 0.009$	$0.137^{a} \pm 0.006$	$0.138^{a} \pm 0.009$	$0.033^{a} \pm 0.003$	$0.047^{a} \pm 0.002$	$0.054^{a} \pm 0.009$	$0.054^{a} \pm 0.004$	$0.064^{a} \pm 0.004$	$0.076^{a} \pm 0.005$
East	$0.092^{a} \pm 0.003$	$0.096^{ab} \pm 0.003$	$0.097^{bc} \pm 0.003$	$0.025^{a} \pm 0.002$	$0.051^{a} \pm 0.002$	$0.084^{a} \pm 0.004$	$0.055^{a} \pm 0.004$	$0.076^{a} \pm 0.004$	$0.112^{a} \pm 0.008$
North	$0.045^{a} \pm 0.004$	$0.064^{b} \pm 0.003$	$0.110^{a} \pm 0.006$	$0.015^{a} \pm 0.004$	$0.023^{a} \pm 0.002$	$0.075^{a} \pm 0.003$	$0.027^{a} \pm 0.005$	$0.044^{a} \pm 0.007$	$0.108^{ab} \pm 0.005$
South	$0.079^{a} \pm 0.003$	$0.091^{a} \pm 0.007$	$0.089^{a} \pm 0.002$	$0.035^{a} \pm 0.004$	$0.046^{a} \pm 0.004$	$0.055^{a} \pm 0.004$	$0.046^{a} \pm 0.004$	$0.067^{a} \pm 0.006$	$0.084^{a} \pm 0.016$
West	$0.064^{b} \pm 0.007$	$0.062^{b} \pm 0.008$	$0.085^{bc} \pm 0.004$	$0.026^{a} \pm 0.003$	$0.035^{a} \pm 0.004$	$0.065^{a} \pm 0.003$	$0.044^{a} \pm 0.002$	$0.058^{a} \pm 0.006$	$0.087^{a} \pm 0.017$

- Values are represented as mean ± SE
- Means with the same letter are not significantly different.
- Tukeys's Honest Significant Difference (HSD) Test was performed at α=0.05 and Cv=4.289

Table 6.5.7a: Seasonal variation in Zinc (mg/g DW) in *Thuidium cyambifolium* at different directions in Thal during the years 2020, 2021, and 2022

Directions	Summer			Rain			Winter		
	2020	2021	2022	2020	2021	2022	2020	2021	2022
Baseline	0.234±0.018	0.326±0.013	0.387±0.010	0.094±0.007	0.135±0.025	0.147±0.013	0.132±0.008	0.165±0.025	0.265±0.011
City Center	0.678 ^{d} ± 0.017	0.734 ^{e} ± 0.013	0.883 ^{d} ± 0.029	0.138 ^{f} ± 0.032	0.234 ^{e} ± 0.015	0.344 ^{d} ± 0.009	0.383 ^{d} ± 0.015	0.437 ^{f} ± 0.010	0.556 ^{d} ± 0.011
East	1.176 ^{c} ± 0.024	1.466 ^{cd} ± 0.023	1.766 ^{c} ± 0.015	0.329 ^{d} ± 0.015	0.661 ^{cd} ± 0.030	0.763 ^{e} ± 0.031	0.836 ^{b} ± 0.011	1.137 ^{d} ± 0.027	1.446 ^{cd} ± 0.023
North	0.850 ^{d} ± 0.018	1.129 ^{e} ± 0.015	1.357 ^{f} ± 0.027	0.333 ^{de} ± 0.021	0.430 ^{e} ± 0.019	0.425 ^{e} ± 0.025	0.646 ^{d} ± 0.016	0.665 ^{e} ± 0.024	0.860 ^{f} ± 0.027
South	0.850 ^{d} ± 0.022	1.339 ^{e} ± 0.024	1.665 ^{bc} ± 0.024	0.488 ^{f} ± 0.013	0.656 ^{e} ± 0.022	1.034 ^{cd} ± 0.018	0.625 ^{e} ± 0.018	1.081 ^{c} ± 0.022	1.442 ^{b} ± 0.013
West	1.150 ^{d} ± 0.025	1.513 ^{c} ± 0.010	1.925 ^{b} ± 0.013	0.326 ^{c} ± 0.017	0.673 ^{cd} ± 0.025	0.948 ^{e} ± 0.018	0.761 ^{d} ± 0.023	1.046 ^{bc} ± 0.020	1.559 ^{b} ± 0.029

Table 6.5.7b: Seasonal variation in Lead (mg/g DW) in *Thuidium cyambifolium* at different directions in Thal during the years 2020, 2021, and 2022

Directions	Summer			Rain			Winter		
	2020	2021	2022	2020	2021	2022	2020	2021	2022
Baseline	0.163±0.019	0.236±0.016	0.264±0.011	0.032±0.007	0.044±0.011	0.057±0.009	0.052±0.008	0.059±0.009	0.088±0.009
City Center	0.650 ^{de} ± 0.033	0.708 ^{d} ± 0.019	0.744 ^{e} ± 0.029	0.283 ^{d} ± 0.019	0.643 ^{bc} ± 0.019	0.772 ^{c} ± 0.022	0.348 ^{e} ± 0.020	0.367 ^{d} ± 0.005	1.065 ^{cd} ± 0.029
East	1.039 ^{c} ± 0.015	1.357 ^{b} ± 0.029	1.663 ^{b} ± 0.028	0.363 ^{c} ± 0.017	0.545 ^{d} ± 0.023	0.898 ^{b} ± 0.026	0.662 ^{bc} ± 0.014	0.864 ^{d} ± 0.030	0.416 ^{d} ± 0.010
North	0.866 ^{cd} ± 0.030	1.166 ^{cd} ± 0.013	1.562 ^{c} ± 0.020	0.365 ^{d} ± 0.025	0.533 ^{de} ± 0.017	0.342 ^{d} ± 0.018	0.645 ^{de} ± 0.010	0.838 ^{c} ± 0.033	1.258 ^{b} ± 0.027
South	0.553 ^{d} ± 0.019	0.828 ^{f} ± 0.023	1.814 ^{b} ± 0.029	0.136 ^{f} ± 0.028	0.356 ^{d} ± 0.027	0.582 ^{d} ± 0.012	0.304 ^{f} ± 0.020	1.247 ^{a} ± 0.024	0.854 ^{ef} ± 0.017
West	1.143 ^{a} ± 0.021	1.460 ^{b} ± 0.026	1.269 ^{cd} ± 0.028	0.468 ^{b} ± 0.027	0.321 ^{d} ± 0.016	0.983 ^{b} ± 0.019	0.884 ^{a} ± 0.018	0.572 ^{e} ± 0.032	1.472 ^{a} ± 0.024

- Values are represented as mean ± SE
- Means with the same letter are not significantly different.
- Tukeys's Honest Significant Difference (HSD) Test was performed at α=0.05 and Cv=4.289

Table 6.5.7c: Seasonal variation in Copper (mg/g DW) in *Thuidium cyambifolium* at different directions in Thal during the years 2020, 2021, and 2022

Directions	Summer			Rain			Winter		
	2020	2021	2022	2020	2021	2022	2020	2021	2022
Baseline	0.135±0.017	0.158±0.011	0.165±0.008	0.035±0.008	0.037±0.007	0.046±0.005	0.056±0.008	0.062±0.006	0.076±0.004
City Center	0.732 ^{c} ± 0.019	0.811 ^{d} ± 0.007	1.269 ^{e} ± 0.026	0.535 ^{bc} ± 0.008	0.586 ^{bcd} ± 0.010	0.543 ^{de} ± 0.016	0.544 ^{c} ± 0.012	0.556 ^{c} ± 0.003	0.658 ^{de} ± 0.009
East	1.141 ^{b} ± 0.023	1.361 ^{b} ± 0.027	1.477 ^{c} ± 0.023	0.436 ^{c} ± 0.013	0.670 ^{c} ± 0.015	0.731 ^{c} ± 0.013	0.950 ^{b} ± 0.013	0.1.123 ^{b} ± 0.016	1.234 ^{b} ± 0.025
North	1.258 ^{b} ± 0.021	0.928 ^{e} ± 0.015	0.813 ^{e} ± 0.008	0.279 ^{d} ± 0.026	0.464 ^{e} ± 0.024	0.528 ^{e} ± 0.024	0.569 ^{d} ± 0.020	0.647 ^{e} ± 0.015	0.849 ^{ef} ± 0.014
South	0.853 ^{de} ± 0.019	1.241 ^{c} ± 0.026	1.880 ^{a} ± 0.020	0.258 ^{d} ± 0.022	0.347 ^{e} ± 0.034	0.585 ^{e} ± 0.013	0.609 ^{d} ± 0.024	0.776 ^{e} ± 0.019	1.106 ^{c} ± 0.016
West	0.851 ^{e} ± 0.020	1.541 ^{a} ± 0.025	1.481 ^{d} ± 0.018	0.448 ^{bc} ± 0.031	0.633 ^{c} ± 0.017	0.955 ^{bc} ± 0.014	0.962 ^{b} ± 0.029	1.233 ^{a} ± 0.021	1.406 ^{a} ± 0.020

Table 6.5.7d: Seasonal variation in Cadmium (mg/g DW) in *Thuidium cyambifolium* at different directions in Thal during the years 2020, 2021, and 2022

Directions	Summer			Rain			Winter		
	2020	2021	2022	2020	2021	2022	2020	2021	2022
Baseline	0.010±0.001	0.022±0.006	0.041±0.007	ND	ND	0.006 ± 0.001 ^{a}	0.006±0.001	0.011±0.004	0.017±0.009
City Center	0.051 ^{a} ± 0.003	0.071 ^{ab} ± 0.005	0.077 ^{ab} ± 0.005	0.034 ^{a} ± 0.004	0.047 ^{a} ± 0.002	0.044 ^{a} ± 0.004	0.045 ^{a} ± 0.004	0.052 ^{a} ± 0.003	0.062 ^{a} ± 0.003
East	0.120 ^{a} ± 0.006	0.173 ^{a} ± 0.011	0.225 ^{a} ± 0.003	0.045 ^{a} ± 0.003	0.081 ^{a} ± 0.003	0.139 ^{a} ± 0.011	0.079 ^{a} ± 0.002	0.080 ^{a} ± 0.004	0.098 ^{a} ± 0.003
North	0.121 ^{a} ± 0.005	0.198 ^{a} ± 0.012	0.215 ^{a} ± 0.013	0.063 ^{a} ± 0.004	0.083 ^{a} ± 0.008	0.136 ^{a} ± 0.010	0.098 ^{a} ± 0.004	0.115 ^{a} ± 0.008	0.185 ^{a} ± 0.006
South	0.099 ^{a} ± 0.029	0.132 ^{a} ± 0.013	0.164 ^{a} ± 0.007	0.037 ^{a} ± 0.004	0.064 ^{a} ± 0.005	0.085 ^{a} ± 0.013	0.058 ^{a} ± 0.002	0.086 ^{a} ± 0.003	0.138 ^{a} ± 0.004
West	0.179 ^{a} ± 0.010	0.184 ^{a} ± 0.010	0.221 ^{a} ± 0.007	0.025 ^{a} ± 0.004	0.067 ^{a} ± 0.015	0.089 ^{a} ± 0.014	0.072 ^{a} ± 0.003	0.088 ^{a} ± 0.003	0.128 ^{a} ± 0.004

- Values are represented as mean ± SE
- Means with the same letter are not significantly different.
- Tukeys's Honest Significant Difference (HSD) Test was performed at α=0.05 and Cv=4.289

Table 6.5.8a: Seasonal variation in Zinc (mg/g DW) in *Thuidium cyambifolium* at different directions in Munsiyari during the years 2020, 2021, and 2022

Directions	Summer			Rain			Winter		
	2020	2021	2022	2020	2021	2022	2020	2021	2022
Baseline	0.234±0.018	0.326±0.013	0.387±0.010	0.094±0.007	0.135±0.025	0.147±0.013	0.132±0.008	0.165±0.025	0.265±0.011
City Center	0.707 ^{d} ± 0.007	0.856 ^{d} ± 0.013	0.916 ^{d} ± 0.009	0.311 ^{e} ± 0.015	0.338 ^{de} ± 0.008	0.390 ^{d} ± 0.009	0.383 ^{d} ± 0.020	0.561 ^{e} ± 0.010	0.640 ^{d} ± 0.011
East	0.970 ^{d} ± 0.019	1.206 ^{e} ± 0.023	1.500 ^{e} ± 0.020	0.654 ^{c} ± 0.033	0.771 ^{bc} ± 0.019	0.858 ^{e} ± 0.022	0.665 ^{c} ± 0.025	0.972 ^{e} ± 0.013	1.142 ^{e} ± 0.010
North	0.946 ^{d} ± 0.026	1.303 ^{d} ± 0.029	1.604 ^{e} ± 0.030	0.255 ^{e} ± 0.012	0.412 ^{e} ± 0.020	0.691 ^{d} ± 0.027	0.624 ^{d} ± 0.024	0.746 ^{de} ± 0.032	0.957 ^{f} ± 0.023
South	1.471 ^{b} ± 0.026	2.091 ^{a} ± 0.020	2.314 ^{a} ± 0.017	0.704 ^{c} ± 0.020	1.210 ^{a} ± 0.021	1.406 ^{a} ± 0.013	1.249 ^{b} ± 0.021	1.563 ^{a} ± 0.024	1.861 ^{a} ± 0.029
West	1.010 ^{e} ± 0.019	1.304 ^{e} ± 0.018	1.590 ^{d} ± 0.021	0.370 ^{c} ± 0.020	0.571 ^{d} ± 0.028	0.829 ^{f} ± 0.012	0.737 ^{d} ± 0.015	0.948 ^{c} ± 0.015	1.239 ^{d} ± 0.019

Table 6.5.8b: Seasonal variation in Lead (mg/g DW) in *Thuidium cyambifolium* at different directions in Munsiyari during the years 2020, 2021, and 2022

Directions	Summer			Rain			Winter		
	2020	2021	2022	2020	2021	2022	2020	2021	2022
Baseline	0.163±0.019	0.236±0.016	0.264±0.011	0.032±0.007	0.044±0.011	0.057±0.009	0.052±0.008	0.059±0.009	0.088±0.009
City Center	0.658 ^{cde} ± 0.043	0.758 ^{d} ± 0.009	0.913 ^{d} ± 0.047	0.283 ^{d} ± 0.019	0.317 ^{d} ± 0.006	0.337 ^{d} ± 0.008	0.322 ^{ef} ± 0.020	0.374 ^{de} ± 0.005	0.383 ^{d} ± 0.010
East	0.756 ^{d} ± 0.017	1.052 ^{c} ± 0.014	1.408 ^{c} ± 0.019	0.381 ^{c} ± 0.025	0.544 ^{b} ± 0.024	0.738 ^{e} ± 0.019	0.460 ^{d} ± 0.022	0.743 ^{a} ± 0.017	1.092 ^{c} ± 0.017
North	0.664 ^{ef} ± 0.024	1.084 ^{d} ± 0.016	1.331 ^{e} ± 0.013	0.150 ^{e} ± 0.020	0.361 ^{f} ± 0.025	0.569 ^{ef} ± 0.018	0.365 ^{f} ± 0.023	0.648 ^{d} ± 0.015	1.049 ^{c} ± 0.012
South	0.743 ^{c} ± 0.014	1.084 ^{d} ± 0.017	1.351 ^{cd} ± 0.019	0.344 ^{de} ± 0.022	0.558 ^{c} ± 0.018	0.868 ^{bc} ± 0.022	0.563 ^{c} ± 0.024	0.861 ^{c} ± 0.021	1.051 ^{d} ± 0.023
West	0.965 ^{bc} ± 0.024	1.367 ^{bc} ± 0.020	1.638 ^{c} ± 0.016	0.270 ^{c} ± 0.028	0.581 ^{c} ± 0.027	0.957 ^{bc} ± 0.020	0.537 ^{f} ± 0.015	0.802 ^{d} ± 0.014	1.248 ^{b} ± 0.013

- Values are represented as mean ± SE
- Means with the same letter are not significantly different.
- Tukeys's Honest Significant Difference (HSD) Test was performed at α=0.05 and Cv=4.289

Table 6.5.8c: Seasonal variation in Copper (mg/g DW) in *Thuidium cyambifolium* at different directions in Munsiyari during the years 2020, 2021, and 2022

Directions	Summer			Rain			Winter		
	2020	2021	2022	2020	2021	2022	2020	2021	2022
Baseline	0.135±0.017	0.158±0.011	0.165±0.008	0.035±0.008	0.037±0.007	0.046±0.005	0.056±0.008	0.062±0.006	0.076±0.004
City Center	0.745 ^{c} ± 0.009	0.817 ^{d} ± 0.007	0.837 ^{de} ± 0.008	0.513 ^{bc} ± 0.008	0.536 ^{bc} ± 0.010	0.545 ^{de} ± 0.016	0.544 ^{c} ± 0.012	0.556 ^{c} ± 0.003	0.621 ^{e} ± 0.009
East	0.979 ^{c} ± 0.021	1.276 ^{bc} ± 0.026	1.650 ^{b} ± 0.020	0.155 ^{e} ± 0.010	0.361 ^{d} ± 0.020	0.597 ^{d} ± 0.026	0.468 ^{e} ± 0.019	0.711 ^{e} ± 0.011	1.112 ^{c} ± 0.010
North	1.250 ^{b} ± 0.024	1.415 ^{c} ± 0.028	1.878 ^{b} ± 0.022	0.468 ^{c} ± 0.020	0.678 ^{cd} ± 0.020	0.965 ^{c} ± 0.020	0.962 ^{b} ± 0.017	1.253 ^{b} ± 0.027	1.579 ^{b} ± 0.022
South	1.263 ^{a} ± 0.022	1.562 ^{a} ± 0.020	1.761 ^{b} ± 0.023	0.329 ^{d} ± 0.004	0.541 ^{d} ± 0.014	0.852 ^{bc} ± 0.022	1.036 ^{b} ± 0.019	1.355 ^{b} ± 0.026	1.551 ^{a} ± 0.018
West	0.949 ^{c} ± 0.018	1.257 ^{a} ± 0.027	1.567 ^{c} ± 0.018	0.377 ^{cd} ± 0.013	0.584 ^{c} ± 0.025	0.963 ^{b} ± 0.024	0.640 ^{c} ± 0.013	0.966 ^{b} ± 0.021	1.258 ^{b} ± 0.019

Table 6.5.8d: Seasonal variation in Cadmium (mg/g DW) in *Thuidium cyambifolium* at different directions in Munsiyari during the years 2020, 2021, and 2022

Directions	Summer			Rain			Winter		
	2020	2021	2022	2020	2021	2022	2020	2021	2022
Baseline	0.010±0.001	0.022±0.006	0.041±0.007	ND	ND	0.006 ± 0.001^{a}	0.006±0.001	0.011±0.004	0.017±0.009
City Center	0.052 ^{a} ± 0.003	0.072 ^{ab} ± 0.005	0.079 ^{ab} ± 0.005	0.035 ^{a} ± 0.004	0.043 ^{a} ± 0.002	0.053 ^{a} ± 0.003	0.042 ^{a} ± 0.004	0.051 ^{a} ± 0.003	0.062 ^{a} ± 0.004
East	0.135 ^{a} ± 0.004	0.159 ^{a} ± 0.006	0.186 ^{ab} ± 0.004	0.033 ^{a} ± 0.010	0.049 ^{a} ± 0.010	0.064 ^{a} ± 0.005	0.065 ^{a} ± 0.004	0.084 ^{a} ± 0.003	0.114 ^{a} ± 0.005
North	0.085 ^{a} ± 0.004	0.102 ^{ab} ± 0.003	0.113 ^{a} ± 0.005	0.022 ^{a} ± 0.006	0.034 ^{a} ± 0.004	0.057 ^{a} ± 0.005	0.055 ^{a} ± 0.004	0.068 ^{a} ± 0.003	0.084 ^{ab} ± 0.004
South	0.091 ^{a} ± 0.004	0.102 ^{a} ± 0.031	0.115 ^{a} ± 0.005	0.020 ^{a} ± 0.006	0.033 ^{a} ± 0.003	0.057 ^{a} ± 0.004	0.044 ^{a} ± 0.031	0.055 ^{a} ± 0.041	0.076 ^{a} ± 0.004
West	0.077 ^{ab} ± 0.005	0.083 ^{ab} ± 0.005	0.114 ^{abc} ± 0.005	0.016 ^{a} ± 0.009	0.030 ^{a} ± 0.008	0.059 ^{a} ± 0.004	0.039 ^{a} ± 0.003	0.045 ^{a} ± 0.041	0.076 ^{a} ± 0.005

- Values are represented as mean ± SE
- Means with the same letter are not significantly different.
- Tukeys's Honest Significant Difference (HSD) Test was performed at α=0.05 and Cv=4.289

Much work has been performed on seasonal metal accumulation in the north zone under Asian temperate climatic conditions in the central Himalayan belt, which shares the characteristics of both the Eastern and Western Himalayas (Saxena et al., 2008; Srivastava et al., 2014 and Chaturvedi et al. 2023). Different species have been used in research to assess the quality of air, water, and soil (De Oliveira et al., 2019; Oishi, 2018). Mosses are widely used as biomonitors for assessing atmospheric aerosols and are considered key bioindicators of air pollution (Korzeniowska & Panek, 2012; Salo & Makinen, 2019; Kosior et al., 2020). Therefore, the utilization of bryophytes, especially mosses, has been explored as a biomonitor for assessing atmospheric metal deposition throughout the world (Makholm & Mladenoff, 2005; Muller et al., 2020; Van Laaten et al., 2020; Dollery et al., 2022). However, the present investigation explores the seasonal metal accumulation and Seasonal metal load of Zn, Pb, Cu, and Cd in moss *Thuidium cymbifolium* (Dozy & Molk) Dozy & Molk. at different directions of Champawat and Pithoragarh during the study (from 2020 to 2022). Direction-wise, different sites of Champawat and Pithoragarh districts were studied for metal accumulation, i.e., Zinc, Lead, Copper, and Cadmium, seasonally during the study period (i.e., 2020 to 2022).

Therefore, different sites, i.e., City center, East, North, South, and West directions in Chamapawat, Lohagat, Khetikhan, and Barakote regions of Champawat district and similar direction sites of Pithogarh, Ghat, Thal, and Munsiyari of Pithoragarh district were explored for the deposition of selected metals in moss *T. cymbifolium*.

By comparing the obtained results of different sampling stations of Champawat district and Pithoragarh from the baseline level of Zn in different seasons was measured, it was noted that the maximum zinc accumulation was reported during the summer season, followed by the winter season, with the lowest accumulation observed in the rainy season across all study sites (Figures 6.5.1a- 6.5.8l) during the study. Therefore, the results supported previous workers (Saxena et al., 2008; Paliulis, 2021). It was noticed during this study that the accumulation of zinc was found to fluctuate seasonally, with the highest value during summer and the lowest value in the rainy season.

Chaturvedi et al. (2023) also highlighted a notable increase in metal load across all surveyed sites in the Kumaon region of Uttarakhand, supporting the present findings. Additionally, accelerated growth (biomass) during the monsoon season might be responsible for a more rapid reduction in the metal deposition in moss than biomass. Findings of Singh et al.

(2017) also support the present findings. The concentration of Zn in these selected sites of the present investigation has potential links to agricultural practices, as the inhabitants most often use Zn to enhance the growth of crops. The present observation was supported by the report of Meylan et al. (2017), who emphasized the significant contribution of anthropogenic activities to the atmospheric deposition of Zinc.

The observations of this study regarding the maximum zinc accumulation during the study supported the investigation of Paliulis (2021), who reported that there is an inverse relationship between wind speed and Zn accumulation, i.e., the slower the wind speed, the higher the concentration of zinc in moss.

Direction-wise, Zn accumulation in Champawat and Pithoragarh districts was also studied. In the Champawat district, northern and southern sampling sites were recorded as the highest zinc accumulation sites, whereas in the Pithoragarh district, southern, eastern, and western sampling sites showed maximum zinc accumulation in the first, second, and third orders. The highest zinc accumulation observed at various sampling sites may be attributed to dry deposition of metal spewed from vehicles, motor oil, wear and tear of vehicle components, and abrasion of tires. This finding is consistent with previous research confirming this phenomenon (Ares et al., 2015; Salo et al., 2016; Chaturvedi et al., 2023).

The present study found that Lead (Pb) accumulation during the summer season was reported to be the maximum, followed by the winter season. In contrast, during the rainy season, there was less accumulation of lead during the rainy season in all transplanted sites. The lowest accumulation was observed in the rainy season across all study sites, as shown in the figures throughout the study and, thus, previous research (Srivastava et al., 2014; Macedo-Miranda et al., 2016; Hu et al., 2018) also supports the present study findings.

The accumulation of lead (Pb), as shown in the tables and figures, represents each season over three consecutive years (2020 to 2022). In Champawat District, northern and eastern sampling sites showed maximum lead accumulation; however, in Pithoragarh districts, eastern and western sampling sites had the most significant Pb values. Variations in seasonal lead accumulation in different direction sites of Champawat and Pithoragarh districts were sharply observed, and present findings are in agreement with some of the previous workers (Limo et al., 2018; Hu et al., 2018; Dalupang et al., 2023).

A comparison of the results from different sampling stations of Champawat and Pithoragarh districts with the baseline level of Copper (Cu) across various seasons revealed that the highest copper (Cu) accumulation occurred during the summer, followed by the winter season. The lowest accumulation was observed in the rainy season across all study sites, as shown in the figures throughout the study. Previous research supported the present study findings (Srivastava et al., 2014; Hu et al., 2018).

Seasonal accumulation of copper at different sampling sites of Champawat and Pithoragarh districts was investigated during three consecutive years, i.e., 2020, 2021, and 2022. In Champawat District, southern and northern sampling sites showed maximum copper accumulation, whereas in Pithoragarh district, a similar pattern was recorded. Current observations align with the findings of previous researchers (Saxena et al., 2008; Ares et al., 2015; Salo et al., 2016; Chaturvedi et al., 2023).

A comparison of the results from different sampling stations with the baseline level of Cadmium (Cd) across various seasons revealed that the highest Cadmium (Cd) accumulation occurred during the summer, followed by the winter season. The lowest accumulation was observed in the rainy season across all study sites, as shown in the figures throughout the study. Previous research supports the present study findings (Saxena et al., 2008; Srivastava et al., 2014; Miranda et al., 2016).

The concentration of Cd in control sites throughout monsoon and winter was below the detection limit (Table 6.5.1d to 6.5.8d). Furthermore, the moss exhibited a relatively low measurement of Cadmium in comparison to the other metals. Cd is leached out easily from the surface, and this quick leaching property could be the reason for its low value in the control site (Saxena & Arfeen, 2010).

Seasonal Cadmium (Cd) metal accumulation data for different sampling sites of Champawat and Pithoragarh revealed that the highest Cadmium (Cd) value was recorded in the eastern sites in both districts. In contrast, the western and northern direction sites of Champawat were marked as the second largest cadmium accumulated sites. In the Pithoragarh city center, sites were recorded in the second order. That might be due to the high use of fertilizers and increased e wastage. Khan et al., 2022 also reported that anthropogenic activities such as using batteries, burning fossil fuels, high-phosphate fertilizers, and burning sewage and municipal waste are potential sources of Cd in the environment. Discarded rechargeable batteries are also a source of Cd in the environment since they now constitute substantial elements of every mobile device.

These batteries will be disposed of later (Recknagel et al., 2014). Cadmium is also found in households, such as in the cadmium plating of domestic refrigerator ice trays, the use of enamels containing cadmium compounds, and the utilization of cadmium pigments in the production of plastic. Individuals commonly and carelessly employ these practices for storing food items (Rahimzadeh et al., 2017).

The study by Srivastava et al. (2014) emphasized the notable increase in zinc concentration in moss compared to the control site. Additionally, the researchers reported that the zinc concentration was higher towards the west during all three seasons: summer, monsoon, and winter, following the present findings. The sites studied in the present study are well-known as tourist places and for producing essential agricultural practices. The seasonal increasing zinc concentration might be due to these possible factors, and some of the previous research findings also support the present study's findings (Gerdol et al., 2000; Otvos et al., 2003; Srivastava et al., 2014).

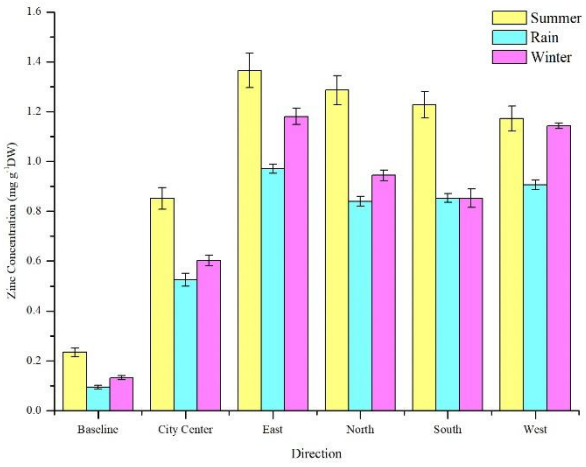

Figure 6.5.1a: Seasonal monitoring of Zinc (mg/g DW) at Champawat during 2020 in *Thuidium cyambifolium*

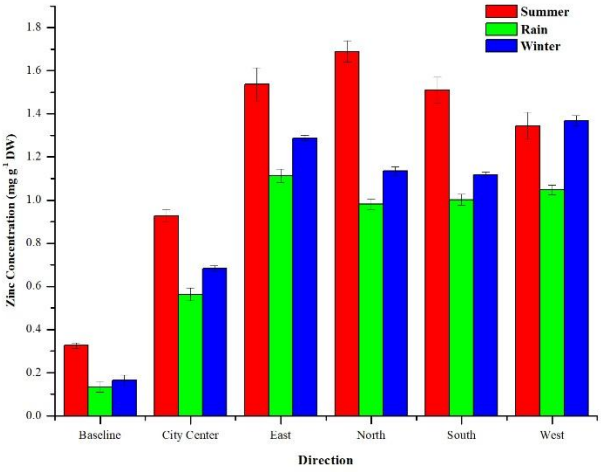

Figure 6.5.1b: Seasonal monitoring of Zinc (mg/g DW) at Champawat during 2021 *Thuidium cyambifolium*

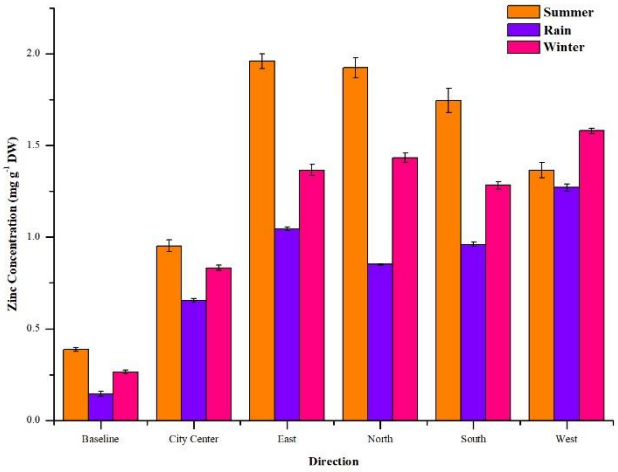

Figure 6.5.1c: Seasonal monitoring of Zinc (mg/g DW) at Champawat during 2022 *Thuidium cyambifolium*

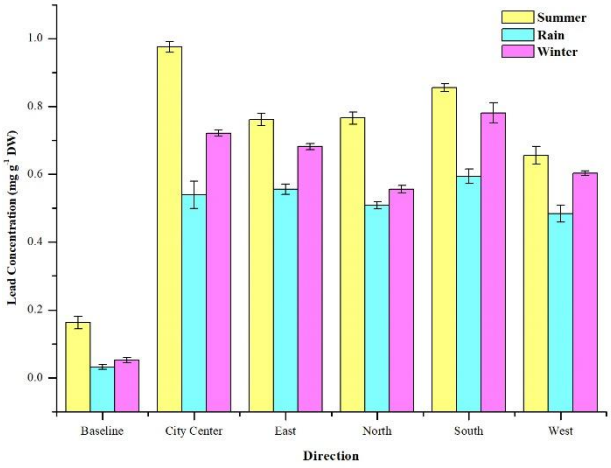

Figure 6.5.1d: Seasonal monitoring of Lead (mg/g DW) at Champawat during 2020 *Thuidium cyambifolium*

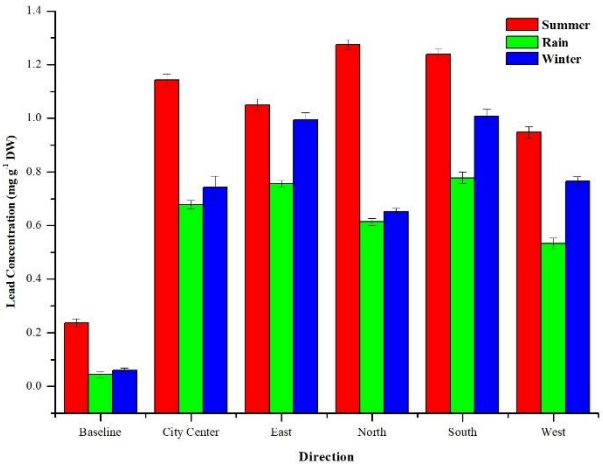

Figure 6.5.1e: Seasonal monitoring of Lead (mg/g DW) at Champawat during 2021 *Thuidium cyambifolium*

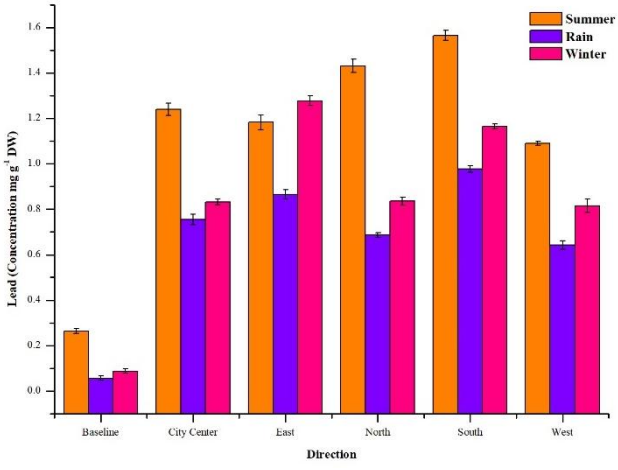

Figure 6.5.1f: Seasonal monitoring of Lead (mg/g DW) at Champawat during 2022 *Thuidium cyambifolium*

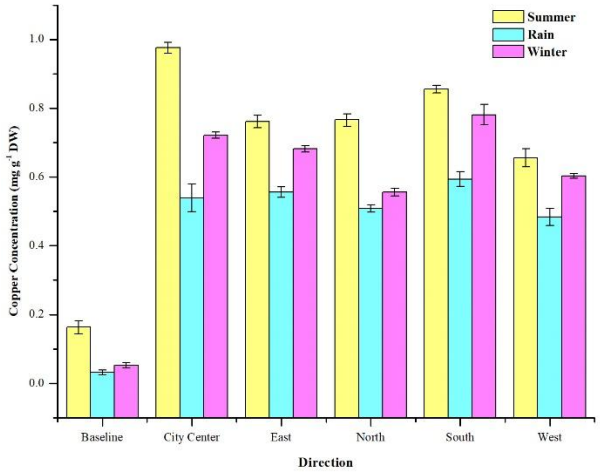

Figure 6.5.1g: Seasonal monitoring of copper (mg/g DW) at Champawat during 2020 *Thuidium cyambifolium*

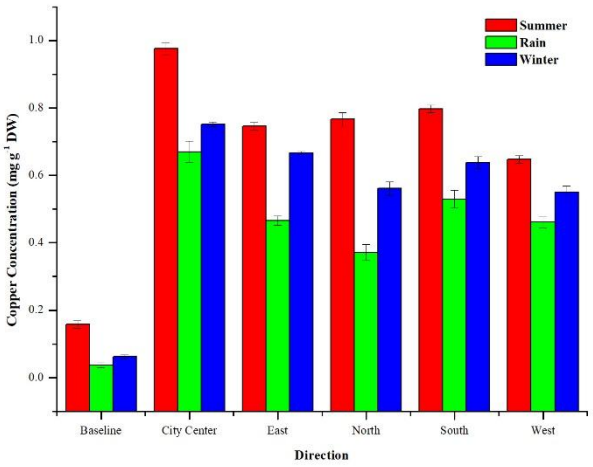

Figure 6.5.1h: Seasonal monitoring of Copper (mg/g DW) at Champawat during 2021 *Thuidium cyambifolium*

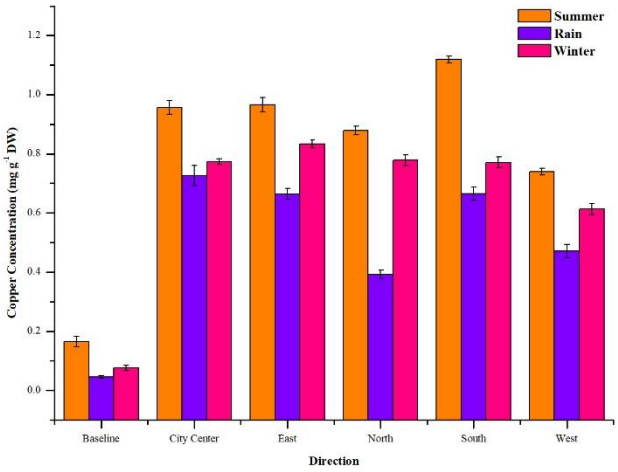

Figure 6.5.1i: Seasonal monitoring of Copper (mg/g DW) at Champawat during 2022 *Thuidium cyambifolium*

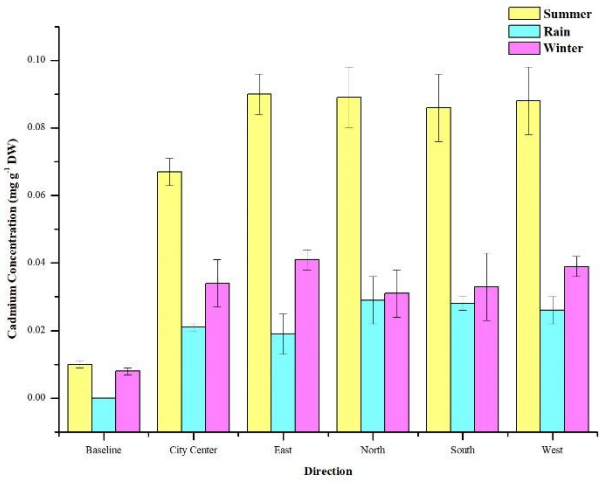

Figure 6.5.1j: Seasonal monitoring of Cadmium (mg/g DW) at Champawat during 2020 *Thuidium cyambifolium*

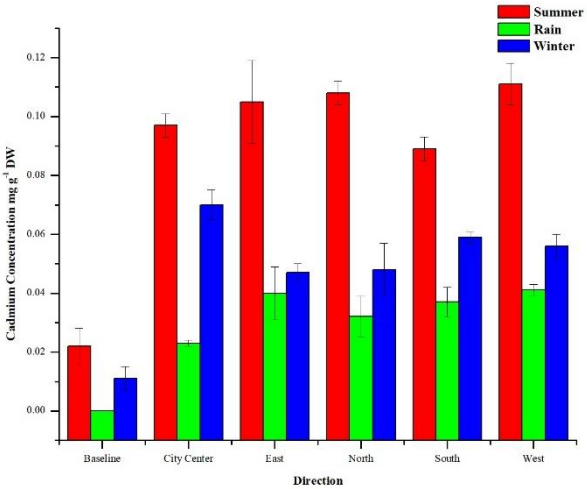

Figure 6.5.1k: Seasonal monitoring of Cadmium (mg/g DW) at Champawat during 2021 *Thuidium cyambifolium*

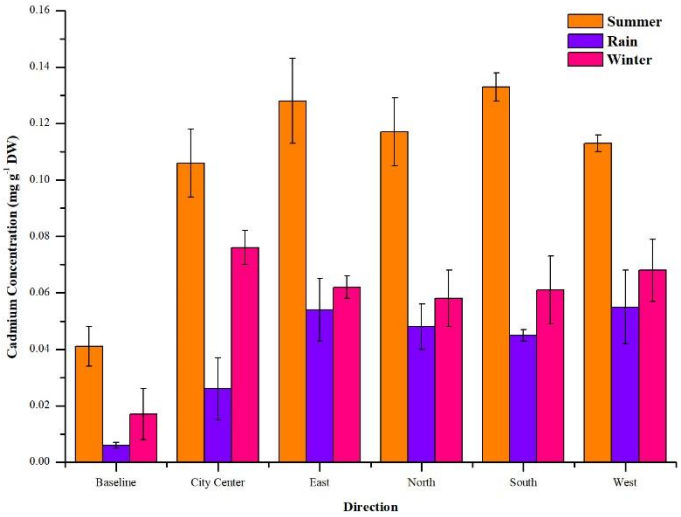

Figure 6.5.1l: Seasonal monitoring of Cadmium (mg/g DW) at Champawat during 2022 *Thuidium cyambifolium*

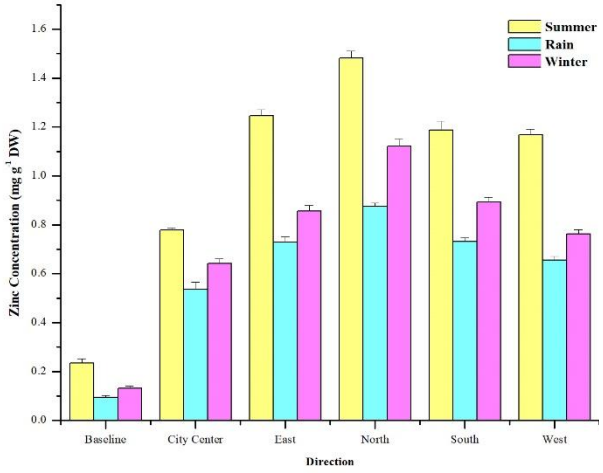

Figure 6.5.2a: Seasonal monitoring of Zinc (mg/g DW) at Lohaghat during 2020 in *Thuidium cyambifolium*

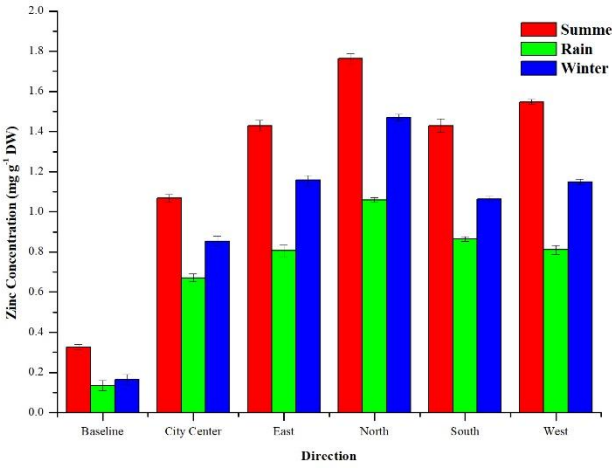

Figure 6.5.2b: Seasonal monitoring of Zinc (mg/g DW) at Lohaghat during 2021 *Thuidium cyambifolium*

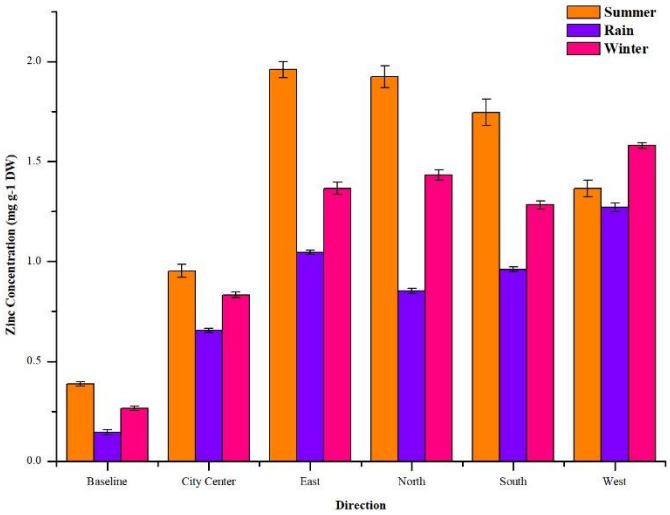

Figure 6.5.2c: Seasonal monitoring of Zinc (mg/g DW) at Lohaghat during 2022 *Thuidium cyambifolium*

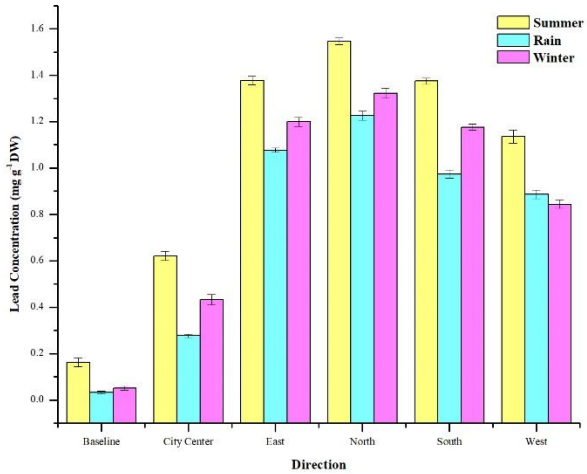

Figure 6.5.2d: Seasonal monitoring of Lead (mg/g DW) at Lohaghat during 2020 *Thuidium cyambifolium*

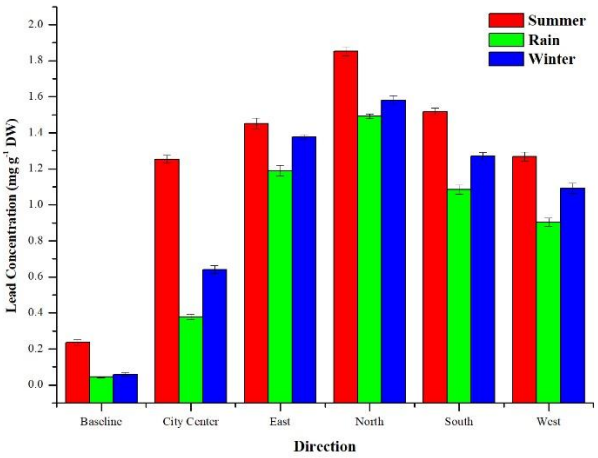

Figure 6.5.2e: Seasonal monitoring of Lead (mg/g DW) at Lohaghat during 2021 *Thuidium cyambifolium*

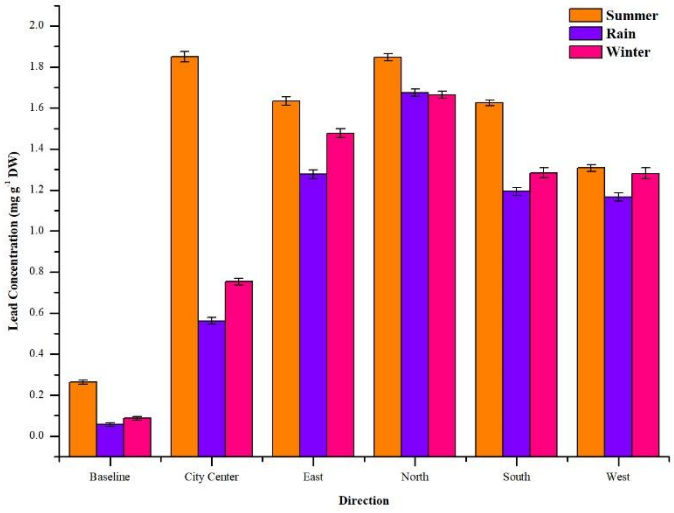

Figure 6.5.2f: Seasonal monitoring of Lead (mg/g DW) at Lohaghat during 2022 *Thuidium cyambifolium*

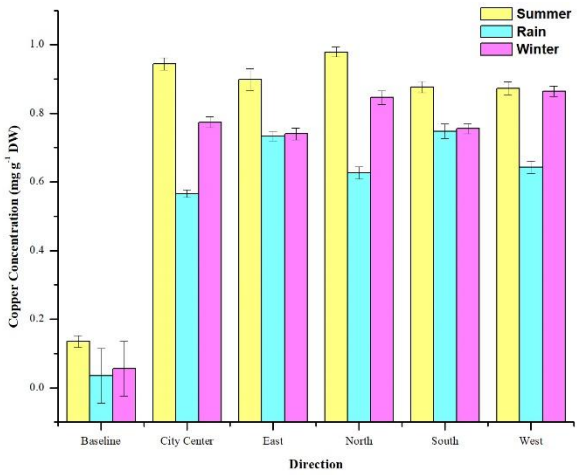

Figure 6.5.2g: Seasonal monitoring of copper (mg/g DW) at Lohaghat during 2020 *Thuidium cyambifolium*

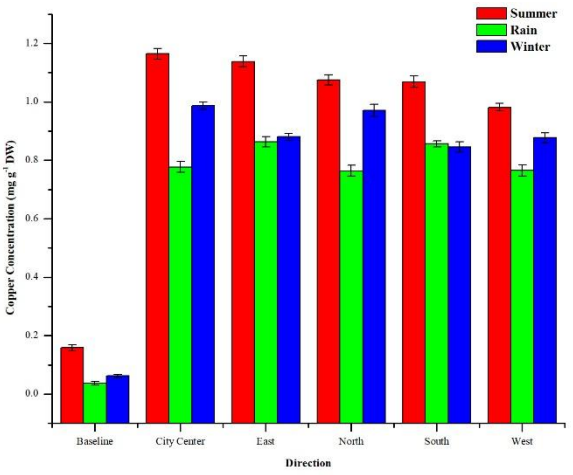

Figure 6.5.2h: Seasonal monitoring of Copper (mg/g DW) at Lohaghat during 2021 *Thuidium cyambifolium*

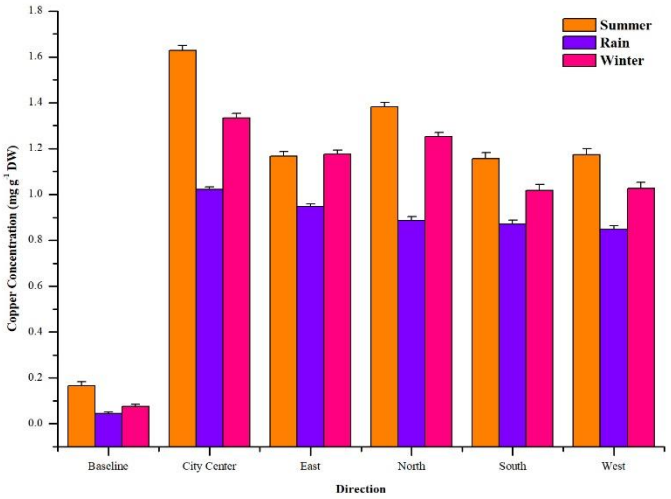

Figure 6.5.1i: Seasonal monitoring of Copper (mg/g DW) at Lohaghat during 2022 *Thuidium cyambifolium*

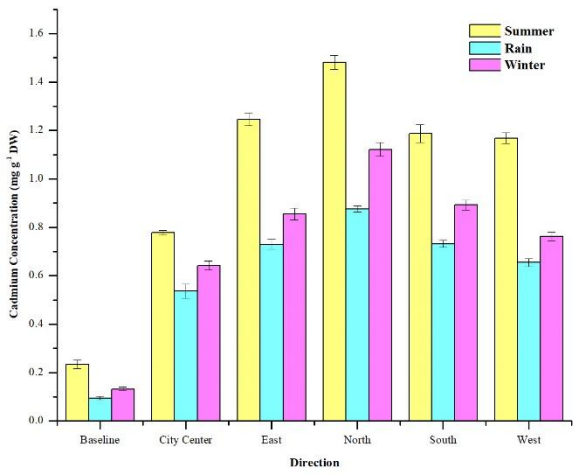

Figure 6.5.2j: Seasonal monitoring of Cadmium (mg/g DW) at Lohaghat during 2020 *Thuidium cyambifolium*

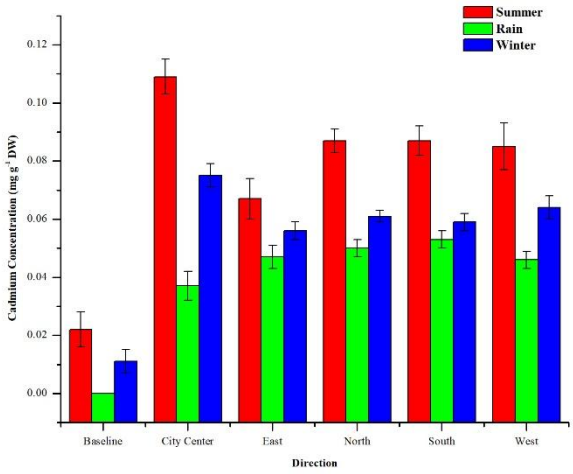

Figure 6.5.2k: Seasonal monitoring of Cadmium (mg/g DW) at Lohaghat during 2021 *Thuidium cyambifolium*

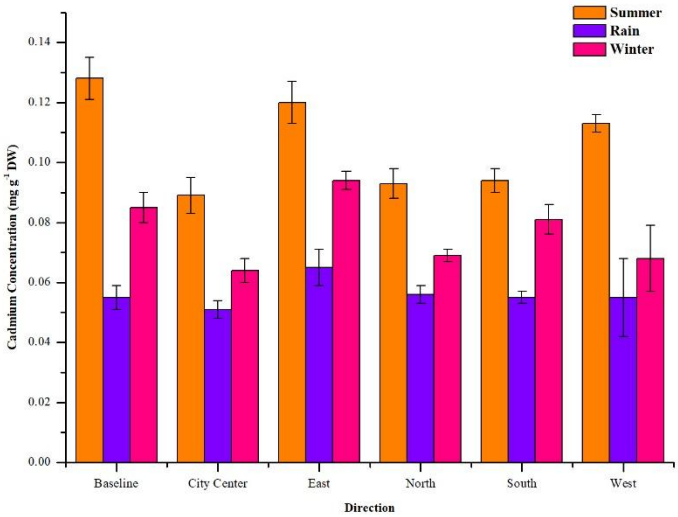

Figure 6.5.2l: Seasonal monitoring of Cadmium (mg/g DW) at Lohaghat during 2022 *Thuidium cyambifolium*

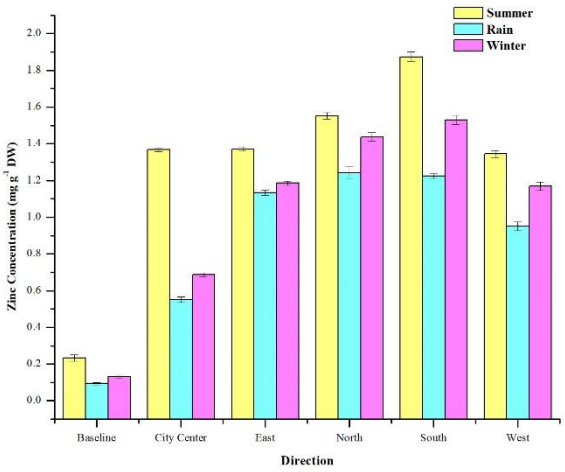

Figure 6.5.3a: Seasonal monitoring of Zinc (mg/g DW) at Khetikhan during 2020 in *Thuidium cyambifolium*

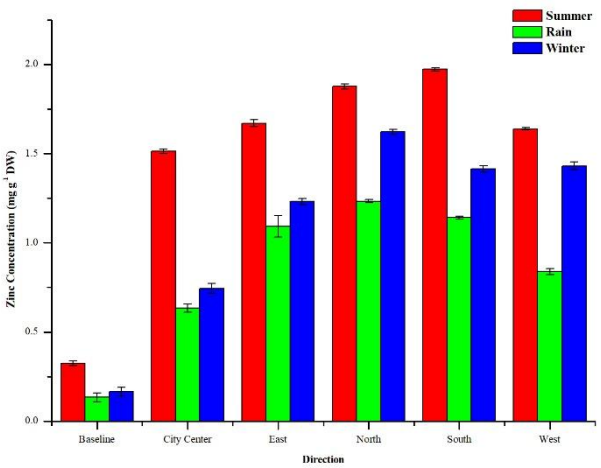

Figure 6.5.3b: Seasonal monitoring of Zinc (mg/g DW) at Khetikhan during 2021 *Thuidium cyambifolium*

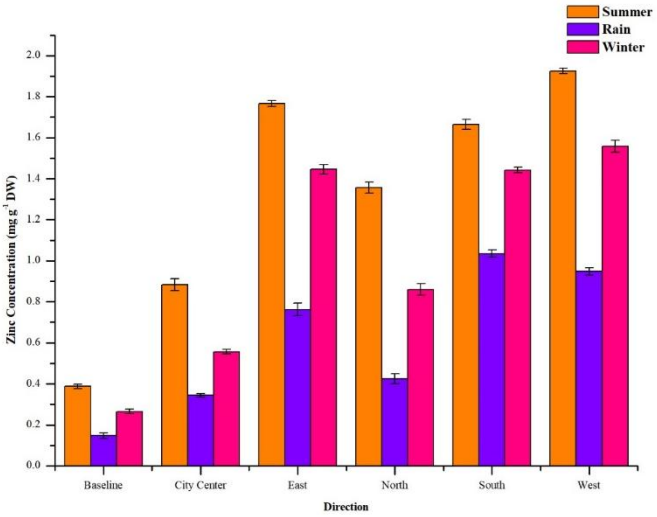

Figure 6.5.3c: Seasonal monitoring of Zinc (mg/g DW) at Khetikhan during 2022 *Thuidium cyambifolium*

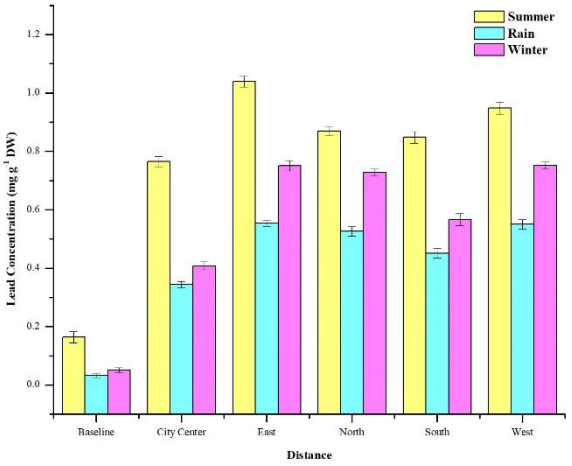

Figure 6.5.3d: Seasonal monitoring of Lead (mg m^{-1} DW) at Khetikhan during 2020 *Thuidium cyambifolium*

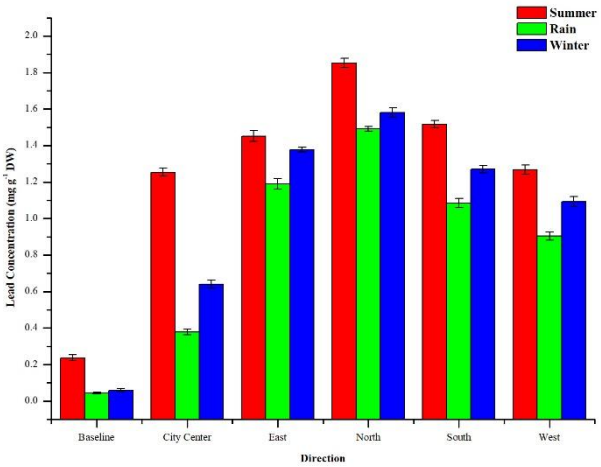

Figure 6.5.3e: Seasonal monitoring of Lead (mg/g DW) at Khetikhan during 2021 *Thuidium cyambifolium*

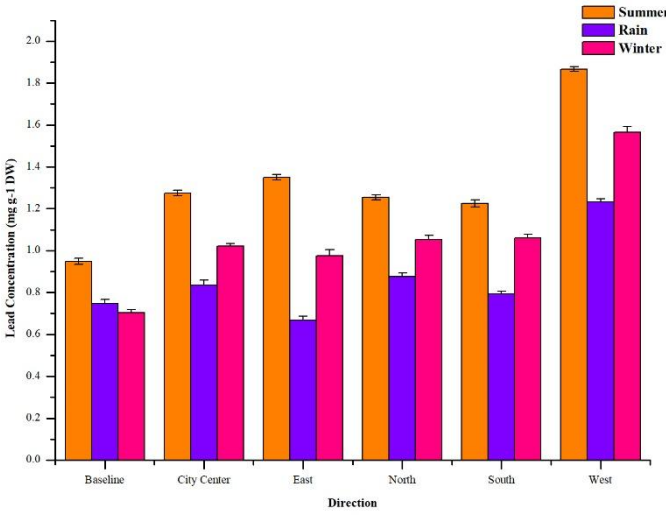

Figure 6.5.3f: Seasonal monitoring of Lead (mg/g DW) at Khetikhan during 2022 *Thuidium cyambifolium*

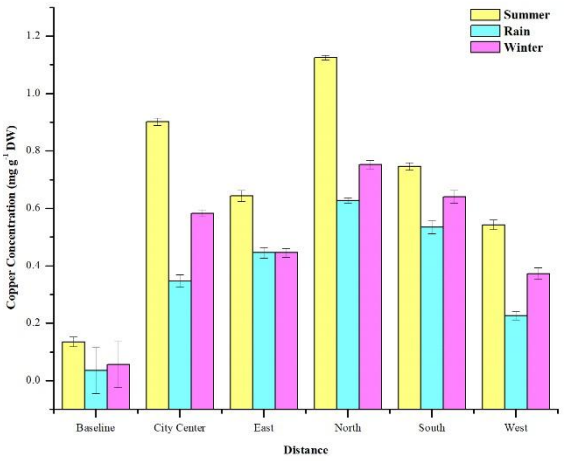

Figure 6.5.3g: Seasonal monitoring of copper (mg/g DW) at Khetikhan during 2020 *Thuidium cyambifolium*

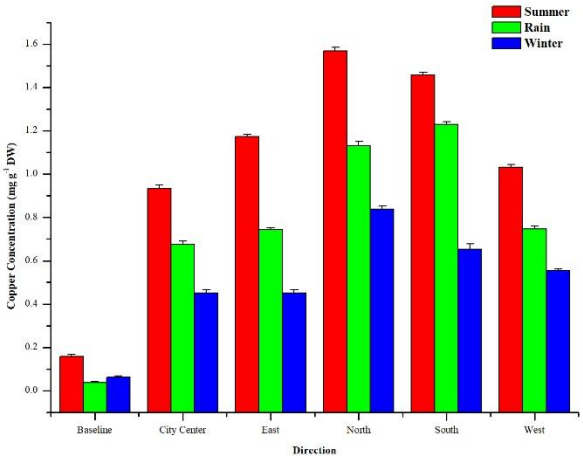

Figure 6.5.3h: Seasonal monitoring of Copper (mg/g DW) at Khetikhan during 2021 *Thuidium cyambifolium*

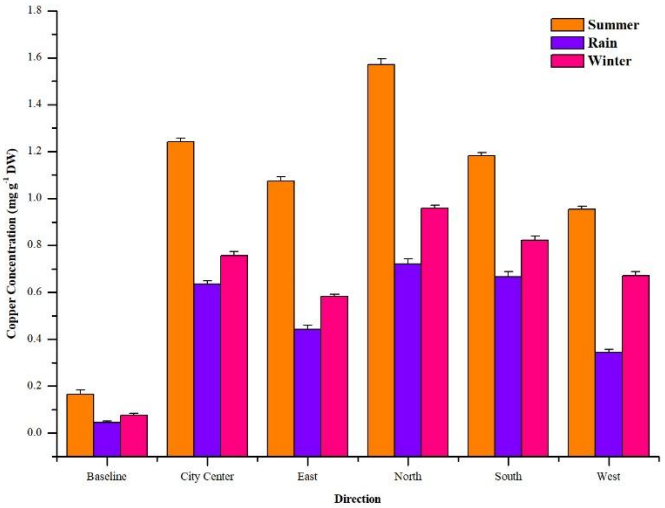

Figure 6.5.3i: Seasonal monitoring of Copper (mg/g DW) at Khetikhan during 2022 *Thuidium cyambifolium*

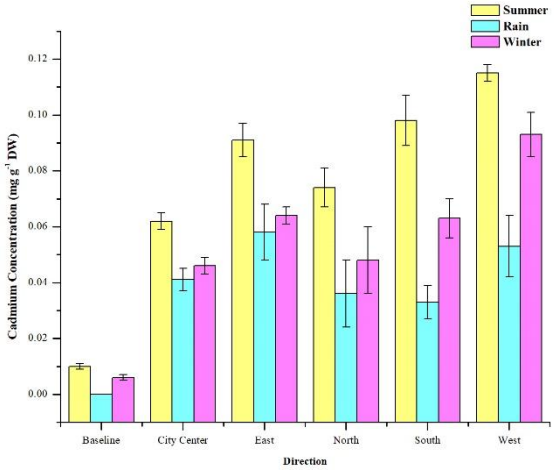

Figure 6.5.3j: Seasonal monitoring of Cadmium (mg/g DW) at Khetikhan during 2020 *Thuidium cyambifolium*

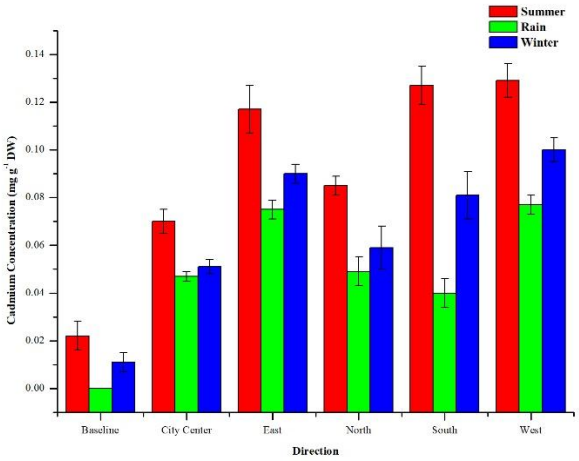

Figure 6.5.3k: Seasonal monitoring of Cadmium (mg/g DW) at Khetikhan during 2021 *Thuidium cyambifolium*

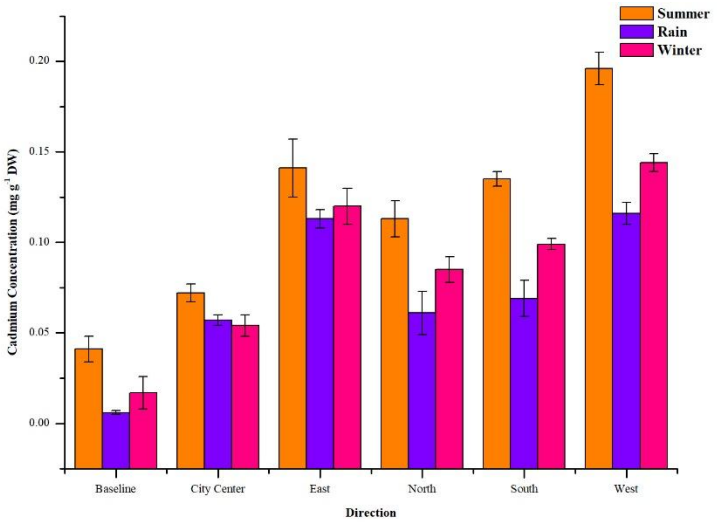

Figure 6.5.3l: Seasonal monitoring of Cadmium (mg/g DW) at Khetikhan during 2022 *Thuidium cyambifolium*

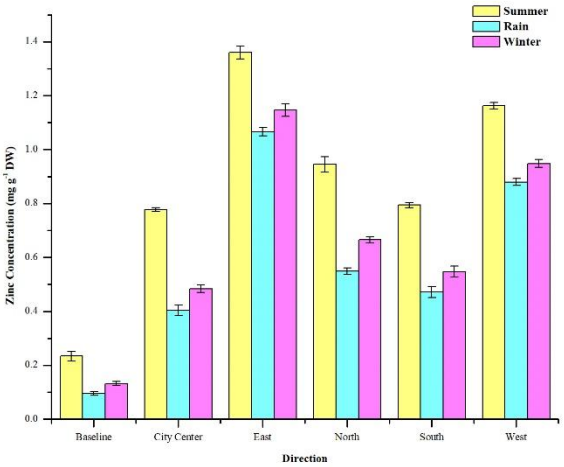

Figure 6.5.4a: Seasonal monitoring of Zinc (mg/g DW) at Barakote during 2020 in *Thuidium cyambifolium*

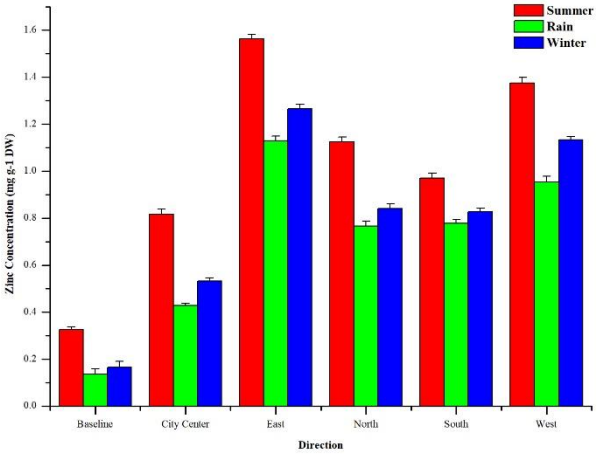

Figure 6.5.4b: Seasonal monitoring of Zinc (mg/g DW) at Barakote during 2021 *Thuidium cyambifolium*

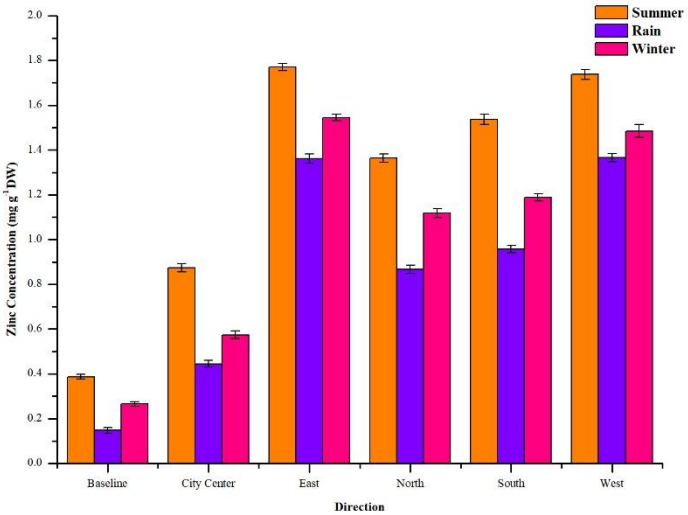

Figure 6.5.4c: Seasonal monitoring of Zinc (mg/g DW) at Barakote during 2022 *Thuidium cyambifolium*

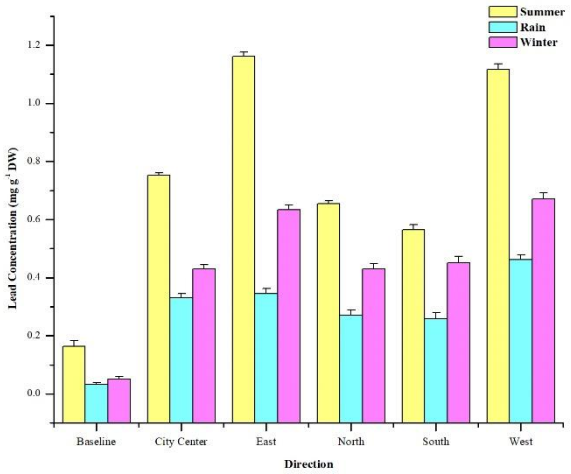

Figure 6.5.4d: Seasonal monitoring of Lead (mg m^{-1} DW) at Barakote during 2020 *Thuidium cyambifolium*

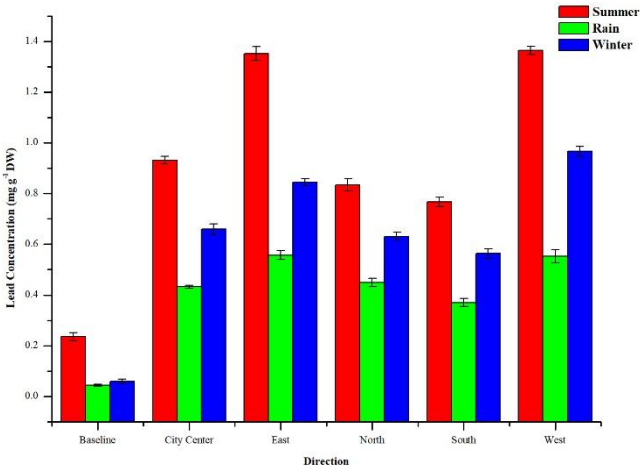

Figure 6.5.4e: Seasonal monitoring of Lead (mg/g DW) at Barakote during 2021 *Thuidium cyambifolium*

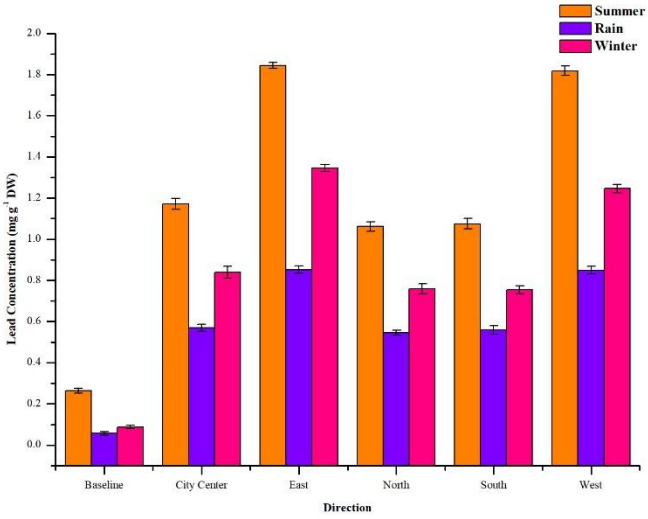

Figure 6.5.4f: Seasonal monitoring of Lead (mg/g DW) at Barakote during 2022 *Thuidium cyambifolium*

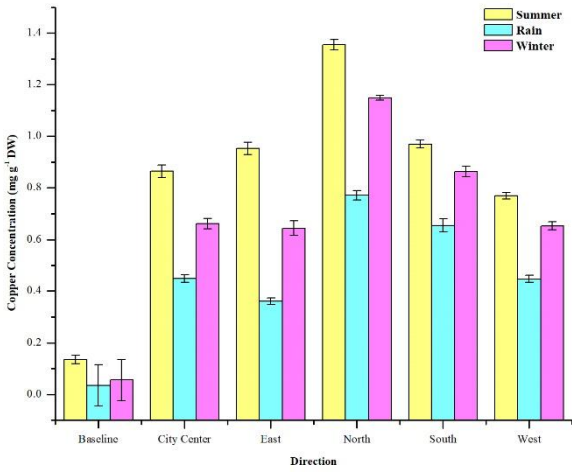

Figure 6.5.4g: Seasonal monitoring of copper (mg/g DW) at Barakote during 2020 *Thuidium cyambifolium*

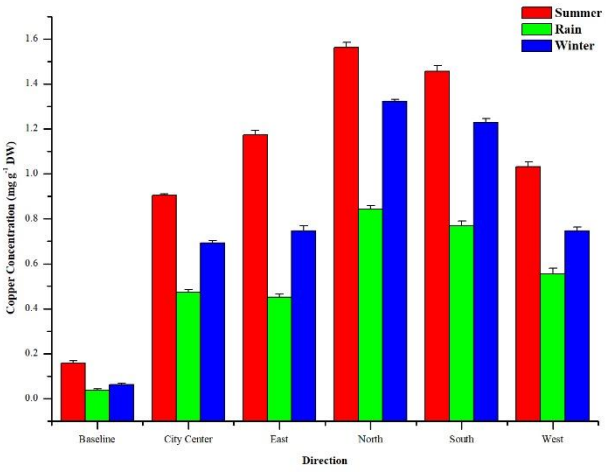

Figure 6.5.4h: Seasonal monitoring of Copper (mg/g DW) at Barakote during 2021 *Thuidium cyambifolium*

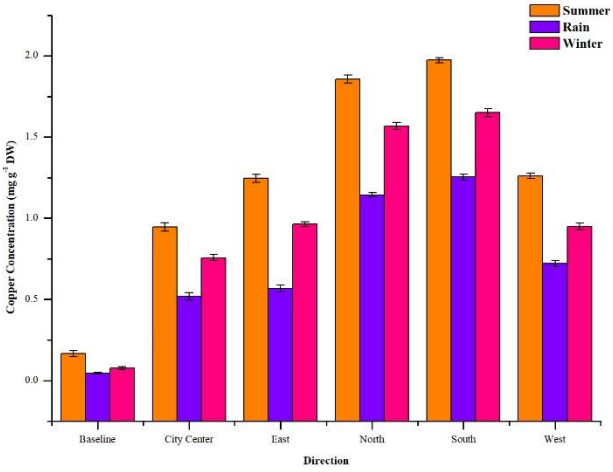

Figure 6.5.4i: Seasonal monitoring of Copper (mg/g DW) at Barakote during 2022 *Thuidium cyambifolium*

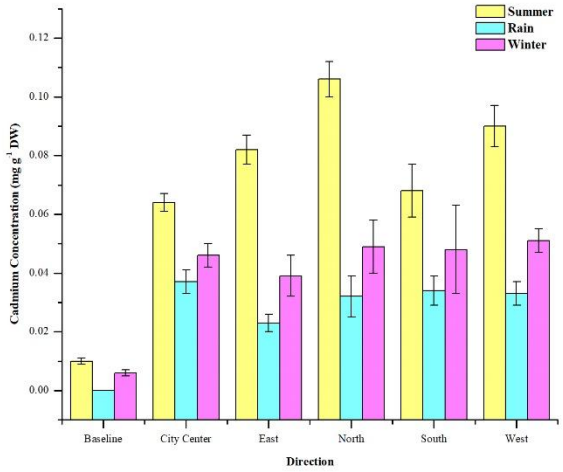

Figure 6.5.4j: Seasonal monitoring of Cadmium (mg/g DW) at Barakote during 2020 *Thuidium cyambifolium*

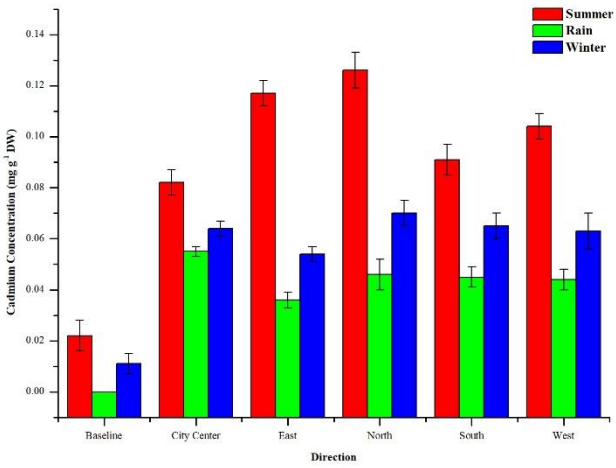

Figure 6.5.4k: Seasonal monitoring of Cadmium (mg/g DW) at Barakote during 2021 *Thuidium cyambifolium*

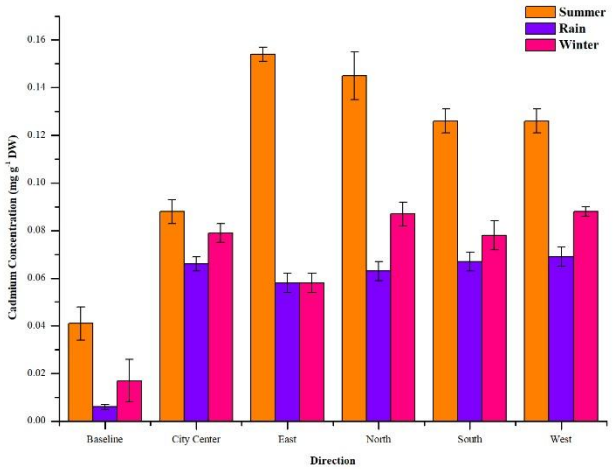

Figure 6.5.4l: Seasonal monitoring of Cadmium (mg/g DW) at Barakote during 2022 *Thuidium cyambifolium*

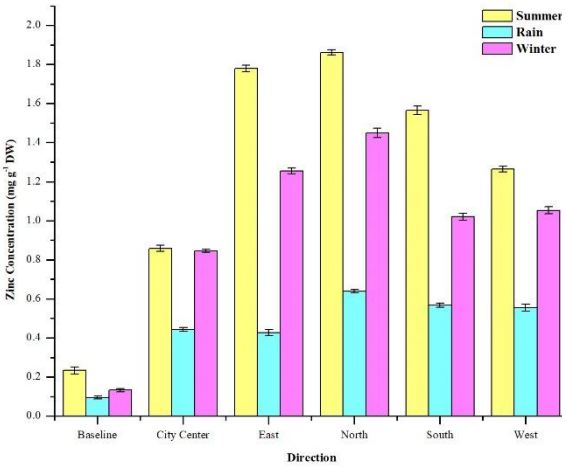

Figure 6.5.5a: Seasonal monitoring of Zinc (mg/g DW) at Pithoragrh during 2020 in *Thuidium cyambifolium*

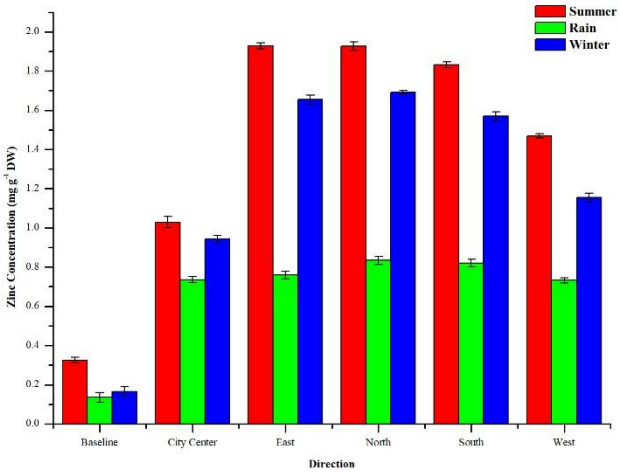

Figure 6.5.5b: Seasonal monitoring of Zinc (mg/g DW) at Pithoragrh during 2021 *Thuidium cyambifolium*

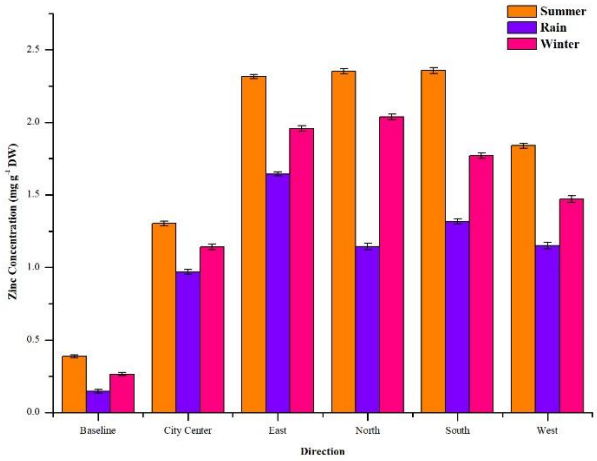

Figure 6.5.5c: Seasonal monitoring of Zinc (mg/g DW) at Pithoragrh during 2022 *Thuidium cyambifolium*

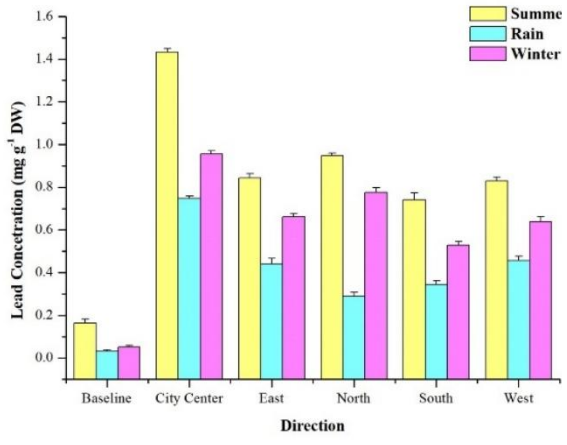

Figure 6.5.5d: Seasonal monitoring of Lead (mg m^{-1} DW) at Pithoragrh during 2020 *Thuidium cyambifolium*

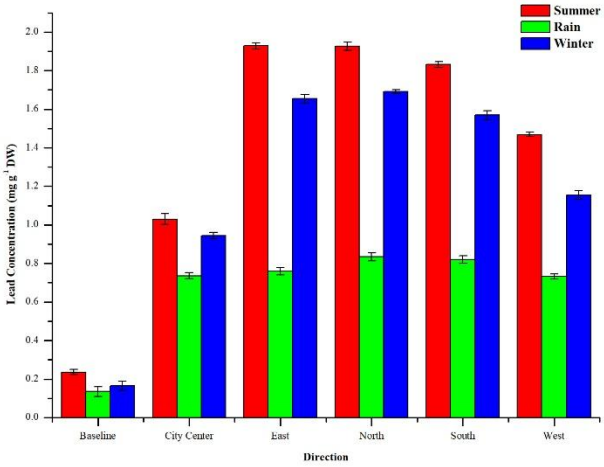

Figure 6.5.5e: Seasonal monitoring of Lead (mg/g DW) at Pithoragrh during 2021 *Thuidium cyambifolium*

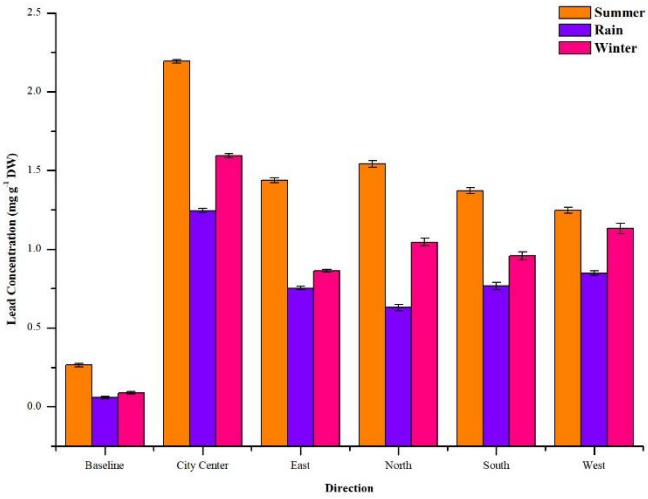

Figure 6.5.5f: Seasonal monitoring of Lead (mg/g DW) at Pithoragrh during 2022 *Thuidium cyambifolium*

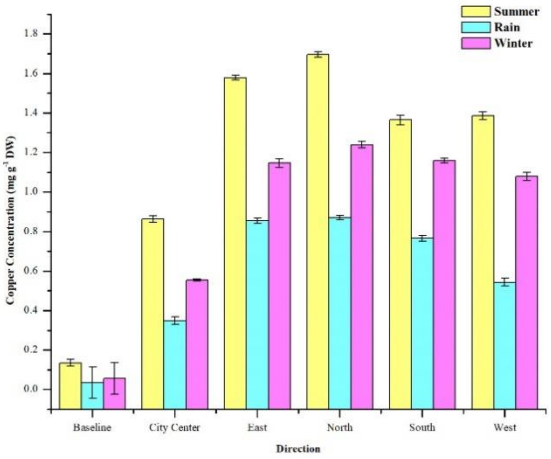

Figure 6.5.5g: Seasonal monitoring of copper (mg/g DW) at Pithoragrh during 2020 *Thuidium cyambifolium*

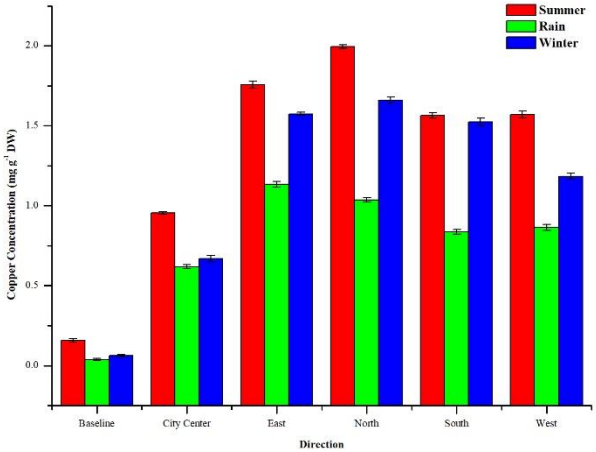

Figure 6.5.5h: Seasonal monitoring of Copper (mg/g DW) at Pithoragrh during 2021 *Thuidium cyambifolium*

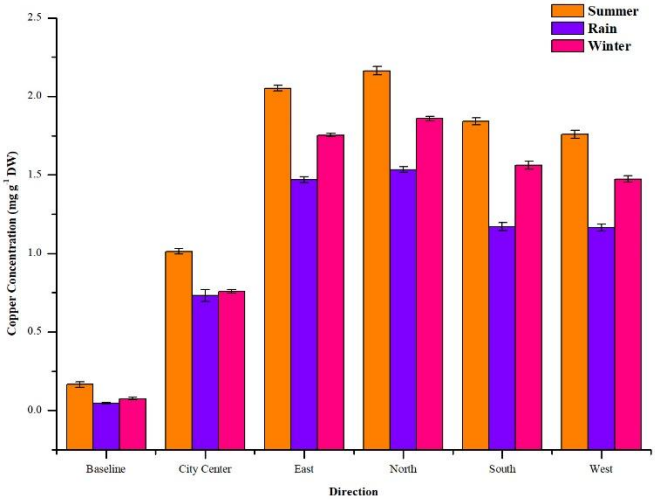

Figure 6.5.5i: Seasonal monitoring of Copper (mg/g DW) at Pithoragrh during 2022 *Thuidium cyambifolium*

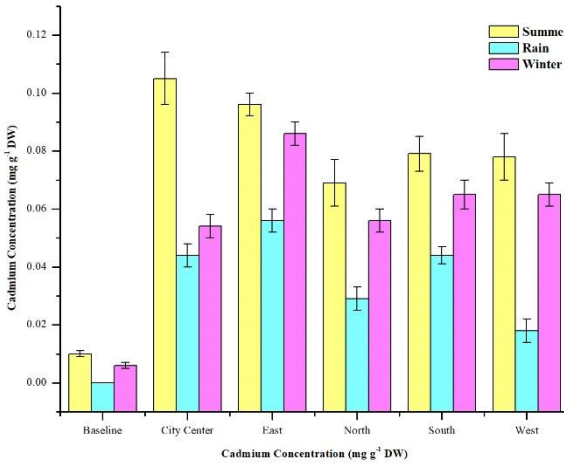

Figure 6.5.5j: Seasonal monitoring of Cadmium (mg/g DW) at Pithoragrh during 2020 *Thuidium cyambifolium*

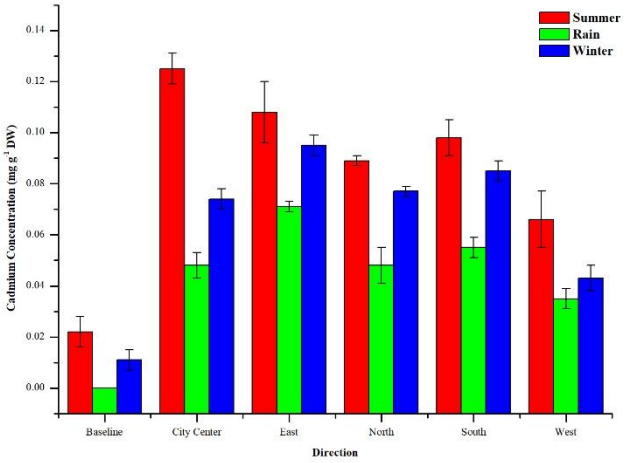

Figure 6.5.5k: Seasonal monitoring of Cadmium (mg/g DW) at Pithoragrh during 2021 *Thuidium cyambifolium*

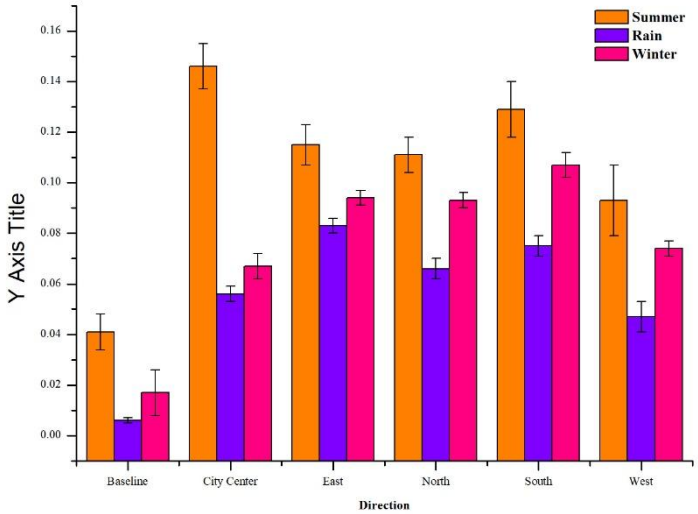

Figure 6.5.5l: Seasonal monitoring of Cadmium (mg/g DW) at Pithoragrh during 2022 *Thuidium cyambifolium*

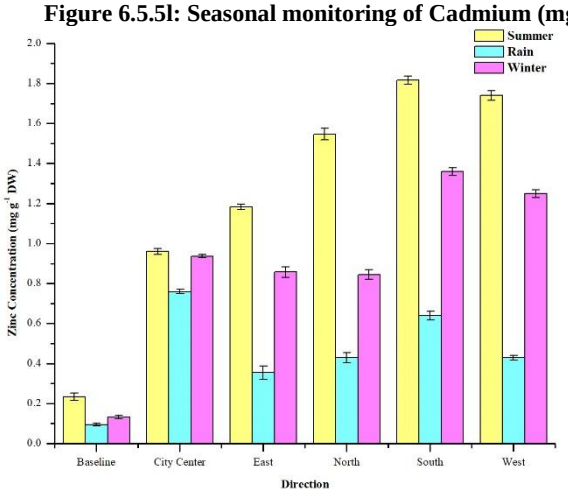

Figure 6.5.6a: Seasonal monitoring of Zinc (mg/g DW) at Ghat during 2020 in *Thuidium cyambifolium*

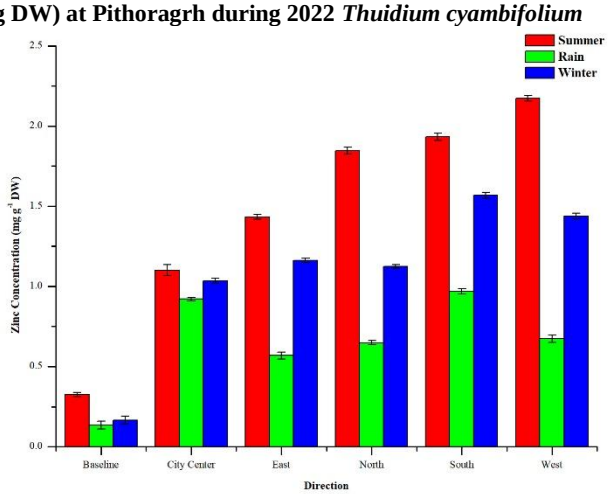

Figure 6.5.6b: Seasonal monitoring of Zinc (mg/g DW) at Ghat during 2021 *Thuidium cyambifolium*

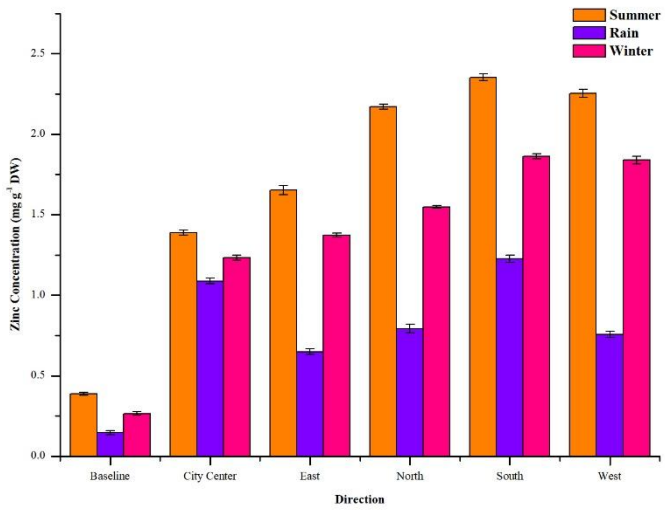

Figure 6.5.6c: Seasonal monitoring of Zinc (mg/g DW) at Ghat during 2022 *Thuidium cyambifolium*

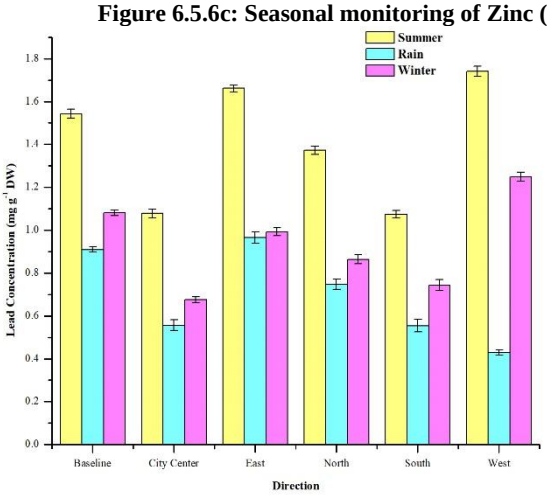

Figure 6.5.6d: Seasonal monitoring of Lead (mg/g DW) at Ghat during 2020 *Thuidium cyambifolium*

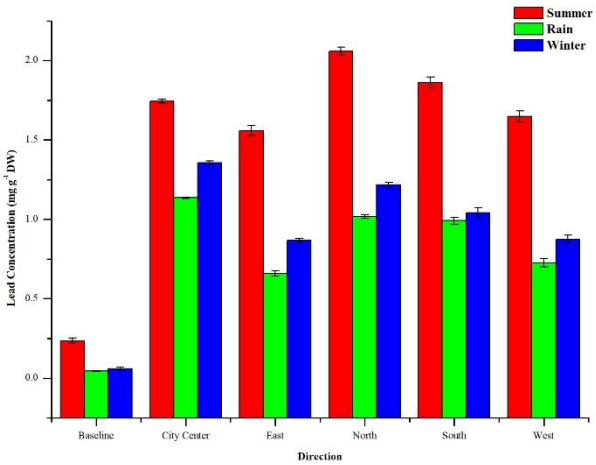

Figure 6.5.6e: Seasonal monitoring of Lead (mg/g DW) at Ghat during 2021 *Thuidium cyambifolium*

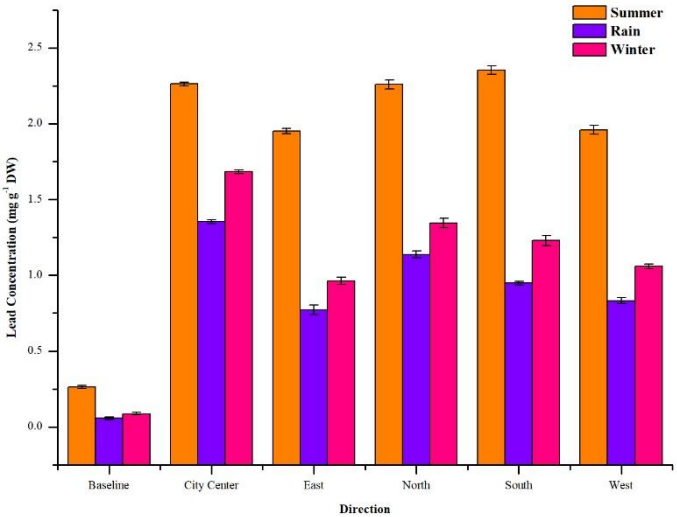

Figure 6.5.6f: Seasonal monitoring of Lead (mg/g DW) at Ghat during 2022 *Thuidium cyambifolium*

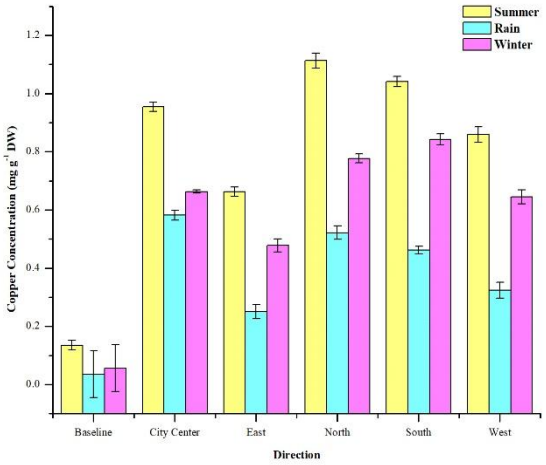

Figure 6.5.6g: Seasonal monitoring of copper (mg/g DW) at Ghat during 2020 *Thuidium cyambifolium*

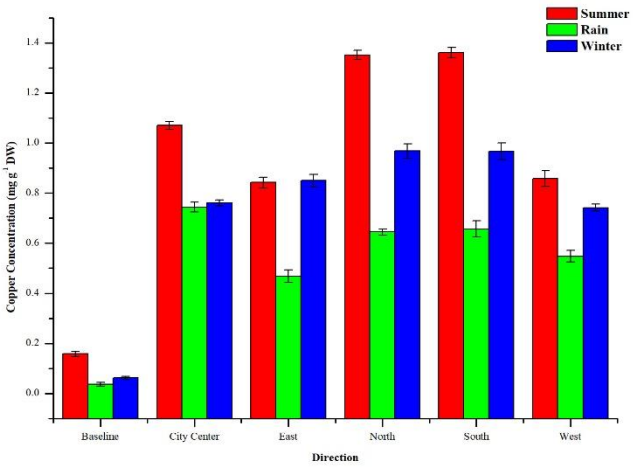

Figure 6.5.6h: Seasonal monitoring of Copper (mg/g DW) at Ghat during 2021 *Thuidium cyambifolium*

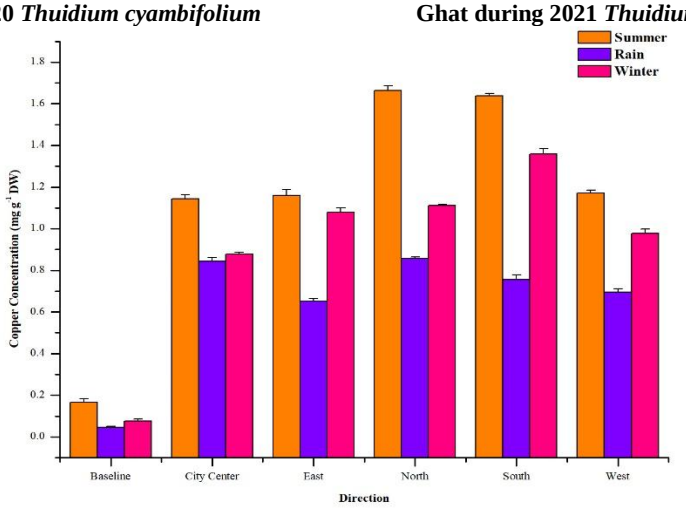

Figure 6.5.6i: Seasonal monitoring of Copper (mg/g DW) at Ghat during 2022 *Thuidium cyambifolium*

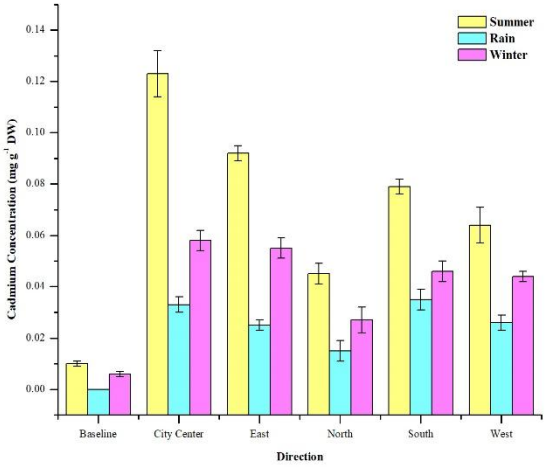

Figure 6.5.6j: Seasonal monitoring of Cadmium (mg/g DW) at Ghat during 2020 *Thuidium cyambifolium*

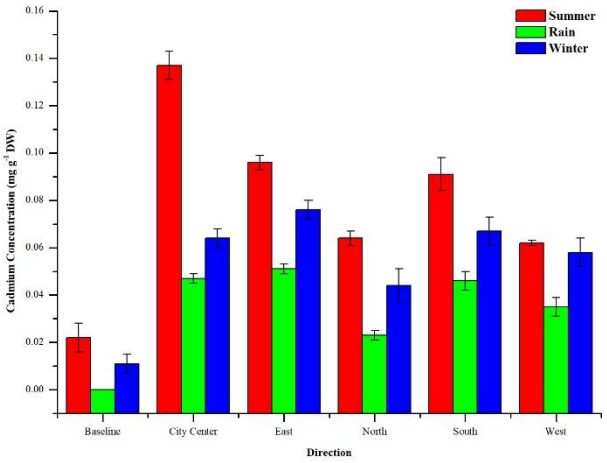

Figure 6.5.6k: Seasonal monitoring of Cadmium (mg/g DW) at Ghat during 2021 *Thuidium cyambifolium*

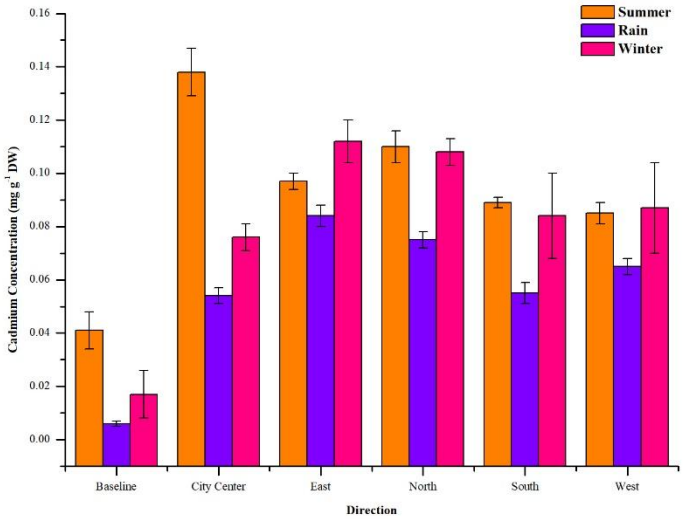

Figure 6.5.6l: Seasonal monitoring of Cadmium (mg/g DW) at Ghat during 2022 *Thuidium cyambifolium*

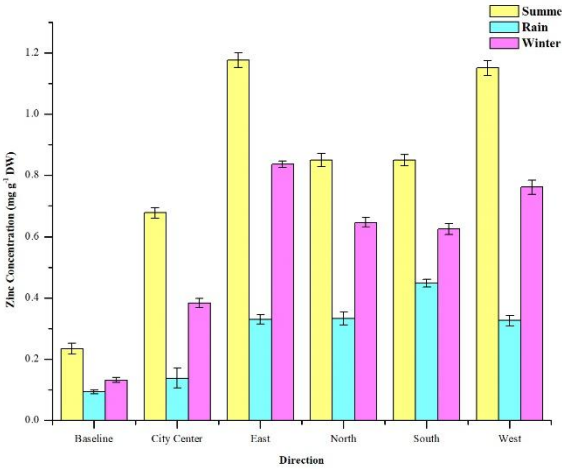

Figure 6.5.7a: Seasonal monitoring of Zinc (mg/g DW) at Thal during 2020 in *Thuidium cyambifolium*

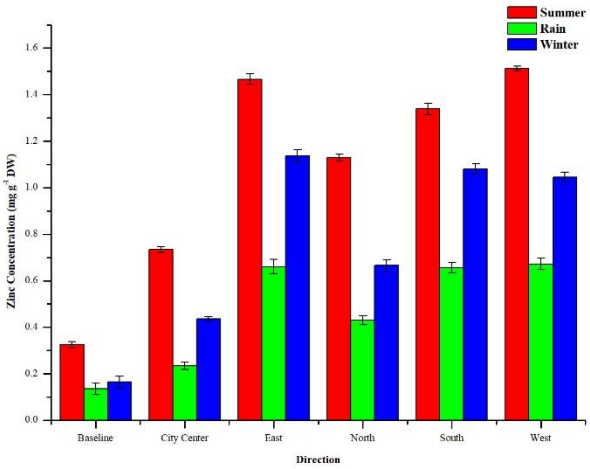

Figure 6.5.7b: Seasonal monitoring of Zinc (mg/g DW) at Thal during 2021 *Thuidium cyambifolium*

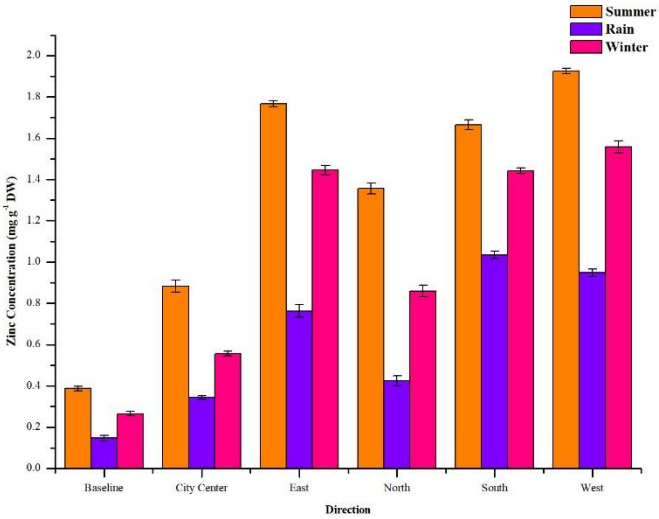

Figure 6.5.7c: Seasonal monitoring of Zinc (mg/g DW) at Thal during 2022 *Thuidium cyambifolium*

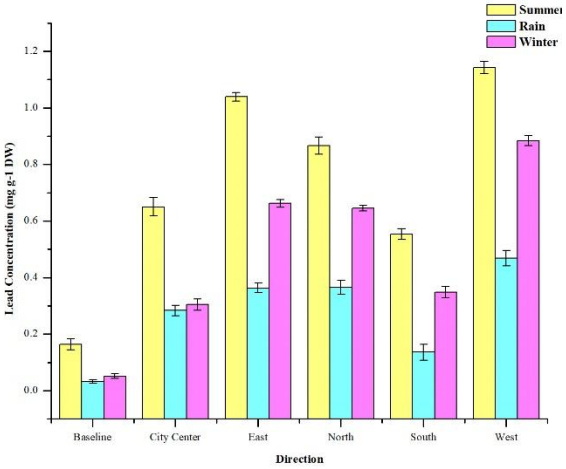

Figure 6.5.7d: Seasonal monitoring of Lead (mg m^{-1} DW) at Thal during 2020 *Thuidium cyambifolium*

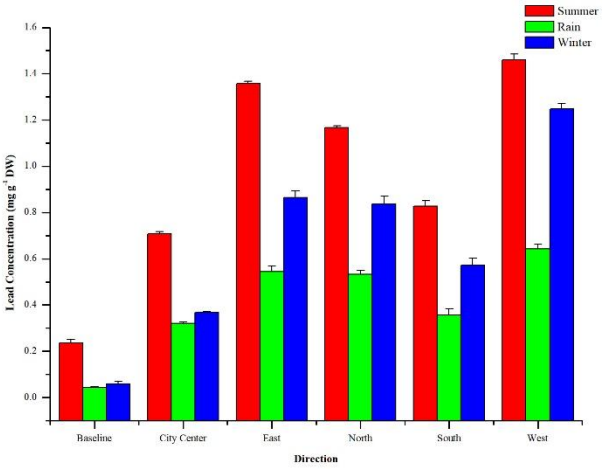

Figure 6.5.7e: Seasonal monitoring of Lead (mg/g DW) at Thal during 2021 *Thuidium cyambifolium*

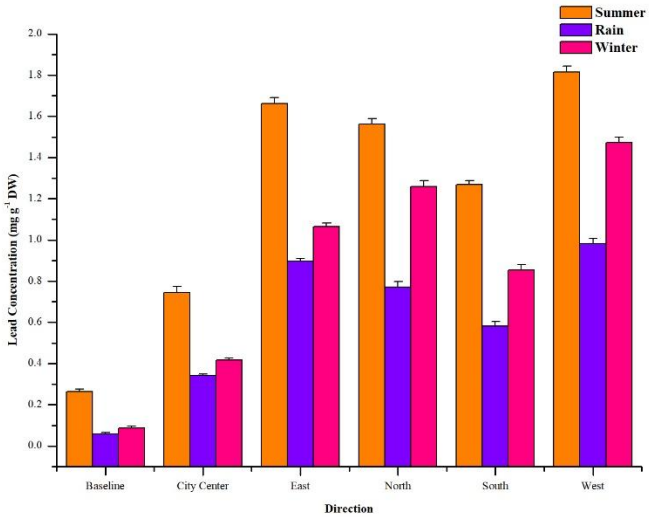

Figure 6.5.7f: Seasonal monitoring of Lead (mg/g DW) at Thal during 2022 *Thuidium cyambifolium*

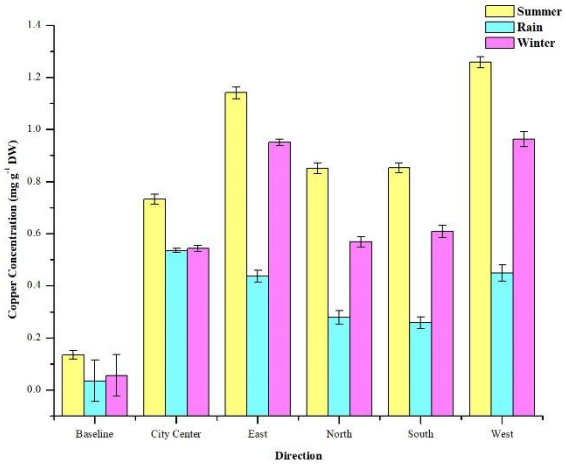

Figure 6.5.7g: Seasonal monitoring of copper (mg/g DW) at Thal during 2020 *Thuidium cyambifolium*

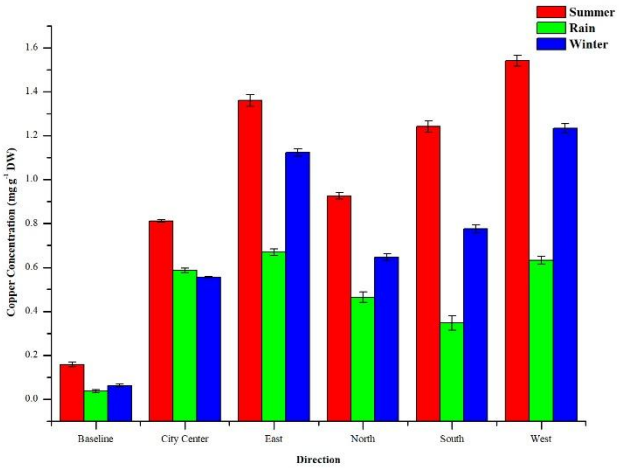

Figure 6.5.7h: Seasonal monitoring of Copper (mg/g DW) at Thal during 2021 *Thuidium cyambifolium*

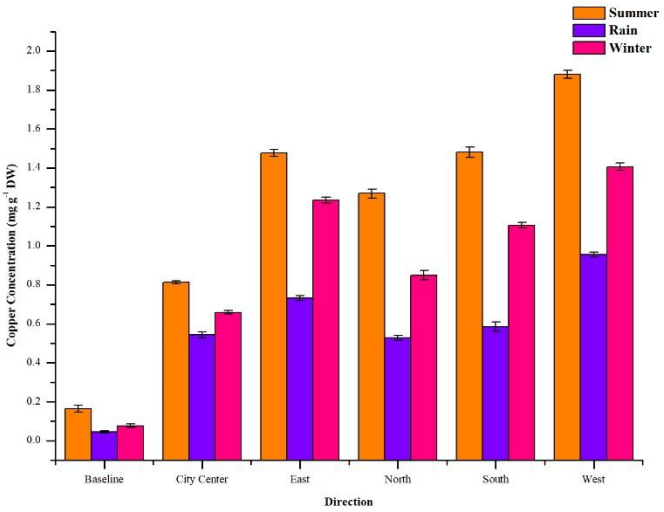

Figure 6.5.7i: Seasonal monitoring of Copper (mg/g DW) at Thal during 2022 *Thuidium cyambifolium*

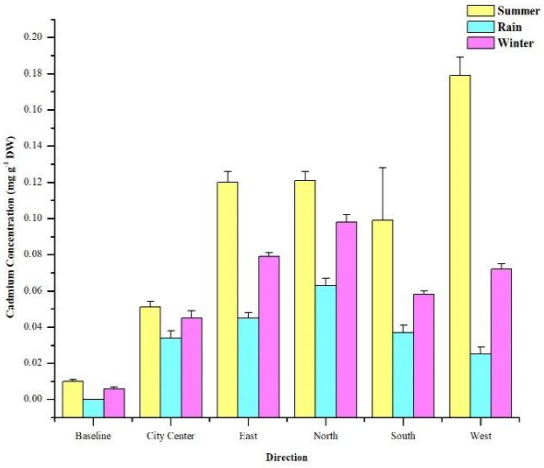

7j: Seasonal monitoring of Cadmium (mg/g DW) at Thal during 2020 *Thuidium cyambifolium*

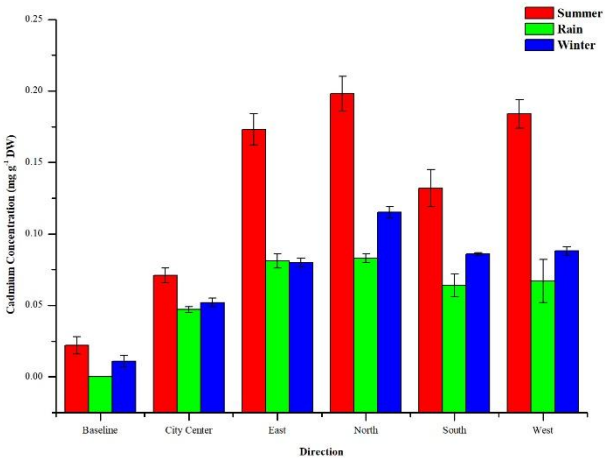

Figure 6.5.7k: Seasonal monitoring of Cadmium (mg/g DW) at Thal during 2021 *Thuidium cyambifolium*

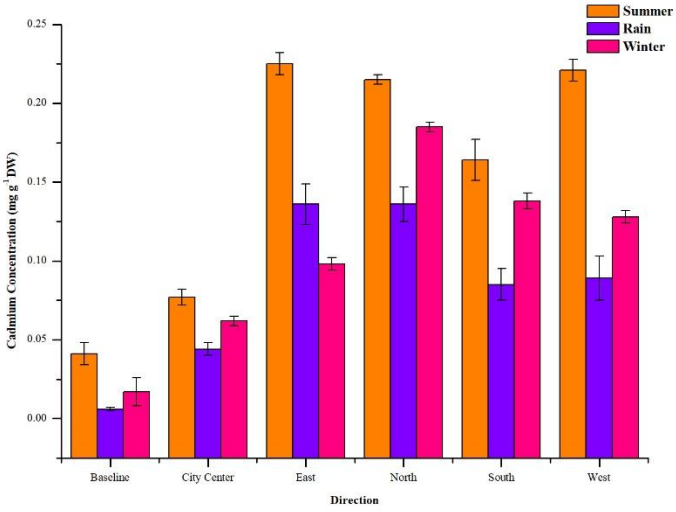

Figure 6.5.7l: Seasonal monitoring of Cadmium (mg/g DW) at Thal during 2022 *Thuidium cyambifolium*

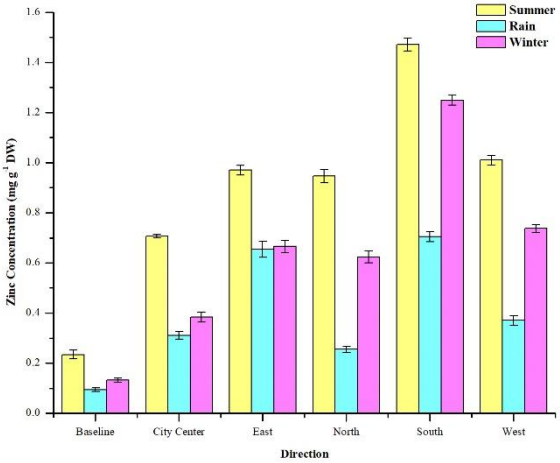

Figure 6.5.8a: Seasonal monitoring of Zinc (mg/g DW) at Munsiyari during 2020 in *Thuidium cyambifolium*

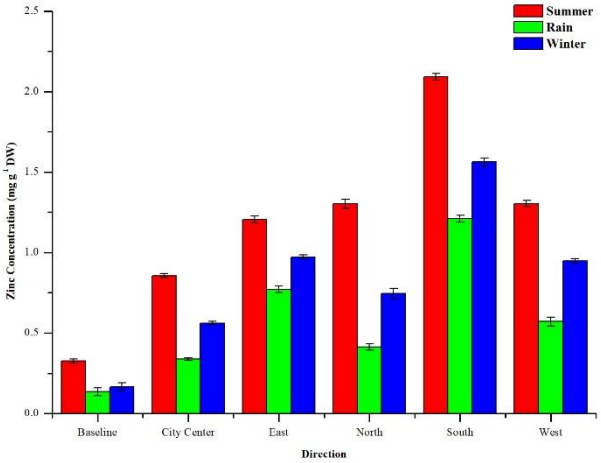

Figure 6.5.8b: Seasonal monitoring of Zinc (mg/g DW) at Munsiyari during 2021 *Thuidium cyambifolium*

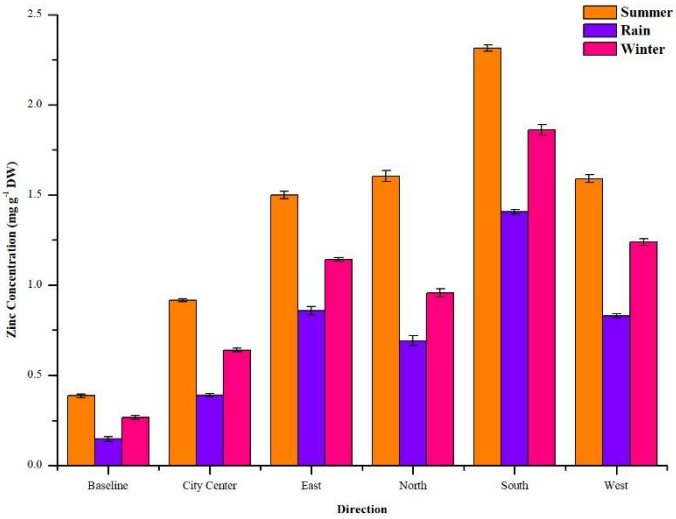

Figure 6.5.8c: Seasonal monitoring of Zinc (mg/g DW) at Munsiyari during 2022 *Thuidium cyambifolium*

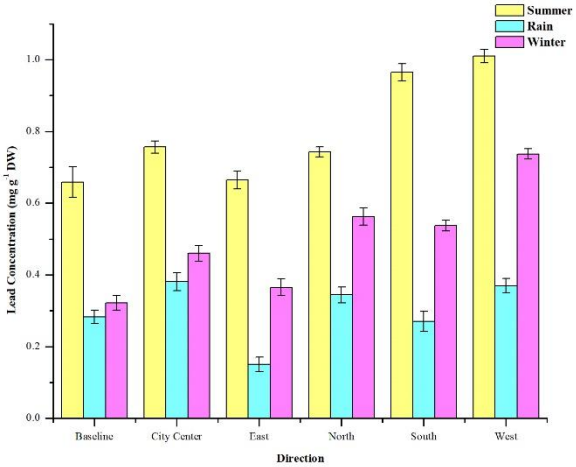

Figure 6.5.8d: Seasonal monitoring of Lead (mg m^{-1} DW) at Munsiyari during 2020 *Thuidium cyambifolium*

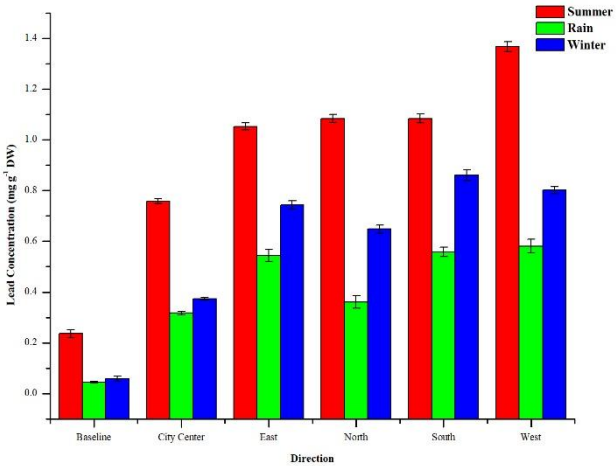

Figure 6.5.8e: Seasonal monitoring of Lead (mg/g DW) at Munsiyari during 2021 *Thuidium cyambifolium*

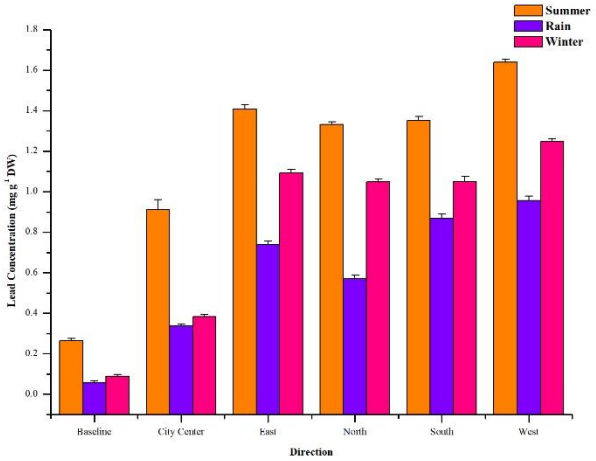

Figure 6.5.8f: Seasonal monitoring of Lead (mg/g DW) at Munsiyari during 2022 *Thuidium cyambifolium*

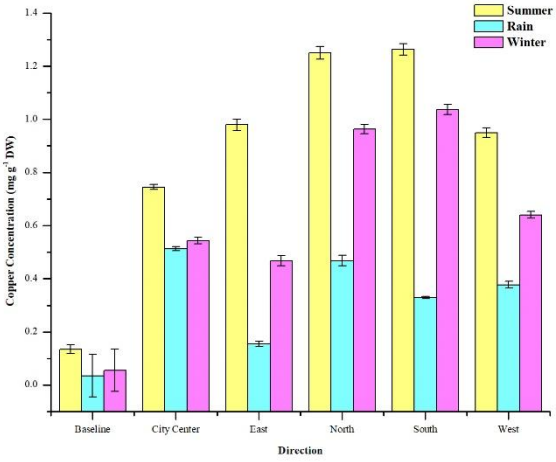

Figure 6.5.8g: Seasonal monitoring of copper (mg/g DW) at Munsiyari during 2020 *Thuidium cyambifolium*

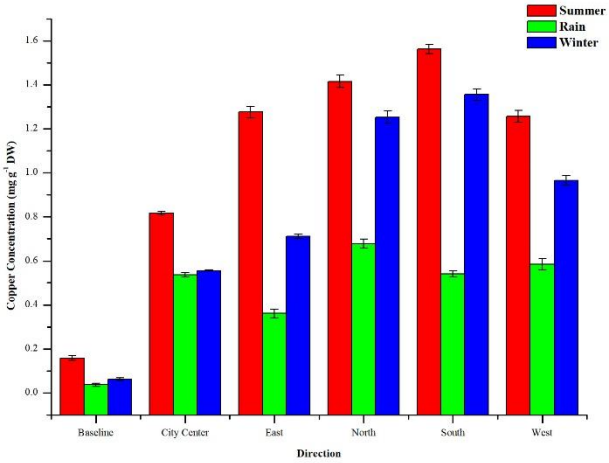

Figure 6.5.8h: Seasonal monitoring of Copper (mg/g DW) at Munsiyari during 2021 *Thuidium cyambifolium*

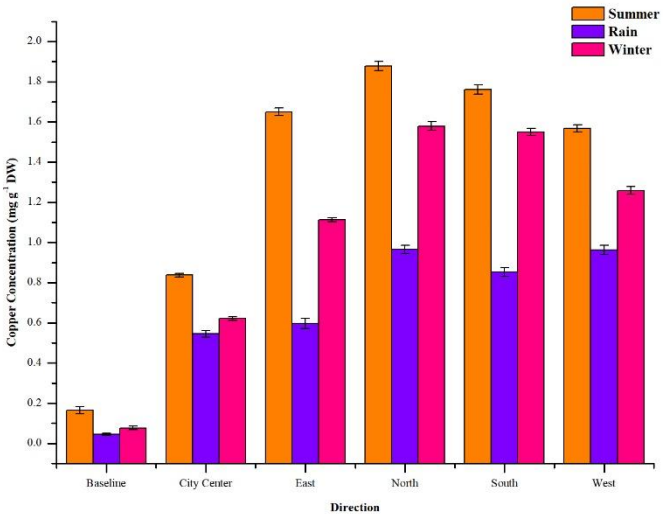

Figure 6.5.8i: Seasonal monitoring of Copper (mg/g DW) at Munsiyari during 2022 *Thuidium cyambifolium*

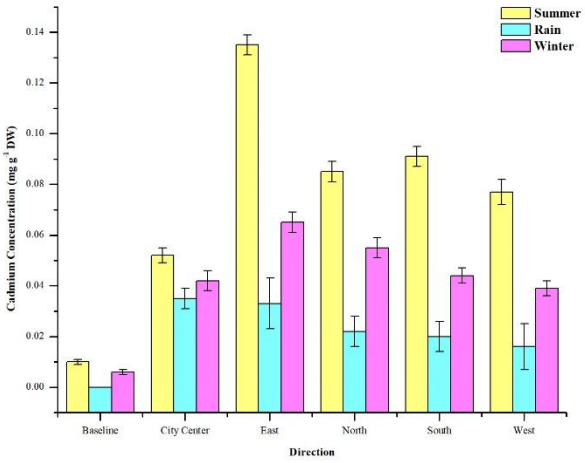

Figure 6.5.8j: Seasonal monitoring of Cadmium (mg/g DW) at Munsiyari during 2020 *Thuidium cyambifolium*

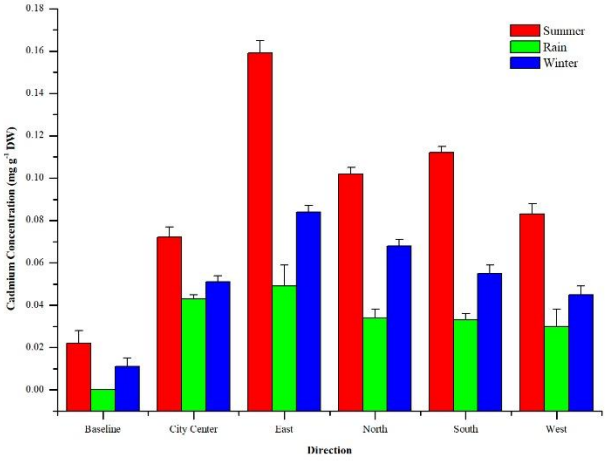

Figure 6.5.8k: Seasonal monitoring of Cadmium (mg/g DW) at Munsiyari during 2021 *Thuidium cyambifolium*

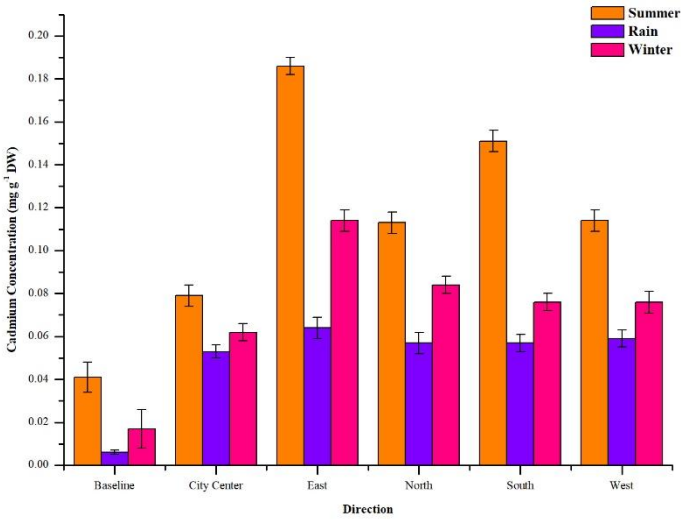

Figure 6.5.8l: Seasonal monitoring of Cadmium (mg/g DW) at Munsiyari during 2022 *Thuidium cyambifolium*

6.6. ANNUAL METAL ACCUMULATION AT DIFFERENT STUDY SITES FROM DIFFERENT DIRECTIONS IN 2020, 2021 and 2022

6.6.1 CHAMPAWAT

The annual metal load of different studied metals, i.e., Zinc (Zn), Lead (Pb), Copper (Cu), and Cadmium (Cd) in moss *Thuidium cymbifolium* (Dozy & Molk) Dozy & Molk. at different directions from Champawat during the study (from 2020 to 2022) is presented in Table (6.6.1) and Figures (6.6.1a to 6.6.1c).

6.6.1a Zinc:

In 2020, the maximum Zn accumulation was measured in the East direction from 2020 (1.172

mg/g DW), 2021 (1.313 mg/g DW), and 2022 (1.457 mg/g DW). During the study period, the minimum concentration was analyzed in the moss from the city center (0.660 mg/g DW, 0.724 mg/g DW, and 0.813 mg/g DW).

6.6.1b. Lead:

The comparative study during three years of the study showed that a high value of Pb was reported from the city center (0.745 mg/g DW) in 2020, while the same was reported high from the south in 2021 (1.008 mg/g DW) and 2022 (1.236 mg/g DW). The lowest concentration was measured towards the west (0.581 mg/g DW, 0.749 mg/g DW, and 0.850 mg/g DW) in 2020, 2021, and 2022, respectively.

6.6.1c. Copper:

Results revealed that maximum Cu accumulation was recorded from the city center in 2020 (0.652 mg/g DW) and 2021 (0.799 mg/g DW), respectively, while it was maximum from the south direction (0.851 mg/g DW) during 2022. Furthermore, minimum values were found from the west direction in 2020 (0.484 mg/g DW), 2021 (0.553 mg/g DW), and 2022 (0.608 mg/g DW).

6.6.1d. Cadmium:

Observation of annual accumulations of Cd in moss *T. cymbifolium* at different collection sites of Champawat City during the years 2020, 2021, and 2022 revealed that maximum Cd accumulation in the moss occurred from the west during 2020 (0.051 mg/g DW) in 2021 (0.069 mg/g DW), and 2022 (0.0.090 mg/g DW). A decrease in Cd accumulation was observed in transplants collected from the city center in 2020 (0.038 mg/g DW) and 2022 (0.069 mg/g DW), while it was reported lower from the south direction in 2021 (0.062 mg/g DW) in the moss analyzed.

6.6.2. Lohaghat:

Results of the annual accumulation of different metals (Zn et al.) in moss *T. cymbifolium* to varying directions in Lohaghat during the years 2020, 2021, and 2022 are presented in Table (6.6.2) and also presented in Figures (6.6.2a to 6.6.2c).

6.6.2a. Zinc:

Observations show that maximum zinc accumulation was recorded from the north direction in 2020 (1.160 mg g^{-1}), 2021 (1.431 mg g^{-1}), and 2022 (1.685 mg g^{-1}). The minimum Zn level was found at the city center in all three consecutive years of study, i.e., 0.652 mg/g DW, 0.863 mg/g DW,

and 1.052 mg/g DW, respectively.

6.6.2b. Lead:

Pb accumulation was highest from the north direction in 2020 (1.365 mg/g DW), 2021 (1.642 mg/g DW), and in 2022 (1.728 mg/g DW). Additionally, minimal values were recorded at the city center in 2020 (0.444 mg/g DW), 2021 (0.757 mg/g DW), and in 2022 (1.055 mg/g DW).

6.6.2c. Copper:

The highest metal accumulation was measured in the north direction of the city during 2020 (0.817 mg/g DW), while the same was reported highest from the city center during 2021 (0.976 mg/g DW) and 2022 (1.328 mg/g DW). The lowest values were found from the city center (0.873 mg/g DW) from the west direction (0.874 mg/g DW) in 2020 and the south direction during 2022 (1.015 mg/g DW).

6.6.2d. Cadmium:

Results revealed that moss *T. cymbifolium* accumulated the high Cd from the west direction in 2020 (0.054 mg/g DW) in the city center during 2021 (0.074 mg/g DW) and 2022 (0.093 mg/g DW). However, during 2020, the lowest values were reported from the north (0.040 mg/g DW), and in 2021 and 2022, the same was reported lowest from the east direction (0.057 mg/g DW and 0.068 mg/g DW).

6.6.3. Khetikhan:

Results of annual accumulation of Zn, Pb, Cu, and Cd in moss *T. cymbifolium* at different sampling sites of Nainital during the years 2020, 2021, and 2022 are presented in Table (6.6.3) and also presented in Figures (6.6.3a to 6.6.3c).

6.6.3a. Zinc:

Data revealed that *T. cymbifolium* accumulates Zn at its highest in the south in 2020 (1.542 mg/g DW) and 2022 (1.845 mg/g DW) and at its lowest in the north in 2021 (1.577 mg/g DW). However, minimum accumulations were found in the city center in 2020 (0.868 mg/g DW), 2021 (0.964 mg/g DW), and 2022 (1.077 mg/g DW).

6.6.3b. Lead:

The results of bio mapping of lead through moss *T. cymbifolium* at different directions of

Khetikhan during 2020, 2021 and 2022 show that the east direction recorded the maximum metal accumulation in the years 2020 (0.781 mg/g DW) and 2021 (1.319 mg/g DW), while towards the south, it was reported highest in 2022 (1.061 mg/g DW). The lowest Pb level was found at the city center in the three years, i.e., 0.506 mg/g DW (2020), 0.589 mg/g DW (2021), and 0.800 mg/g DW (2022).

6.6.3c. Copper:

Annual accumulation of copper in moss *T. cymbifolium* at different sampling sites of Khetikhan during 2020, 2021, and 2022 depicted that the highest concentration of metal was reported from the north direction during 2020 (0.835 mg/g DW), 2021 (1.179 mg/g DW) and 2022 (1.084 mg/g DW). Whereas the minimum deposition was reported in moss samples harvested from the west direction during 2020 (0.380 mg/g DW), from the city center during 2021 (0.687 mg/g DW), and again from the west direction during 2022 (0.656 mg/g DW).

6.6.3d. Cadmium:

Results show that maximum Cd accumulation in the moss occurred from the west during 2020 (0.087 mg g^{-1}DW), 2021 (0.102 mg g^{-1}DW), and 2022 (0.152 mg g^{-1}DW). Minimum Cd values were reported from the moss collected from the city centre in 2020 (0.050 mg g^{-1}DW), 2021 (0.056 mg g^{-1}DW), and 2022 (0.061 mg g^{-1}DW).

6.6.4. Barakote:

The results of biomapping of studied metals (Zn, Pb, Cu and Cd) through moss *T. cymbifolium* at different collection sites of Barakote during the years 2020, 2021 and 2022 are presented in table (6.6.4) and Figures (6.6.4a to 6.6.4c).

6.6.4a. Zinc:

In summer, the east direction recorded the maximum metal accumulation in 2020 (1.191 mg g^{-1}DW), 2021 (1.319 mg/g DW), and 2022 (1.559 mg/g DW). The minimum Zn level was found at city center in 2020 (0.555 mg/g DW), in 2020 (0.593 mg/g DW) and 2021 (0.630 mg/g DW).

6.6.4b. Lead:

The maximum lead accumulation was recorded in the west direction in 2020 (0.750 mg/g DW) and in 2021 (0.961 mg/g DW), while it was reported high from the east direction during 2022

(1.347 mg/g DW). The minimum lead accumulation was reported from the south (0.424 mg/g DW) in 2020 and 2021 (0.567 mg/g DW), while during 2022, it was reported high from the north direction (0.788 mg/g DW).

6.6.4c. Copper:

In the summer season, the maximum Cu accumulation was recorded in the north direction in 2020 (1.092 mg/g DW), in 2021 (1.241 mg/g DW), and in the south direction in 2022 (1.626 mg/g DW). Transplants collected from the west direction during 2020 (0.623 mg/g DW) and from the city centre during 2021 (0.691 mg/g DW) and 2022 (0.740 mg/g DW) accumulated the minimum metal.

6.6.4d. Cadmium:

The amount of Cd accumulated in moss *T. cymbifolium* at different sampling stations of Barakote during different seasons of the years 2020, 2021, and 2022 was high from the north direction during 2020 (0.063 mg/g DW), 2021 (0.081 mg/g DW) and 2022 (0.098 mg/g DW). In addition, minimum values were recorded at the east in 2020 (0.048 mg/g DW), from the city centre and south direction in 2021 (0.067 mg/g DW) and the city centre in 2022 (0.078 mg/g DW).

6.6.5. Pithoragarh:

Table 6.6.5 and Figures (6.6.5a to 6.6.5c) show the outcomes of biomonitoring for Zn, Pb, Cu, and Cd using moss *T. cymbifolium* in different directions at Pithoragarh in the years 2020, 2021, and 2022.

6.6.5a. Zinc:

Observations showed a consistent trend for the maximum and minimum zinc accumulation. The highest concentration was recorded in the north direction in 2020 (1.317 mg/g DW) and 2021 (1.484 mg/g DW), while from the east direction in 2022 (1.972 mg/g DW). Furthermore, minimum values were found at the city center during 2020 (0.716 mg/g DW), 2021 (0.903 mg/g DW), and 2022 (1.137 mg/g DW).

6.6.5b. Lead:

The city center recorded the maximum metal accumulation in 2020 (1.046 mg/g DW), 2021 (1.307 mg/g DW), and 2022 (1.676 mg/g DW). The minimum Pb level was found in the south direction in 2020 (0.538 mg/g DW) and 2021 (0.780 mg g-1), while in 2022, the same was reported as minimal

from the east direction (1.018 mg/g DW).

6.6.5c. Copper:

The peak concentration of Cu was found to be maximum in the north direction in 2020 (1.268 mg/g DW) and 2022 (1.564 mg/g DW) and from the east direction in 2021 (1.852 mg/g DW). Meanwhile, the minimum accumulation was reported in moss collected from the city centre (0.588 mg/g DW) in 2020, (0.747 mg/g DW) in 2021, and (0.834 mg/g DW) in 2022.

6.6.5d. Cadmium:

Results show that maximum Cd accumulation in the moss was found high in the east direction during 2020 (0.079 mg/g DW), 2021 (0.092 mg/g DW), and in the south in 2022 (0.104 mg/g DW). The minimum load was found in the north in 2020 (0.051 mg/g DW) and in the west direction in 2021 (0.048 mg/g DW) and 2022 (0.071 mg/g DW).

6.6.6. Ghat:

The biomonitoring for Zn, Pb, Cu, and Cd through moss T. cymbifolium at different collection sites of Ghat during the years 2020, 2021, and 2022 are depicted in Table (6.6.6) and figures (6.6.6a- 6.6.6c).

6.6.6a. Zinc:

The highest values were evaluated from the south in 2020 (1.271 mg/g DW), 2021 (1.570 mg/g DW), and 2022 (1.813 mg/g DW). At the same time, the lowest concentration was found in the east during 2020 (0.798 mg/g DW) and in the city center during 2021 (1.091 mg/g DW) and 2022 (1.237 mg/g DW).

6.6.6b. Lead:

The highest values were recorded from the north direction in 2020 (1.206 mg/g DW), in 2021 (1.431 mg/g DW), and from the city center in 2022 (1.767 mg/g DW). The lowest values were observed in the east direction (0.770 mg/g DW) during 2020, 1.028 mg/g DW during 2021, and 1.229 mg/g DW during 2022.

6.6.6c. Copper:

Results revealed that maximum Cu accumulation was towards the north in 2020 (0.804

mg/g DW), towards the south in 2021 (0.995 mg/g DW), and in the west direction in 2022 (1.250 mg/g DW). Minimum values were found at the east in 2020 (0.463 mg/g DW), from the west in 2021 (0.716 mg/g DW), and in 2022 (0.948 mg/g DW).

6.6.6d. Cadmium:

Results of annual accumulation of Cd in moss *T. cymbifolium* at different sampling sites of Ghat during the years 2020, 2021 and 2022 showed that the maximum Cd concentration was reported from the city centre during 2020 (0.071 mg/g DW) and 2021 (0.082 mg/g DW) while it was reported high from east direction in 2022 (0.098 mg/g DW). While the maximum Cd values were reported from the moss collected from the north direction in 2020 (0.029 mg/g DW) and 2021 (0.044 mg/g DW), while it was minimum from the south direction in 2022 (0.076 mg/g DW).

6.6.7. Thal:

Table (6.6.7) and Figures (6.6.7a to 6.6.7c) depict the annual variations for Zn, Pb, Cu and Cd concentration in moss *T. cymbifolium* at different collection sites of Thal for the three consecutive years (2020, 2021, and 2022).

6.6.7a. Zinc:

The highest values were evaluated in the north direction in 2020 (0.780 mg/g DW) and from the east direction in 2021 (1.090 mg/g DW), while the maximum was reported from the west direction in 2022 (1.437 mg/g DW). At the same time, the lowest concentration was found in the city centre in 2020 (0.400 mg/g DW), 2021 (0.451 mg/g DW), and 2021 (0.512 mg/g DW).

6.6.7b. Lead:

The Pb value was maximum in the west direction (0.832 mg/g DW, 1.118 mg/g DW, and 1.408 mg/g DW) in 2020, 2021, and 2022, respectively. Its minimum concentration was measured in transplants harvested in the east direction (0.346 mg/g DW) in 2020, from the city center in 2021 (0.447 mg/g DW), and in 2022 (0.489 mg/g DW).

6.6.7c. Copper:

Observations revealed that maximum Cu accumulation was reported from the west direction in 2020 (0.890 mg/g DW), in 2021 (1.137 mg/g DW) and in 2022 (1.278 mg/g DW). It was reported lowest from the south direction in 2020 (0.566 mg/g DW) from the city centre in 2021 (0.620 mg/g DW), and in 2022 (0.651 mg/g DW).

6.6.7d. Cadmium:

The maximum Cd concentration in the south direction in 2020 (0.094 mg/g DW) while in the north direction in 2021 (0.125 mg/g DW) and 2022 (0.177 mg/g DW). Concentration declined to 0.043 mg/g DW in 2020, 0.055 mg/g DW in 2021, and 0.063 mg/g DW in 2022 at the city center.

6.6.8. Munsiyari:

The results of biomapping of all four studied metals i.e. Zinc, Lead, Copper and Cadmium, through moss *T. cymbifolium* at different collection sites of Munsiyari during the years 2020, 2021, and 2022 are presented in Table (6.6.8a) and Figures (6.6.8a to 6.6.8 c).

6.6.8a. Zinc:

The south direction recorded the maximum metal accumulation in 2020 (1.141 mg/g DW), 2021 (1.622 mg/g DW), and 2022 (1.860 mg/g DW). However, the lowest values were observed at the city centre in 2020 (0.467 mg/g DW), 2021 (0.585 mg/g DW), and 2022 (0.649 mg/g DW).

6.6.8b. Lead:

In the monsoon, the consistent peak concentration of Pb was reported from the west direction in 2020 (0.591 mg/g DW), in 2021 (0.916 mg/g DW), and in 2022 (1.281 mg/g DW). In contrast, the concentration was measured at the minimum in moss samples harvested from the north direction during 2020 (0.393 mg/g DW) and from the city centre in 2021 (0.483 mg/g DW) and 2022 (0.544 mg/g DW).

6.6.8c. Copper:

The highest concentration was observed at different sites in different years, i.e., in the north direction during 2020 (0.893 mg/g DW) and 2022 (1.474 mg/g DW), and in 2021 (1.153 mg/g DW), same was high from the south direction. The same diversified trend was observed for the minimum concentration towards the east direction in 2020 (0.534 mg/g DW) (2020), while at the city centre, it was 0.637 mg/g DW in 2021 and 0.668 mg/g DW in 2022.

6.6.8d. Cadmium:

The maximum cadmium level was found at different sites in all three years: towards the north in 2020 (0.054 mg/g DW), and from the east direction in 2021 (0.097 mg/g DW), and 2022

(0.121 mg/g DW). In addition, minimum values were recorded from the city center in 2020 (0.043 mg/g DW), in 2021 (0.052 mg/g DW), and 2022 (0.077 mg/g DW).

Table 6.6.1: Annual variation of different metals (mg/g DW) in *Thuidium cyambifolium* at various transplant sites of Champawat during the years 2020, 2021 and 2022

Sampling Sites	Zinc			Lead			Copper			Cadmium		
	2020	2021	2022	2020	2021	2022	2020	2021	2022	2020	2021	2022
Control	0.153 ± 0.011	0.209 ± 0.021	0.266 ± 0.011	0.082 ± 0.011	0.113 ± 0.012	0.136 ± 0.010	0.075 ± 0.05	0.086 ± 0.008	0.096 ± 0.011	0.006 ± 0.001	0.011 ± 0.003	0.021 ± 0.006
City Center	0.660^{d} ± 0.030	0.724 ± 0.015	0.813 ± 0.019	0.745^{a} ± 0.018	0.854 ± 0.026	0.942 ± 0.020	0.652 ± 0.023	0.799 ± 0.022	0.819 ± 0.022	0.038 ± 0.003	0.063 ± 0.003	0.069 ± 0.003
East	1.172^{a} ± 0.040	1.313 ^{a} ± 0.032	1.457 ^{a} ± 0.027	0.666^{b} ± 0.014	0.932 ± 0.022	1.108 ± 0.025	0.515 ± 0.035	0.626 ± 0.010	0.821 ± 0.019	0.050 ± 0.005	0.064 ± 0.005	0.081 ± 0.006
North	1.023^{b} ± 0.033	1.269 ^{a} ± 0.028	1.403^{a} ± 0.031	0.610 ± 0.013	0.847 ± 0.015	0.984 ± 0.019	0.511 ± 0.015	0.566 ± 0.021	0.683 ± 0.016	0.046 ± 0.005	0.063 ± 0.006	0.072 ± 0.010
South	0.978 ^{c} ± 0.036	1.210 ± 0.029	1.329^{b}± 0.033	0.744^{ab} ± 0.021	1.008 ± 0.023	1.236 ± 0.015	0.591 ± 0.025	0.655 ± 0.018	0.851 ± 0.018	0.049 ± 0.008	0.062 ± 0.004	0.079 ± 0.006
West	1.074^{b} ± 0.027	1.253^{b} ± 0.033	1.405^{ab} ± 0.025	0.581 ± 0.019	0.749 ± 0.019	0.850 ± 0.019	0.484 ± 0.014	0.553 ± 0.015	0.608 ± 0.018	0.051 ± 0.004	0.069 ± 0.004	0.090 ± 0.09

Table 6.6.2: Annual variation of different metals (mg/g DW) in *Thuidium cyambifolium* at various transplant sites of Lohaghat during the years 2020, 2021 and 2022

Sampling Sites	Zinc			Lead			Copper			Cadmium		
	2020	2021	2022	2020	2021	2022	2020	2021	2022	2020	2021	2022
Control	0.153 ± 0.011	0.209 ± 0.021	0.266 ± 0.011	0.082 ± 0.011	0.113 ± 0.012	0.136 ± 0.010	0.075 ± 0.05	0.086 ± 0.008	0.096 ± 0.011	0.006 ± 0.001	0.011 ± 0.003	0.021 ± 0.006
City Center	0.652 ± 0.019	0.863 ± 0.021	1.052 ± 0.017	0.444 ± 0.017	0.757 ± 0.016	1.055 ± 0.019	0.762 ± 0.015	0.976 ± 0.017	1.328 ± 0.018	0.046 ± 0.004	0.074 ± 0.005	0.089 ± 0.005
East	0.943 ± 0.024	1.131 ± 0.026	1.434 ± 0.015	1.218 ± 0.016	1.339 ± 0.011	1.463 ± 0.014	0.791 ± 0.020	0.961 ± 0.016	1.096 ± 0.016	0.052 ± 0.003	0.057 ± 0.005	0.068 ± 0.004
North	1.160 ± 0.020	1.431 ± 0.018	1.685 ± 0.017	1.365 ± 0.019	1.642 ± 0.015	1.728 ± 0.017	0.817 ± 0.017	0.936 ± 0.019	1.173 ± 0.018	0.040 ± 0.003	0.066 ± 0.003	0.093 ± 0.005
South	0.937 ± 0.013	1.119 ± 0.019	1.355 ± 0.021	1.175 ± 0.015	1.291 ± 0.015	1.368 ± 0.012	0.793 ± 0.017	0.923 ± 0.016	1.015 ± 0.017	0.040 ± 0.005	0.066 ± 0.003	0.072 ± 0.003
West	0.861 ± 0.012	1.169 ± 0.016	1.332 ± 0.024	0.955 ± 0.021	1.088 ± 0.014	1.252 ± 0.014	0.793 ± 0.017	0.874 ± 0.016	1.016 ± 0.022	0.055 ± 0.004	0.065 ± 0.005	0.077 ± 0.004

- Values are represented as mean ± SE
- Means with the same letter are not significantly different.
- Tukeys's Honest Significant Difference (HSD) Test was performed at α=0.05 and Cv=4.289

Table 6.6.3: Annual variation of different metals (mg/g DW) in *Thuidium cyambifolium* at various transplant sites of Khetikhan during years 2020, 2021 and 2022

Sampling Sites	Zinc			Lead			Copper			Cadmium		
	2020	**2021**	**2022**	**2020**	**2021**	**2022**	**2020**	**2021**	**2022**	**2020**	**2021**	**2022**
Control	0.153 ± 0.011	0.209 ± 0.021	0.266 ± 0.011	0.082 ± 0.011	0.113 ± 0.012	0.136 ± 0.010	0.075 ± 0.05	0.086 ± 0.008	0.096 ± 0.011	0.006 ± 0.001	0.011 ± 0.003	0.021 ± 0.006
City Center	0.868 ± 0.013	0.964 ± 0.021	1.077 ± 0.018	0.506 ± 0.014	0.589 ± 0.016	0.800 ± 0.017	0.610 ± 0.016	0.687 ± 0.015	0.878 ± 0.015	0.050 ± 0.003	0.056 ± 0.003	0.061 ± 0.004
East	1.230 ± 0.012	1.331 ± 0.032	1.580 ± 0.016	0.781 ± 0.016	1.319 ± 0.014	1.043 ± 0.017	0.511 ± 0.018	0.790 ± 0.010	0.700 ± 0.014	0.071 ± 0.006	0.094 ± 0.006	0.125 ± 0.010
North	1.411 ± 0.025	1.577 ± 0.012	1.810 ± 0.022	0.708 ± 0.015	0.913 ± 0.014	0.998 ± 0.014	0.835 ± 0.011	1.179 ± 0.016	1.084 ± 0.019	0.053 ± 0.010	0.064 ± 0.006	0.086 ± 0.010
South	1.542 ± 0.021	1.510 ± 0.012	1.854 ± 0.021	0.621 ± 0.019	0.853 ± 0.013	1.061 ± 0.013	0.640 ± 0.020	1.114 ± 0.016	0.891 ± 0.018	0.065 ± 0.007	0.083 ± 0.008	0.101 ± 0.006
West	1.155 ± 0.022	1.303 ± 0.015	1.555 ± 0.017	0.750 ± 0.016	1.155 ± 0.015	1.027 ± 0.015	0.380 ± 0.017	0.777 ± 0.011	0.656 ± 0.015	0.087 ± 0.007	0.102 ± 0.005	0.152 ± 0.007

Table 6.6.4: Annual variation of different metals (mg/g DW) in *Thuidium cyambifolium* at various transplant sites of Barakote during years 2020, 2021 and 2022

Sampling Sites	Zinc			Lead			Copper			Cadmium		
	2020	**2021**	**2022**	**2020**	**2021**	**2022**	**2020**	**2021**	**2022**	**2020**	**2021**	**2022**
Control	0.153 ± 0.011	0.209 ± 0.021	0.266 ± 0.011	0.082 ± 0.011	0.113 ± 0.012	0.136 ± 0.010	0.075 ± 0.05	0.086 ± 0.008	0.096 ± 0.011	0.006 ± 0.001	0.011 ± 0.003	0.021 ± 0.006
City Center	0.555 ± 0.013	0.593 ± 0.014	0.630 ± 0.012	0.504 ± 0.012	0.674 ± 0.014	0.860 ± 0.011	0.658 ± 0.020	0.691 ± 0.009	0.740 ± 0.022	0.049 ± 0.004	0.067 ± 0.003	0.078 ± 0.004
East	1.191 ± 0.021	1.319 ± 0.020	1.559 ± 0.018	0.713 ± 0.018	0.918 ± 0.019	1.347 ± 0.017	0.653 ± 0.022	0.791 ± 0.019	0.926 ± 0.020	0.048 ± 0.005	0.069 ± 0.003	0.090 ± 0.004
North	0.720 ± 0.017	0.911 ± 0.020	1.116 ± 0.016	0.451 ± 0.015	0.638 ± 0.019	0.788 ± 0.020	1.092 ± 0.015	1.241 ± 0.016	1.523 ± 0.020	0.063 ± 0.007	0.081 ± 0.006	0.098 ± 0.006
South	0.604 ± 0.017	0.859 ± 0.018	1.227 ± 0.017	0.424 ± 0.021	0.567 ± 0.018	0.796 ± 0.022	0.830 ± 0.020	1.151 ± 0.021	1.626 ± 0.019	0.050 ± 0.009	0.067 ± 0.005	0.090 ± 0.005
West	0.996 ± 0.013	1.155 ± 0.020	1.529 ± 0.017	0.750 ± 0.018	0.961 ± 0.021	1.304 ± 00.17	0.623 ± 0.014	0.777 ± 0.022	0.976 ± 0.018	0.058 ± 0.005	0.070 ± 0.005	0.094 ± 0.004

- Values are represented as mean ± SE
- Means with the same letter are not significantly different.
- Tukeys's Honest Significant Difference (HSD) Test was performed at α=0.05 and Cv=4.289

Table 6.6.5: Annual variation of different metals (mg/g DW) in *Thuidium cyambifolium* at various transplant sites of Pithoragarh during years 2020, 2021 and 2022

Sampling Sites	Zinc			Lead			Copper			Cadmium		
	2020	2021	2022	2020	2021	2022	2020	2021	2022	2020	2021	2022
Control	0.153 ± 0.011	0.209 ± 0.021	0.266 ± 0.011	0.082 ± 0.011	0.113 ± 0.012	0.136 ± 0.010	0.075 ± 0.05	0.086 ± 0.008	0.096 ± 0.011	0.006 ± 0.001	0.011 ± 0.003	0.021 ± 0.006
City Center	0.716 ± 0.011	0.903 ± 0.013	1.137 ± 0.017	1.046 ± 0.014	1.307 ± 0.011	1.676 ± 0.012	0.588 ± 0.014	0.747 ± 0.014	0.834 ± 0.023	0.068 ± 0.005	0.082 ± 0.005	0.090 ± 0.005
East	1.153 ± 0.015	1.448 ± 0.020	1.972 ± 0.017	0.648 ± 0.021	0.827 ± 0.023	1.018 ± 0.012	1.193 ± 0.015	1.488 ± 0.015	1.757 ± 0.016	0.079 ± 0.004	0.092 ± 0.006	0.097 ± 0.005
North	1.317 ± 0.015	1.484 ± 0.017	1.844 ± 0.20	0.670 ± 0.018	0.828 ± 0.017	1.072 ± 0.022	1.268 ± 0.013	1.564 ± 0.014	1.852 ± 0.020	0.051 ± 0.005	0.071 ± 0.004	0.090 ± 0.005
South	1.051 ± 0.017	1.407 ± 0.019	1.814 ± 0.019	0.538 ± 0.022	0.780 ± 0.014	1.031 ± 0.023	1.096 ± 0.025	1.309 ± 0.018	1.524 ± 0.024	0.063 ± 0.005	0.079 ± 0.005	0.104 ± 0.017
West	0.958 ± 0.018	1.118 ± 0.016	1.487 ± 0.020	0.641 ± 0.020	0.869 ± 0.017	1.075 ± 0.022	1.003 ± 0.020	1.206 ± 0.019	1.466 ± 0.023	0.054 ± 0.005	0.048 ± 0.018	0.071 ± 0.008

Table 6.6.6: Annual variation of different metals (mg/g DW) in *Thuidium cyambifolium* at various transplant sites of Ghat during years 2020, 2021 and 2022

Sampling Sites	Zinc			Lead			Copper			Cadmium		
	2020	2021	2022	2020	2021	2022	2020	2021	2022	2020	2021	2022
Control	0.153 ± 0.011	0.209 ± 0.021	0.266 ± 0.011	0.082 ± 0.011	0.113 ± 0.012	0.136 ± 0.010	0.075 ± 0.05	0.086 ± 0.008	0.096 ± 0.011	0.006 ± 0.001	0.011 ± 0.003	0.021 ± 0.006
City Center	0.885 ± 0.011	1.019 ± 0.011	1.237 ± 0.017	1.177 ± 0.016	1.412 ± 0.011	1.767 ± 0.012	0.767 ± 0.013	0.858 ± 0.016	0.954 ± 0.016	0.071 ± 0.005	0.082 ± 0.004	0.089 ± 0.005
East	0.798 ± 0.024	1.055 ± 0.016	1.255 ± 0.019	0.770 ± 0.020	1.028 ± 0.020	1.229 ± 0.024	0.463 ± 0.017	0.720 ± 0.024	0.963 ± 0.022	0.057 ± 0.003	0.074 ± 0.003	0.098 ± 0.005
North	0.940 ± 0.026	1.206 ± 0.015	1.503 ± 0.017	1.206 ± 0.020	1.431 ± 0.019	1.581 ± 0.028	0.804 ± 0.021	0.988 ± 0.020	1.211 ± 0.011	0.029 ± 0.004	0.044 ± 0.004	0.098 ± 0.005
South	1.271 ± 0.020	1.570 ± 0.019	1.813 ± 0.020	0.994 ± 0.021	1.298 ± 0.028	1.510 ± 0.024	0.782 ± 0.017	0.995 **± 0.028**	1.250 ± 0.019	0.053 ± 0.004	0.068 ± 0.006	0.076 ± 0.007
West	1.139 ± 0.019	1.348 ± 0.019	1.616 ± 0.023	0.790 ± 0.024	1.083 ± 0.029	1.284 ± 0.021	0.609 ± 0.026	0.716 ± 0.023	0.948 ± 0.017	0.045 ± 0.004	0.052 ± 0.003	0.079 ± 0.008

- Values are represented as mean ± SE
- Means with the same letter are not significantly different.
- Tukeys's Honest Significant Difference (HSD) Test was performed at α=0.05 and Cv=4.289

Table 6.6.7: Annual variation of different metals (mg/g DW) in *Thuidium cyambifolium* at various transplant sites of Thal during the years 2020, 2021, and 2022

Sampling Sites	Zinc			Lead			Copper			Cadmium		
	2020	2021	2022	2020	2021	2022	2020	2021	2022	2020	2021	2022
Control	0.153 ± 0.011	0.209 ± 0.021	0.266 ± 0.011	0.082 ± 0.011	0.113 ± 0.012	0.136 ± 0.010	0.075 ± 0.05	0.086 ± 0.008	0.096 ± 0.011	0.006 ± 0.001	0.011 ± 0.003	0.021 ± 0.006
City Center	0.400 ± 0.022	0.451 ± 0.013	0.512 ± 0.009	0.412 ± 0.024	0.447 ± 0.013	0.489 ± 0.016	0.604 ± 0.013	0.620 ± 0.007	0.651 ± 0.011	0.043 ± 0.004	0.055 ± 0.003	0.063 ± 0.004
East	0.641 ± 0.016	1.090 ± 0.027	1.322 ± 0.023	0.346 ± 0.022	0.921 ± 0.021	1.187 ± 0.019	0.574 ± 0.022	1.046 ± 0.020	1.145 ± 0.016	0.065 ± 0.012	0.109 ± 0.004	0.151 ± 0.008
North	0.780 ± 0.016	0.740 ± 0.019	0.883 ± 0.026	0.688 ± 0.015	0.845 ± 0.023	1.189 ± 0.028	0.842 ± 0.020	0.673 ± 0.018	0.873 ± 0.020	0.081 ± 0.003	0.125 ± 0.003	0.177 ± 0.006
South	0.610 ± 0.020	1.025 ± 0.022	1.381 ± 0.018	0.625 ± 0.022	0.598 ± 0.017	0.892 ± 0.023	0.566 ± 0.022	0.776 ± 0.026	1.053 ± 0.022	0.094 ± 0.004	0.097 ± 0.007	0.124 ± 0.009
West	0.746 ± 0.022	1.075 ± 0.018	1.473 ± 0.020	0.832 ± 0.027	1.118 ± 0.022	1.408 ± 0.026	0.890 ± 0.027	1.137 ± 0.021	1.278 ± 0.018	0.092 ± 0.006	0.115 ± 0.009	0.138 ± 0.008

Table 6.6.8: Annual variation of different metals (mg/g DW) in *Thuidium cyambifolium* at various transplant sites of Munsiyari during the years 2020, 2021 and 2022

Sampling Sites	Zinc			Lead			Copper			Cadmium		
	2020	2021	2022	2020	2021	2022	2020	2021	2022	2020	2021	2022
Control	0.153 ± 0.011	0.209 ± 0.021	0.266 ± 0.011	0.082 ± 0.011	0.113 ± 0.012	0.136 ± 0.010	0.075 ± 0.05	0.086 ± 0.008	0.096 ± 0.011	0.006 ± 0.001	0.011 ± 0.003	0.021 ± 0.006
City Center	0.467 ± 0.014	0.585 ± 0.010	0.649 ± 0.009	0.421 ± 0.027	0.483 ± 0.007	0.544 ± 0.021	0. 600 ± 0.010	0.637 ± 0.007	0.668 ± 0.011	0.043 ± 0.004	0.056 ± 0.003	0.065 ± 0.004
East	0.763 ± 0.026	0.983 ± 0.018	1.167 ± 0.017	0.532 ± 0.021	0.780 ± 0.019	1.079 ± 0.018	0.534 ± 0.017	0.783 ± 0.019	1.120 ± 0.018	0.077 ± 0.006	0.097 ± 0.006	0.121 ± 0.005
North	0.608 ± 0.020	0.820 ± 0.027	1.084 ± 0.027	0.393 ± 0.022	0.698 ± 0.018	0.983 ± 0.014	0.893 ± 0.020	1.115 ± 0.025	1.474 ± 0.021	0.054 ± 0.005	0.068 ± 0.003	0.085 ± 0.005
South	1.141 ± 0.023	1.622 ± 0.022	1.860 ± 0.020	0.550 ± 0.020	0.835 ± 0.018	1.090 ± 0.021	0.876 ± 0.015	1.153 ± 0.020	1.388 ± 0.021	0.052 ± 0.004	0.067 ± 0.003	0.095 ± 0.004
West	0.706 ± 0.018	0.941 ± 0.020	1.219 ± 0.017	0591 ± 0.022	0.916 ± 0.020	1.281 ± 0.016	0.655 ± 0.015	0.963 ± 0.024	1.263 ± 0.020	0.044 ± 0.005	0.052 ± 0.005	0.083 ± 0.005

- Values are represented as mean ± SE
- Means with the same letter are not significantly different.
- Tukeys's Honest Significant Difference (HSD) Test was performed at α=0.05 and Cv=4.289

The annual distribution of metals in the eight monitoring sites, including thirty-two sampling sites in District Champawat and Pithoragarh of Uttarakhand, revealed that the annual accumulation pattern of Zinc, Lead, Copper, and Cadmium in moss *T. cymbifolium* was found in the order of summer > winter > monsoon seasons and 2022>2021>2020.

Among these studied sites, zinc concentration was highest during the summer of 2022 in district Champawat from south of Khetikhan (1.854 mg g^{-1}) and lowest from the city center of Barakote (0.555 mg g^{-1}) during 2020 (Tables 6.6.3 and 6.6.4; Figures 6.6.3c and 6.6.4a). in district Pithoragarh, the same was reported high during the summer of 2022 from the east direction of Pithoragarh (1.972 mg g^{-1}) and lowest from the city center of Thal (0.400 mg g^{-1}) in 2020 (Table 6.6.5 and 6.6.7 and Figures 6.6.5c and 6.6.7a). Zinc accumulation in study areas during the summers is attributed to long-range transport, transboundary influences, and tourist inflow (Klos et al., 2009). Deposition rates for Zn differed up to an order of magnitude, probably indicative of local differences in conditions and releases to the atmosphere (Nicholson et al., 2003). The study also reported that some transplants collected near populated areas also have a high Zn concentration. Radziemska et al. (2019) and Swislowski et al. (2022) also reported high Zn concentration in their monitoring study of the Populated area.

Lead (Pb) was reported as the most abundant metal in district Champawat, with the highest concentration of 1.728 mg/g from the north direction of Lohaghat during the summers of 2022 (Table 6.6.2 and Figure 6.6.2c). In the Pithoragarh district, the same was reported to be high in the city center of Ghat (1.767 mg g^{-1}) during the summer of 2022 (Table 6.6.6). According to recent studies on lead contamination of airborne particles, burning leaded gasoline has been a significant source of ongoing lead releases into the environment over the past century. (Flegal et al., 2010; Laidlaw et al., 2012). Pant and Harrison (2013) also reported that the abrasion of tyres significantly contributes to the Pb in the atmosphere.

The deposition of the Pb was reported lowest from the south direction of Barakote (0.424 mg g^{-1}) during the rainy season 2020 from district Champawat. From district Pithoragarh, it was reported lower during the monsoon (0.346 mg g^{-1}) from the east direction of Thal (Table 6.6.7 and Figure 6.6.7a). This may be due to the decreased vehicular and other tourist activities during this season. These results are consistent with the observations of Adachi and Tainosho (2004) as well as Chandra et al. (2014). Lead (Pb) can be transported over long distances, and the influx of tourists during the summer increases Pb accumulation. Nonetheless, atmospheric lead predominantly existed as submicron aerosols (Qarri et al., 2019).

In the summer of 2022, a high deposition of Cu was reported from the northern region of Pithoragarh (1.852 mg g^{-1}) (Table 6.6.5), while the southern region of Barakote had a concentration of 1.626 mg/g (Table 6.6.4). In 2020, the districts of Champawat and Pithoragarh had a reduction in the amount of rainfall, so the eastern direction of Ghat in Pithoragarh district (0.463 mg g-1) and the western direction of Khetikhan in Champawat district (0.380 mg g-1) have been identified as having the lowest deposition rates, as shown in Table 6.6.3 and 6.6.6.

Cu pollution is thought to be closely related to vehicle emissions and mainly from agriculture (the primary constituent of pesticides or fungicides) and household burning (Kapusta et al., 2019). Combustion of coal and organic matter can generate bioluminescent insects known as fireflies, potentially contributing to the observed rise in copper (Cu) levels at the research locations. Conversely, the elevated levels of Cu in the experimental sites can be attributed to the disposal of domestic waste, washing activities, and using kerosene oil to prevent contamination. The present study observed that the high concentration of copper aligns with Eisler's (1998) report, indicating that garbage can also serve as a source of copper.

The annual deposition of the Cd was reported to be high in the summer of 2022 from the west direction of Khetikhan (0.152 mg g^{-1}) in district Champawat (Table 6.6.3 and Figure 6.6.3c) and from the North direction of Thal (0.177 mg g^{-1}) during summer of 2022 in district Pithoragarh (Table 6.6.7 and Figure 6.6.7c). The Cd pollution is caused by a combination of mechanisms, including the transport of cadmium emissions caused by human activities through the air and the subsequent deposition of these emissions. Anthropogenically, phosphate fertilizers released through municipal wastewater are sources of Cd in the atmosphere (Smolders & Mertens, 2013). Tourism activities and amenities, such as hotel wastewater and increased traffic also significant sources of Cd pollution in the study area. These results also agree with the study conducted by Mikhailenko et al. (2020).

Cd deposition was reported to be low in the rainy season of 2020 in both districts. It was low in the city center of Champwat (0.038 mg g^{-1}) (Table 6.6.1 and Figure 6.6.1a) from district Champawat and the north direction from Ghat (0.029 mg g^{-1}) in district Pithoragarh (Table 6.6.5 and Figure 6.6.5a). According to the study by Heindel et al. (2020), atmospheric dust fall was reported to be the highest during the summer compared to the other seasons. The cadmium concentration is low in the ambivalent environment but is of more significant environmental concern (Mikhailenko et al., 2020; Rahimzadeh et al., 2017). This might be due to the ability of cadmium to leach out easily from the surface. These findings are similar to those of Srivastava et al. (2014).

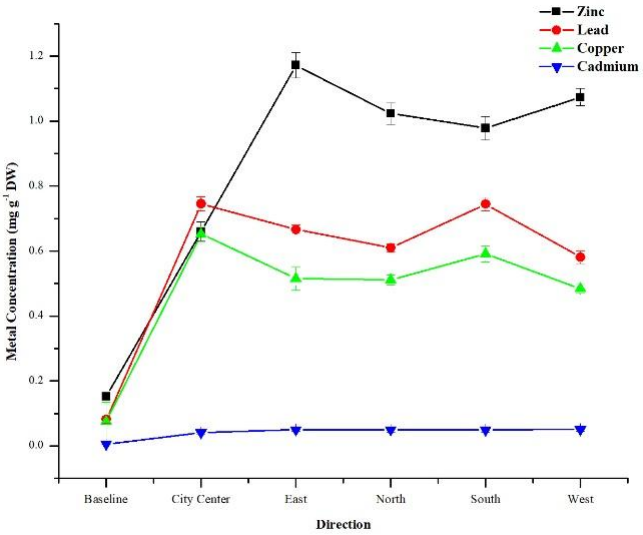

Figure 6.6.1a: Annual concentration of different metals (mg/g DW) at Champawat during 2020 in *Thuidium cyambifolium*

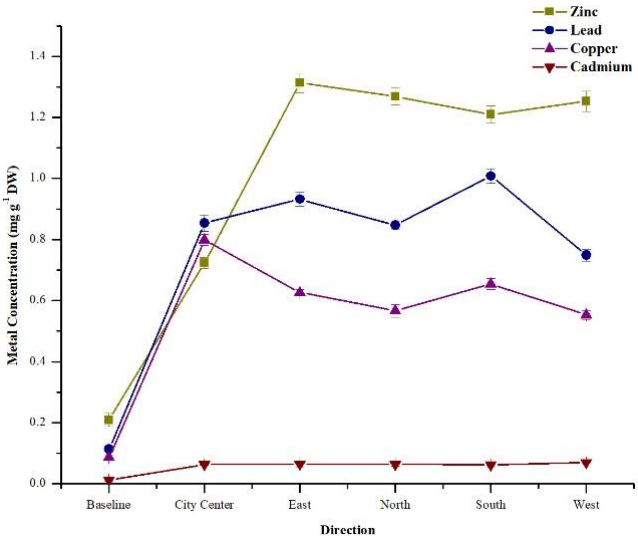

Figure 6.6.1b: Annual concentration of different metals (mg/g DW) at Champawat during 2021 in *Thuidium cyambifolium*

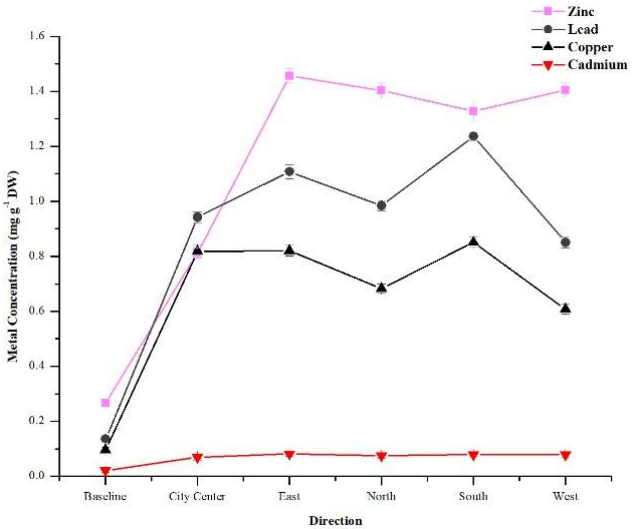

Figure 6.6.1c: Annual concentration of different metals (mg/g DW) at Champawat during 2022 in *Thuidium cyambifolium*

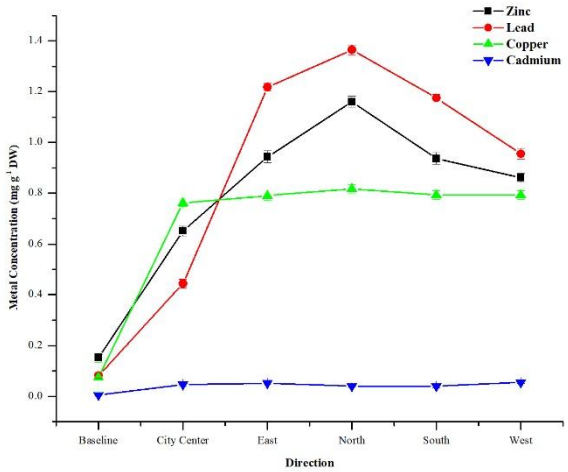

Figure 6.6.2a: Annual concentration of different metals (mg/g DW) at Lohaghat during 2020 in *Thuidium cyambifolium*

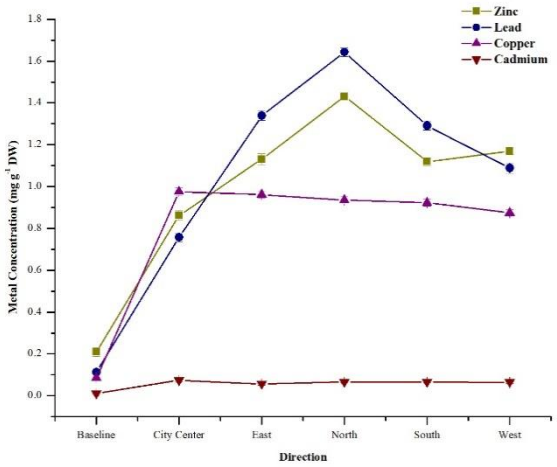

Figure 6.6.2b: Annual concentration of different metals (mg/g DW) at Lohaghat during 2021 in *Thuidium cyambifolium*

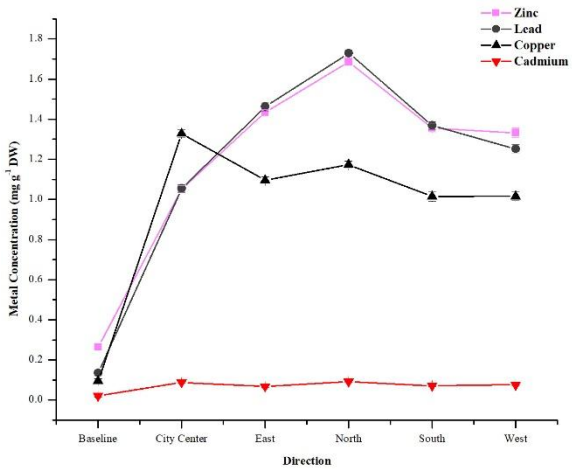

Figure 6.6.2c: Annual concentration of different metals (mg/g DW) at Lohaghat during 2022 in *Thuidium cyambifolium*

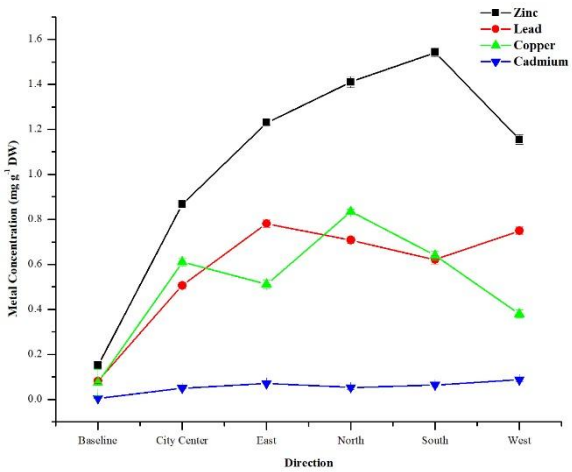

Figure 6.6.3a: Annual concentration of different metals (mg/g DW) at Khetikhan during 2020 in *Thuidium cyambifolium*

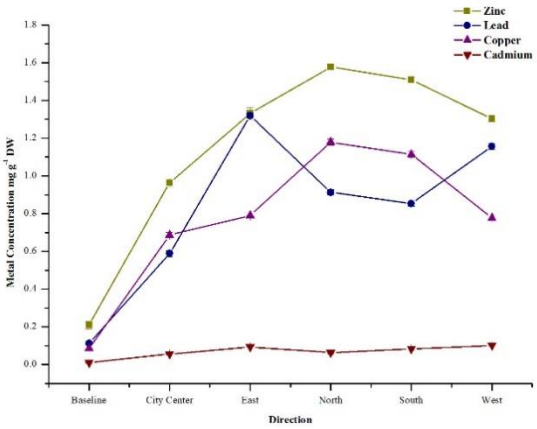

Figure 6.6.3b: Annual concentration of different metals (mg/g DW) at Khetikhan during 2021 in *Thuidium cyambifolium*

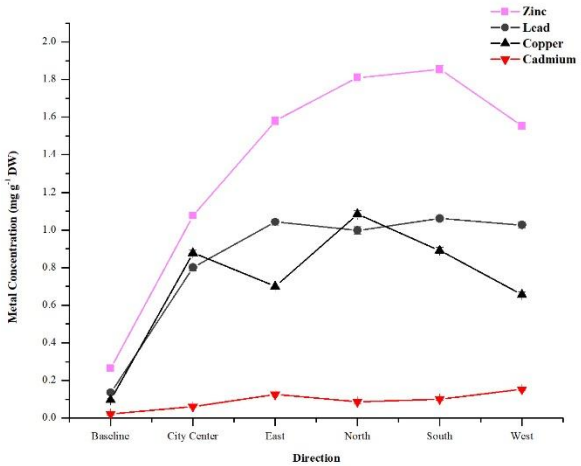

Figure 6.6.3c: Annual concentration of different metals (mg/g DW) at Khetikhan during 2022 in *Thuidium cyambifolium*

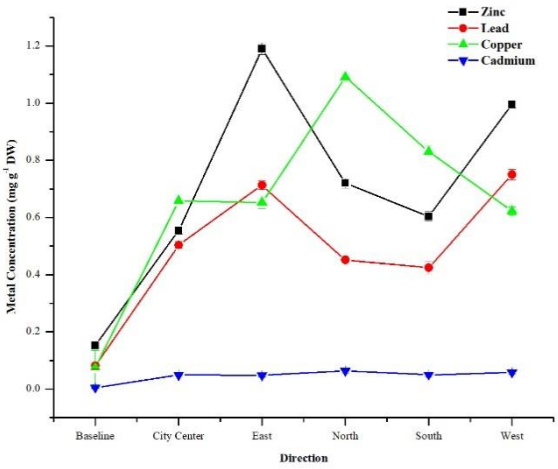

Figure 6.6.4a: Annual concentration of different metals (mg/g DW) at Barakote during 2020 in *Thuidium cyambifolium*

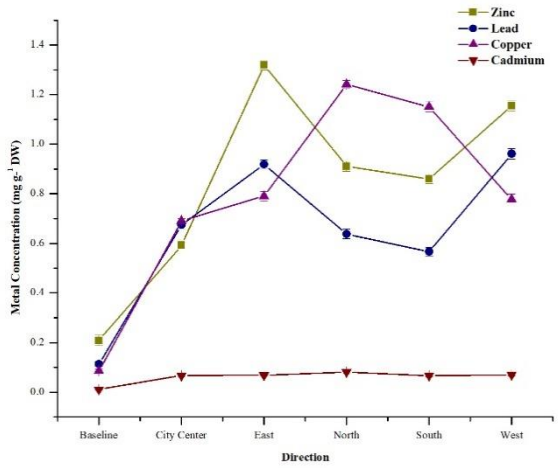

Figure 6.6.4b: Annual concentration of different metals (mg/g DW) at Barakote during 2021 in *Thuidium cyambifolium*

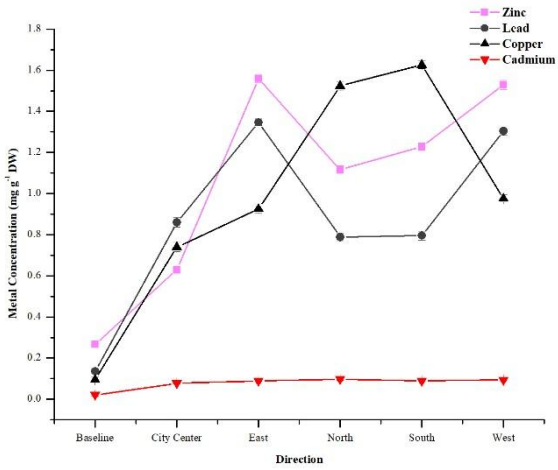

Figure 6.6.4c: Annual concentration of different metals (mg/g DW) at Barakote during 2022 in *Thuidium cyambifolium*

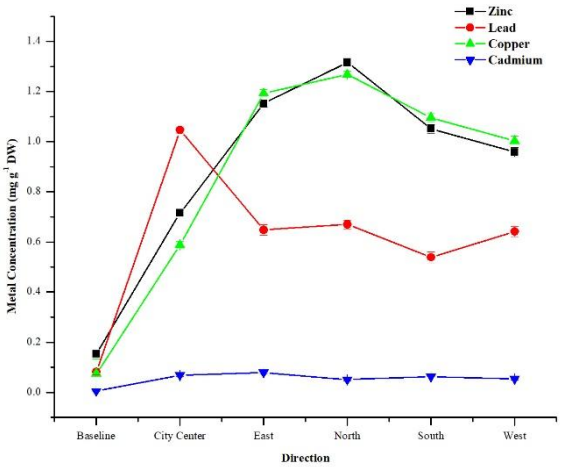

Figure 6.6.5a: Annual concentration of different metals (mg/g DW) at Pithoragarh during 2020 in *Thuidium cyambifolium*

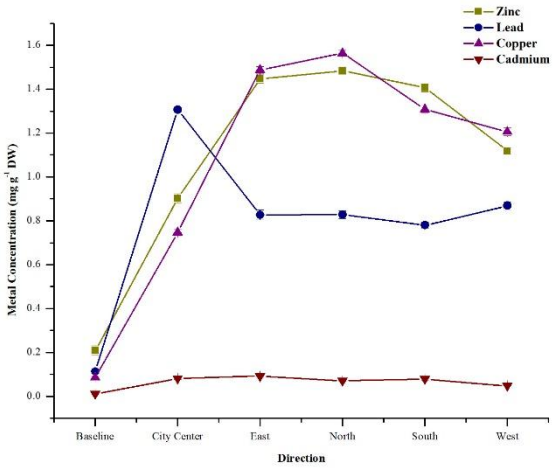

Figure 6.6.5b: Annual concentration of different metals (mg/g DW) at Pithoragarh during 2021 in *Thuidium cyambifolium*

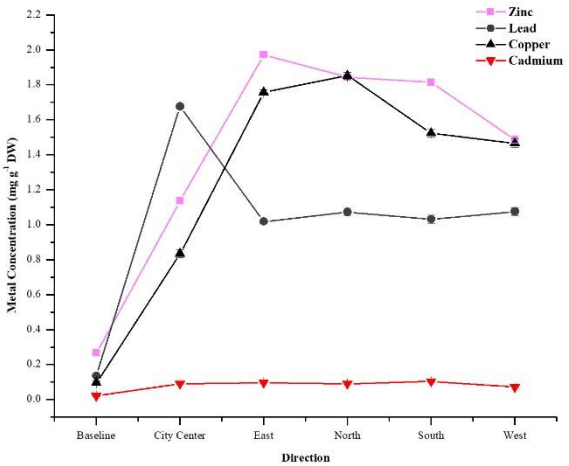

Figure 6.6.5c: Annual concentration of different metals (mg/g DW) at Pithoragarh during 2022 in *Thuidium cyambifolium*

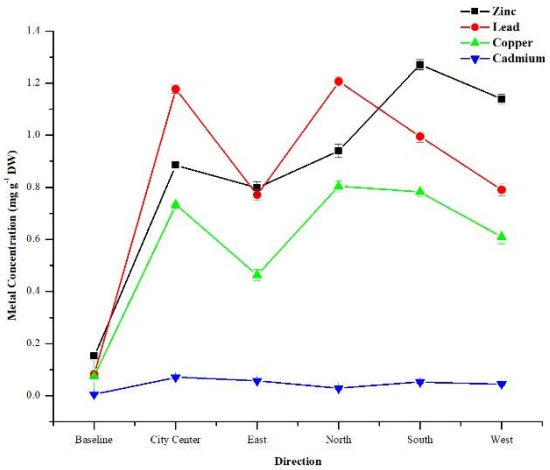

Figure 6.6.6a: Annual concentration of different metals (mg/g DW) at Ghat during 2020 in *Thuidium cyambifolium*

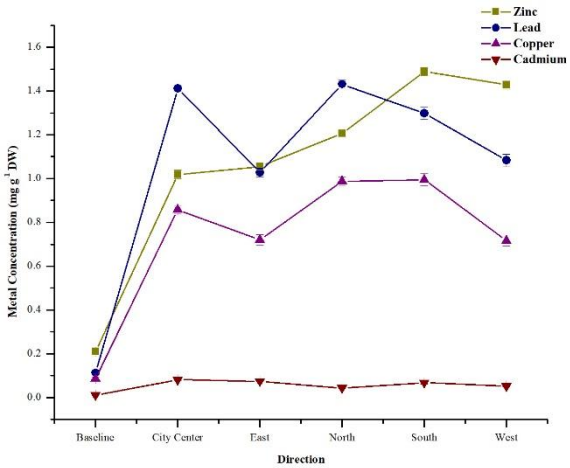

Figure 6.6.6b: Annual concentration of different metals (DW) at Ghat during 2021 in *Thuidium cyambifolium*

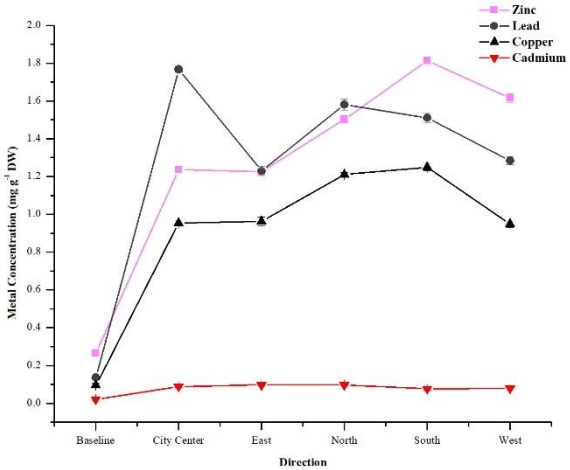

Figure 6.6.6c: Annual concentration of different metals (mg/g DW) at Ghat during 2022 in *Thuidium cyambifolium*

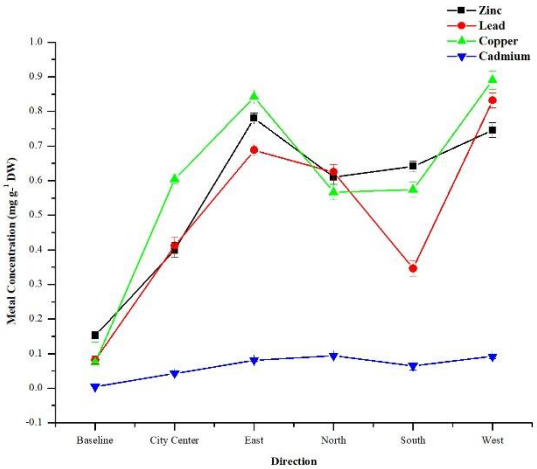

Figure 6.6.7a: Annual concentration of different metals (mg/g DW) at Thal during 2020 in *Thuidium cyambifolium*

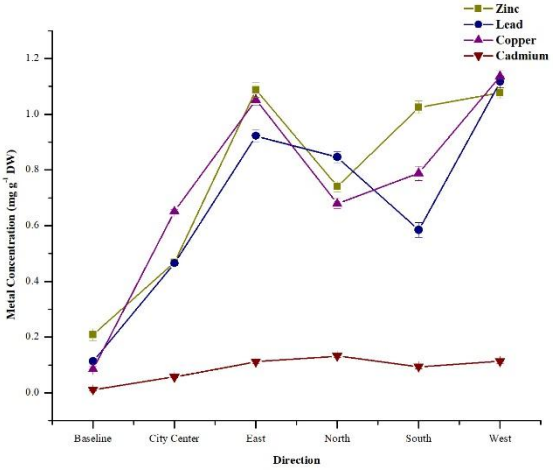

Figure 6.6.7b: Annual concentration of different metals (mg/g DW) at Thal during 2021 in *Thuidium cyambifolium*

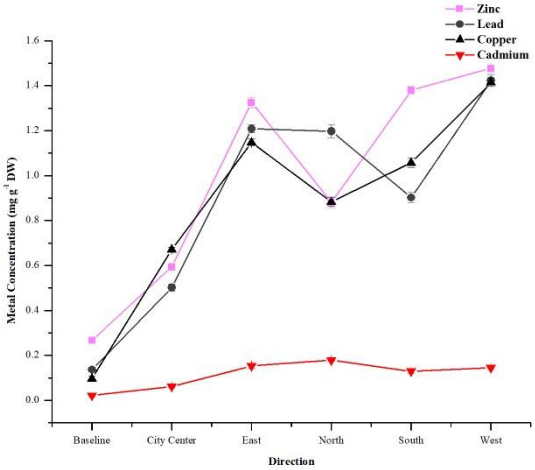

Figure 6.6.7c: Annual concentration of different metals (mg/g DW) at Thal during 2022 in *Thuidium cyambifolium*

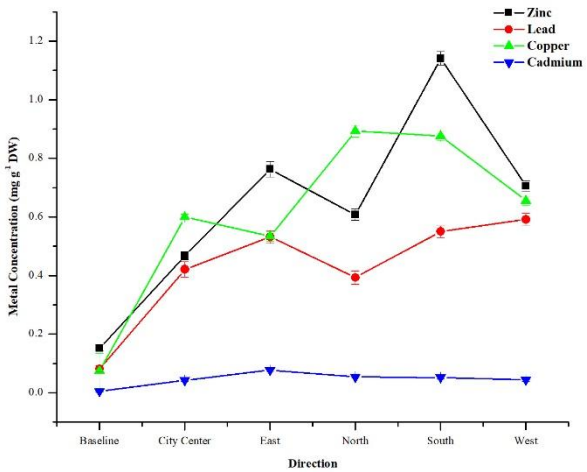

Figure 6.6.8a: Annual concentration of different metals (mg/g DW) at Munsiyari during 2020 in *Thuidium cyambifolium*

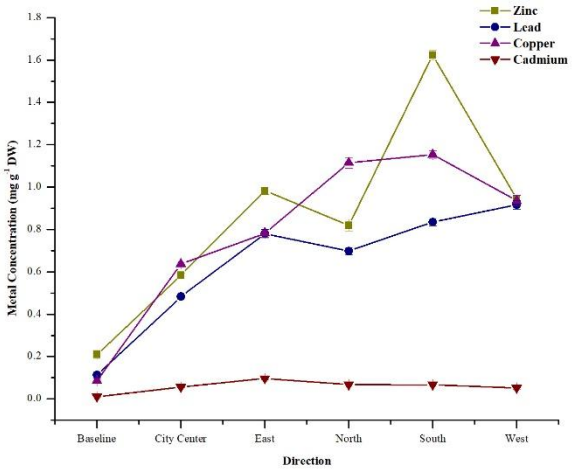

Figure 6.6.8b: Annual concentration of different metals (mg/g DW) at Munsiyari during 2021 in *Thuidium cyambifolium*

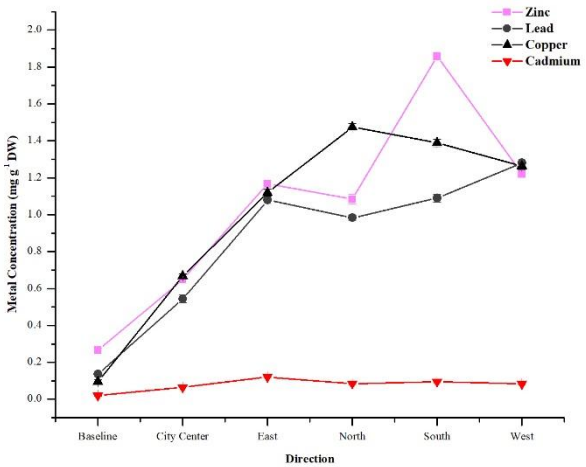

Figure 6.6.8c: Annual concentration of different metals (mg/g DW) at Munsiyari during 2022 in *Thuidium cyambifolium*

6.7 VARIATION OF METAL ACCUMULATION LEVEL AND DEGREE OF CONTAMINATION IN DIFFERENT STUDY SITES OF DISTRICT CHAMPAWAT AND PITHORAGARH IN RELATION TO CONTAMINATION FACTOR IN 2020, 2021 and 2022

The contamination factor (CF) was also calculated for each study site with the grading of contamination caused by different metals. CF showed different contamination categories, indicating that the study sites were not uniformly contaminated by studied heavy metals (Table 6.7 a-c). The scale prepared by Fernández and Carballeira (2002) was used to categorize the level of contamination according to which category C1 represents no pollution if CF is less than 1, and category C2 indicates suspected pollution if CF ranges from 1 to 2. Category C3 denotes slight pollution when CF is between 2 and 3.5, and category C4 indicates moderate pollution levels if CF is between 3.5 and 8.

The analysis from the present study reveals that for Zinc (Zn) during 2020, the degree of contamination was calculated between C1 and C3. The city center of Munsiyari falls under the C1 category, which shows that the site is unpolluted. The north of Lohaghat and Pithoragarh, south of Khetikhan and Ghat, East direction of Barakote and Thal, and east and west direction of Barakote fall under the C3 category with CF in the range of 2-3.5, which shows that these sites had slight pollution (Table 6.7a). In the year 2021, the city center of Thal was under the C1 category with CF > 1. It showed that this site was unpolluted at that time. The rest of the sites fall under the C2 category, which indicates that these sites were suspected of pollution. The east and west of Barakote, north of Pithoragarh, and south of Ghat, Thal, and Munsiyari were under the C3 category, which shows that these sites had a slight level of pollution (Table 6.7b). For the third year of study (2022), the city center of Munsiyari falls under the C1 category, which shows that the site is unpolluted. The east direction of Barakote, Pithoragarh, and Thal, and the south direction of Munsiyari and Thal were in the C3 category with CF in the range of 2-3.5. It indicates that these sites had a slight level of pollution (Table 6.7c). According to Wei et al. (2015), human activities such as metal production, waste incineration, and combustion processes are significant contributors to the atmospheric deposition of zinc (Zn). In some sites where no direct metal source was reported, their transboundary wind movement might be a possible source of pollution.

Paliulis (2021) studied a strong correlation between wind speed and zinc concentration, finding that the higher the zinc concentration in moss transplants, the slower the wind speed. In addition, Srivastava et al. (2014) reported that during the three seasons—summer, monsoon, and winter—the zinc concentration in the moss was significantly higher than that of the control site. They also reported that the zinc concentration was higher towards the west at 0.5 km. The sites studied in the present

study are well-known as tourist places and for producing essential agricultural practices. The seasonal increasing zinc concentration might be due to these possible factors, and some of the previous research findings also support the present findings (Otvos et al., 2003; Srivastava et al., 2014).

The analysis conducted in the current study indicates that the level of contamination for Lead (Pb) in the year 2020 was found to be in the range of C1 and C3. The city center of Lohaghat is classified as C1, indicating that the area is free from pollution. The areas to the north, direction of Lohaghat, Pithoragarh, Ghat, and Munsiyari, south of Lohaghat, Ghat, and Munsiyari, and in the east direction of Lohaghat, Barakote, Pithoragarh, and Thal, as well as the areas in the west direction of Barakote and Thal, were classified as C3 category. This classification indicates that these sites have experienced a slight level of contamination (Table 6.7a). In 2021, most of the sites belong to the C2 category, suggesting that they are suspected of being polluted. In the north direction, Lohagaht, Pithoragarh, and Munsiyari; from the south direction, Lohaghat, and Munsiyari; in the east direction Lohaghat, Khetikhan, Barakote, Pithoragarh, and Thal and from the west Khetikhan, Barakote and Thal were classified as C3, indicating a slight high level of pollution at these locations (Table 6.7b). In 2022, all sites from the city center and south direction fall under the C2 category. It shows that this site was suspected of pollution. Only the south direction of Munsiyari falls under the C3 category. Other sites Lohaghat, Pithoragarh, Thal, and Munsiyari from the north direction, Barakote, Pithoragarh, and Thal and from the west direction Lohaghat, Khetikhan, Barakote, Thal, and Munsiyari fall under C3 category with CF in the rage of 2-3.5 that shows that it has a slight level of pollution (Table 6.7c). Lead (Pb) can also be transboundary and long-range, and summertime tourist inflow contributes to increased Pb accumulation. However, submicron aerosols are the primary form of atmospheric lead (Qarri et al., 2019). Significant sources of lead in the environment were vehicular emission and its atmospheric transport close to the study sites. Luo et al., 2015 also reported similar observations in their findings. Additionally, it was noted that anthropogenic activities like burning coal may be linked to environmental lead sources (Das, 2022).

For Copper (Cu), for most of the sites from each direction, the contamination factor values were in the range of 1-2; thus, these sites fall under the C2 category, which shows that these sites have a slight pollution level. The CF (contamination factor) in the range of 2-3.5 is observed in the city center of Pithoragarh and the areas of Ghat, Khetikhan, Barakote, and Thal from the north, east, and west directions. As a result, these sites are classified under the C3 category, indicating a slight level of pollution (Table 6.7a). During the second year (2021) city center of Champawat and Pithoragarh, the north and south directions of Khetikhan and Barakote, the east direction of Thal, and the west direction of Thal and Munsiyari with CF in the range of 2-3.5; fall under the C3 category, which shows that these sites have a slight pollution level. Rest all study sites with CF in the range of 1-2 fall under

the C2 category (Table 6.7b). In 2022, only the city centers of Thal and Munsiyari fall under the C1 category and show that these sites were unpolluted. The city centers of Pithoragarh and Ghat, the north direction of Khetikhan and Barakote, the south direction of Barakote and Thal, the East and west direction of Thal, and the west direction of Munsiyari have CF in the range of 2-3.5, which shows that the sites were in the C3 category (Table 6.7c). Copper is also considered to be a significant constituent of pesticides or fungicides often released into the environment. Copper released into the environment from various sources, such as the burning of fossil fuels, especially coal, leading to the release of copper in fly and bottom ash, as well as used motor oils, sewage, and sewage sludge, constitutes significant contributors to environmental copper contamination (Singh et al., 2017). Fireflies can be produced by burning coal and organic materials, which could increase high Cu levels in study sites. On the other hand, home waste, washing, and using kerosene oil to prevent adulteration could cause higher Cu values in the experimental sites. It was interesting to see that Eisler, (1998) conclusion that trash can also be a source of copper was supported by the high value of copper found in this study.

Regarding Cadmium (Cd), in 2020, the contamination factor values for the majority of sites in each direction ranged from 1 to 2. Consequently, these sites can be classified within the C2 category, indicating a slight level of pollution. The contamination factor (CF) ranging from 2 to 3.5 is observed in the city center of Ghat, as well as in the areas of Pithoragarh, Ghat, Thal and Munsiyari, which were located in the east direction. Consequently, these sites are categorized as C3, denoting a minor degree of pollution (Table 6.7a). In 2021, the city center, the north and south directions of Champawat, the east direction of Pithoragarh, Ghat, Thal, and Munsiyari, and the west direction of Thal all have a pollution level categorized as C3, with CF ranging from 2 to 3.5. This indicates a slight level of pollution at these sites. All study sites with a CF value between 1 and 2 are classified as belonging to the C2 category (Table 6.7b). By 2022, only the city center of Thal was classified under the C1 category, which shows that the area is unpolluted. The eastern and western directions of Khetikhan and Thal and the north direction of Thal have CFs in the range of 2 to 3.5. This indicates that these locations fall into the C3 category with a slight level of pollution (Table 6.7c). Khan et al. (2022) also reported that anthropogenic activities such as using batteries, burning fossil fuels, high-phosphate fertilizers, and burning sewage and municipal waste are potential sources of Cd in the environment. Discarded rechargeable batteries are also a source of Cd in the environment since they now constitute substantial elements of every mobile device. These batteries will be disposed of later (Recknagel et al., 2014). Cadmium is also found in households, such as in the cadmium plating of domestic refrigerator ice trays, the use of enamels containing cadmium compounds, and the utilization of cadmium pigments in the production of plastic. Individuals commonly and carelessly employ these practices for storing food items (Rahimzadeh et al., 2017).

TABLE 6.7a: Categorization of different study sites of Champawat and Pithoragarh district according to contamination factor (CF) during the year 2020

	Zinc							
	Champawat	**Lohaghat**	**Khetikhan**	**Barakote**	**Pithoragarh**	**Ghat**	**Thal**	**Munsiyari**
City Center	1.11	1.17	1.20	1.27	1.17	1.45	1.03	0.78
North	1.71	2.09	1.95	1.65	2.16	1.54	1.58	1.02
South	1.64	1.69	2.13	1.38	1.73	2.08	1.66	1.91
East	1.96	1.70	1.70	2.72	1.89	1.30	2.02	1.28
West	1.80	1.55	1.59	2.28	1.57	1.86	1.93	1.18
	Lead							
City Center	1.77	0.90	1.18	1.59	1.06	2.01	1.77	1.42
North	1.45	2.78	1.65	1.43	2.28	2.10	1.83	2.12
South	1.76	2.39	1.45	1.34	1.98	2.05	1.01	2.08
East	1.58	2.48	1.82	2.26	2.15	1.21	2.02	1.27
West	1.38	1.95	1.75	2.37	1.81	1.60	2.44	1.55
	Copper							
City Center	1.79	1.40	1.88	1.45	2.49	2.15	1.17	1.41
North	1.58	1.50	2.58	2.41	1.59	2.21	1.60	1.31
South	1.79	1.46	1.98	1.83	1.28	1.82	1.62	1.84
East	1.55	1.45	1.58	1.44	1.54	1.41	2.39	1.78
West	1.29	1.46	1.17	1.38	1.53	1.45	2.52	1.98
	Cadmium							
City Center	0.87	1.60	1.39	1.44	1.83	2.64	1.13	1.38
North	1.88	1.38	1.46	1.84	1.38	1.07	2.48	1.73
South	1.80	1.36	1.80	1.46	1.69	1.97	1.70	1.66
East	1.85	1.79	1.97	1.41	2.14	2.11	2.14	2.50
West	2.02	1.90	2.42	1.71	1.45	1.66	2.42	1.42

Contamination factor (CF) categories:
CF < 1= No contamination (C1) (Green Color); CF = 1-2 Suspected (C2) (Yellow Color); CF = 2 - 3.5 = Slight contamination (C3) (Red Color)

TABLE 6.7b: Categorization of different study sites of Champawat and Pithoragarh district according to contamination factor (CF) during the year 2021

	Zinc							
	Champawat	**Lohaghat**	**Khetikhan**	**Barakote**	**Pithoragarh**	**Ghat**	**Thal**	**Munsiyari**
City Center	1.01	1.18	1.17	1.07	1.22	1.34	0.99	1.09
North	1.78	1.96	1.91	1.64	2.00	1.58	1.57	1.52
South	1.69	1.53	1.83	1.55	1.89	2.06	2.17	3.01
East	1.84	1.55	1.61	2.38	1.95	1.39	2.30	1.83
West	1.75	1.60	1.58	2.08	1.51	1.77	2.28	1.75
	Lead							
City Center	1.52	1.18	1.16	1.57	1.10	1.69	1.48	1.27
North	1.51	2.55	1.79	1.48	2.30	1.95	1.92	2.22
South	1.80	2.00	1.68	1.32	1.92	1.96	1.33	2.30
East	1.66	2.08	2.59	2.13	2.19	1.42	2.09	1.56
West	1.33	1.69	2.27	2.24	1.77	1.41	2.53	1.86
	Copper							
City Center	2.11	1.53	1.31	1.31	2.28	1.91	1.11	1.12
North	1.21	1.47	2.24	2.36	1.44	1.93	1.62	1.62
South	1.80	1.45	2.12	2.18	1.36	1.75	1.88	1.94
East	1.63	1.51	1.50	1.50	1.44	1.39	2.51	1.81
West	1.43	1.37	1.48	1.47	1.51	1.46	2.71	2.13
	Cadmium							
City Center	2.63	1.67	1.40	1.40	1.91	2.29	1.06	1.39
North	1.19	1.50	1.68	1.68	1.66	1.21	2.44	1.71
South	1.36	1.50	1.39	1.39	1.84	1.89	1.74	1.67
East	2.98	1.29	1.44	1.44	2.13	2.06	2.07	2.43
West	2.26	1.48	1.46	1.46	1.11	1.44	2.09	1.31

Contamination factor (CF) categories:
CF < 1= No contamination (C1) (Green Color); CF = 1-2 Suspected (C2) (Yellow Color); CF = 2 - 3.5 = Slight contamination (C3) (Red Color)

TABLE 6.7c: Categorization of different study sites of Champawat and Pithoragarh district according to contamination factor (CF) during the year 2022

	Zinc							
	Champawat	**Lohaghat**	**Khetikhan**	**Barakote**	**Pithoragarh**	**Ghat**	**Thal**	**Munsiyari**
City Center	1.01	1.19	1.11	0.94	1.18	1.36	1.02	0.97
North	1.75	1.91	1.87	1.66	1.92	1.65	1.52	1.63
South	1.66	1.53	1.92	1.83	1.88	1.99	2.38	2.79
East	1.81	1.62	1.64	2.32	2.05	1.35	2.28	1.75
West	1.75	1.51	1.61	2.28	1.54	1.78	2.55	1.83
	Lead							
City Center	1.50	1.32	1.27	1.53	1.04	1.43	1.21	1.06
North	1.56	2.16	1.58	1.41	2.32	1.82	2.15	2.35
South	1.96	1.71	1.68	1.42	1.91	1.88	1.62	2.21
East	1.76	1.83	1.65	2.41	2.20	1.45	2.17	1.78
West	1.35	1.56	1.63	2.33	1.84	1.42	2.56	2.01
	Copper							
City Center	1.68	1.84	1.77	1.23	2.30	2.00	0.99	0.98
North	1.38	1.62	2.18	2.53	1.47	1.79	1.74	1.77
South	1.50	1.41	1.79	2.71	1.42	1.71	2.09	1.97
East	1.58	1.52	1.41	1.54	1.40	1.39	2.27	1.95
West	1.30	1.41	1.32	1.62	1.48	1.45	2.79	2.31
	Cadmium							
City Center	2.29	1.65	1.10	1.23	1.47	1.51	0.87	1.15
North	1.34	1.72	1.54	1.56	1.48	1.66	2.55	1.52
South	1.55	1.34	1.81	1.43	1.70	1.29	1.84	1.69
East	1.14	1.26	2.23	1.43	1.60	1.65	2.19	2.16
West	1.24	1.42	2.72	1.50	1.17	1.34	2.09	1.48

Contamination factor (CF) categories:
CF < 1= No contamination (C1) (Green Color); CF = 1-2 Suspected (Yellow Color); CF = 2 - 3.5 = Slight contamination (C3) (Red Color)

Chapter 7: SUMMARY AND CONCLUSION

Metals are considered an essential part of the Earth's geochemical systems; thus, nature is a primary source of metals in the atmosphere. Metals are ubiquitous in the environment, with differing concentrations in parent rock, soil, water, air, and all biological matter. With increased industrial and urban growth, various metals, such as zinc, arsenic, lead, cadmium, and others, seriously threaten the ecosystem and lead to heavy metal pollution. Different organisms are being explored for research to assess air, water, and soil conditions as biomonitors. Biomonitors like mosses are extensively utilized to estimate atmospheric aerosols and are considered bioindicators of air pollution.

The present investigation explores the capabilities of *Thudium cyambifolium* as a biomonitor for monitoring the atmospheric metal deposition across various directions in the Champawat (29.2783° N, 80.0535° E) and Pithoragarh districts (30.085° N 80.03659° E) of Uttarakhand state of India. The whole work has been conceived into four major parts: ecological study, physiological tolerance study, taxonomic study for identification, and biomonitoring study for heavy metal accumulation.

Before introducing the moss species for the biomonitoring study, the study area was surveyed thoroughly. Sample collection was done as per the protocol of ICP vegetation. During sample collection, Growing moss was collected from the forest core and treated as a control because the forest core is least affected by anthropogenic activity and, therefore, least affected by contamination.

A thorough sampling of 45 moss genera from 18 families was conducted at various collection sites in Mayawati and Kranteshwar in the Champawat Chandak and Thalkedar districts of Pithoragarh. This study aimed to illustrate these diverse mosses occurrence and distributional pattern. During the study, Thalkedar reported a maximum of 35 species of mosses, followed by Kranteshwar (31 species), Chandak (29 species), and Mayawati (26 species). Significantly, four mosses, namely *Thuidium cyambifolium, Rhynchostegiella divericatifolia, Fissidens anomalus,* and *Isopterygium elegens*, were identified as the most abundant species in all four control sites and selected for their tolerance activity against metals.

As mentioned earlier, to assess the tolerance of mosses against heavy metals (Zinc, Lead, Copper, and Cadmium), their physiological response to chlorophyll and total chlorophyll content, nitrate reductase enzyme activity, and peroxidase enzyme activity were analyzed.

A minimal decrease in total chlorophyll content was reported in *T. cyambifolium* compared to other studied mosses—except for *R. divericatifolia*, which exhibited the second-highest tolerance to copper. It may be concluded that the deposition of heavy metals, including Cd, Cu, Zn, and Pb, in mosses leads to stress and reduction of chlorophyll.

The nitrate reductase activity of the examined mosses against the Zn, Cu, Pb, and Cd was in order of *T. cyambifolium> R. divericatifolia> F. anomalus> I. elegens.* Compared to *T. cyambifolium*, the other three mosses showed a significant decrease in NR activity when exposed to heavy metal treatments.

During this study, it was noted that Cd, Zn, Cu, and Pb treatments generally suppress POD activity in moss plants, with the effect becoming more pronounced over time, except for the unique response seen in *T. cyambifolium.* POD activity was found to be decreased consistently as observations were taken on the third, sixth, and fifteenth days. It was also observed that firstly, the value increased, then it started to decrease. The rise in enzyme activity may be a protective mechanism against excessive peroxide generation when exposed to low concentrations of heavy metals. The peroxidase activity of the examined mosses against the Zn, Cu, Pb, and Cd was in order of *T. cyambifolium> R. divericatifolia> F. anomalus> I. elegens.*

The moss *Thuidium cyambifolium* was introduced to monitor atmospheric heavy metal contamination and was subsequently used in a biomonitoring study involving moss bag transplantation. Each season, three sets of moss bags were strategically positioned at various research locations to examine their accumulation of heavy metals.

The moss was collected over three consecutive years in winter, summer, and rainy seasons. The present investigation examined the accumulation of Zinc, Copper, Lead, and Cadmium in eight distinct study sites in the Champawat and Pithoragarh districts.

Moss bags containing *T. cymbifolium* were transplanted at nearly equal heights to cover different sites, varying in direction and seasonal placement, to analyze the accumulation of heavy metals in the moss. After the end of the season, the transplanted bags were collected and subjected to acid digestion to extract the metals using the atomic absorption spectrophotometer (AAS).

Direction-wise, different sites of Campawat and Pithoragarh district were studied for metal accumulation, i.e., Zinc, Lead, Copper, and Cadmium, seasonally during the study period (i.e., 2020 to 2022). Various locations, such as the City center, East, North, South, and West directions in

Chamapawat, Lohagat, Khetikhan, and Barakote regions of Champawat district, as well as similar direction sites of Pithogarh, Ghat, Thal, and Munsiyari in Pithoragarh district, were investigated for the existence of specific heavy metals accumulation.

The study compared the results of various sampling stations in Champawat district and Pithoragarh to the baseline levels of Zn, Cu, Pb, and Cd in different seasons. It was discovered that the highest accumulation of these heavy metals occurred during the summer season, followed by the winter season. The lowest accumulation was observed during the rainy season at all study sites.

The concentrations of these heavy metals exhibited considerable variation and outliers in decreasing order across the three seasons: summer, winter, and rain. Summer exhibited the highest accumulation of Zinc (1.972 mg/g) from the east direction of Pithorgarh and the south direction of Khetikhan, compared to the other two seasons (1.854 mg/g). Simultaneously, the winter and rainy seasons exhibited the lowest zinc accumulation (0.400 mg/g and 0.555 mg/g) measured from the city center of Thal and Champawat. The recorded levels of Pb contamination in Champawat and Pithoragarh districts were 1.767 mg/g and 1.728 mg/g as measured from the east direction of Thal and the north direction of Lohaghat during the summer, rainy, and winter seasons, respectively. Copper metal accumulation was minimal during the rainy season from the east direction of Ghat (0.463 mg/g) and from the west direction of Khetikhan (0.380 mg/g). Cadmium showed remarkable differences in accumulation compared to the other three studied metals in the summer, winter, and rainy seasons. Maximum accumulation from the north direction from the Thal and minimum accumulation from the north direction from the Ghat of district Pithoragarh were reported.

The findings from this study lead to the following conclusions:

- Oxidative stress parameters are essential biomarkers of environmental pollution and indicate plant tolerance.
- Mosses can accumulate pollutants over a long period, which makes them a promising and cost-effective alternative for conducting long-term atmospheric research.
- Seasonal monitoring has shown that air pollution, climatic factors, topography, and other environmental stress have had a negative impact on the moss species by decreasing physiological parameters and biochemical activities.
- The concentration of each metal accumulated in moss varied significantly throughout different seasons. Zn and Pb were recorded at their maximum in all the seasons, and sites in the Pithoragarh and Champawat region could be due to the proximity of the road or town of

the study area. At the same time, Cu and Cd exhibited a high concentration from the sites dominant with agricultural practices.

- The findings revealed that, despite limited industrialization, the metal concentration rises, raising concerns regarding the urban metal load at various catchment sites in both hilly districts. The current study discovered that vehicle exhaust emissions are a substantial contributor in densely populated urban areas, where the majority of vehicles and generators are primarily responsible for pollution.
- Compared to other locations, the areas to the east and north of Pithoragarh, as well as the south direction of Khetikhan and Barakote, experienced high annual accumulations of zinc (Zn) and copper (Cu). The presence of high levels of Zn and Cu in this area could be related to the extensive agricultural practices, where the use of pesticides and fertilizers may contribute to the accumulation of these elements.
- The city center of Ghat, the northern direction of Pithoragarh from district Pithoragarh and west of Khetikhan, the north direction in Lohaghat from Champawat district exhibited significant levels of lead (Pb) and cadmium (Cd) contamination. This could be attributed to the fact that these locations serve as significant commercial hubs and popular tourist destinations, resulting in a substantial concentration of vehicles and a high level of pollution. Automobiles, specifically buses, cars, and other motor vehicles, serve as the sole means of transportation for tourists and goods, linking the foothills to these regions.
- Microclimatic and microenvironmental factors profoundly impact mosses due to their lack of cuticle, thin epidermis, and ability to actively absorb substances from their surface. These factors significantly affect the amount and rate at which mosses take up metals from precipitation. Current research indicates that Mosses serve as long-term integrators of atmospheric metal accumulation. The current study initially investigates metal precipitation by moss and confirms the function of moss *T. cymbifolium* as an effective biomonitor.
- The unique feature of this study is that it provides data on atmospheric deposition in the Champawat and Pithoragarh districts, which is currently lacking in this particular area of the research. Hence, this discovery addresses a knowledge gap.

Based on the present work, moss *T. cymbifolium* is strongly recommended as an excellent biomonitor or accumulator of metal precipitations. The increase in metal in moss is alarming, and the study will help policymakers prepare mitigation strategies and keep the environment clean.

There is a growing need for effective and dependable techniques for monitoring heavy metal contamination to safeguard our environment and public health. One innovative and ecologically sensitive approach that has garnered increasing attention is using bryophytes, a diverse group of non-vascular plants encompassing mosses as bioindicators for heavy metal contamination.

Variation of metal accumulation level and degree of contamination in different study sites of district Champawat and Pithoragarh regarding contamination factors was also studied. During three consecutive years, For Zinc, the city center of Munsiyari and the city center of Thal were reported under the C1 category with CF > 1, showing that this site were recorded as unpolluted during the course of the study. The areas north of Lohaghat and Pithoragarh, south of Khetikhan and Ghat, and east of Barakote and Thal, along with the east and west directions of Barakote, fall under the C3 category. The contamination factor (CF) in these regions ranges from 2 to 3.5, indicating slight pollution.

The city center of Lohaghat is classified as C1, indicating that the area is free from Pb pollution. The areas to the north, direction of Lohaghat, Pithoragarh, Ghat, and Munsiyari, south of Lohaghat, Ghat, and Munsiyari, and in the east direction of Lohaghat, Barakote, Pithoragarh, and Thal, as well as the areas in the west direction of Barakote and Thal, were classified as C3 category showing that these sites had slight Pb pollution.

With reference to Cu, the CF (contamination factor) in the range of 2-3.5 is observed in the city centers of Pithoragarh and Ghat, Khetikhan, Barakote, and Thal from the north, east, and west directions. As a result, these sites were classified under the C3 category, indicating a slight level of pollution. The city centers of Thal and Munsiyari fall under the C1 category and show that they were unpolluted with Copper.

Regarding Cadmium (Cd), the contamination factor values for most sites in each direction ranged from 1 to 2. Consequently, these sites can be classified within the C2 category, indicating a slight pollution level. The contamination factor (CF) ranging from 2 to 3.5 is observed in the city center of Ghat and in the areas of Pithoragarh, Ghat, Thal, and Munsiyari, which were located in the east direction. Consequently, these sites are categorized as C3, denoting a minor degree of pollution, which shows that the area is unpolluted. The eastern and western directions of Khetikhan and Thal and the north direction of Thal have CFs in the range of 2 to 3.5. This indicates that these locations fall into the C3 category with a slight level of pollution

The present study's outcome emphasized the origins of pollution and the degree of contamination in the Champawat and Pithoragarh districts. It has been noted that, despite limited industrialization, there is a rise in metal concentration. This has raised concerns regarding the increasing metal load in urban areas throughout several district catchment sites. The current study revealed that the tourist inflow significantly contributes to air pollution in densely populated urban areas, where many vehicles and generators release considerable pollutants.

The present study recommends using the moss *T. cyambifolium* as a reliable biomonitor or accumulator of metal precipitation. The significant increase in metal accumulation in moss from study sites is alarming, and this investigation will help policymakers develop strategies to mitigate the problem and enhance environmental purity. Furthermore, it is highly recommended that biomapping studies be carried out in other hill stations to anticipate forthcoming levels of pollution from heavy metals. This data will aid in managing tourist activity, monitoring current traffic levels, facilitating modernization efforts, and promoting industrialization.

BIBLIOGRAPHY

Abas, A. (2021). A systematic review on biomonitoring using lichen as the biological indicator: A decade of practices, progress and challenges. *Ecological Indicators*, *121*, 107197.

Adachi, K., & Tainosho, Y. (2004). Characterization of heavy metal particles embedded in tire dust. *Environment International*, *30*(8), 1009-1017.

Adnan, M., Xiao, B., Xiao, P., Zhao, P., Li, R., & Bibi, S. (2022). Research progress on heavy metals pollution in the soil of smelting sites in China. *Toxics*, *10*(5), 231.

Agarwal, A., Satsangi, A., Lakhani, A., & Kumari, K. M. (2020). Seasonal and spatial variability of secondary inorganic aerosols in PM2.5 at Agra: Source apportionment through receptor models. *Chemosphere*, *242*, 125132.

Agnan, Y., Probst, A., & Sejalon-Delmas, N. (2017). Evaluation of lichen species resistance to atmospheric metal pollution by coupling diversity and bioaccumulation approaches: A new bioindication scale for French forested areas. *Ecological Indicators*, *72*, 99-110.

Al-Mutairi, A., Smallbone, A., Al-Salem, S. M., & Roskilly, A. P. (2017). The first carbon atlas of the state of Kuwait. *Energy*.

Amundsen, C. E., Almaas, A., & Singh, B. R. (2000). Cadmium in soil, soil solution and plants. Data as basis for risk assessment of Cd in mineral fertilisers. *Report-Jordforsk*.

Ares, A., Fernandez, J. A., Aboal, J. R., & Carballeira, A. (2011). Study of the air quality in industrial areas of Santa Cruz de Tenerife (Spain) by active biomonitoring with *Pseudoscleropodium purum*. *Ecotoxicology and environmental safety*, *74*(3), 533-541.

Ares, A., Aboal, J. R., Carballeira, A., Giordano, S., Adamo, P., & Fernández, J. A. (2012). Moss bag biomonitoring: a methodological review. *Science of the Total Environment*, *432*, 143-158.

Ares, A., Varela, Z., Aboal, J. R., Carballeira, A., & Fernández, J. A. (2015). Active biomonitoring with the moss Pseudoscleropodium purum: comparison between different types of transplants and bulk deposition. Ecotoxicology and environmental safety, 120, 74-79.

Ascaso, C. & Galvan, J. (1976). The ultrastructure of the symbionts of *Rhizocarpon geographicum, Parmelia conspersa* and *Vmbilicaria pustulat*a growing under dryness conditions. *Protoplasma 87:* 409-418

Aydogan, s., Erdag, B., & Aktaş, L. (2017). Bioaccumulation and oxidative stress impact of Pb, Ni, Cu, and Cr heavy metals in two bryophyte species, *Pleurochaete squarrosa* and *Timmiella barbuloides*. *Turkish Journal of Botany*, *41*(5), 464-475.

Backor, M., Goga, M., Rucova, D., Urminska, D., Backorova, M., & Klejdus, B. (2023). Allelopathic effects of three lichen secondary metabolites on cultures of apo symbiotically grown lichen photobionts and free-living alga *Scenedesmus quadricauda*. *South African Journal of Botany*, *162*, 688-693.

Badamasi, H. (2017). Biomonitoring of air pollution using plants. *MAYFEB Journal of Environmental Science*, *2*.

Bajpai, R., Upreti, D. K., Dwivedi, S. K., & Nayaka, S. (2009). Lichen as quantitative biomonitors of atmospheric heavy metals deposition in Central India. *Journal of atmospheric chemistry*, *63*, 235-246.

Bansal, P., Verma, S., & Srivastava, A. (2016). Biomonitoring of air pollution using antioxidative enzyme system in two genera of family Pottiaceae (Bryophyta). *Environmental Pollution*, *216*, 512-518.

Bansal, P., Joshi, Y., & Sharma, R. A. (2024). Physiological responses shown by the apical (green) and basal (brown) leaves of seven taxa of moss family Pottiaceae (Bryophyta): A comparative study from India. *Vegetos*, 1-10.

Barenyi, B., & Krause, G. H. (1985). Inhibition of photosynthetic reactions by light: A study with isolated spinach chloroplasts. *Planta*, *163*(2), 218-226.

Bargagli, R. (2016). Moss and lichen biomonitoring of atmospheric mercury: a review. *Science of the Total Environment*, *572*, 216-231.

Barukial, J., & Hazarika, P. (2023). Bryophytes as an accumulator of toxic elements from the environment: recent advances. *Bioactive Compounds in Bryophytes and Pteridophytes*, 165-182.

Basha, S., Jhala, J., Thorat, R., Goel, S., Trivedi, R., Shah, K., Menon, G., Gaur, P. S., Mody, K. H. & Jha, B. (2010). Assessment of heavy metal content in suspended particulate matter of coastal industrial town, Mithapur, Gujarat, India. *Atmospheric Research*, *97*(1-2), 257-265.

Benitez, Á., Armijos, L., & Calva, J. (2021). Monitoring air quality with transplanted bryophytes in a neotropical Andean city. Life, 11(8), 821.

Berg, T., Royset, O., & Steinnes, E. (1995). Moss (*Hylocomium splendens*) used as biomonitor of atmospheric trace element deposition: estimation of uptake efficiencies. *Atmospheric Environment*, *29*(3), 353-360.

Brown, D. H., & Bates, J. W. (1990). Bryophytes and nutrient cycling. *Botanical Journal of the Linnean Society*, *104*(1-3), 129-147.

Bian, Z., Wang, Y., Zhang, X., Li, T., Grundy, S., Yang, Q., & Cheng, R. (2020). A review of environment effects on nitrate accumulation in leafy vegetables grown in controlled environments. *Foods*, *9*(6), 732.

Budke, J. M., & Goffinet, B. (2016). Comparative cuticle development reveals taller sporophytes are covered by thicker calyptra cuticles in mosses. *Frontiers in plant science*, *7*, 832.

Cabral, J. P. (2003). Copper toxicity in five *Parmelia* lichen in vitro. *Environ. Exp. Bot*. *49:* 237-250.

Carginale, V., Sorbo, S., Capasso, C., Trinchella, F., Cafiero, G., & Basile, A. (2004). Accumulation, localisation, and toxic effects of cadmium in the liverwort *Lunularia cruciata*. *Protoplasma*, *223*, 53-61.

Cesa, M., Baldisseri, A., Bertolini, G., Dainese, E., Dal Col, M., Dalla Vecchia, U., Marchesini P. & Nimis, P. L. (2013). Implementation of an active 'bryomonitoring' network for chemical status and temporal trend assessment under the Water Framework Directive in the Chiampo Valley's tannery district (NE Italy). *Journal of Environmental Management, 114,* 303-315.

Chakrabortty, S., & Paratkar, G. T. (2006). Biomonitoring of trace element air pollution using mosses. *Aerosol and air quality research*, *6*(3), 247-258.

Chandra, S., Kulshrestha, M. J., & Singh, R. (2014). Temporal variation and concentration weighted trajectory analysis of lead in PM10 aerosols at a site in Central Delhi, India. *International Journal of Atmospheric Sciences*, *2014*(1), 323040.

Chaturvedi, P., Singh, S., & Rathore, K. S. (2023). Multivariant Assessment of Metals Using Liverworts as an Appealing Tool in Catchment Sites of Uttarakhand, India. *Nature Environment and Pollution Technology*, *22*(4), 1921-1930.

Chaudhuri, S., & Roy, M. (2024). Global ambient air quality monitoring: Can mosses help? A systematic meta-analysis of literature about passive moss biomonitoring. *Environment, Development and Sustainability*, *26*(3), 5735-5773.

Chettri, M. K., Cook, C. M., Vardaka, E., Sawidis, T., & Lanaras, T. (1998). The effect of Cu, Zn and Pb on the chlorophyll content of the lichens *Cladonia convoluta* and *Cladonia rangiformis*. *Environmental and experimental botany*, *39*(1), 1-10.

Chmielowska-Bąk, J., & Deckert, J. (2021). Plant recovery after metal stress—A review. *Plants*, *10*(3), 450.

Chrysargyris, A., Maggini, R., Incrocci, L., Pardossi, A., & Tzortzakis, N. (2021). Copper Tolerance and Accumulation on Pelargonium graveolens L'Hér. Grown in Hydroponic Culture. Plants 2021, 10, 1663.

Cimboláková, I., Uher, I., Laktičová, K. V., Vargová, M., Kimáková, T., & Papajová, I. (2020). Heavy metals and the environment. *Environ. Factors Affect. Hum. Heal*, *10*.

Conti, M. E. (2008). Environmental biological monitoring. *WIT Transactions on State-of-the-art in Science and Engineering*, 30.

Cuny, D. (2012). Air pollution biomonitoring with plants and fungi: concepts and uses. In *Annales Pharmaceutiques Françaises* (Vol. 70, No. 4, pp. 182-187).

Dalupang, X. P. P., Matias, H. A. N., Rivera, M. L. D., & Viz, J. A. (2023). Biomonitoring of Atmospheric Lead (Pb) Pollutants Using Sphagnum Moss in Bantay, Ilocos Sur, Philippines. *Philippine Journal of Science*, 152.

De Nicola, F., Murena, F., Costagliola, M. A., Alfani, A., Baldantoni, D., Prati, M. V., Sessa, L., Spagnuolo, V., & Giordano, S. (2013). A multi-approach monitoring of particulate matter,

metals and PAHs in an urban street canyon. *Environmental Science and Pollution Research*, *20*, 4969-4979.

De Oliveira, R. H., Carneiro, C. D. C., De Almeida, F. G. V., de Oliveira, B. M., Nunes, E. H. M., & dos Santos, Chaturved A. S. (2019). Multivariate air pollution classification in urban areas using mobile sensors and self-organizing maps. *International Journal of Environmental Science and Technology*, *16*(10), 5475-5488.

Decker, E. L., & Reski, R. (2020). Mosses in biotechnology. *Current opinion in biotechnology*, *61*, 21-27.

Demirevska-Kepova, K., Simova-Stoilova, L., Stoyanova, Z., Hölzer, R., & Feller, U. (2004). Biochemical changes in barley plants after excessive supply of copper and manganese. *Environmental and Experimental Botany*, *52*(3), 253-266.

Ding, C., Yang, Q., Zhao, X., Xu, L., Tang, H., Liu, Z., Zhai, J., & Zhang, Q. (2024). A review of 210Pb and 210Po in moss. *Journal of Environmental Radioactivity*, *276*, 107448.

Dołęgowska, S., & Migaszewski, Z. M. (2014). terrestrial mosses as trace element bioindicators: a review. *classification, development and growth and functional role in ecosystems*, 25-69.

Dollery, R., Bowie, M. H., & Dickinson, N. M. (2022). The ecological importance of moss ground cover in dry shrubland restoration within an irrigated agricultural landscape matrix. *Ecology and Evolution*, *12*(4), e8843.

Eisler, R. (1998). *Copper hazards to fish, wildlife, and invertebrates: a synoptic review* (No. 33). US Department of the Interior, US Geological Survey.

El Morabet, R. (2019). Effects of outdoor air pollution on human health.

Eldridge, D. J., Guirado, E., Reich, P. B., Ochoa-Hueso, R., et al. (2023). The global contribution of soil mosses to ecosystem services. *Nature Geoscience*, *16*(5), 430-438.

Elstner, E. F., & Osswald, W. (1994). Mechanisms of oxygen activation during plant stress. *Proceedings of the Royal Society of Edinburgh, Section B: Biological Sciences*, *102*, 131-154.

Fatoba, P. O., & Udoh, E. G. (2008). Effects of some heavy metals on chlorophyll accumulation

in *Barbula lambarenensis*. *Ethnobotanical leaflets*, *2008*(1), 107.

Faus-Kessler, T., Dietl, C., Tritschler, J., & Peichl, L. (1999). Temporal and spatial trends of metal contents of Bavarian mosses Hypnum cupressiforme. *Science of the total environment*, *232*(1-2), 13-25.

Fernandez, J. A. and Carballeria, A. (2002). Biomonitoring metal deposition in Glacia (NW Spain) with mosses: factors affecting bioconcentration. *Chemosphere*. *46*: 535-542.

Fernández, J. A., Real, C., Couto, J. A., Aboal, J. R., & Carballeira, A. (2005). The effect of sampling design on extensive bryomonitoring surveys of air pollution. *Science of the total environment*, *337*(1-3), 11-21.

Filova, A., Fargasova, A., & Molnárová, M. (2021). Cu, Ni, and Zn effects on basic physiological and stress parameters of *Raphidocelis subcapitata* algae. *Environmental Science and Pollution Research*, *28*(41), 58426-58441.

Flegal, A. R., Gallon, C., Hibdon, S., Kuspa, Z. E., & Laporte, L. F. (2010). Declining-but Persistent-Atmospheric Contamination in Central California from the Resuspension of Historic Leaded Gasoline Emissions as Recorded in the Lace Lichen (*Ramalina menziesii* Taylor) from 1892 to 2006. *Environmental science & technology*, *44*(14), 5613–5618.

Frati, L., & Brunialti, G. (2023). Recent trends and future challenges for lichen biomonitoring in forests. *Forests*, *14*(3), 647.

Frontasyeva, M., Harmens, H., Uzhinskiy, A., & Chaligava, O. (2020). *Mosses as biomonitors of air pollution: 2015/2016 survey on heavy metals, nitrogen and POPs in Europe and beyond* (Doctoral dissertation, PatriNat (OFB-CNRS-MNHN)).

Gahtori, D., Singh, J., & Vyas, A. (2024). Assessment of atmospheric metal deposition by moss Thuidium cymbifolium (Dozy & Molk.) Dozy & Molk. At Champawat Hills, India. *Vegetos*, 1-13.

Gao, G., Zeng, H., & Zhou, Q. (2022). Biomonitoring atmospheric pollution of polycyclic aromatic hydrocarbons using mosses. *Atmosphere*, *14*(1), 26.

Gautam, A. S., Kumar, S., Gautam, S., Ram, K., Siingh, D., Ambade, B., & Sharma, M. (2021). Regional Air Quality: Forest Fires Impacts of SO_2 Emissions on Air Pollutants in the Himalayan Region of Uttarakhand, India.

Ghorani-Azam, A., Riahi-Zanjani, B., & Balali-Mood, M. (2016). Effects of air pollution on human health and practical measures for prevention in Iran. *Journal of research in medical sciences: the official journal of Isfahan University of Medical Sciences*, *21*.

Giordano, S., Admo, P., Sorbo, S. and Vingiani, S. (2005). Atmospheric trace metal pollution in the Naples urban area based on results from moss and lichen bags. *Environ. Pollut. 136*: 431-442.

Gorelova, S. V., & Frontasyeva, M. V. (2017). The use of higher plants in biomonitoring and environmental bioremediation. *Phytoremediation: Management of Environmental Contaminants, Volume 5*, 103-155.

Gou, T., Yang, L., Hu, W., Chen, X., Zhu, Y., Guo, J., & Gong, H. (2020). Silicon improves the growth of cucumber under excess nitrate stress by enhancing nitrogen assimilation and chlorophyll synthesis. *Plant physiology and biochemistry*, *152*, 53-61.

Gouia, H., Ghorbal, M. H., & Meyer, C. (2000). Effects of cadmium on activity of nitrate reductase and on other enzymes of the nitrate assimilation pathway in bean. *Plant Physiology and Biochemistry*, *38*(7-8), 629-638.

Goyal, P. (2003). Present scenario of air quality in Delhi: a case study of CNG implementation. *Atmospheric Environment*, *37*(38), 5423-5431.

Grodzinska, K., Szarek-Lukaszewska, G., & Godzik, B. (1999). Survey of heavy metal deposition in Poland using mosses as indicators. *Science of the Total Environment*, *229*(1-2), 41-51.

Grodzińska, K., Frontasyeva, M., Szarek-Łukaszewska, G., Klich, M., Kucharska-Fabiś, A., Gundorina, S. F., & Ostrovnaya, T. M. (2003). Trace element contamination in industrial regions of Poland studied by moss monitoring. *Environmental Monitoring and Assessment*, *87*, 255-270.

Gupta, A. (1995). Heavy metal accumulation by three species of mosses in Shillong, North-Eastern India. *Water, Air, and Soil Pollution*, *82*, 751-756.

Gurjar, B. R. (2021). Air pollution in India: Major issues and challenges. *Energy Future, Magzter*.

Guttikunda, S. K., & Mohan, D. (2014). Re-fueling road transport for better air quality in India. *Energy Policy*, *68*, 556-561.

Hajek, M., Pleskova, Z., Syrovatka, V., Peterka, T., Laburdova, J., Kintrova, K., Jirousek M., & Hájek, T. (2014). Patterns in moss element concentrations in fens across species, habitats, and regions. *Perspectives in Plant Ecology, Evolution and Systematics*, *16*(5), 203-218.

Harmens, H., Norris, D., & Mills, G. (2013). *Heavy metals and nitrogen in mosses: spatial patterns in 2010/2011 and long-term temporal trends in Europe*. NERC/Centre for Ecology & Hydrology.

Hasanuzzaman, M., Bhuyan, M. B., Zulfiqar, F., Raza, A., Mohsin, S. M., Mahmud, J. A., Fujita, M. & Fotopoulos, V. (2020). Reactive oxygen species and antioxidant defense in plants under abiotic stress: Revisiting the crucial role of a universal defense regulator. *Antioxidants*, *9*(8), 681.

Hassan, M. J., Ali Raza, M., Ur Rehman, S., Ansar, M., Gitari, H., Khan, I., Wajid, M., Ahmed, M., Shah, G. A., Peng, Y., & Li, Z. (2020). Effect of cadmium toxicity on growth, oxidative damage, antioxidant defence system and cadmium accumulation in two sorghum cultivars. *Plants*, *9*(11), 1575.

Heindel, R. C., Putman, A. L., Murphy, S. F., Repert, D. A., & Hinckley, E. L. (2020). Atmospheric dust deposition varies by season and elevation in the Colorado Front Range, USA—Journal of Geophysical Research: Earth Surface, 125(5), e2019JF005436.

Herpin. U., Berlekamp, B., Markert, B., Wolterbeek, B., Grodzinska, K., Siewers, U., Lieth, H. and Weekert, V. (1996). The distribution of heavy metals in a transect of the three states Netherlands, Germany and Poland, determined with the aid of moss monitoring. *Sci. Tot. Environ*. *187*: 185-198.

Herrmann, R. (1990). Biomonitoring of organic and inorganic trace pollutants by means of mosses. *Bryophytes. Their chemistry and chemical taxonomy. Proceedings of the Phytochemical Society of Europe*, *29*, 319-333.

Hiscox, J. D., & Israelstam, G. F. (1979). A method for the extraction of chlorophyll from leaf tissue without maceration. *Canadian journal of botany*, *57*(12), 1332-1334.

Hodson, M. E. (2004). Heavy metals—geochemical bogey men?. *Environmental Pollution*, *129*(3), 341-343.

Hu, Y., You, J., & Liang, X. (2015). Nitrate reductase-mediated nitric oxide production is involved in copper tolerance in shoots of hulless barley. *Plant cell reports*, *34*, 367-379.

Hu, R., Yan, Y., Zhou, X., Wang, Y., & Fang, Y. (2018). Monitoring heavy metal contents with *Sphagnum junghuhnianum* moss bags in relation to traffic volume in Wuxi, China. *International journal of environmental research and public health*, *15*(2), 374.

Hussain, S., Khaliq, A., Noor, M. A., Tanveer, M., Hussain, H. A., Hussain, S., Shah T. & Mehmood, T. (2020). Metal toxicity and nitrogen metabolism in plants: an overview. *Carbon and nitrogen cycling in soil*, 221-248.

Isaza, D. F. G., Cramp, R. L., & Franklin, C. E. (2020). Living in polluted waters: A meta-analysis of the effects of nitrate and interactions with other environmental stressors on freshwater taxa. *Environmental Pollution*, *261*, 114091.

Jafarova, M., Grifoni, L., Aherne, J., & Loppi, S. (2023). Comparison of lichens and mosses as biomonitors of airborne microplastics. *Atmosphere*, *14*(6), 1007.

Jayasri, M. A., & Suthindhiran, K. (2017). Effect of zinc and lead on the physiological and biochemical properties of aquatic plant Lemna minor: its potential role in phytoremediation. *Applied Water Science*, *7*, 1247-1253.

Jiang Y, Liu X, Tian R, Shao X. Field-sampling methods for investigating ground-bryophyte populations in forest vegetation. Pol J Ecol. 2011;59(2):317-27.

Jiang, T., Yang, X., Zhong, Y., Tang, Q., Liu, Y., & Su, Z. (2018). Species composition and diversity of ground bryophytes across a forest edge-to-interior gradient. *Scientific Reports*, *8*(1), 11868.

Jiang, Y., Fan, M., Hu, R., Zhao, J., & Wu, Y. (2018). Mosses are better than leaves of vascular plants in monitoring atmospheric heavy metal pollution in urban areas. *International journal of environmental research and public health*, *15*(6), 1105.

Jiang, Y., Zhang, X., Hu, R., Zhao, J., Fan, M., Shaaban, M., & Wu, Y. (2020). Urban atmospheric environment quality assessment by naturally growing bryophytes in Central China. *International journal of environmental research and public health*, *17*(12), 4537.

Joshi, N. (2021). Caught Between a Rock and a Hard Place. *Mountain Research and Development*, *41*(1), R13-R21.

Joshi, S., & Afroz, A. (2023). Bryomonitoring of atmospheric elements in Sphagnum sp. commonly growing bryophyte in the Indian Himalayan region of Uttarakhand. *Nova Geodesia*, *3*(2), 127-127.

Jozwiak, M., & Jozwiak, M. (2009). Influence of cement industry on accumulation of heavy metals in bioindicators. *Ecol chem Eng*, *16*(3), 323-34.

Kapusta, P., Stanek, M., Szarek-Łukaszewska, G., & Godzik, B. (2019). Long-term moss monitoring of atmospheric deposition near a large steelworks reveals the growing importance of local non-industrial sources of pollution. *Chemosphere, 230*, 29-39.

Khan, Z., Elahi, A., Bukhari, D. A., & Rehman, A. (2022). Cadmium sources, toxicity, resistance and removal by microorganisms-A potential strategy for cadmium eradication. *Journal of Saudi Chemical Society*, *26*(6), 101569.

Klos, A., Rajfur, M., Wacławek, M., & Wacławek, W. (2009). Impact of roadway particulate matter on deposition of pollutants in the vicinity of main roads. *Environ Prot Eng, 3*, 105-121.

Korzeniowska, J., & Panek, E. (2012). The Content of Trace Metals (Cd, Cr, Cu, Ni, Pb, Zn) in Selected Plant Species (Moss *Pleurozium Schreberi,* Dandelion *Taraxacum Officianale*, Spruce *Picea Abies*) along the Road Cracow–Zakopane. *Geomatics and Environmental Engineering*, *6*(1), 43-50.

Kosior, G., Frontasyeva, M., Ziembik, Z., Zincovscaia, I., Dolhanczuk-Srodka, A., & Godzik, B.

(2020). The moss biomonitoring method and neutron activation analysis in assessing pollution by trace elements in selected Polish national parks. *Archives of environmental contamination and toxicology*, *79*, 310-320.

Kumar, P., Patel, A., Rai, J., & Kumar, P. (2023). Environmental Challenges and Concurrent Trend of Weather Extremes over Uttarakhand Himalaya. 10.1007/s00704-023-04690-z

Kumar, V., Pandita, S., Sidhu, G. P. S., Sharma, A., Khanna, K., Kaur, P., Bali, A. S. & Setia, R. (2021). Copper bioavailability, uptake, toxicity and tolerance in plants: A comprehensive review. *Chemosphere*, *262*, 127810.

Kuttippurath, J., Patel, V. K., Pathak, M., & Singh, A. (2022). Improvements in SO2 pollution in India: role of technology and environmental regulations. *Environmental Science and Pollution Research*, *29*(52), 78637-78649.

Laidlaw, M. A., Zahran, S., Mielke, H. W., Taylor, M. P., & Filippelli, G. M. (2012). Re-suspension of lead contaminated urban soil as a dominant source of atmospheric lead in Birmingham, Chicago, Detroit and Pittsburgh, USA. *Atmospheric environment*, *49*, 302-310.

Lazo, P., Kika, A., Qarri, F., Bekteshi, L., Allajbeu, S., Stafilov, T. (2022). Air quality assessment by moss biomonitoring and trace metals atmospheric deposition. *Aerosol Air Qual. Res.* 22, 220008.

Lepneva, O. M., Sluka, Z. A., Abramova, L. I., & Obukhov, A. I. (1987, January). Mosses as bioindicators of heavy metal pollution of the urban environment. In *Nauchnye Doklady Vysshei Shkoly. Biologicheskie Nauki* (No. 8, pp. 87-91).

Li, L., Zheng, B., & Liu, L. (2010). Biomonitoring and bioindicators used for river ecosystems: definitions, approaches and trends. *Procedia environmental sciences*, *2*, 1510-1524.

Limo, J., Paturi, P., & Makinen, J. (2018). Magnetic biomonitoring with moss bags to assess stop-and-go traffic induced particulate matter and heavy metal concentrations. *Atmospheric Environment*, *195*, 187-195.

Lopez-Luna, J., Gonzalez-Chavez, M. C., Esparza-Garcia, F. J., & Rodriguez-Vazquez, R. (2012). Fractionation and availability of heavy metals in tannery sludge-amended soil and toxicity

assessment on the fully–grown Phaseolus vulgaris cultivars. *Journal of Environmental Science and Health, Part A*, *47*(3), 405-419.

Luna, C. M., Casano, L. M., & Trippi, V. S. (2000). Inhibition of wheat nitrate reductase activity by zinc. *Biologia Plantarum*, *43*, 257-262.

Luo, X. S., Xue, Y., Wang, Y. L., Cang, L., Xu, B., & Ding, J. (2015). Source identification and apportionment of heavy metals in urban soil profiles. *Chemosphere, 127*, 152-157.

Macedo-Miranda, G., Avila-Pérez, P., Gil-Vargas, P., Zarazúa, G., Sánchez-Meza, J. C., Zepeda-Gómez, C., & Tejeda, S. (2016). Accumulation of heavy metals in mosses: a biomonitoring study. *SpringerPlus*, *5*, 1-13.

Magurran, A. E. (2003). *Measuring biological diversity*. John Wiley & Sons.

Mahapatra, B., Dhal, N. K., Dash, A. K., Panda, B. P., Panigrahi, K. C. S., & Pradhan, A. (2019). Perspective of mitigating atmospheric heavy metal pollution: using mosses as biomonitoring and indicator organism. *Environmental Science and Pollution Research*, *26*(29), 29620-29638.

Makholm, M. M., & Mladenoff, D. J. (2005). Efficacy of a biomonitoring (moss bag) technique for determining element deposition trends on a mid-range (375 km) scale. *Environmental Monitoring and Assessment*, *104*, 1-18.

Manisalidis, I., Stavropoulou, E., Stavropoulos, A., & Bezirtzoglou, E. (2020). Environmental and health impacts of air pollution: a review. *Frontiers in public health*, *8*, 14.

Marć, M., Tobiszewski, M., Zabiegała, B., de la Guardia, M., & Namieśnik, J. (2015). Current air quality analytics and monitoring: A review. *Analytica chimica acta*, *853*, 116-126.

Markert, B. (1993). Plants as biomonitors.

Markert, B. A., Breure, A. M. and Zechmeister, H. G. (2003). Definitions, strategies and principles for bioindication/Biomonitoring of the environment. Elsevier, *oxford*. pp. 3-39.

Markert, B. and Weckert, V. (1989). Fluctuations of element concentrations during the growing season of *Polytrichum formosum* (Hedw.). *Water, Air, Soil pollut*. *43*: 177-189.

Meng, W., Dai, Q., Ren, Q., Tu, N., & Leng, T. (2021). Ecological stoichiometric characteristics of soil-moss C, N, and P in restoration stages of karst rocky desertification. *PloS one*, *16*(6), e0252838.

Meylan, G., & Reck, B. K. (2017). The anthropogenic cycle of zinc: Status quo and perspectives. *Resources, Conservation and Recycling, 123,* 1-10.

Mikhailenko, A. V., Ruban, D. A., Ermolaev, V. A., & Van Loon, A. J. (2020). Cadmium pollution in the tourism environment: A literature review. *Geosciences, 10*(6), 242.

Mitra, S., Chakraborty, A. J., Tareq, A. M., Emran, T. B., Nainu, F., Khusro, A., Idris A. M., Khandaker M. U., Osman H., Alhumaydhi F. A. & Simal-Gandara, J. (2022). Impact of heavy metals on the environment and human health: Novel therapeutic insights to counter the toxicity. *Journal of King Saud University-Science*, *34*(3), 101865.

Mittler, R., & Zilinskas, B. A. (1994). Regulation of pea cytosolic ascorbate peroxidase and other antioxidant enzymes during the progression of drought stress and following recovery from drought. *The Plant Journal*, *5*(3), 397-405.

Monaci, F., Ancora, S., Bianchi, N., Bonini, I., Paoli, L., & Loppi, S. (2021). Combined use of native and transplanted moss for post-mining characterization of metal (loid) river contamination. *Science of the Total Environment*, *750*, 141669.

Mukhopadhyay, S., Dutta, R., & Das, P. (2020). A critical review on plant biomonitors for determination of polycyclic aromatic hydrocarbons (PAHs) in air through solvent extraction techniques. *Chemosphere*, *251*, 126441.

Munne-Bosch, S., & Alegre, L. (2002). Plant aging increases oxidative stress in chloroplasts. *Planta*, *214*, 608-615.

Negi, M. S. & Bisht, P. S. (2018). Social and economic determinants of migration and economic development of Uttarakhand: with special reference to Kumaun region. *Journal of Acharaya Narendra Dev Research Institute*, *26*(2), 15-22.

Nicholson, S. E., Some, B., McCollum, J., Nelkin, E., Klotter, D., Berte, Y., Diallo, B. M., Gaye, I., Kpabeba, G., Ndiaye, O., Noukpozounkou, J. N., Tanu, M. M., Thiam, A., Toure, A. A. & Traore, A. K. (2003). Validation of TRMM and other rainfall estimates with a high-

density gauge dataset for West Africa. Part II: Validation of TRMM rainfall products. *Journal of Applied Meteorology*, *42*(10), 1355-1368.

Nordstrom, U. (2019). *Moss*. Penguin UK.

Oishi, Y. (2018). Comparison of moss and pine needles as bioindicators of transboundary polycyclic aromatic hydrocarbon pollution in central Japan. *Environmental Pollution*, *234*, 330-338.

Ojo, F. P., Oluseye, O. C., & Abiola, O. G. (2012). Mosses as biomonitors of heavy metal deposition in the atmosphere. *International Journal of Environmental Sciences*, *1*(2), 56-62.

Okamoto, O. K., Pinto, E., Latorre, L. R., Bechara, E. J. H., & Colepicolo, P. (2001). Antioxidant modulation in response to metal-induced oxidative stress in algal chloroplasts. *Archives of Environmental Contamination and Toxicology*, *40*, 18-24.

Okamoto, O. K., Pinto, E., Latorre, L. R., Bechara, E. J. H., & Colepicolo, P. (2001). Antioxidant modulation in response to metal-induced oxidative stress in algal chloroplasts. *Archives of Environmental Contamination and Toxicology*, *40*, 18-24.

Onele, A. O., Chasov, A. V., Viktorova, L. V., Minibayeva, F. V., & Beckett, R. P. (2021). Characterization and expression analysis of ascorbate peroxidase from the moss *Dicranum scoparium* during abiotic stresses. *The Bryologist*, *124*(1), 68-84.

Onianwa, P. C. (2001). Monitoring atmospheric metal pollution: A review on the use of mosses as indicators. *Env. Monit. Assses*. *71:* 13-50.

Otvos, E., Pazmandi, T. and Tuba, Z. (2003). First national survey of atmospheric heavy metal deposition in Hungary by the analysis of mosses. S*ci. Tot. Environ. 309*: 151-160.

Ouzounidou, G. (1993). Changes in variable chlorophyll fluorescence as a result of Cu-treatment: dose-response relations in Silene and Thlaspi. *Photosynthetica, 29*:455-462.

Pagotto, C., Remy, N., Legret, M., & Le Cloirec, P. (2001). Heavy metal pollution of road dust and roadside soil near a major rural highway. *Environmental technology*, *22*(3), 307-319.

Paliulis, D. (2021). Removal of lead (II) and zinc (II) from aqueous solutions applying Fibber

Hemp (L.). *Ecological Chemistry and Engineering S*, *28*(2), 229-239.

Panda, S. K., Chaudhury, I., & Khan, M. H. (2003). Heavy metals induce lipid peroxidation and affect antioxidants in wheat leaves. *Biologia Plantarum*, *46*(2), 289-294.

Panda, S. K., & Choudhury, S. (2005). Chromium stress in plants. *Brazilian journal of plant physiology*, *17*, 95-102.

Pant, P., & Harrison, R. M. (2013). Estimation of the contribution of road traffic emissions to particulate matter concentrations from field measurements: A review. *Atmospheric environment*, *77*, 78-97.

Patsikka, E., Kairavuo, M., Sersen, F., Aro, E. M. & Tyystjarvi, E. (2002). Excess copper predisposes photosystem II to photoinhibition in vivo by outcompeting iron and causing decrease in leaf chlorophyll. *Plant Physiology*, *129*(3), 1359-1367.

Pavlikova, I., Motyka, O., Plasek, V., & Bitta, J. (2021). Monitoring of heavy metals and nitrogen concentrations in mosses in the vicinity of an integrated iron and steel plant: Case study in Czechia. *Applied Sciences*, *11*(17), 8262.

Perera, F. (2018). Pollution from fossil-fuel combustion is the leading environmental threat to global pediatric health and equity: Solutions exist. *International journal of environmental research and public health*, *15*(1), 16.

Popper, Z. A., & Fry, S. C. (2003). Primary cell wall composition of bryophytes and charophytes. *Annals of botany*, *91*(1), 1-12.

Putter, J. (1974). *In Methods of Enzymatic Analysis*. 2 (ed.) Bergmeyer Academic Press, New York, pp 685.

Qarri, F., Lazo, P., Allajbeu, S., Bekteshi, L., Kane, S., & Stafilov, T. (2019). The evaluation of air quality in Albania by moss biomonitoring and metals atmospheric deposition. *Archives of environmental contamination and toxicology*, *76*, 554-571.

Quartacci, M. F., Cosi, E. and Navari Izzo, F. (2001). Lipids and NADPH dependnt superoxide production in plasma membrane vesicle from roots of wheat grown under copper

deficiency or excess. *J. Exp. Bot. 52*: 77-84.

Radziemska, M., Mazur, Z., Bes, A., Majewski, G., Gusiatin, Z. M., & Brtnicky, M. (2019). Using mosses as bioindicators of potentially toxic element contamination in ecologically valuable areas located in the vicinity of a road: a case study. *International journal of environmental research and public health*, *16*(20), 3963.

Rahimzadeh, M. R., Rahimzadeh, M. R., Kazemi, S., & Moghadamnia, A. A. (2017). Cadmium toxicity and treatment: An update. *Caspian journal of internal medicine*, *8*(3), 135.

Rai, P. K. and Panda, L. L. S. (2005). Roadside plants as bio indicators of air pollution in an industrial region, Rourkela, India. *Int. J. of Advancements in Res. & Tech., 4*(1), 14-36.

Rajfur, M. (2013). Algae as a source of information on surface waters contamination with heavy metals. *Ecological Chemistry and Engineering. A*, *20*(10).

Rajfur, M., Stoica, A. I., Swisłowski, P., Stach, W., Ziegenbalg, F., & Mattausch, E. M. (2024). Assessment of Atmospheric Pollution by Selected Elements and PAHs during 12-Month Active Biomonitoring of Terrestrial Mosses. *Atmosphere*, *15*(1), 102.

Rashid, M. H., Babu, D., & Siraki, A. G. (2021). Interactions of the antioxidant enzymes NAD (P) H: Quinone oxidoreductase 1 (NQO1) and NRH: Quinone oxidoreductase 2 (NQO2) with pharmacological agents, endogenous biochemicals and environmental contaminants. *Chemico-Biological Interactions*, *345*, 109574.

Recknagel, S., Radant, H., & Kohlmeyer, R. (2014). Survey of mercury, cadmium and lead content of household batteries. *Waste management*, *34*(1), 156-161.

Reguera, P., Couceiro, L., & Fernández, N. (2018). A review of the empirical literature on the use of limpets *Patella* sp. (Mollusca: Gastropoda) as bioindicators of environmental quality. *Ecotoxicology and environmental safety*, *148*, 593-600.

Reimann, C., Niskavaara, H., Kashulina, G., Filzmoser, P., Boyd, R., Volden, T., Tomilina, O & Bogatyrev, I. (2001). Critical remarks on the use of terrestrial moss (*Hylocomium splendens* and *Pleurozium schreberi*) for monitoring of airborne pollution. *Environmental pollution*, *113*(1), 41-57.

Rippy, J. F., Nelson, P. V., & Bilderback, T. (2005). Cation Exchange Capacity and Base Saturation of 64 Peat Mosses. *HortScience*, *40*(4), 1124D-1124.

Rissman, J., Bataille, C., Masanet, E., Aden, N., Morrow III, W. R., Zhou, N., Elliott N., Dell R., Heeren N., Huckestein B., Cresko J., Miller S. A., Roy J., Fennell P., Cremmins B, Blank T.K., Hone D, Williams E.D., Rue du Can S., Sisson B., Williams M., Katzenberger J., Burtraw D., Sethi G., Ping H., Danielson D., Lu H., Lorber T., Dinkel J. & Helseth, J. (2020). Technologies and policies to decarbonize global industry: Review and assessment of mitigation drivers through 2070. *Applied energy*, *266*, 114848.

Ross, H. B. (1990). On the use of the mosses *Hylocomium splendens* and *Pleurozium schreberi* for estimating atmospheric trace metal deposition. *Water, Air, Soil Pollut*. *50*: 63-76.

Ruhling, Å., & Tyler, G. (1970). Sorption and retention of heavy metals in the woodland moss *Hylocomium splendens* (Hedw.) Br. et Sch. Oikos, 92-97.

Ruhling, A. and Tyler, G. (1973). Heavy metal deposition in Scandinavia. *Water, Air, Soil Pollut. 2*: 445-455.

Ruhling, A. and Tyler, G. (1984). Recent changes in deposition of heavy metals in Northern Europe. *Water, Air, Soil Pollut*. *22*: 173-180.

Ruhling, A. (Ed.). (1994). Atmospheric heavy metal deposition in Europe .Estimations Based on Moss Analysis , vol. 9.Nordic Council of Ministers , Copenhagen, NORD. pp. 1-53.

Sahu, V., & Asthana, A. K. (2015). Diversity in mosses of Pithoragarh and its neighbouring areas, Western Himalaya, India. *Indian Forester*, *141*(11), 1183-1193.

Sainger, M., Sharma, A., Bauddh, K., Sainger, P. A., & Singh, R. P. (2014). Remediation of nickel-contaminated soil by Brassica juncea L. cv. T-59 and effect of the metal on some metabolic aspects of the plant. *Bioremediation journal*, *18*(2), 100-110.

Salo, H., Paturi, P., & Makinen, J. (2016). Moss bag (*Sphagnum papillose*) magnetic and elemental properties for characterizing seasonal and spatial variation in urban pollution. *International journal of environmental science and technology*, *13*, 1515–1524.

Salo, H., & Makinen, J. (2019). Comparison of traditional moss bags and synthetic fabric bags in magnetic monitoring of urban air pollution. *Ecological indicators*, *104*, 559-566.

Sawant, K., Prakash, R., & Mishra, N. (2021). Effect of Urban Land Use on Agriculture, Forest, and River Beds: A Case Study of Dehradun City, Uttarakhand, India. In *Advances in Civil Engineering and Infrastructural Development: Select Proceedings of ICRACEID 2019* (pp. 187-196). Springer Singapore.

Saxena, D. K., & Saxena, A. (2000). Uptake of metals in Plagiochasma and their uses in pollution monitoring. *Geophytology*, *28*(1&2), 129-137.

Saxena, D. K. & Arfeen, S. (2010). Metal deposition pattern in Kumaon hills (India) through active monitoring using moss *Racomitrium crispulum*. *Iran. J. Environ. Health. Sci. Eng.*, 7(2), 103-114

Saxena, D. K. and Arfeen, M. S. (2006b). Response of nitrate Reductase activity and antioxidative defense system in moss *Racomitrium crispulum* (Hook. F. et Wils.) Hook. F. et Wils. To lead and zinc toxicity. *Physiol. Mol. Biol. Plants.* 12 (4): 303-306.

Saxena, D. K., & Arfeen, M. S. (2009). Effect of Cu and Cd on oxidative enzymes and chlorophyll content of moss Racomitrium crispulum. *Taiwania*, *54*(4), 365-374.

Saxena, D. K., Janajreh, I., & Gahtori, D. (2014). Monitoring of Metal Dispersion in Kumaon Hills (INDIA) Through Active Monitoring Using Moss. *Int. J. of Sustainable Water and Environmental Systems*, *6*(1), 1-15.

Saxena, D. K., Saxena, A., & Srivastava, H. S. (2000). Biomonitoring of metal precipitation at petrol pumps and their effects on moss *Sphagnum cuspidatum* Hoffm. *Journal of environmental studies and policy*, *3*(2), 95-102.

Saxena, D. K., Singh, S. O., & Srivastava, K. (2006). Distribution of some mosses in Nainital, Almora and Pithoragarh district of Kumaon region, India. *Environment Conservation Journal*, *7*(1&2), 83-87.

Saxena, D. K., Singh, S., & Srivastava, K. (2008). Atmospheric heavy metal deposition in Garhwal hill area (India): Estimation based on native moss analysis. *Aerosol and Air Quality Research*, *8*(1), 94-111.

Saxena, D. K., Singh, S., & Srivastava, K. (2008). Atmospheric heavy metal deposition in Garhwal hill area (India): Estimation based on native moss analysis. *Aerosol and Air Quality Research*, *8*(1), 94-111.

Shakya, K., Chettri, M. K., & Sawidis, T. (2008). Impact of heavy metals (copper, zinc, and lead) on the chlorophyll content of some mosses. *Archives of Environmental Contamination and Toxicology*, *54*, 412-421.

Shankar, N.; Kamakshi; Saxena, A., & Saxena, D. K. (2000). Variations in some metabolites and nitrate reductase activity in *Plagiochasma appendiculatum* in polluted urban environment. *Physiol. Mol. Biol. Plants, 6:* 89-91.

Singh, S., Srivastava, K., Gahtori, D., & Saxena, D. K. (2017). Bryomonitoring of atmospheric elements in *Rhodobryum giganteum* (Schwaegr.) Par., growing in Uttarakhand region of Indian Himalayas. *Aerosol and Air Quality Research, 17*(3), 810-820.

Sheoran, I. S., Aggarwal, N., & Singh, R. (1990). Effects of cadmium and nickel on in vivo carbon dioxide exchange rate of pigeon pea (*Cajanus cajan* L.). *Plant and soil*, *129*, 243-249.

Sheue, C. R., Sarafis, V., Kiew, R., Liu, H. Y., Salino, A., Kuo-Huang, L. L., Yang, Y. P., Tsai, C. C., Lin, C. H., Yong, J. W. H. & Ku, M. S. (2007). Bizonoplast, a unique chloroplast in the epidermal cells of microphylls in the shade plant *Selaginella erythropus* (Selaginellaceae). *American Journal of Botany*, *94*(12), 1922-1929.

Shvetsova, M. S., Kamanina, I. Z., Frontasyeva, M. V., Madadzada, A. I., Zinicovscaia, I. I., Pavlov, S. S., Vergel, N., & Yushin, N. S. (2019). Active moss biomonitoring using the "moss bag technique" in the park of Moscow. *Physics of Particles and Nuclei Letters*, *16*, 994-1003.

Singh, P. D., Salgotra, A. K., & Manhas, A. S. (2019). Causes and consequences of environment degradation in Uttarakhand. *Indian Journal of Economics and Development*, *7*(4), 1-9.

Singh, S., Parihar, P., Singh, R., Singh, V. P., & Prasad, S. M. (2016). Heavy metal tolerance in plants: role of transcriptomics, proteomics, metabolomics, and ionomics. *Frontiers in plant science*, *6*, 1143.

Singh, S., Srivastava, K., Gahtori, D., & Saxena, D. K. (2017). Bryomonitoring of atmospheric elements in *Rhodobryum giganteum* (Schwaegr.) Par., growing in Uttarakhand region of Indian Himalayas. *Aerosol and Air Quality Research*, *17*(3), 810-820.

Sinha, S., Singh, A., Sinha, D., & Chatterjee, R. (2021). A review on bryophytes as key bio-indicators to monitor heavy metals in the atmosphere. *International Journal of Plant and Environment*, *7*(01), 49-62.

Słonina, N., Świsłowski, P., & Rajfur, M. (2021). Passive and active biomonitoring of atmospheric aerosol with the use of mosses. *Ecological Chemistry and Engineering S*, *28*(2), 163-172.

Sloof, J. E., Wolterbeek, H. Th. (1991). National trace-element air pollution monitoring survey using epipjhytic lichens. *Lichenologist. 23*: 139-165.

Smolders, E., Mertens, J. (2013). Cadmium. In heavy metals in soils: trace metals and metalloids in soils and their bioavailability; Alloway, B.J., Ed.; Springer: Dordrecht, The Netherlands, pp. 283–311.

Snedecor, G. W. and Cochran W. G. (1967). *Statistical methods*. Lowa State University, U. S. A. Oxford and I. B. H. Publishing Co., New Delhi.

Soudzilovskaia, N. A., Cornelissen, J. H. C., During, H. J., Van Logtestijn, R. S. P., Lang, S. I., & Aerts, R. (2010). Similar cation exchange capacities among bryophyte species refute a presumed mechanism of peatland acidification. *Ecology*, *91*(9), 2716-2726.

Srivastava, H.S. (1975). Distribution of nitrate reductase ageing bean seedlings. *Plants Cell Physio., 16*: 995-999.

Srivastava, H. S. (2004). Plant Physiology: A textbook for University students. Rastogi publications. India. pp-167-181.

Srivastava, K., Singh, S., & Saxena, D. K. (2014). Monitoring of metal deposition by moss *Barbula constricta* J. Linn., from Mussoorie Hills in India. *Environmental Research, Engineering and Management*, *67*(1), 54-62.

Ştefanuţ, S., Manole, A., Ion, M. C., Constantin, M., Banciu, C., Onete, M., Manu M., Vicol I., Moldoveanu M. M., Maican S., Cobzaru I., Nicoara R. G., Florescu L. I., Mogildea E. D., Purice D. M., Nicolae C. D., Catana R. D., Teodosiu G., Dumitrache C. A., Maria G. M., Vatca C., Oanţa M. & Öllerer, K. (2018). Developing a novel warning-informative system

as a tool for environmental decision-making based on biomonitoring. *Ecological Indicators*, *89*, 480-487.

Steinnes, E. (1993). In some aspects of Biomonitoring of air pollutants using mosses as illustrated by the 1976 Norwegian Survey. Markert, B. (Ed). VHC, weinheim. pp 381-394.

Steinnes, E. (1995). A critical evaluation of the use of naturally growing moss to monitor the deposition of atmospheric metals. *Sci Tot. Environ*. *161*: 243-249.

Subramoniam, A. and Subhisha, S. (2005). Bryophytes of India: A potential source of anti-microbial agents. In: Khan, I.A., Khanum, A. editors. Role of biotechnology in medicinal and aromatic plants. Vol.11. Hyderabad, India: Ukaaz Publications.

Sujetoviene, G., & Galinyte, V. (2016). Effects of the urban environmental conditions on the physiology of lichen and moss. *Atmospheric Pollution Research*, *7*(4), 611-618.

Sulistiyorini, D., Walgraeve, C., & Van Langenhove, H. (2022). Biomonitoring of polycyclic aromatic hydrocarbons in the ambient air using plants: a review. In *Proceedings of the International Conference on Radioscience, Equatorial Atmospheric Science and Environment and Humanosphere Science, 2021* (pp. 457-494). Singapore: Springer Nature Singapore.

Swisłowski, P., Ziembik, Z., & Rajfur, M. (2021). Air quality during new year's eve: A biomonitoring study with moss. *Atmosphere*, *12*(8), 975.

Swislowski, P., Vergel, K., Zinicovscaia, I., Rajfur, M., & Waclawek, M. (2022). Mosses as a biomonitor to identify elements released into the air as a result of car workshop activities. *Ecological Indicators*, *138*, 108849.

Tan, B. C., Ho, B. C., Linis, V., Iskandar, E. A., Nurhasanah, I., Mulyati, S., & Haerida, I. (2006). Mosses of Gunung Halimun National Park, West Java, Indonesia. *Reinwardtia*, *12*(3), 205-214.

Tiwari, S., & Agrawal, S. B. (Eds.). (2022). *New Paradigms in Environmental Biomonitoring Using Plants*. Elsevier.

Turetsky, M. R., Mack, M. C., Hollingsworth, T. N., & Harden, J. W. (2010). The role of mosses in ecosystem succession and function in Alaska's boreal forest. *Canadian Journal of Forest Research*, *40*(7), 1237-1264.

Tyler, G. (1990). Bryophytes and heavy metals: a literature review. *Bot. J. Linn. Soc. 104:* 231-253.

Uka, U. N., Belford, E. J., & Elebe, F. A. (2021). Effects of road traffic on photosynthetic pigments and heavy metal accumulation in tree species of Kumasi Metropolis, Ghana. *SN Applied Sciences*, *3*, 1-12.

Vajpayee, P., Tripathi, R. D., Rai, U. N., Ali, M. B., & Singh, S. N. (2000). Chromium (VI) accumulation reduces chlorophyll biosynthesis, nitrate reductase activity and protein content in Nymphaea alba L. *Chemosphere*, *41*(7), 1075-1082.

Van Assche, F. & Clijsters, H., (1990). Effect of metal on enzyme activity in plants. *Plant Cell Environ., 13:*195-206.

Van Laaten, N., Merten, D., von Tümpling, W., Schäfer, T., & Pirrung, M. (2020). Comparison of spider web and moss bag biomonitoring to detect sources of airborne trace elements. *Water, Air, & Soil Pollution*, *231*, 1-17.

Vats, S. K., Singh, A., Koul, M., & Uniyal, P. L. (2010). Study on the metal absorption by two mosses in Delhi Region (India). *J Am Sci*, *6*(3), 176-181.

Vieille, B., Albert, I., Leblond, S., Couvidat, F., Parent, É., & Meyer, C. (2021). Are Grimmia mosses good biomonitors for urban atmospheric metallic pollution? Preliminary evidence from a French case study on cadmium. *Atmosphere*, *12*(4), 491.

Vincent, W. F. (1980). Mechanisms of rapid photosynthetic adaptation in natural phytoplankton communities II. Changes in photochemical capacity as measured by DCMU-induced chlorophyll fluorescence. *Journal of Phycology*, *16*(4), 568-577.

Vyas, J. & Puranik, R. G. (1995). Inhibition of nitrate Reductase activity by arcenate in excised leaf segments. *Indian J. Plant Physiol.* 38: 143-147.

Wahid, A., Ghani, A., Ali, I., & Ashraf, M. Y. (2007). Effects of cadmium on carbon and nitrogen assimilation in shoots of mungbean [*Vigna radiata* (L.) Wilczek] seedlings. *Journal of*

agronomy and crop science, *193*(5), 357-365.

Wang, J. J., Chen, Q. Y., Liu, L., Yang, L., Zhang, Z., Zhang, Q., & Cao, D. J. (2022). Effects of lead on Cladophora rupestris: localization, subcellular distribution, and cell ultrastructure. *Bioremediation Journal*, *26*(1), 20-30.

Wang, M., Xiao, Y., Song, B., Zhang, X., & Zhuang, W. (2024). Pb-N complex stress mitigates the physiological damage of a single stress (Pb or N) on bryophytes. *Acta Physiologiae Plantarum*, *46*(6), 68.

Wei, Z., Gu, H., Van Le, Q., Peng, W., Lam, S. S., Yang, Y., Li, C. & Sonne, C. (2021). Perspectives on phytoremediation of zinc pollution in air, water and soil. *Sustainable Chemistry and Pharmacy*, *24*, 100550.

Wiersma, G. B., Bruns, D. A., Boelcke, C., Whitworth, C., & McAnulty, L. (1990). Elemental composition of mosses from a remote Nothofagus forest site in southern Chile. *Chemosphere*, *20*(5), 569-583.

Wilkie, D., & La Farge, C. (2011). Bryophytes as heavy metal biomonitors in the Canadian High Arctic. *Arctic, Antarctic, and Alpine Research*, *43*(2), 289-300.

Wolterbeek, H. T., & Bode, P. (1995). Strategies in sampling and sample handling in the context of large-scale plant biomonitoring surveys of trace element air pollution. *Science of the Total Environment*, *176*(1-3), 33-43.

Wolterbeek, B. (2002). Biomonitoring of trace element air pollution: principles, possibilities, and perspectives. *Environmental pollution*, *120*(1), 11-21.

Wu, Q., Wang, X., & Zhou, Q. (2014). Biomonitoring persistent organic pollutants in the atmosphere with mosses: performance and application. *Environment International*, *66*, 28-37.

Yadav, S., Tripathi, S. N., & Rupakheti, M. (2022). Current status of source apportionment of ambient aerosols in India. *Atmospheric Environment*, *274*, 118987.

Yarragunta, Y., Srivastava, S., Mitra, D., & Chandola, H. C. (2020). Influence of forest fire episodes on the distribution of gaseous air pollutants over Uttarakhand, India. *GIScience & Remote Sensing*, *57*(2), 190-206.

Yushin, N., Chaligava, O., Zinicovscaia, I., Vergel, K., & Grozdov, D. (2020). Mosses as bioindicators of heavy metal air pollution in the lockdown period adopted to cope with the COVID-19 pandemic. *Atmosphere*, *11*(11), 1194.

Zechmeister, H.G., Grodzinska, K. and Szarek-Lukaszewska, G. (2003). Bryophytes. In: Markert, B. A., Breure, A. M., and Zechmeister, H. G. (Eds) bioindicators and biomonitors. Elsevier, Oxford. Pp 329-375.

Zeng, J., Tang, J., Zhang, F., Wang, Y., Kang, H., Chen, G., Zhang, Z., Yuan, S. & Zhou, Y. (2021). Ammonium regulates redox homeostasis and photosynthetic ability to mitigate copper toxicity in wheat seedlings. *Ecotoxicology and Environmental Safety*, *226*, 112825.

Zhou, J., Jiang, Z., Ma, J., Yang, L., & Wei, Y. (2017). The effects of lead stress on photosynthetic function and chloroplast ultrastructure of Robinia pseudoacacia seedlings. *Environmental Science and Pollution Research*, *24*, 10718-10726.

Zinicovscaia, I., Urosevic, M. A., Vergel, K., Vieru, E., Frontasyeva, M. V., Povar, I., & Duca, G. (2018). Active moss biomonitoring of trace elements air pollution in Chisinau, Republic of Moldova. *Ecological Chemistry and Engineering S*, *25*(3), 361-372.

LIST OF APPENDICES

APPENDIX 1

भारत सरकार
GOVERNMENT OF INDIA
पर्यावरण, वन और जलवायु परिवर्तन मंत्रालय
MINISTRY OF ENVIRONMENT, FOREST & CLIMATE CHANGE
फैक्स/ Fax: (033)26686226
दूरभाष/ Phone: (033)26683235/3364
इमेल/ E-mail: calherbarium@yahoo.co.in

सत्यमेव जयते

भारतीय वनस्पति सर्वेक्षण
BOTANICAL SURVEY OF INDIA
केंद्रीय राष्ट्रीय पादपालय
CENTRAL NATIONAL HERBARIUM
हावड़ा / HOWRAH – 711 103

संख्या/No.: CNH/Tech.II/2023/28 दिनांक/Date: 16-03-2023

To,
Mr. Dheeraj Gahtori
Research Scholar
Lovely Professional University
Jalandhar

Sub.: Identification of one plant specimen – reg.

Dear Mr. Gahtori,

Please refer to your letter dated 11th November 2022 along with a moss specimen for identification. It is to inform you that the specimen has been identified by the concerned expert as:

Sl. No.	Specimen No.	Scientific Name	Family
1.	LPU/DG–01	**Thuidium cymbifolium** (Dozy & Molk.) Dozy & Molk.	Thuidiaceae

The receipt of ₹ 500/- (Rupees Five hundred only) Transaction Ref. No. 0511220000979 dated 5-11-2022, payment made via bharatkosh.gov.in is enclosed herewith.

Please send someone for collecting the specimen within three months from the date of receipt of this letter failing which it will be discarded.

Yours sincerely

16/03/2023

(K. KARTHIGEYAN)
Scientist –'E'
वैज्ञानिक 'ई' Scientist- 'E'
केन्द्रीय राष्ट्रीय पादपालय
Central National Herbarium
भारतीय वनस्पति सर्वेक्षण
Botanical Survey of India
हावड़ा/Howrah-711 103

APPENDIX 2

"जैव विविधता संरक्षण.....प्रकृति के साथ जीने की कला"

कार्यालय उत्तराखण्ड जैव विविधता बोर्ड, देहरादून।

ई–मेल : sbbuttarakhand@gmail.com
वेबसाइट : www.sbb.uk.gov.in
423, इन्दिरा नगर कॉलोनी (निकट मलिक चौक),
देहरादून–248006 (टेलीफैक्स - 0135-2769886)

पत्रांक : 660 /जै०वि०बो०–16–25 दिनांक 10 जून, 2020

सेवा में,

डा० जोगिन्दर सिंह,
प्रोफेसर,
Climate Mitigation and Sustainbale Agriculture Research lab (CMaSAR)
Division of Research and Development.
Lovely Campus, Jalandhar-Delhi G.T. Road (NH-1),
Phagwara, Punjab.

विषयः जनपद चम्पावत एवं पिथौरागढ के वनों में शोध कार्य की अनुमति प्रदान करने के सम्बन्ध में।

सन्दर्भः आपका पत्र दिनांक 03.06.2020.

महोदय,

आपने अपने दिनांक 03.06.2020 द्वारा सूचित किया है कि आपके दिशा–निर्देशन में श्री धीरज गहतोडी शोध कार्य कर रहे हैं जिनका शोध शीर्षक "Potential of Mosses as heavy metal pollution indicators of the Kumaon Region of Uttarakhand India" है। आपके द्वारा चम्पावत एवं पिथौरागढ जनपद में मोस को एकत्रित करने एवं शोध कार्य की अनुमति मांगी गई है, के संबंध में निम्नानुसार अवगत करना है :–

- किसी भारतीय नागरिक अथवा संस्थान को किसी जैव विविधता/जैव सम्पदा पर **अकादमिक शोध कार्य** करने हेतु राज्य जैव विविधता बोर्ड अथवा राष्ट्रीय जैव विविधता प्राधिकरण से पूर्वानुमति लेने की आवश्यकता नहीं है बशर्ते कि शोध कार्य किसी जैव संसाधन का **वाणिज्यिक उपयोग से सम्बन्धित न हो और ना ही शोध कार्य में किसी विदेशी व्यक्ति अथवा संस्थान की सहभागिता हो।**
- यदि शोध कार्य का वर्तमान उद्देश्य किसी जैव संसाधन का वाणिज्यिक उपयोग करना नहीं है परन्तु शोध के निष्कर्ष को भविष्य में वाणिज्यिक उपयोग में लाया जा सकता है तो उचित होगा कि शोध कार्य करने से पूर्व राज्य जैव विविधता बोर्ड से पूर्वानुमति ली जाये।

कृपया इस सम्बन्ध में और अधिक जानकारी प्राप्त करने के लिये जैव विविधता अधिनियम, 2002 की धारा–2, 4, 5 व 6 का अध्ययन करने का कष्ट करें। उक्त अधिनियम उत्तराखण्ड जैव विविधता बोर्ड की वैबसाईट www.ssb.uk.gov.in में उपलब्ध है।

अतः कृपया उपरोक्तानुसार अग्रेतर कार्यवाही करने का कष्ट करें।

भवदीय,
10/06/2020
(एस०एस० रसाईली)
सदस्य–सचिव,
उत्तराखण्ड जैव विविधता बोर्ड,
देहरादून।

APPENDIX 3

DEPARTMENT OF BOTANY
H.N.B. POST GRADUATE COLLLEGE KHATIMA
UDHAM SINGH NAGAR (UTTARAKHAND)

NO OBJECTION CERTIFICATE

This is to certify that :-

a. The department has No objection in allowing Mr. Dheeraj Gahtori to pursue his Research work in the Department of Botany of HNBPG College, Khatima.

b. General Physical facilities, such as furniture/space etc. Are available in the related department and shall be provided to the candidate mentioned above for his Doctoral Research.

डा०..... 17/03/20
एसो० / असि० प्रोफेसर
एच.एन.बी. राजकीय स्ना०महाविद्यालय
खटीमा (ऊधम सिंह नगर)

Dr. Anjana Chandola Bhatt
Head
Department of Botany

APPENDIX 4

PUBLICATIONS:

1. Gahtori, D., Singh, J., & Vyas, A. (2024). Assessment of atmospheric metal deposition by moss Thuidium cymbifolium (Dozy & Molk.) Dozy & Molk. At Champawat Hills, India. *Vegetos*, 1-13. DOI: https://doi.org/10.1007/s42535-024-00937-w Scopus indexed

CONFERENCES:

1. Presented a paper entitled "*An assessment of atmospheric metal deposition by moss Thulium cyambifolium (Dozy & Molk.) Dozy & Molk.*" in the 2nd International Conference on Plant Physiology and Biotechnology(ICPPB) held from April 20 to 21, 2023, and was organized by the School of bioengineering and, in Lovely Professional University Punjab.

2. Presented a paper entitled "*Large scale atmosphere monitoring by mosses in district Champawat, Uttarakhand, India*" at the International Conference on Global Efforts on Agriculture, Forestry, Environment, and Food Security (Theme Climate change and its impact-GAFEF-2022) held at Tribhuvan University, Pokhara Campus, Nepal from 17 to 19 August 2021.

APPENDIX 5

PHOTO GALLARY

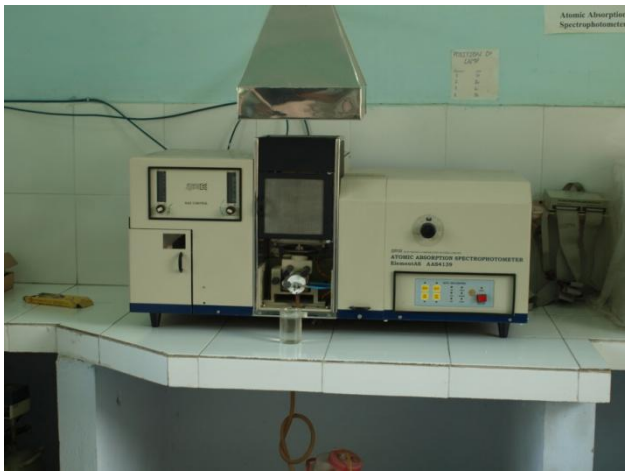

Atomic Absorption Spectrophotometer

Digestion Samples

Transplant Bags

A study Site

Collection of Moss